



US 20170001170A1

(19) United States

(12) Patent Application Publication (10) Pub. No.: US 2017/0001170 A1  
Ghosh et al. (43) Pub. Date: Jan. 5, 2017

---

(54) METHOD, SYNTHESIS, ACTIVATION PROCEDURE AND CHARACTERIZATION OF AN OXYGEN RICH ACTIVATED POROUS CARBON SORBENT FOR SELECTIVE REMOVAL OF CARBON DIOXIDE WITH ULTRA HIGH CAPACITY

(71) Applicants: **William Marsh Rice University**, Houston, TX (US); **Apache Corporation**, Houston, TX (US)

(72) Inventors: **Saunab Ghosh**, Houston, TX (US); **Andrew R. Barron**, Houston, TX (US); **Jason Ho**, Houston, TX (US)

(73) Assignees: **William Marsh Rice University**, Houston, TX (US); **Apache Corporation**, Houston, TX (US)

(21) Appl. No.: 15/200,632

(22) Filed: Jul. 1, 2016

#### Related U.S. Application Data

(60) Provisional application No. 62/187,744, filed on Jul. 1, 2015.

#### Publication Classification

(51) Int. Cl.  
**B01J 20/20** (2006.01)  
**C10L 3/10** (2006.01)

**B01J 20/30** (2006.01)  
**B01D 53/04** (2006.01)  
**C01B 31/12** (2006.01)  
**B01J 20/28** (2006.01)  
(52) U.S. Cl.  
CPC ..... **B01J 20/20** (2013.01); **C01B 31/12** (2013.01); **B01J 20/28066** (2013.01); **B01J 20/28076** (2013.01); **B01J 20/3078** (2013.01); **B01D 53/04** (2013.01); **C10L 3/104** (2013.01); **C10L 2290/541** (2013.01)

(57)

#### ABSTRACT

The present disclosure pertains to materials for CO<sub>2</sub> adsorption at pressures above 1 bar, where the materials include a porous carbon material with a surface area of at least 2800 m<sup>2</sup>/g, a total pore volume of at least 1.35 cm<sup>3</sup>/g, and a carbon content of 80%-95%. The porous carbon material is prepared by heating organic polymer precursors or biological materials in the presence of KOH at 700° C.-800° C. The present disclosure also pertains to materials for the separation of CO<sub>2</sub> from natural gas at partial pressures above 1 bar, where the material includes a porous carbon material with a surface area of at least 2000 m<sup>2</sup>/g, a total pore volume of at least 1.00 cm<sup>3</sup>/g, and a carbon content of greater than 90%. The porous carbon materials can be prepared by heating organic polymer precursors or biological materials in the presence of KOH at 600° C.-700° C.

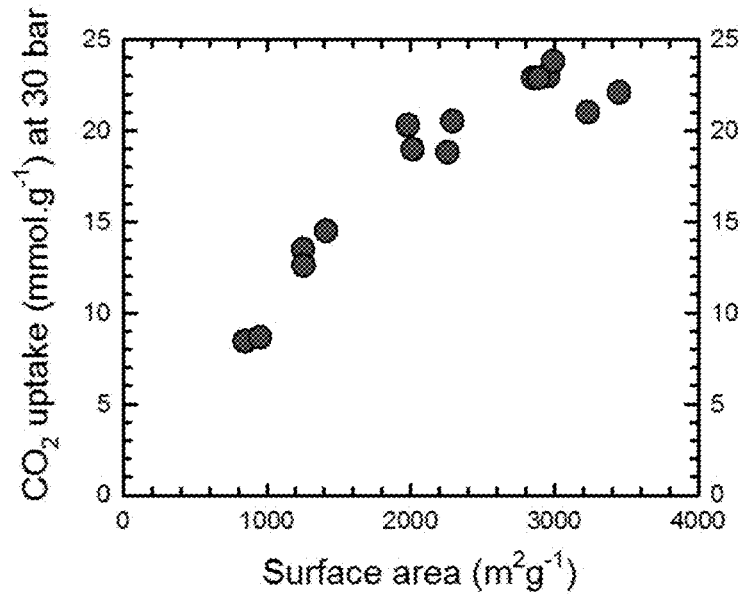


**FIG. 1A**

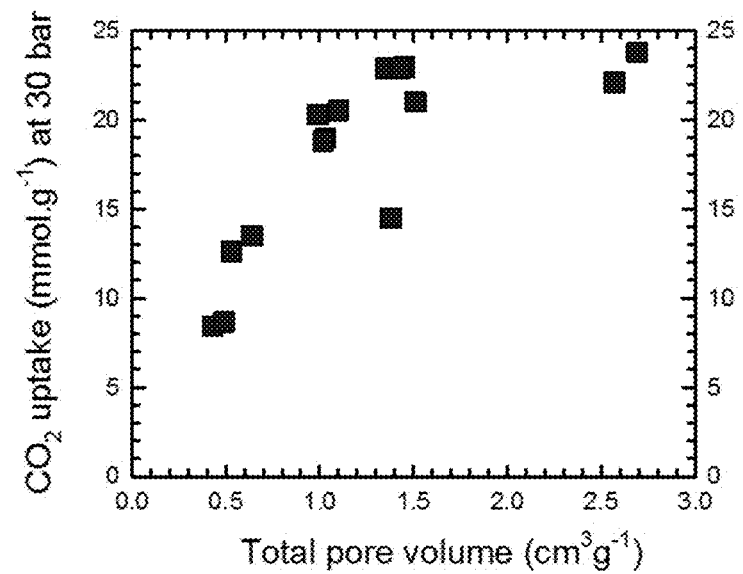


**FIG. 1B**

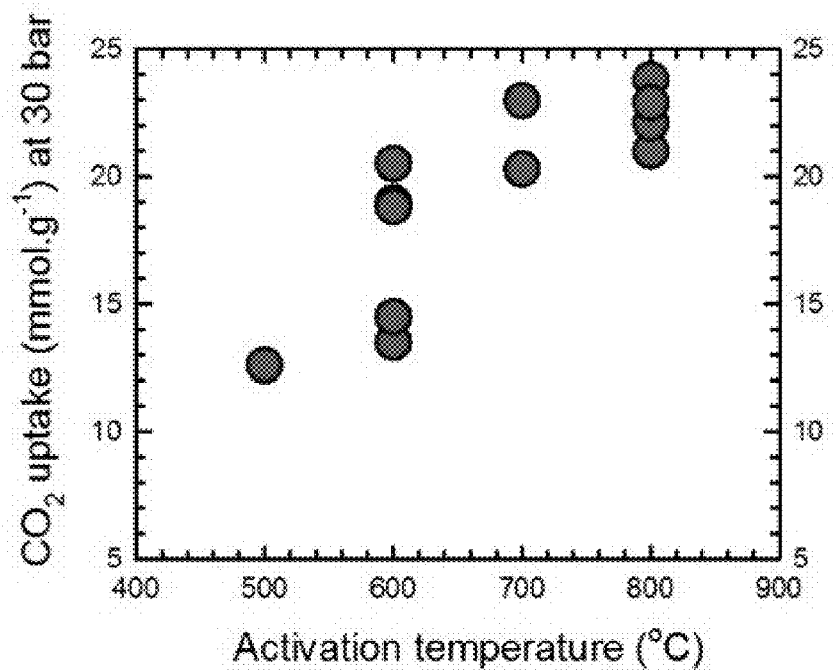


**FIG. 2**

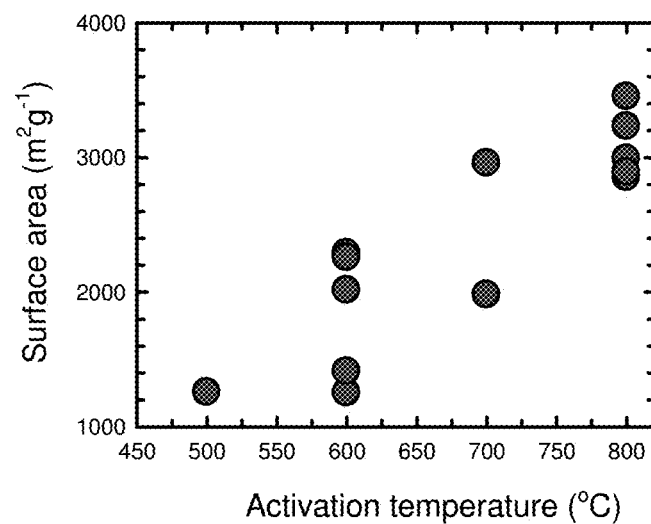


**FIG. 3A**

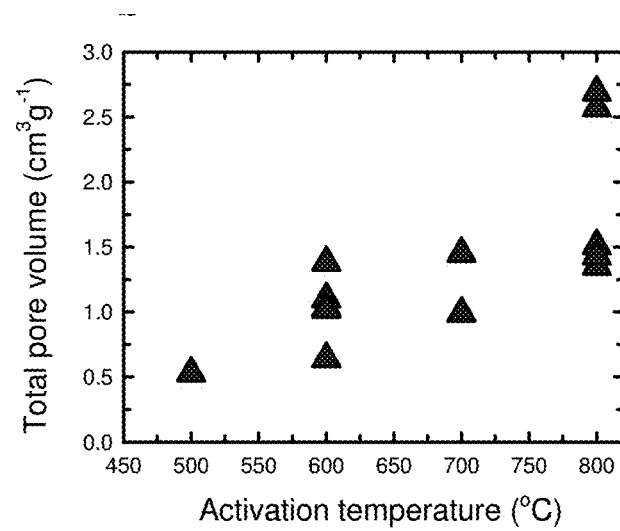


**FIG. 3B**

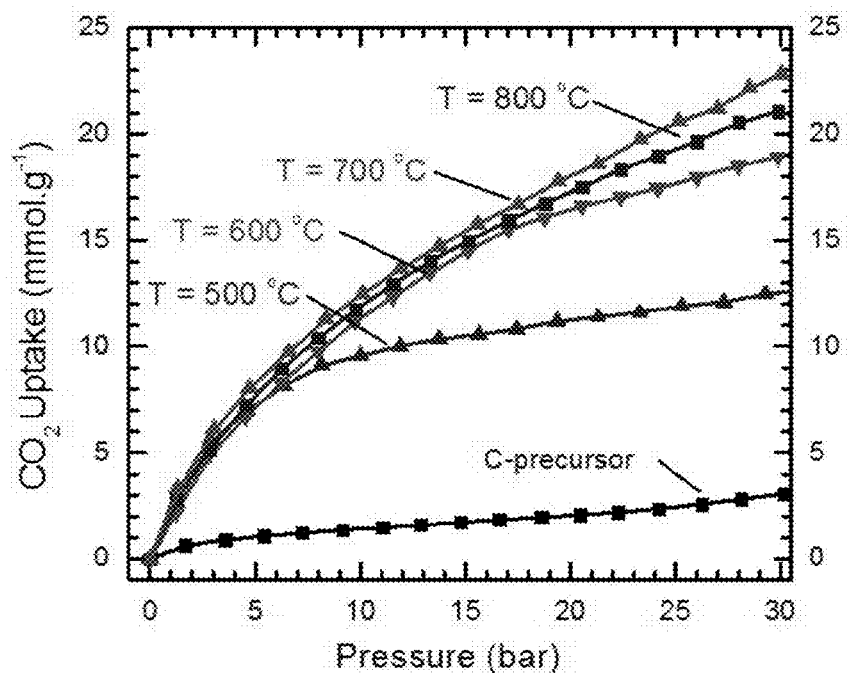
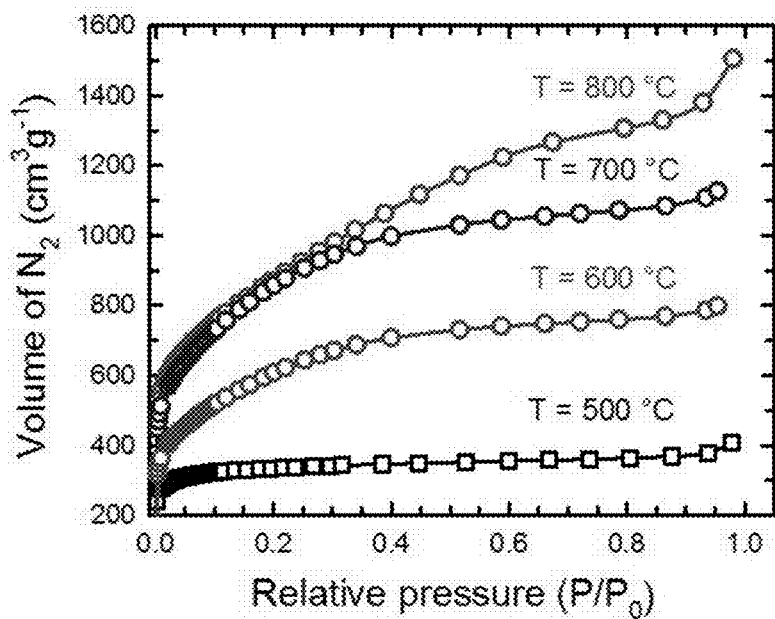
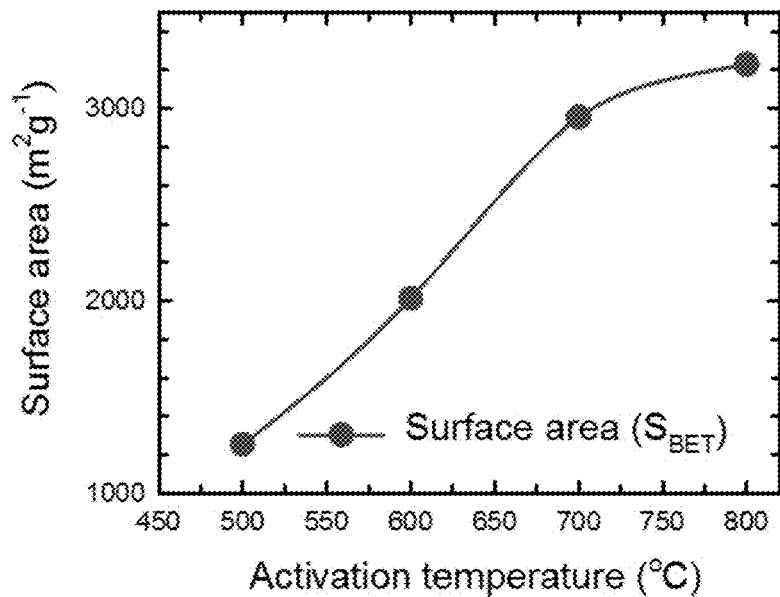


FIG. 4



**FIG. 5**



**FIG. 6A**

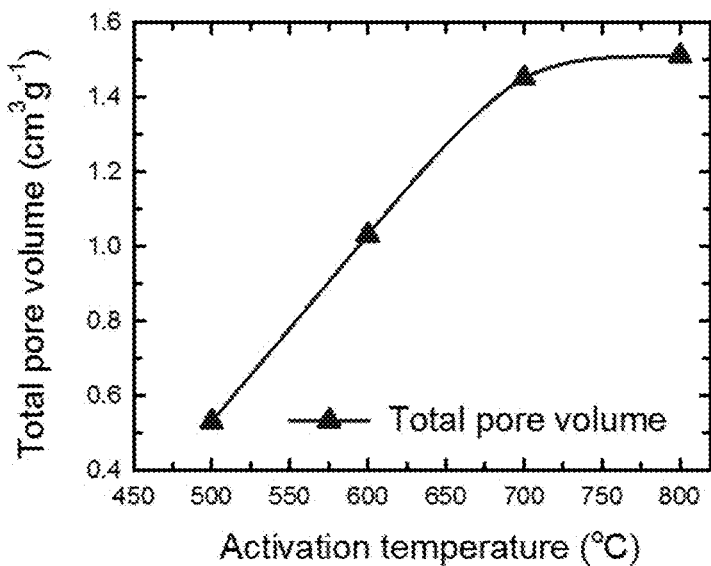


**FIG. 6B**

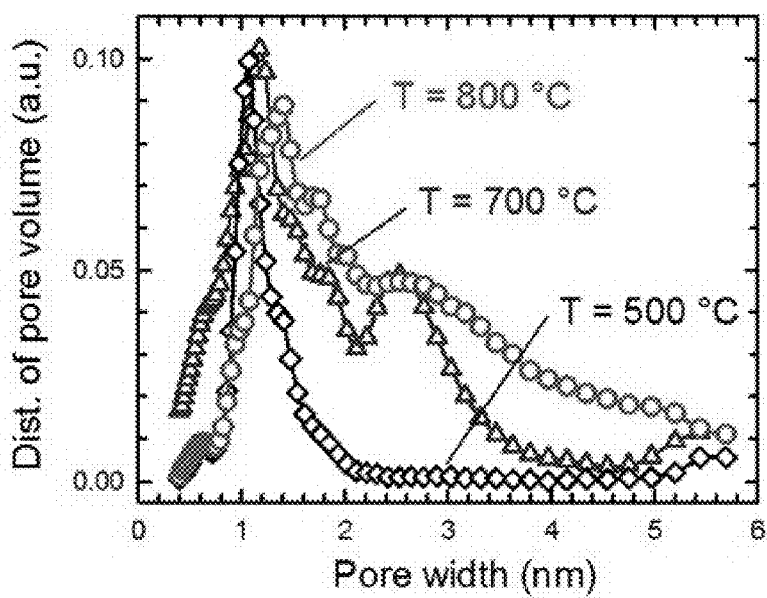
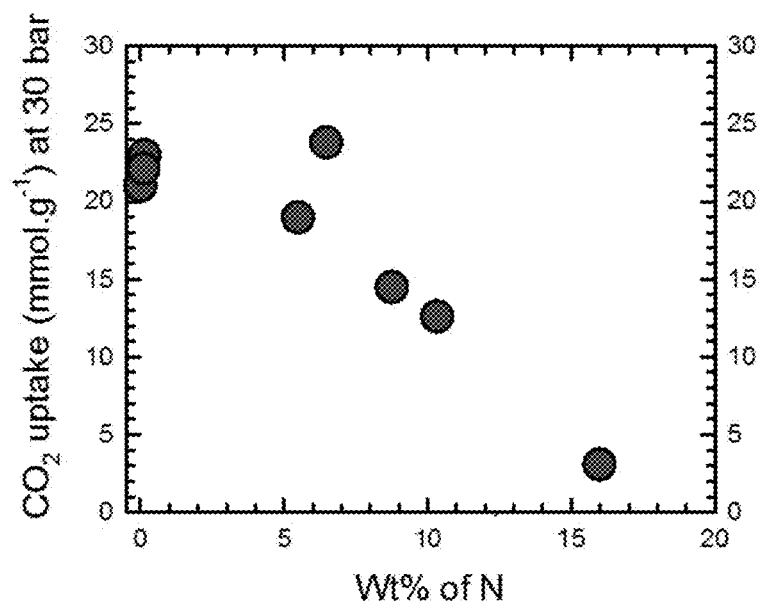
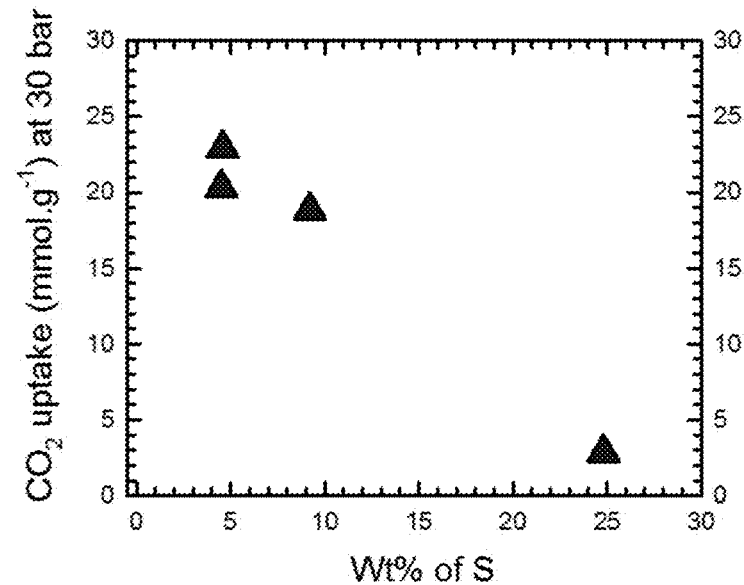
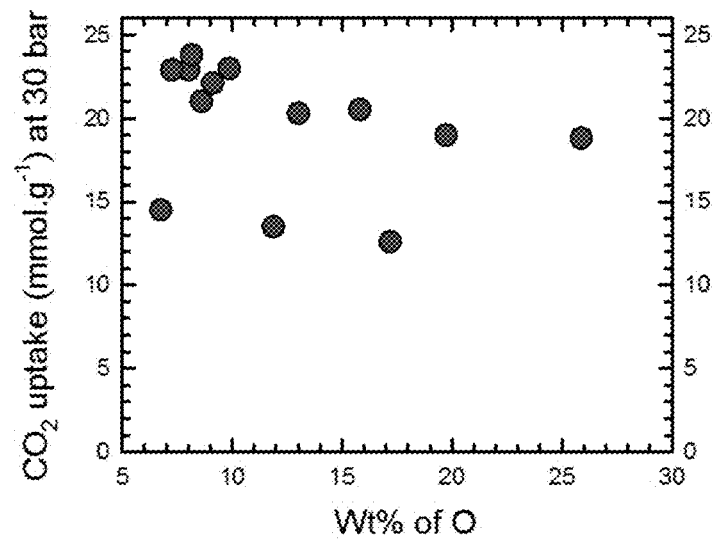
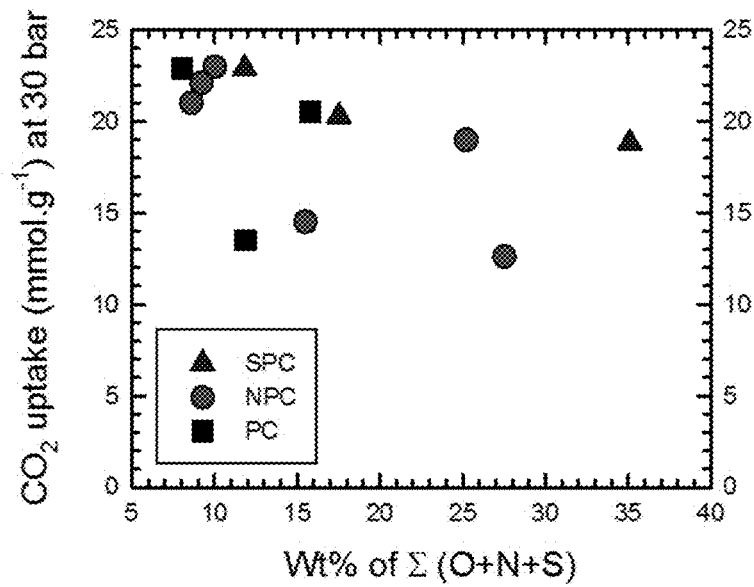


FIG. 7

**FIG. 8A****FIG. 8B**



**FIG. 9A**



**FIG. 9B**

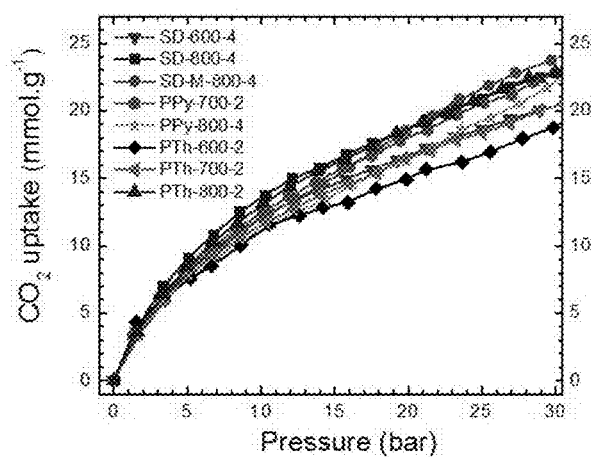


**FIG. 10A**

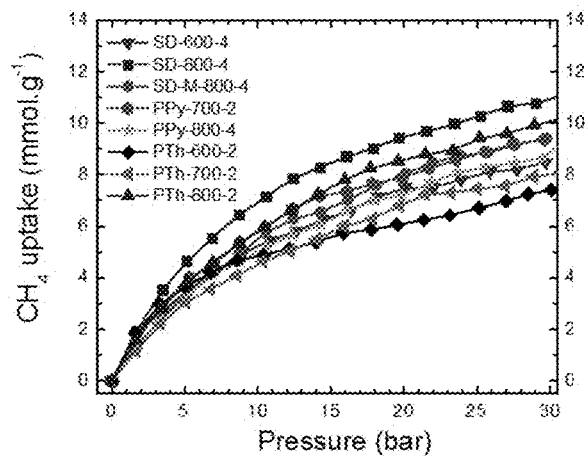


**FIG. 10B**

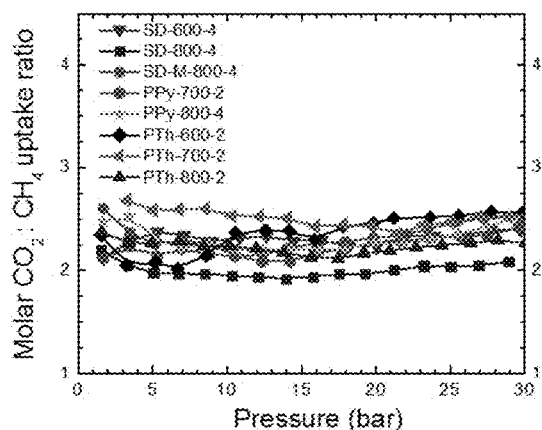


**FIG. 10C**

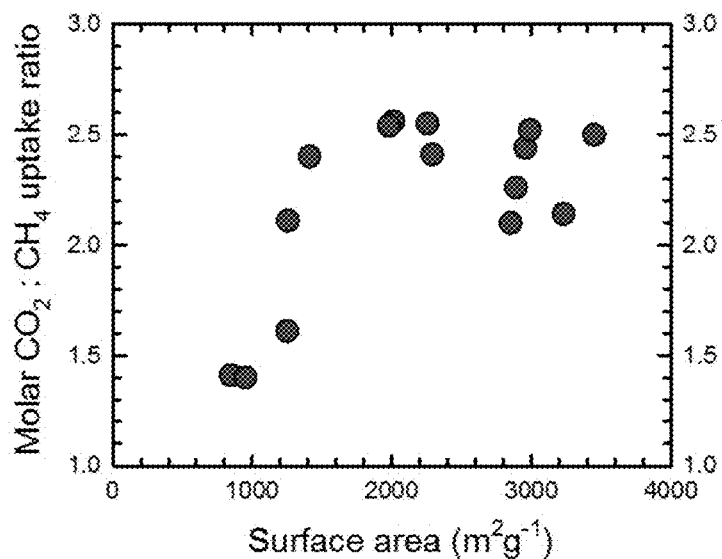


**FIG. 11A**

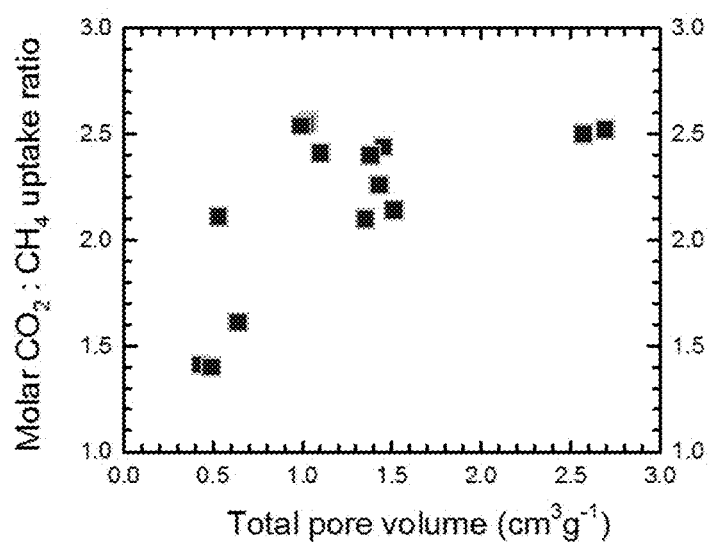


**FIG. 11B**

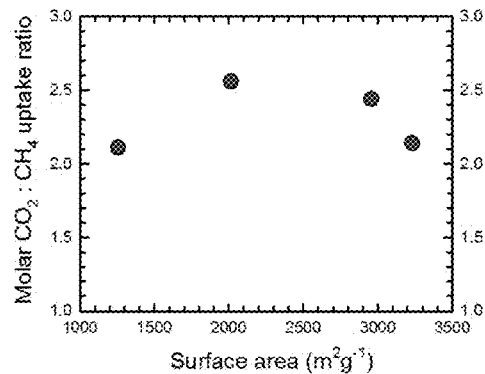


FIG. 12A

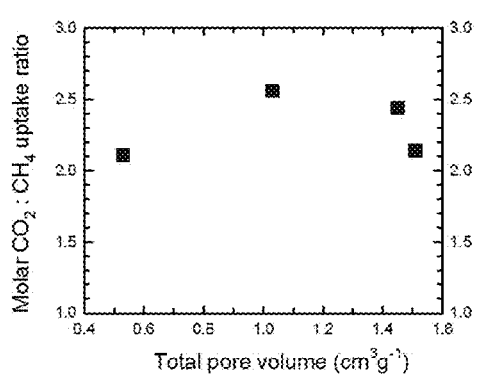


FIG. 12B

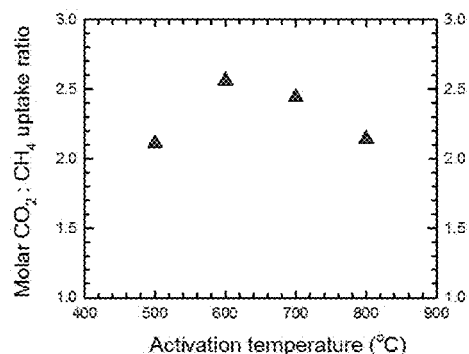


FIG. 12C

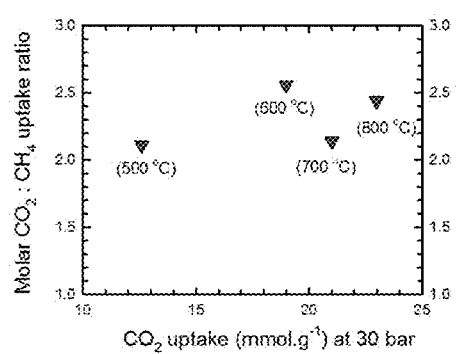


FIG. 12D

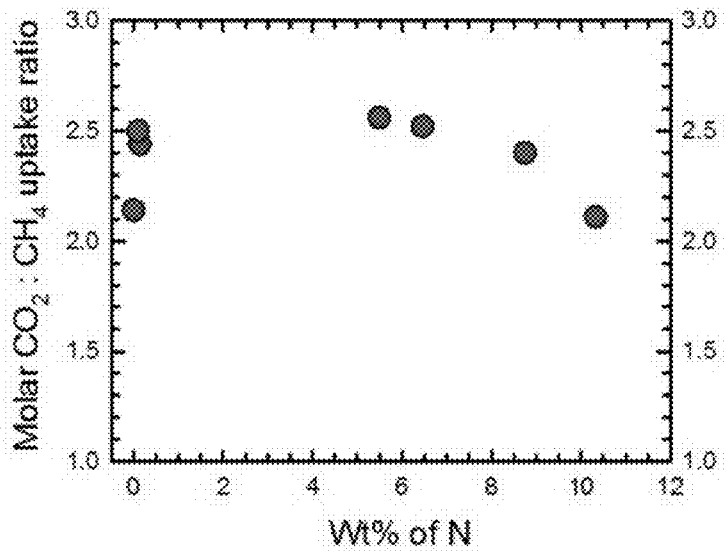


FIG. 13

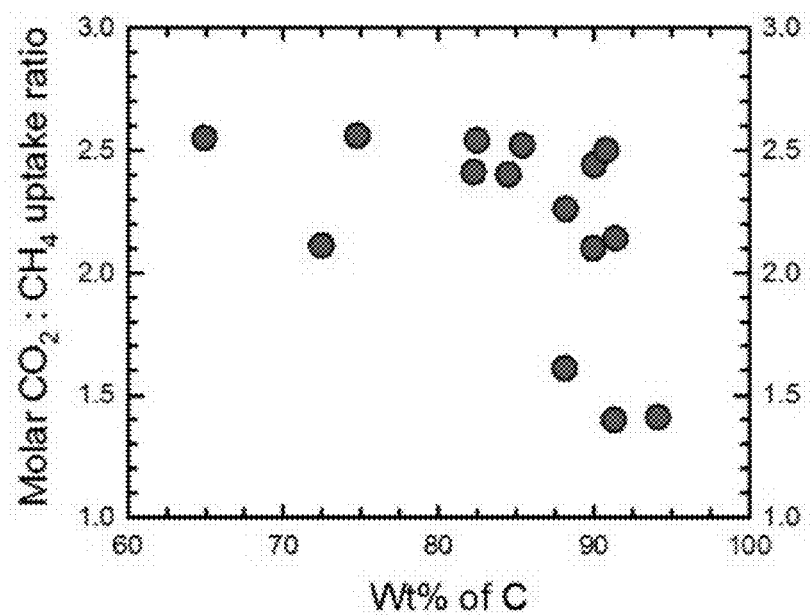


FIG. 14

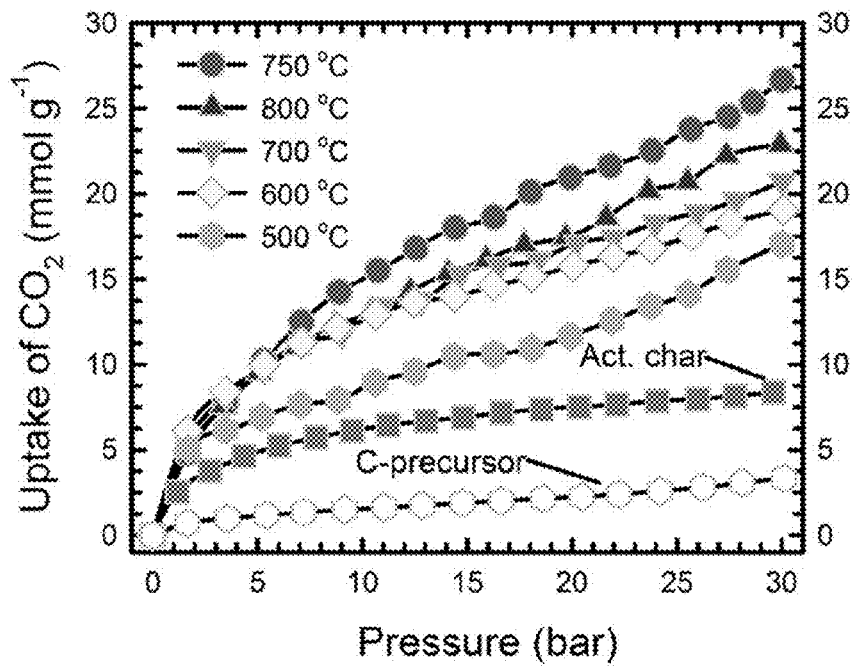
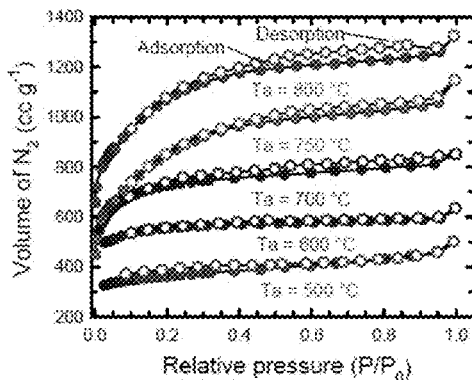
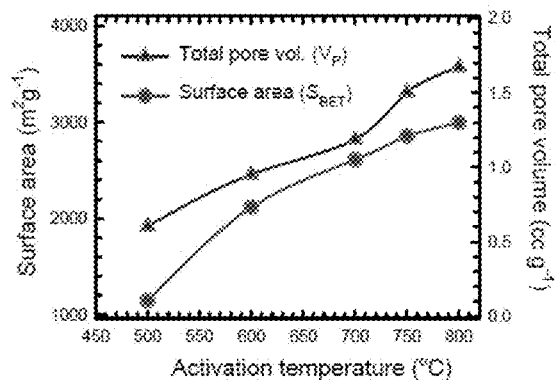


FIG. 15



**FIG. 16A**



**FIG. 16B**

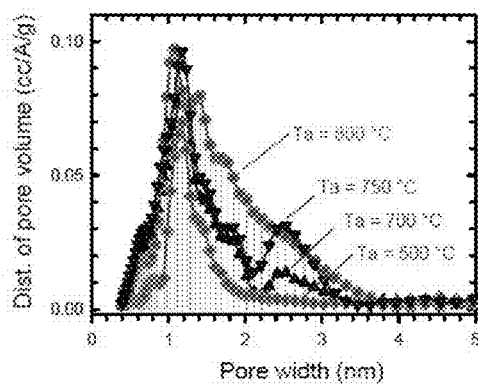


**FIG. 16C**

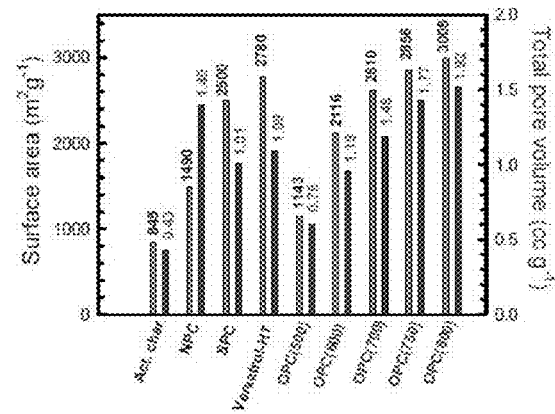


**FIG. 16D**

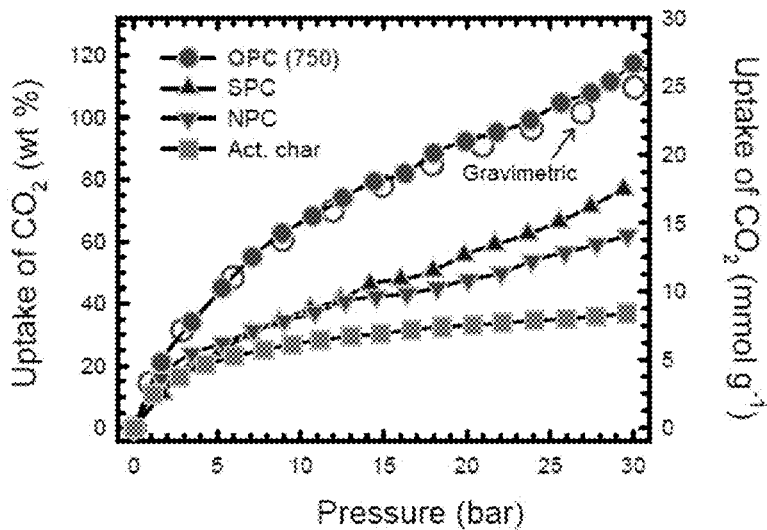


FIG. 17A

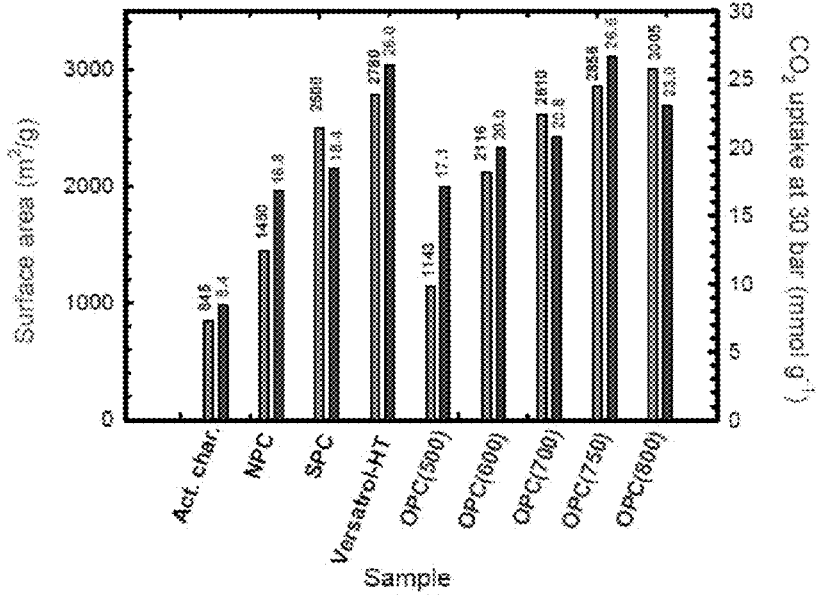


FIG. 17B

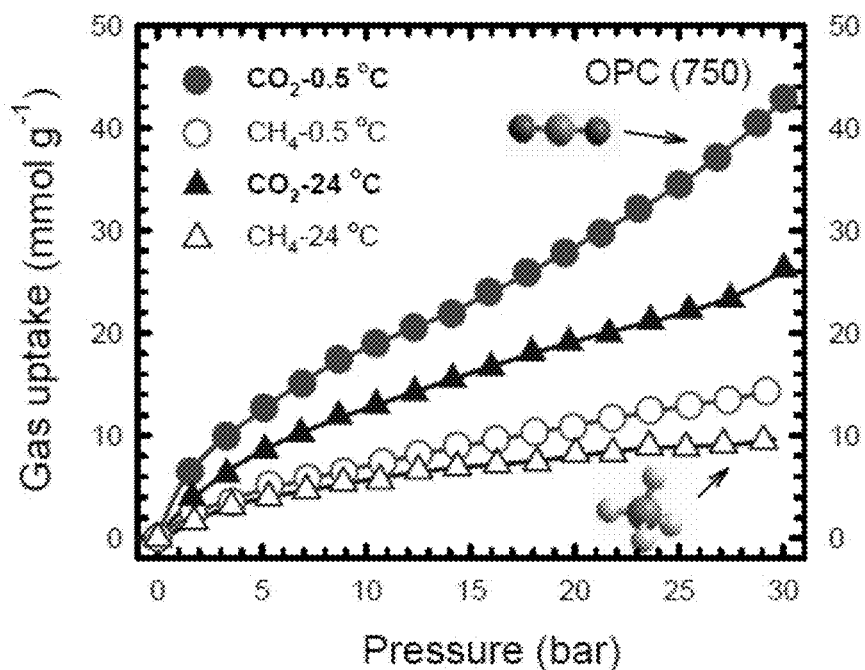


FIG. 18A

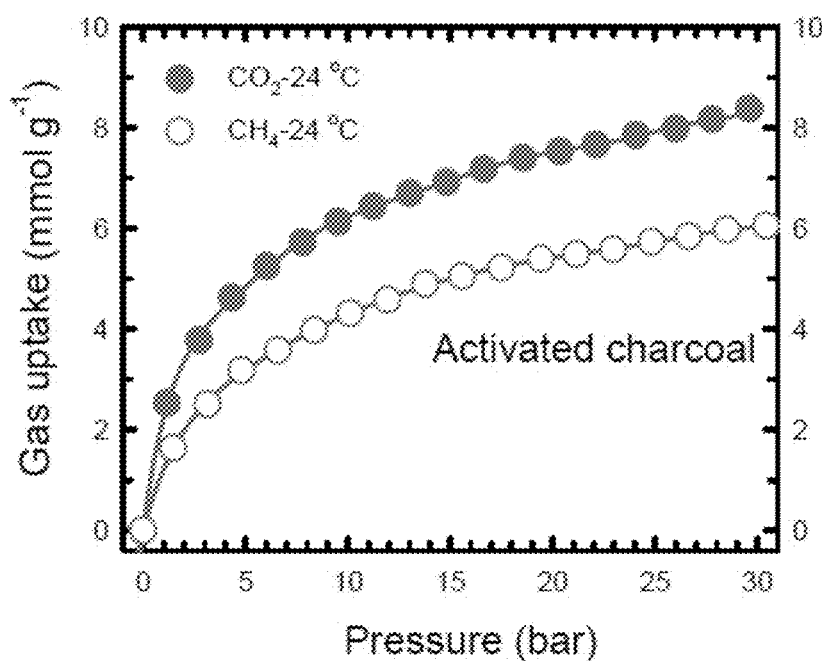


FIG. 18B

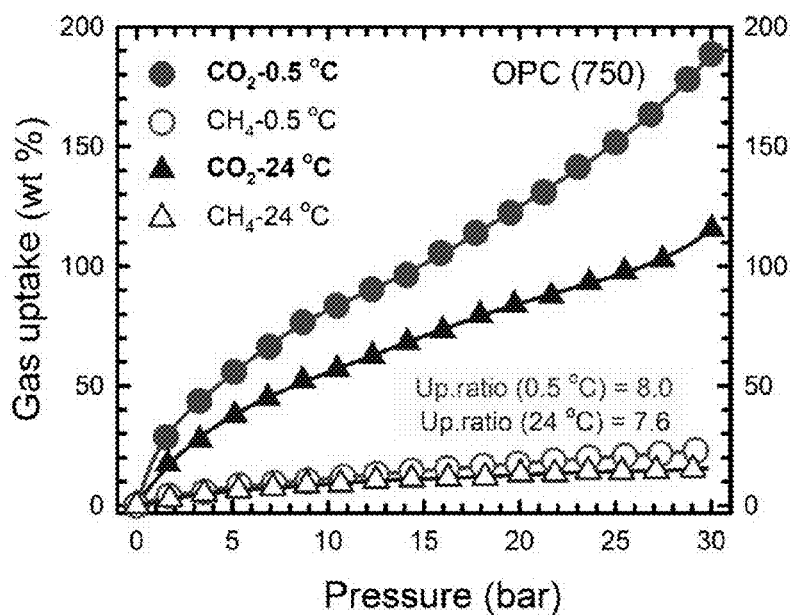
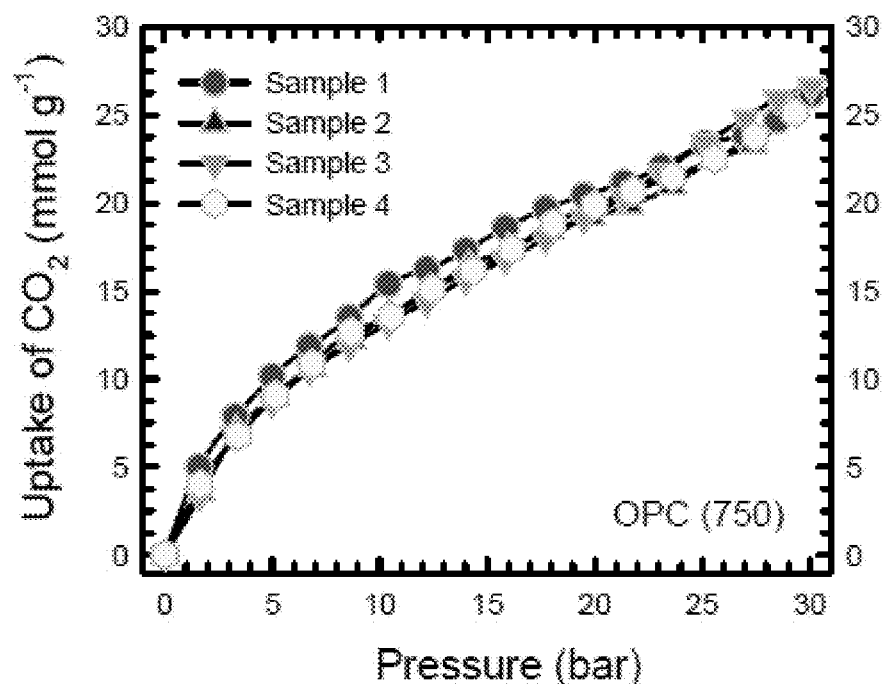
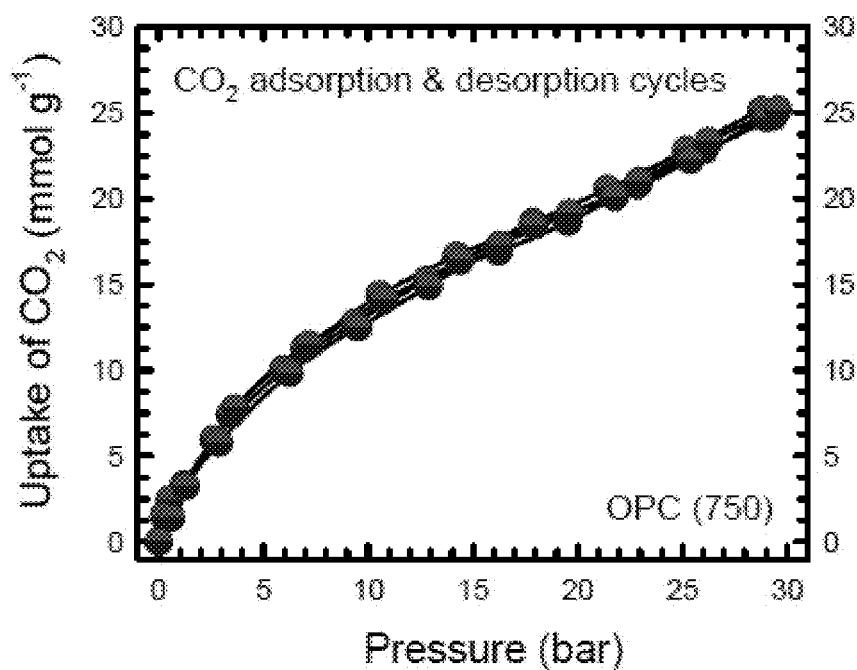


FIG. 19



**FIG. 20A**



**FIG. 20B**

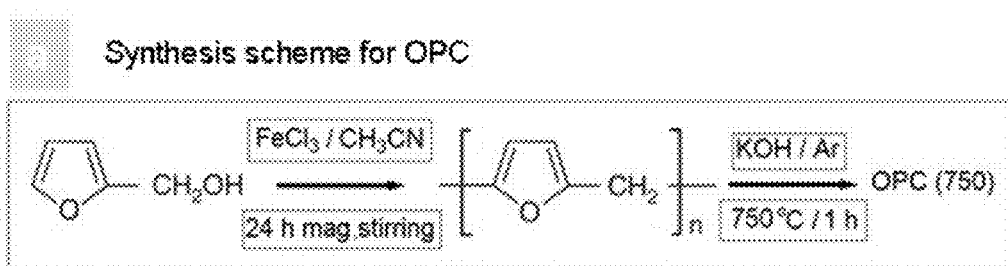


FIG. 21A

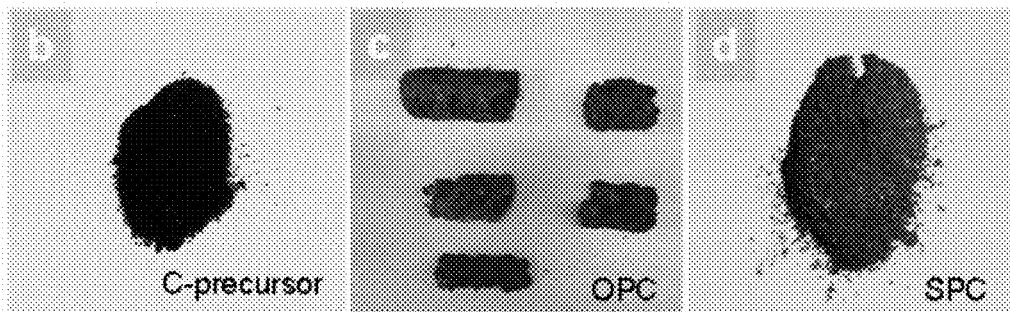


FIG. 21B

FIG. 21C

FIG. 21D

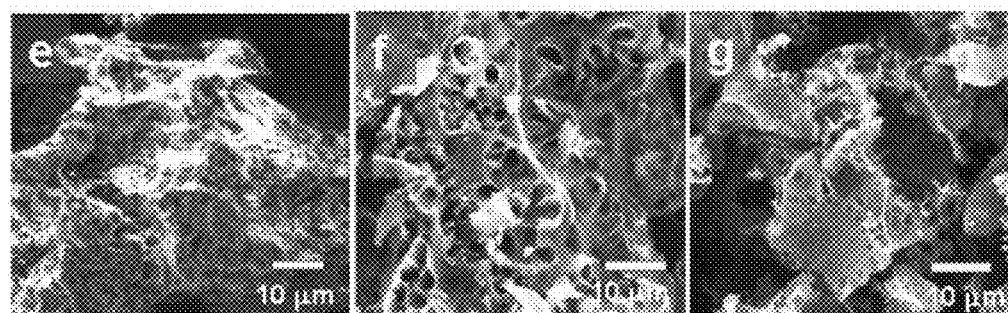


FIG. 21E

FIG. 21F

FIG. 21G

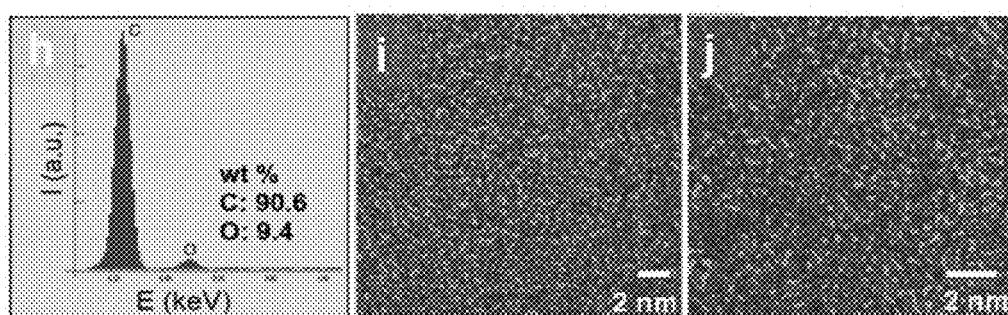
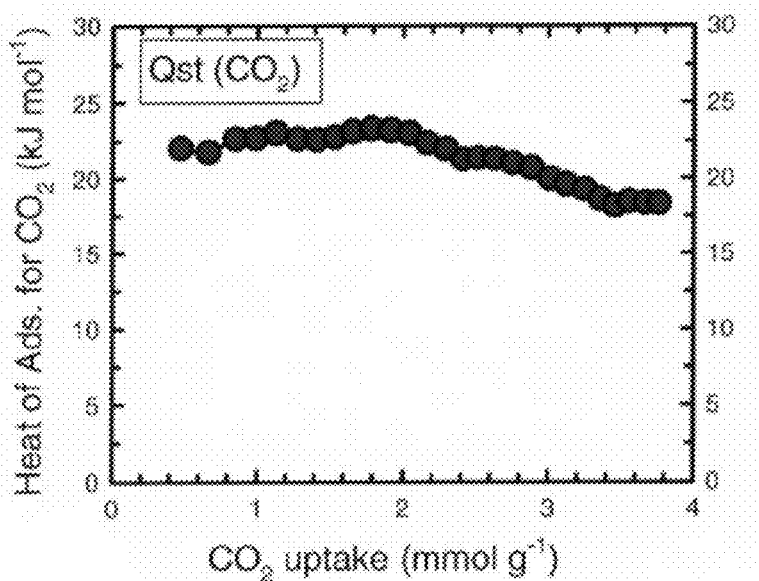


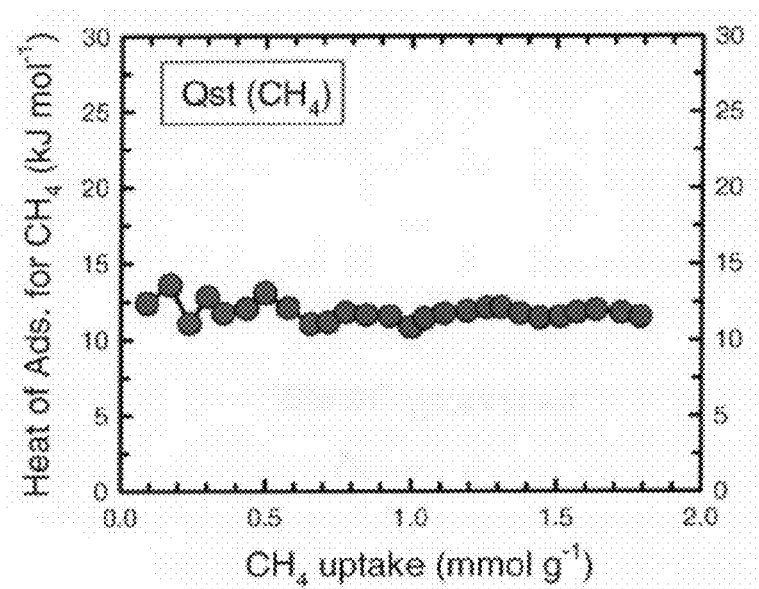
FIG. 21H

FIG. 21I

FIG. 21J



**FIG. 22A**



**FIG. 22B**

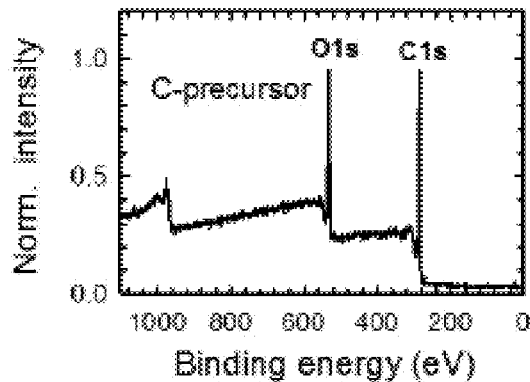


FIG. 23A

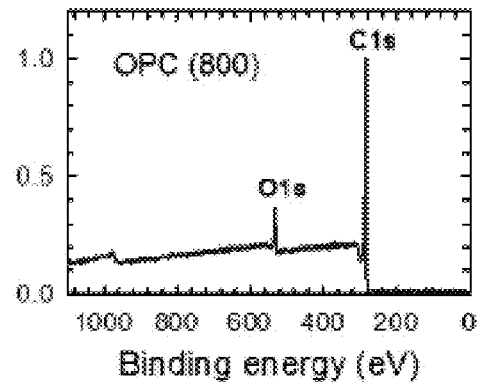


FIG. 23B

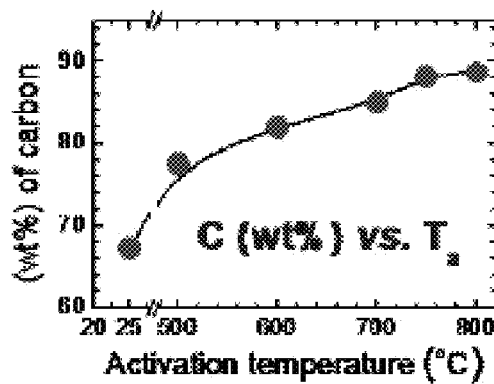


FIG. 23C

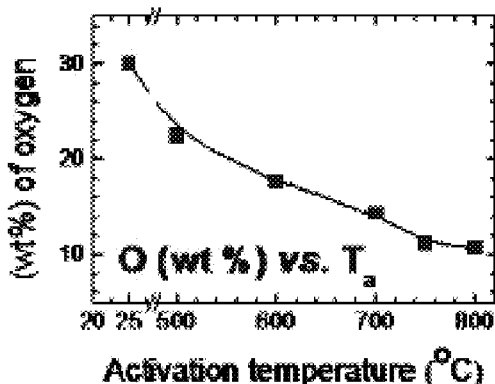
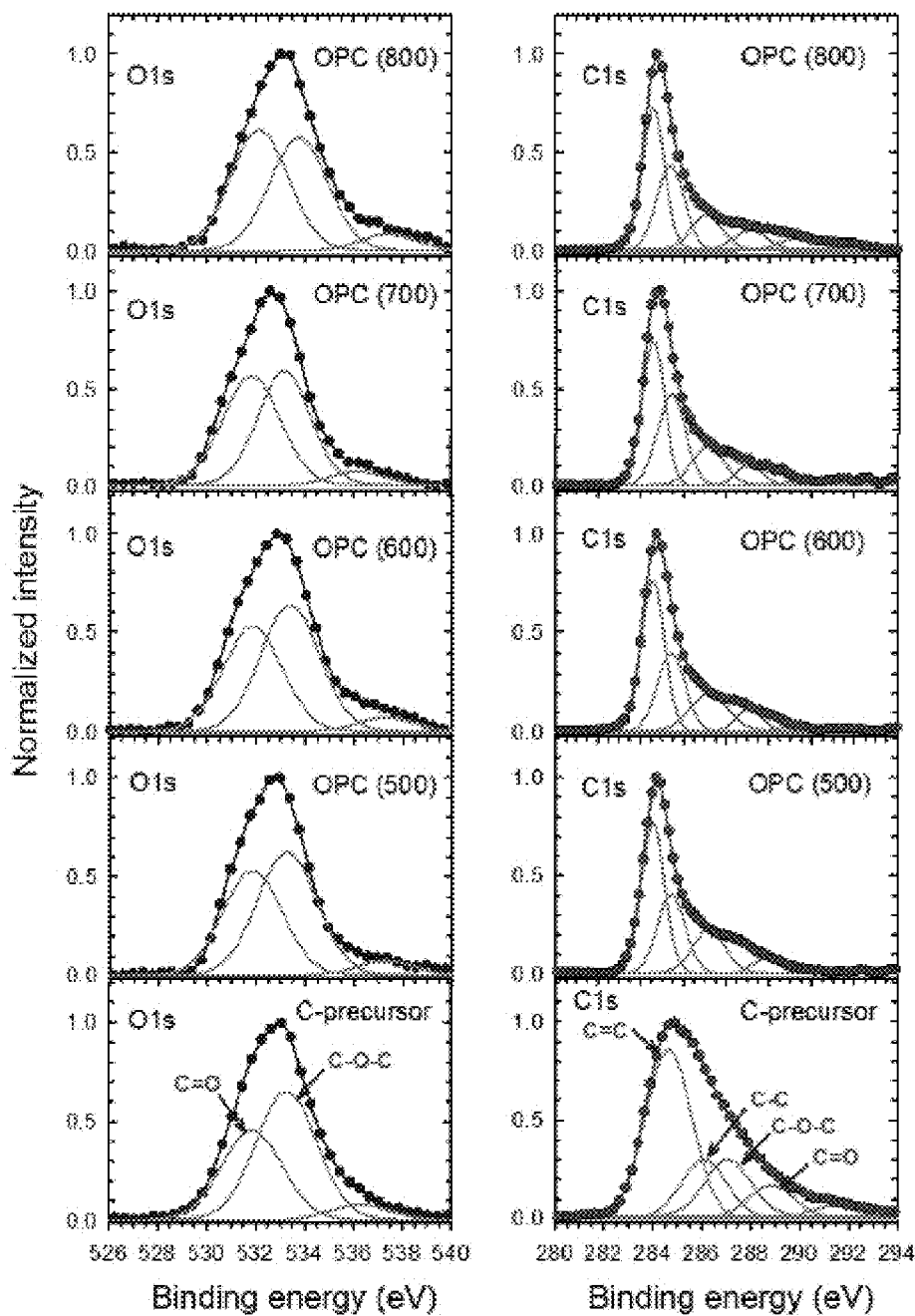


FIG. 23D



**FIG. 23E**

**FIG. 23F**

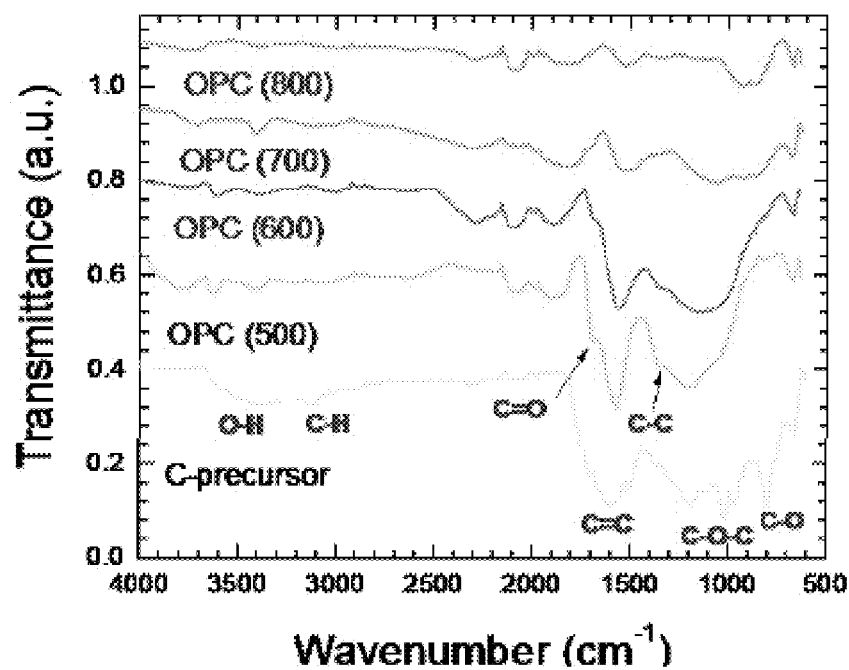


FIG. 23G

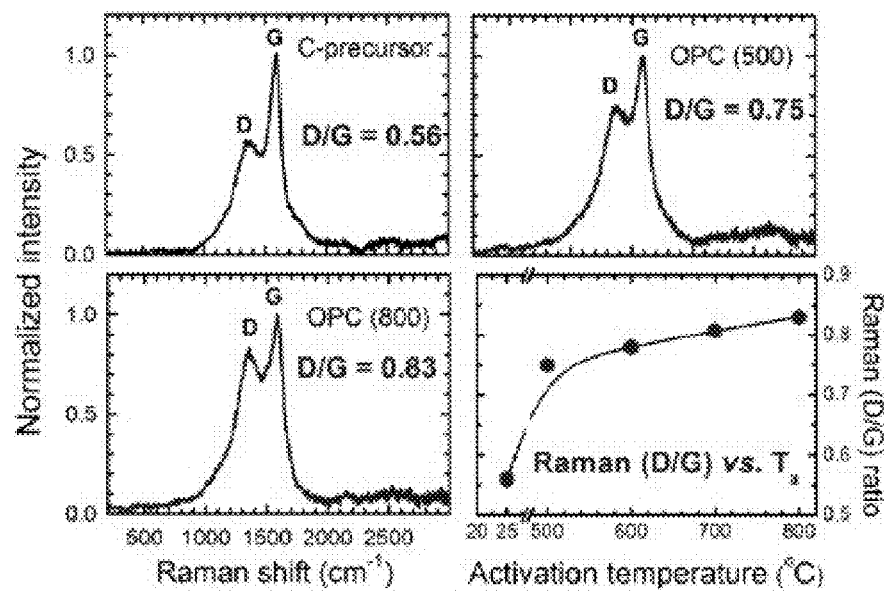


FIG. 23H

**METHOD, SYNTHESIS, ACTIVATION  
PROCEDURE AND CHARACTERIZATION  
OF AN OXYGEN RICH ACTIVATED POROUS  
CARBON SORBENT FOR SELECTIVE  
REMOVAL OF CARBON DIOXIDE WITH  
ULTRA HIGH CAPACITY**

**CROSS-REFERENCE TO RELATED  
APPLICATIONS**

[0001] This application claims priority to U.S. Provisional Patent Application No. 62/187,744, filed on Jul. 1, 2016. The entirety of the aforementioned application is incorporated herein by reference.

**STATEMENT REGARDING FEDERALLY  
SPONSORED RESEARCH**

[0002] Not applicable.

**BACKGROUND**

[0003] Current materials for capturing carbon dioxide ( $\text{CO}_2$ ) suffer from numerous limitations, including limited  $\text{CO}_2$  sorption capacity and selectivity. Various embodiments of the present disclosure address these limitations.

**SUMMARY**

[0004] In some embodiments, the present disclosure pertains to materials for  $\text{CO}_2$  adsorption at pressures above 1 bar. In some embodiments, the materials include a porous carbon material with a surface area of at least 2800  $\text{m}^2/\text{g}$ , a total pore volume of at least 1.35  $\text{cm}^3/\text{g}$ , and a carbon content of between 80% and 95% as measured by X-ray photoelectron spectroscopy. In some embodiments, the porous carbon material is prepared by heating an organic polymer precursor or biological material in the presence of potassium hydroxide (KOH). In some embodiments, the temperature of activation is between 700° C. and 800° C.

[0005] In additional embodiments, the present disclosure pertains to materials for the separation of  $\text{CO}_2$  from natural gas at partial pressures of either component above 1 bar. In some embodiments, the materials include a porous carbon material with a surface area of at least 2000  $\text{m}^2/\text{g}$ , a total pore volume of at least 1.00  $\text{cm}^3/\text{g}$ , and a carbon content of greater than 90% as measured by X-ray photoelectron spectroscopy. In some embodiments, the porous carbon material is prepared by heating an organic polymer precursor or biological material in the presence of KOH. In some embodiments, the temperature of activation is between 600° C. and 700° C.

[0006] The porous carbon materials of the present disclosure can be prepared in various manners. For instance, in some embodiments, the porous carbon materials of the present disclosure are prepared by heating an organic polymer precursor. In some embodiments, the organic polymer precursor includes oxygen in a functional group. In some embodiments, the functional group is a furyl. In some embodiments, the organic polymer precursor is furfuryl alcohol. In some embodiments, the organic polymer precursor polymerizes to form polyfurfuryl alcohol (PFA). In some embodiments, PFA is prepared by the polymerization of furfuryl alcohol with a catalyst. In some embodiments, the catalyst is iron(III) chloride.

[0007] In some embodiments, the porous carbon materials of the present disclosure are prepared by heating a biological

material. In some embodiments, the biological material includes, without limitation, sawdust, coconut husk, and combinations thereof.

[0008] Additional embodiments pertain to methods of making the materials of the present disclosure. Further embodiments pertain to utilizing the materials of the present disclosure for the capture of  $\text{CO}_2$  from various environments.

**DESCRIPTION OF THE FIGURES**

[0009] FIG. 1 provides data relating to high pressure  $\text{CO}_2$  uptake (at 30 bar and 24° C.) as a function of the surface area (FIG. 1A) and total pore volume (FIG. 1B), for a range of porous carbons (PCs), including N-containing PCs (NPCs) and S-containing PCs (SPCs).

[0010] FIG. 2 provides a plot of  $\text{CO}_2$  uptake at 30 bar and 24° C. as a function of activation temperature for PC NPC and SPC samples.

[0011] FIG. 3 provides estimated surface area (FIG. 3A) and total pore volume (FIG. 3B) as a function of activation temperature for PC, NPC and SPC samples.

[0012] FIG. 4 provides comparative data relating to  $\text{CO}_2$  uptake as a function of  $\text{CO}_2$  pressure on N-containing polymer polypyrrole (PPy) precursors and PPy precursors activated at different temperatures (PPy-T-2). Sorption measurements were performed at 24° C.

[0013] FIG. 5 provides  $\text{N}_2$  adsorption isotherms for four different NPC samples of PPy-T-2 prepared from polypyrrole and activated at the labelled temperature (T). Sorption measurements were performed at 24° C.

[0014] FIG. 6 provides data relating to the determination of pore structures by  $\text{N}_2$  physisorption isotherms of PPy-T-2 samples activated at different temperatures by  $\text{N}_2$  physisorption isotherms. Shown are the estimated surface area (FIG. 6A) and total pore volume (FIG. 6B) versus activation temperature.

[0015] FIG. 7 shows the pore size distributions of PPy-T-2 samples prepared at the three activation temperatures shown, as determined by the non-local density functional theory (NLDFT) method.

[0016] FIG. 8 shows high pressure (30 bar)  $\text{CO}_2$  uptake as a function of N wt % (FIG. 8A) and S wt % (FIG. 8B) in NPC and SPC samples, respectively. Sorption measurements were performed at 24° C.

[0017] FIG. 9 shows high pressure (30 bar)  $\text{CO}_2$  uptake as a function of 0 wt % (FIG. 9A) and  $\Sigma(\text{O}, \text{N}, \text{S})$  wt % (FIG. 9B) in PC, NPC and SPC samples. Sorption measurements were performed at 24° C.

[0018] FIG. 10 shows room temperature volumetric  $\text{CO}_2$  (FIG. 10A) and methane ( $\text{CH}_4$ ) (FIG. 10B) adsorption isotherms for PC, NPC, and SPC samples. FIG. 10C shows the molar  $\text{CO}_2:\text{CH}_4$  uptake ratio as a function of gas pressure for PC, NPC, and SPC samples.

[0019] FIG. 11 shows plots of molar  $\text{CO}_2:\text{CH}_4$  uptake ratio (@ 30 bar) as a function of the surface area (FIG. 11A) and total pore volume (FIG. 11B) for a range of PC, NPC and SPC samples. Sorption measurements were performed at 24° C.

[0020] FIG. 12 shows plots of molar  $\text{CO}_2:\text{CH}_4$  uptake ratio (@ 30 bar) as a function of the surface area (FIG. 12A), total pore volume (FIG. 12B), activation temperature (FIG. 12C), and  $\text{CO}_2$  uptake (FIG. 12D) for PPy-T-2 ( $T=500, 600, 700$  and 800° C.) NPC samples. Sorption measurements were performed at 24° C.

[0021] FIG. 13 shows high pressure (30 bar) molar CO<sub>2</sub>:CH<sub>4</sub> uptake ratio as a function of N wt % in NPC samples. Sorption measurements were performed at 24° C.

[0022] FIG. 14 shows the high pressure (30 bar) molar CO<sub>2</sub>:CH<sub>4</sub> uptake ratio as a function of C wt % in PC, NPC, and SPC samples. Sorption measurements were performed at 24° C.

[0023] FIG. 15 shows volumetric CO<sub>2</sub> uptake of different OPCs activated at increasing temperature, activated carbon and carbon precursor.

[0024] FIG. 16 provides an analysis of the porous structure of OPC samples activated at different temperatures. FIG. 16A shows N<sub>2</sub> adsorption and desorption isotherms for a PC (800) sample. FIG. 16B shows estimated surface area and total pore-volume vs. activation temperature. FIG. 16C shows the distribution of pore volumes as a function of activation temperature as estimated by NLDFT. FIG. 16D shows the surface area (blue bars) and total pore volume (purple) for activated charcoal and eight different PC samples known for high CO<sub>2</sub> uptakes (>14 mmol g<sup>-1</sup> at 30 bar).

[0025] FIG. 17 provides additional data relating to the CO<sub>2</sub> uptake of porous carbons. FIG. 17A shows the volumetric CO<sub>2</sub> uptake of various porous carbons prepared from different carbon precursors, including O-rich PC (OPC), N-rich PC (NPC) and S-rich PC (SPC). Measurements were performed in a PCTPRO instrument at 24° C. FIG. 17B shows the graphical representation of surface areas and maximum CO<sub>2</sub> uptake capacities at 30 bar for nine different porous carbon sorbents. The highest CO<sub>2</sub> uptake property (26.6 mmol g<sup>-1</sup>) is demonstrated by Applicants' newly discovered OPC (750) sample (second bar to the right).

[0026] FIG. 18 provides a demonstration of optimal gas uptake selectivity of OPC samples for CO<sub>2</sub> over CH<sub>4</sub>. FIG. 18A shows volumetric CO<sub>2</sub> and CH<sub>4</sub> uptake measurements on OPC (750) sorbents up to a pressure range of 30 bar at 0.5 and 24° C. FIG. 18B shows volumetric CO<sub>2</sub> and CH<sub>4</sub> uptake measurements on commercially available activated charcoal. The molar uptake ratios (CO<sub>2</sub>/CH<sub>4</sub>) at 30 bar for OPC(750) and activated charcoal are 2.74 and 1.4, respectively.

[0027] FIG. 19 provides a demonstration of optimal gas uptake selectivity of OPC samples for CO<sub>2</sub> over CH<sub>4</sub>. Volumetric CO<sub>2</sub> and CH<sub>4</sub> uptake measurements on OPC (750) sorbents up to a pressure range of 30 bar at 0.5° C. and 24° C. are shown. The mass uptake ratios (CO<sub>2</sub>/CH<sub>4</sub>) at 30 bar for OPC(750) are 8.0 and 7.6, respectively.

[0028] FIG. 20 provides a demonstration of the reproducibility of sample preparation and gas uptake properties of OPCs. FIG. 20A shows volumetric CO<sub>2</sub> uptake measurements on four different OPC (750) samples synthesized and activated the same way. FIG. 20B shows two successive CO<sub>2</sub> adsorption and desorption cycles.

[0029] FIG. 21 provides various schemes and data relating to the synthesis and characterization of OPCs. FIG. 21A provides a synthesis scheme for OPC. Photographs of carbon precursor (FIG. 21B), as-synthesized OPC (FIG. 21C), and as-synthesized SPC samples (FIG. 21D) are also shown. OPC samples are pellet like compared to SPC and other PC materials. Scanning electron microscopy (SEM) images of carbon precursor (FIG. 21E), OPC (600) (FIG. 21F) and OPC (800) samples (FIG. 21G) are also shown. FIG. 21H shows an energy-dispersive X-ray spectroscopy (EDS) elemental scan for OPC (800). Also shown are high reso-

lution transmission electron microscopy (TEM) images of OPC (600) (FIG. 21I) and OPC (800) samples (FIG. 21J) showing nm sized micro porous structures.

[0030] FIG. 22 shows the isosteric heat of absorption of CO<sub>2</sub> (FIG. 22A) and CH<sub>4</sub> (FIG. 22B) as a function molar gas uptakes.

[0031] FIG. 23 shows the characterization of chemical compositions of carbon precursor and porous carbon samples activated at increasing temperatures. Shown are X-ray photoelectron spectroscopy (XPS) survey scans for C-precursor (FIG. 23A) and OPC (800) (FIG. 23B). Also shown are the wt % of elemental carbon (FIG. 23C) and oxygen (FIG. 23D) vs. activation temperature. XPS elemental scanning for carbon C1s (FIG. 23E) and oxygen O1s (FIG. 23F) are also shown. FIG. 23G shows the Fourier transform infrared spectroscopy (FTIR) spectra of C-precursor and activated OPCs. FIG. 23H shows the Raman spectra and Raman disorder (D) to graphene (G) band intensity ratio vs. activation temperature. KOH/Polymer weight ratio=3 in all cases. IR spectra are base line corrected and vertically offset for clarity.

#### DETAILED DESCRIPTION

[0032] It is to be understood that both the foregoing general description and the following detailed description are illustrative and explanatory, and are not restrictive of the subject matter, as claimed. In this application, the use of the singular includes the plural, the word "a" or "an" means "at least one", and the use of "or" means "and/or", unless specifically stated otherwise. Furthermore, the use of the term "including", as well as other forms, such as "includes" and "included", is not limiting. Also, terms such as "element" or "component" encompass both elements or components comprising one unit and elements or components that comprise more than one unit unless specifically stated otherwise.

[0033] The section headings used herein are for organizational purposes and are not to be construed as limiting the subject matter described. All documents, or portions of documents, cited in this application, including, but not limited to, patents, patent applications, articles, books, and treatises, are hereby expressly incorporated herein by reference in their entirety for any purpose. In the event that one or more of the incorporated literature and similar materials defines a term in a manner that contradicts the definition of that term in this application, this application controls.

[0034] There are generally two classes of materials employed for carbon dioxide (CO<sub>2</sub>) separation: reactants and adsorbents. The former includes amine and other reactive species such as ionic liquids and alkali-metal-based oxides. At present, monoethanolamine (MEA) is the industry standard. However, regeneration, degradation and corrosion, together with health and environmental issues, still affect its large scale implementation.

[0035] Impregnation of CO<sub>2</sub> capture materials onto supports has been investigated, but it is only recently that the regeneration temperature has been lowered by their combination with carbon nanomaterials. Ionic liquids, suitable for high pressure capture are expensive and toxic, while cheap alkali metal oxides suffer from severe deactivation upon cycling.

[0036] Although the aforementioned materials show optimal selectivity between CO<sub>2</sub> and methane (CH<sub>4</sub>), their myriad drawbacks have meant that much effort has been

invested into the study of solid porous sorbents, such as porous carbons (PC), metal-organic frameworks (MOFs), microporous zeolites, and porous silica-based sorbents with high surface area.

[0037] MOFs outperform zeolites in terms of maximum capacity at high pressure, but are expensive since they require complex multistep synthesis procedures. In addition, their gas adsorption capacity degrades after several cycles of usage. Carbonaceous materials, such as activated carbon and charcoal, are cheaper and less sensitive to moisture than zeolites and MOFs, but their adsorption capacity generally increases with loss of selectivity at high pressure.

[0038] Chemically activated porous carbon adsorbents have large surface areas and pore volumes associated with micro- and meso-porous structure. As a result, such materials show significantly improved CO<sub>2</sub> capturing capacity as compared to traditional carbonaceous materials.

[0039] It has been suggested that the presence of nitrogen or sulphur dopants is responsible for improved CO<sub>2</sub> uptake in porous carbon materials (e.g., *Nat Commun.*, 2014, 5, 3961 and U.S. Pat. Pub. No. 2015/0111024). These studies were undertaken at 30 bar (1 bar=100,000, Pa=750.06 mmHg) using compounds previously reported to show improved results over activated carbon at 1 bar (e.g., *Adv. Funct. Mater.*, 2011, 21, 2781-2787; and *Microporous Mesoporous Mater.*, 2012, 158, 318-323). The improved high pressure results were proposed to be due to the S or N centers acting as a Lewis base to facilitate the ambient polymerization of the CO<sub>2</sub>. However, previous investigations of the role of N-doping in CO<sub>2</sub> capture by PCs up to 1 bar pressure shows no correlation (e.g., *ACS Appl. Mater. Interfaces*, 2013, 5, 6360-6368).

[0040] The conventional goal in synthesizing a porous carbon material with optimal CO<sub>2</sub> adsorption is to focus on increased surface area and pore volume (e.g., U.S. Pat. Pub. No. 2016/0136613). The same approach is presumed to also work for the separation of CO<sub>2</sub> from natural gas.

[0041] However, the present disclosure demonstrates that increasing the surface area and pore volume of a carbon material do not guarantee the best adsorbent. Instead a combination of factors is involved in defining the ideal porous carbon absorbent material.

[0042] In some embodiments, the present disclosure pertains to novel materials for CO<sub>2</sub> capture. In additional embodiments, the present disclosure pertains to methods of making the materials of the present disclosure. In further embodiments, the present disclosure pertains to methods of utilizing the materials of the present disclosure for the capture of CO<sub>2</sub> from various environments. As set forth in more detail herein, the present disclosure can have various embodiments.

#### [0043] Materials for CO<sub>2</sub> Capture

[0044] In some embodiments, the present disclosure pertains to materials for CO<sub>2</sub> adsorption at pressures above 1 bar. In some embodiments, the materials include a porous carbon material with a surface area of at least 2800 m<sup>2</sup>/g, a total pore volume of at least 1.35 cm<sup>3</sup>/g, and a carbon content of between 80% and 95% as measured by X-ray photoelectron spectroscopy. In some embodiments, the porous carbon material is prepared by heating an organic polymer precursor or biological material in the presence of potassium hydroxide (KOH). In some embodiments, the temperature of activation is between 700° C. and 800° C.

[0045] In additional embodiments, the present disclosure pertains to materials for the separation of CO<sub>2</sub> from natural gas at partial pressures of either component above 1 bar. In some embodiments, the materials include a porous carbon material with a surface area of at least 2000 m<sup>2</sup>/g, a total pore volume of at least 1.00 cm<sup>3</sup>/g, and a carbon content of greater than 90% as measured by X-ray photoelectron spectroscopy. In some embodiments, the porous carbon material is prepared by heating an organic polymer precursor or biological material in the presence of KOH. In some embodiments, the temperature of activation is between 600° C. and 700° C.

[0046] In some embodiments, the materials of the present disclosure are rich in oxygen. As such, in some embodiments, the materials of the present disclosure are referred to as oxygen rich activated porous carbons (OPCs). In some embodiments, the materials of the present disclosure have an oxygen content of more than about 10 wt %. In some embodiments, the materials of the present disclosure have an oxygen content between about 10 wt % and about 25 wt %.

[0047] In some embodiments, the materials of the present disclosure may lack other heteroatoms, such as nitrogen or sulfur. For instance, in some embodiments, the total heteroatom content of the materials of the present disclosure may range from about 0 wt % to about 1 wt %. In some embodiments, the total heteroatom content of the materials of the present disclosure may be less than about 1 wt %.

[0048] The materials of the present disclosure can have various advantageous properties. For instance, in some embodiments, the materials of the present disclosure have high surface areas. In some embodiments, the materials of the present disclosure have surface areas of more than about 1,000 m<sup>2</sup>/g. In some embodiments, the materials of the present disclosure have surface areas that range from about 1,000 m<sup>2</sup>/g to about 5000 m<sup>2</sup>/g (Table 5). In some embodiments, the materials of the present disclosure have surface areas of about 3005 m<sup>2</sup>/g (e.g., in OPC samples chemically activated at 800° C.) (FIG. 16D).

[0049] In some embodiments, the materials of the present disclosure have high CO<sub>2</sub> adsorption capacities. In some embodiments, the materials of the present disclosure have a CO<sub>2</sub> adsorption capacity of more than about 100 wt %. In some embodiments, the materials of the present disclosure have CO<sub>2</sub> adsorption capacities between about 117 wt % and about 189 wt %.

[0050] In some embodiments, the materials of the present disclosure have a CO<sub>2</sub> adsorption capacity of up to 117 wt % (26.6 mmol/g) at a pressure of 30 bar, a number that is higher than any reported uptake values for activated porous carbon (PC) adsorbents (FIG. 17 and Table 5). In some embodiments, the materials of the present disclosure capture CO<sub>2</sub> from a natural gas containing environment that is rich in CH<sub>4</sub> at a maximum molar uptake ratio of 2.75 (7.5 by mass ratio) at a pressure of 30 bar (FIGS. 18-19).

[0051] In some embodiments, the materials of the present disclosure (e.g., OPCs that are activated at 750° C., referred to herein as OPC (750)) outperform most of the existing porous carbons for high pressure uptake of CO<sub>2</sub> (e.g., 26.6 mmol/g; 117 wt % at 30 bar) and demonstrate optimal selectivity for CO<sub>2</sub> capture over CH<sub>4</sub> uptake (e.g., V<sub>CO2</sub>/V<sub>CH4</sub> ratio ~2.7 (molar) and ~7.5 (by wt) at 30 bar) at room temperature. Additionally, OPC (750) demonstrates ultrahigh CO<sub>2</sub> uptake (43 mmol g<sup>-1</sup>; 189 wt %) at 0.5° C., a value that was never reported previously (FIG. 18A).

[0052] In some embodiments, the materials of the present disclosure exhibit remarkable thermal stability and reproducible gas uptake properties for many cycles (FIG. 20). Unlike other fine powder type activated porous carbon materials, the materials of the present disclosure can be clumpy and pelletized in some embodiments. Such properties can in turn make the materials of the present disclosure better candidates for preparing solid pellet-like adsorbents (FIG. 21C).

[0053] Formation of Materials

[0054] The materials of the present disclosure can be prepared in various manners. Additional embodiments of the present disclosure pertain to methods of making the materials of the present disclosure.

[0055] In some embodiments, a carbon precursor is first synthesized. Next, the carbon precursor is activated to form porous carbon materials. Various methods may be utilized to optimize sample preparation to synthesize activated porous carbon materials with very high CO<sub>2</sub> uptake.

[0056] In some embodiments, a carbon precursor is activated by chemical activation. In some embodiments, the chemical activation includes heating the carbon precursor in a mixture. In some embodiments, the carbon precursor is heated in a mixture that contains a base, such as KOH. In some embodiments, the heating temperature ranges from about 500° C. to about 800° C. (FIG. 15). In some embodiments, the activation temperature is about 750° C.

[0057] In some embodiments, the carbon precursor is synthesized by polymerizing a carbon source. In some embodiments, the polymerization occurs by exposing the carbon source to an oxidant, such as iron (III) chloride (FeCl<sub>3</sub>) in the presence of acetonitrile (CH<sub>3</sub>CN).

[0058] In some embodiments, the materials of the present disclosure are prepared from affordable and readily available carbon sources. In some embodiments, the carbon sources include oxygen-containing carbons. In some embodiments, the oxygen containing carbon sources are rich in alcohol. In some embodiments, the carbon sources lack heteroatoms such as nitrogen, sulfur, and combinations thereof. As such, in some embodiments, the formed materials of the present disclosure also lack such heteroatoms.

[0059] In some embodiments, the materials of the present disclosure are prepared by heating a biological material. In some embodiments, the biological material includes, without limitation, sawdust, coconut husk, and combinations thereof.

[0060] In some embodiments, the carbon source that is utilized to make the materials of the present disclosure is furfuryl alcohol (FFA) (purchasable from Sigma Aldrich at a price of \$354 for 25 kg with purity>98%) (Table 4). In some embodiments where the carbon source is FFA, the formed carbon precursor is polyfurfuryl alcohol (PFFA).

[0061] In some embodiments, the materials of the present disclosure are prepared by heating an organic polymer precursor. In some embodiments, the organic polymer precursor includes oxygen in a functional group. In some embodiments, the functional group is a furyl. In some embodiments, the organic polymer precursor is FFA. In some embodiments, the organic polymer precursor polymerizes to form polyfurfuryl alcohol (PFFA). In some embodiments, PFFA is prepared by the polymerization of furfuryl alcohol with a catalyst. In some embodiments, the catalyst is FeCl<sub>3</sub>.

[0062] A more specific method of making the materials of the present disclosure is illustrated in FIG. 21A. In this illustration, the FFA is polymerized by using FeCl<sub>3</sub> as the oxidant. In a typical synthesis, a solution of FeCl<sub>3</sub> is prepared by solubilizing FeCl<sub>3</sub> in CH<sub>3</sub>CN. FFA is then mixed with CH<sub>3</sub>CN and slowly added to the FeCl<sub>3</sub> solution. The mixture is then magnetically stirred for 24 hours at room temperature. The polymerized product, brown colored PFFA, is then separated by filtration over a sintered glass funnel, washed thoroughly with abundant distilled water, and then with acetone. This is followed by drying at 40° C. for 12 hours. The yield of the final product was ~98%.

[0063] Next, the porous carbon was chemically activated by heating a PFFA-KOH mixture (KOH/PFFA at a weight ratio of 3) in inert atmosphere. The mixture was then placed inside a quartz tube/tube furnace setup and heated for 1 hour at a fixed temperature in the 500-800° C. range, under a flow of Ar. The activated OPC sample was then thoroughly washed several times with diluted HCl and distilled water and dried on a hot plate at 70° C. for 12 hours.

[0064] In some embodiments, the KOH/PFFA ratio can be varied. In some embodiments, the activation temperatures and the PFFA-KOH mixing procedure can be varied.

[0065] Use of Materials for Gas Capture

[0066] The materials of the present disclosure can be utilized to capture and selectively remove various gases (e.g., CO<sub>2</sub>, CH<sub>4</sub>, and combinations thereof) from various environments. Additional embodiments of the present disclosure pertain to methods of utilizing the materials of the present disclosure for the separation of a mixture of gases by preferential adsorption and selective desorption. Further embodiments of the present disclosure pertain to methods of utilizing the materials of the present disclosure for the capture of CO<sub>2</sub> from various environments. In some embodiments, the environments include an atmosphere or an environment that contains a mixture of gases. In some embodiments, the methods of the present disclosure pertain to processes for separating CO<sub>2</sub> from natural gas by exposing the natural gas to the materials of the present disclosure.

[0067] In some embodiments, the methods of the present disclosure utilize the materials of the present disclosure in a process in which selectivity and separation of two gases (such as CH<sub>4</sub> and CO<sub>2</sub>) is accomplished by a combination of an adsorption process that favors one of the components (e.g., selectivity of CO<sub>2</sub> over CH<sub>4</sub>). Thereafter, the desorption of the two components from the carbon materials can be significantly different by control over various parameters, such as temperature, pressure, and combinations thereof. In some embodiments, such control allows for the specific desorption of one of the components prior to the other (e.g., CH<sub>4</sub> over CO<sub>2</sub>). In some embodiments, the overall process allows for the selective separation of at least two gaseous components.

[0068] In some embodiments, the materials of the present disclosure differentiate between CH<sub>4</sub> and CO<sub>2</sub> adsorption as well as desorption. In some embodiments, the selectivity of adsorption is further enhanced since the pressure/temperature dependencies of the desorption of CH<sub>4</sub> and the desorption of CO<sub>2</sub> are distinct from each other such that they may be used to improve separation. Thus, in some embodiments, a mixture of adsorbed CH<sub>4</sub> and CO<sub>2</sub> will desorb under different conditions: the CH<sub>4</sub> first and the CO<sub>2</sub> second. In

some embodiments, this difference means that the overall adsorption/desorption selectivity of CH<sub>4</sub> and CO<sub>2</sub> is higher than prior materials.

[0069] In some embodiments, the materials of the present disclosure can be used for the selective capture of CO<sub>2</sub> from various environments. In some embodiments, the materials of the present disclosure can be utilized for the selective capture of CO<sub>2</sub> over hydrocarbons in the environment (e.g., CH<sub>4</sub>). In some embodiments, the adsorption of CO<sub>2</sub>/CH<sub>4</sub> mixtures and measurement of the desorption selectivity can be varied.

#### [0070] Applications and Advantages

[0071] The methods and materials of the present disclosure can provide numerous advantages. For instance, in some embodiments, the methods and materials of the present disclosure can be utilized for the selective removal of CO<sub>2</sub> from natural gas (e.g., methane) that contains various amounts of CO<sub>2</sub> (e.g., 10-20 mol % of CO<sub>2</sub>). Such an application is an important goal in the field of oil and natural gas, since contaminant CO<sub>2</sub> decreases its power efficiency. For an ideal gas adsorbing material, the major requirements are as follows: it should be cheap, simple to synthesize, demonstrate reproducible and high gas uptake property, and complete desorption of CO<sub>2</sub> at low pressure. In various embodiments, the materials of the present disclosure possess all of these properties.

[0072] In some embodiments, the methods and materials of the present disclosure can be utilized for the separation of CO<sub>2</sub> from natural gas at a source where low to medium levels of CO<sub>2</sub> are present. In some embodiments, the methods and materials of the present disclosure can be used as a secondary recovery method for treating CH<sub>4</sub>/CO<sub>2</sub> mixtures in which CO<sub>2</sub> is the major component. In some embodiments, such mixtures include high-pressure samples that are the result of an initial CH<sub>4</sub>/CO<sub>2</sub> separation using traditional methods.

[0073] The materials of the present disclosure can also provide numerous advantages. In particular, among the most efficient solid sorbents for capturing CO<sub>2</sub> from natural gas or atmosphere, MOFs and KOH aided chemically activated PC materials with large surface areas and micro pores have been investigated for decades. PC composites demonstrate remarkable thermal stability and repeatability for selective gas uptake measurements.

[0074] However, to date, most of the researchers have synthesized porous carbons from carbon rich precursors that contain heteroatoms, such as nitrogen or sulfur. For sulfur rich precursors, the most common feedstock for synthesizing PCs are polythiophene or poly(2-thiophenemethanol), whereas, pyrrole or acrylonitrile are being utilized for the production of nitrogen containing PCs.

[0075] Unfortunately, the high cost of both chemicals hinders the industrial scale use of PCs produced from these materials. Based upon an analysis of the best PC materials in terms of selectivity and CO<sub>2</sub> uptake, Applicants have noted that the common link is not the presence of strong Lewis base species such as N or S, but the presence of oxygen. Thus, Applicants envision that oxygen is an important component for selectivity and high adsorption of gases (e.g., CO<sub>2</sub> and/or CH<sub>4</sub>) in the materials of the present disclosure.

#### Additional Embodiments

[0076] Reference will now be made to more specific embodiments of the present disclosure and experimental results that provide support for such embodiments. However, Applicants note that the disclosure below is for illustrative purposes only and is not intended to limit the scope of the claimed subject matter in any way.

#### Example 1

##### Preparation of Porous Carbon Materials

[0077] This Example provides processes for the preparation of various porous carbon materials.

#### Example 1.1

##### Synthesis of Activated Porous Carbon (PC) from Coconut Shell

[0078] Pieces of dry coconut shell were placed inside a quartz tube/tube furnace setup and carbonized for 1 hour at 450° C., under a flow of Ar (flow rate 500 sccm). The carbonized product (500 mg) was thoroughly mixed with potassium hydroxide (KOH) powder (1.0 g). The mixture was then placed inside a quartz tube/tube furnace setup, dried for 20 minutes and then heated for 1 hour at a fixed temperature of 600° C. under continuous flow of Argon (flow rate of about 600 sccm), washed with distilled water (ca. 4 L) and then with acetone (ca. 1 L) and dried at 80° C. for 12 hours.

#### Example 1.2

##### Synthesis of Nitrogen-Containing Porous Carbon (NPC) from Polypyrrole

[0079] The polymerized carbon precursor polypyrrole was synthesized using FeCl<sub>3</sub> as a catalyst following a modification of Applicants' previous methods. In a typical synthesis, a solution of FeCl<sub>3</sub> (50 g) in CH<sub>3</sub>CN (200 mL) was prepared. Next, a solution of pyrrole (5.0 g) in CH<sub>3</sub>CN (50 mL) was slowly added to the previous solution. The mixture was stirred for 24 hours. The polymerized product was then separated by filtration, washed thoroughly with distilled water (ca. 4 L) and then with acetone (ca. 1 L) and dried at 80° C. for 12 hours. The yield of the final product was ~98%. The polypyrrole was chemically activated by heating with an excess (2 or 4 fold by weight) of KOH in inert atmosphere. In a typical activation process, polypyrrole (500 mg) was thoroughly mixed with KOH (1.0 g) that had been crushed to a fine powder in a mortar. The mixture was then placed inside a quartz tube within a tube furnace, dried for 20 minutes and then heated for 1 hour at a fixed temperature in the 500-800° C. range, under a flow of Ar (flow rate 600 sccm). The activated samples were then thoroughly washed with diluted HCl (1.4 M, 100 mL) and several times with distilled water until the filtrate attained neutral pH 7. Finally, the activated PC was dried on a hot plate at 70° C. for 12 hours.

#### Example 1.3

##### Synthesis of Polyfurfuryl Alcohol (PFFA)

[0080] In a typical synthesis, a solution was prepared by dissolving FeCl<sub>3</sub> (50 g) in CH<sub>3</sub>CN (200 mL). To this a

solution of furfuryl alcohol (5 g, Sigma Aldrich, 98%) mixed with CH<sub>3</sub>CN (50 mL) was slowly added. The mixture was stirred for 24 hours under continuous argon purging. The polymerized product, brown colored polyfurfuryl alcohol (PFFA) was separated by filtration, washed thoroughly with DI water (ca. 4 L) and acetone (500 mL), before being dried at 40° C. for 12 hours under vacuum (Yield=98%).

#### Example 1.4

##### Conversion of PFFA to Oxygenated Porous Carbon (OPC)

**[0081]** In a typical activation process, PFFA (500 mg) was thoroughly mixed with KOH powder (1.5 g, crushed previously) in a mortar for 10 minutes. The mixture was then placed inside a quartz tube/tube furnace, dried for 20 minutes and then heated for 1 hour at 500, 600, 700 or 750° C., under a flow of Ar (99.9%, flow rate 600 sccm). The activated samples were then washed with HCl (100 mL, 1.4 M) and DI water until the filtrate attained pH=7. The product was dried at 70° C. for 12 hours under vacuum. The yield of

for 1.5 hours under high vacuum. The free volume inside the sample cell was determined by a series of calibration procedures done under helium. Gas uptake experiments were carried out with high purity research grade CO<sub>2</sub> (99.99%) and CH<sub>4</sub> (99.9%) at 24° C.

**[0084]** FIG. 1A shows a plot of the uptake of CO<sub>2</sub> at 30 bar as a function of the apparent Brunauer-Emmett-Teller (BET) surface area (S<sub>BET</sub>) for all the PC adsorbent measured. As expected, an increase in surface area correlates with an increase in CO<sub>2</sub> uptake. However, any value above 2800 m<sup>2</sup>g<sup>-1</sup> does not appear to improve adsorption. Thus, continued attempts to create even higher surface area materials may not result in any further improvements in CO<sub>2</sub> uptake.

**[0085]** It is envisioned that increased total pore volume (V<sub>p</sub>) will facilitate increased CO<sub>2</sub> adsorption. However, as shown in FIG. 1B, it appears that for pore volumes over 1.35 cm<sup>3</sup>g<sup>-1</sup>, there is not a resulting greater uptake.

**[0086]** FIG. 2 shows the relationship between the activation temperature and the CO<sub>2</sub> uptake for the porous carbon samples listed in Table 1. The general trend is increasing uptake with increased activation temperature with a possible maximum between 700 and 800° C.

TABLE 1

Sample <sup>a</sup>	C (wt %) <sup>b</sup>	O (wt %) <sup>b</sup>	N (wt %) <sup>b</sup>	S (wt %) <sup>b</sup>	Surface area S <sub>BET</sub> (m <sup>2</sup> g <sup>-1</sup> )	Total pore volume (cm <sup>3</sup> g <sup>-1</sup> ) <sup>c</sup>	CO <sub>2</sub> uptake at 30 bar and 24° C. (mmol · g <sup>-1</sup> )
Activated charcoal	94.10	5.90	0.00	0.00	845	0.43	8.45
BPL <sup>d</sup>	91.3	8.7	0.00	0.00	951	0.49	8.66
SD-600-4	82.24	15.80	0.00	0.00	2290	1.10	20.52
SD-800-4	89.96	8.03	0.00	0.00	2850	1.35	22.90
CN-600-2	88.13	11.87	0.00	0.00	1250	0.64	13.50
PPy-500-2	72.47	17.19	10.33	0.00	1255	0.53	12.60
PPy-600-2	74.78	19.72	5.49	0.00	2013	1.03	18.98
PPy-700-2	90.01	9.87	0.14	0.00	2956	1.45	22.98
PPy-800-2	91.39	8.60	0.00	0.00	3230	1.51	21.01
PPy-800-4	90.78	9.11	0.10	0.00	3450	2.57	22.10
PAn-600-3	84.50	6.75	8.75	0.00	1410	1.38	14.50
SD-M-800-4	85.39	8.15	6.46	0.00	2990	2.69	23.80
PTh-600-2	64.91	25.88	0.00	9.21	2256	1.02	18.81
PTh-700-2	82.47	13.01	0.00	4.51	1980	0.99	20.32
PTh-800-2	88.18	7.24	0.00	4.58	2890	1.43	22.87

<sup>a</sup>Precursor-temperature-KOH:precursor ratio.

<sup>b</sup>Determined by XPS.

<sup>c</sup>Determined at P/P<sub>0</sub> ~0.99.

<sup>d</sup>Purchased from Calgon Carbon Corp.

activated PC materials depended on the activation temperature: OPC<sub>500</sub>=55%, OPC<sub>600</sub>=40%, OPC<sub>700</sub>=30%, and OPC<sub>750</sub>=25-27%.

#### Example 2

##### Characterization of the Porous Carbon Materials

**[0082]** This example provides various data relating to the characterization of the porous carbon materials in Example 1.

**[0083]** The volumetric uptake measurements (sorption and desorption) of CO<sub>2</sub> and CH<sub>4</sub> by the porous carbons were performed in an automated Sievert instrument (Setaram PCTPRO). Various PC samples were first crushed into powders and packed in a stainless steel autoclave sample cell. Initial sample pre-treatment was carried out at 130° C.

**[0087]** Given the relationships between surface area and pore volume with CO<sub>2</sub> uptake, it is not surprising that their relationship with activation temperature is also similar (FIG. 3). The analysis of a series of samples prepared from N-containing polymer polypyrrole (PPy) at different activation temperatures (i.e., PPy-T-2), but otherwise under identical conditions, allows for a convenient direct comparison of the effects of temperature.

**[0088]** The CO<sub>2</sub> uptake plot for each sample as a function of CO<sub>2</sub> pressures is shown in FIG. 4, whereas FIG. 5 shows their corresponding N<sub>2</sub> adsorption isotherms at 77 K. It may be noticed that the shape of these isotherms is dependent on the activation temperature. The isotherm for PPy-800-2 is much steeper than that of PPy-500-2 between relative pressures of 0.4 and 1.0, indicating the variation in mesoporosity and adsorption capacity. For the homologous series of NPC

materials, the estimated surface area ( $S_{BET}$ ) and the total pore volume ( $V_p$ ) gradually increase with activation temperature (FIGS. 6A-B), describing the incremental trend for mildly to strongly activated samples. Between 500 and 700° C., the surface area and total pore volume increases systematically, whereas for temperatures above 700° C. no significant increment is noticed.

[0089] Besides the surface area and pore volume, another important characteristic that can be obtained from the  $N_2$  adsorption isotherms is the pore size distribution (PSD) of the porous solid. FIG. 7 depicts the PSDs for three different PPy-based PCs prepared under mild ( $T=500^\circ\text{C}$ .) to strong ( $T=800^\circ\text{C}$ .) activation conditions. The distribution plot for  $T=500^\circ\text{C}$ . indicates that the activated PC mainly consists of micropores in the 1-2 nm range, whereas the plot for PPy-700-2 clearly shows signature of some larger pores in the 2-3.5 nm range. The most strongly activated PC and PPy-800-2 even shows a significant number of mesopores in the 3-6 nm range, in agreement with the steeper adsorption registered for relative pressures of more than 0.4.

[0090] A comparison of the variation in pore size and distribution (FIG. 7) with the  $\text{CO}_2$  uptake for the same samples (FIG. 4 and Table 1) was also made. From 500° C. to 700° C., there is a dramatic increase in the high pressure uptake, which can be associated with the generation of pores in the range of 2-3 nm. However, as may be seen from FIG. 4, there is a slight (but significant) decrease upon further activation to 800° C., even though there is an increase in the presence of larger pores. This suggests that larger pores are not necessarily ideal for a high  $\text{CO}_2$  adsorption. The pore size distribution for the other top adsorbents studied shows a similar bi-modal pore structure centered on 1 nm and 1.5-2 nm.

[0091] The  $\text{CO}_2$  uptake for NPC and SPC samples as a function of their N or S content is shown in FIG. 8. For both NPC and SPC samples, the  $\text{CO}_2$  uptake is at a maximum with the heteroatom content of less than 5 wt %. Based upon these results, it would appear that the presence of neither N nor S correlates in a positive manner with the  $\text{CO}_2$  uptake, although in the present case a higher heteroatom content is associated to lower surface area and pore volume, hence the corresponding lower  $\text{CO}_2$  uptake. Nonetheless, the limited effect of the presence of heteroatoms on  $\text{CO}_2$  uptake is in line with previous results, and Applicants' proposal that the

presence of N or S is not responsible for any stabilization of poly- $\text{CO}_2$  that has been proposed to be responsible for high  $\text{CO}_2$  adsorption at 30 bar.

[0092] Both NPC and SPC samples contain significant O, as do the PC samples produced from non-heteroatom containing precursors. Given that some of the PC samples perform in a comparable manner to those of NPC or SPC, N and S composition cannot be the sole key to high adsorption. While the presence of more than 5 wt % of either N or S appears to significantly lower the uptake of  $\text{CO}_2$ , although this could be related to the lower surface area of the heteroatom-rich samples, the O content is far more effective for the high  $\text{CO}_2$  adsorption observed with 3-16 wt % O (FIG. 9A).

[0093] In support of this observation, there are also some significant findings on the  $\text{CO}_2$  capture capacity of activated PCs obtained from the carbonization of asphalt with KOH. The reduction with  $\text{H}_2$  of asphalt-derived N-doped PCs causes a significant increase of capture capacity up to 26  $\text{mmol}\cdot\text{g}^{-1}$ . The XPS elemental analysis of the sample before and after  $\text{H}_2$  treatment shows that the sample with higher  $\text{CO}_2$  capacity undergoes a significant increase of O content while the N content and type is only slightly changed. This finding supports Applicants' hypothesis that O plays a major role in establishing the  $\text{CO}_2$  capture capacity of PCs. However, what appears to be more important is the combined presence of a heteroatom (i.e.,  $\Sigma(\text{O}, \text{N}, \text{S})$ , FIG. 9B). This can be alternatively stated that the C content should be between 80-95 wt %.

[0094] Based upon the forgoing, it is possible to identify the parameters that define a PC material for maximum  $\text{CO}_2$  uptake: have a surface area > 2800  $\text{m}^2\cdot\text{g}^{-1}$ , a pore volume > 1.35  $\text{cm}^3\cdot\text{g}^{-1}$ , and a C content between 80-95 wt %. To achieve these performance parameters it is necessary to activate above 700° C. and to ensure full mixing of the KOH with the precursor. It is significant that the first two of these suggest that developing higher and higher surface area materials is unproductive, and that understanding the third may lead to the design of new PC materials. Furthermore, these values offer additional variance when the uptake of  $\text{CO}_2$  is required at lower pressures.

[0095] Applicants have also investigated the  $\text{CO}_2/\text{CH}_4$  selectivity by measuring  $\text{CO}_2$  and  $\text{CH}_4$  uptake isotherms up to a high pressure limit of 10, 20 and 30 bar at 24° C. A summary of the data is shown in Table 2.

TABLE 2

Summary of PC, NPC, and SPC samples studied with their molar gas uptakes and selectivity for  $\text{CO}_2$  over  $\text{CH}_4$  at different uptake pressures.

Sample <sup>a</sup>	$\text{CO}_2$ uptake ( $\text{mmol}\cdot\text{g}^{-1}$ ) at			$\text{CH}_4$ uptake ( $\text{mmol}\cdot\text{g}^{-1}$ ) at			Molar ( $\text{CO}_2:\text{CH}_4$ ) uptake ratio		
	10 bar	20 bar	30 bar	10 bar	20 bar	30 bar	10 bar	20 bar	30 bar
Activated charcoal	6.27	7.51	8.45	4.28	5.44	6.03	1.46	1.38	1.41
BPL	6.30	7.87	8.66	3.24	4.96	6.18	1.94	1.59	1.40
SD-600-4	12.06	16.77	20.52	5.23	7.54	8.52	2.31	2.22	2.41
SD-800-4	13.61	18.78	22.90	6.65	9.45	10.92	2.05	1.99	2.10
CN-600-2	10.91	12.65	13.50	5.94	7.24	7.96	1.83	1.74	1.70
PPy-500-2	9.51	11.27	12.60	4.11	5.06	5.98	2.31	2.23	2.11
PPy-600-2	11.37	16.45	18.98	5.39	6.33	7.41	2.11	2.60	2.56
PPy-700-2	12.50	18.12	22.98	5.75	7.92	9.41	2.17	2.29	2.44
PPy-800-2	11.94	17.21	21.01	5.78	8.23	9.82	2.07	2.09	2.14
PPy-800-4	11.18	16.51	22.11	5.10	7.33	8.83	2.19	2.25	2.50

TABLE 2-continued

Summary of PC, NPC, and SPC samples studied with their molar gas uptakes and selectivity for CO<sub>2</sub> over CH<sub>4</sub> at different uptake pressures.

Sample <sup>a</sup>	CO <sub>2</sub> uptake (mmol · g <sup>-1</sup> ) at			CH <sub>4</sub> uptake (mmol · g <sup>-1</sup> ) at			Molar (CO <sub>2</sub> :CH <sub>4</sub> ) uptake ratio		
	10 bar	20 bar	30 bar	10 bar	20 bar	30 bar	10 bar	20 bar	30 bar
PAn-600-3	8.19	10.84	14.50	4.04	5.26	6.03	2.03	2.06	2.40
SD-M-800-4	12.09	18.70	23.76	5.58	8.12	9.41	2.17	2.30	2.52
PTh-600-2	11.17	15.42	18.81	4.77	6.12	7.37	2.34	2.52	2.55
PTh-700-2	11.51	16.67	20.32	4.62	6.87	8.01	2.49	2.43	2.54
PTh-800-2	13.10	18.80	22.87	5.81	8.55	10.14	2.25	2.20	2.26

<sup>a</sup>Precursor-temperature-KOH:precursor ratio.

[0096] FIG. 10A shows the CO<sub>2</sub> uptake plots along with the corresponding CH<sub>4</sub> uptake results in FIG. 10B. Additionally, the molar uptake selectivity (CO<sub>2</sub>/CH<sub>4</sub>) is defined by the molar ratio of adsorbed CO<sub>2</sub> and CH<sub>4</sub> at a certain pressure, i.e., at 30 bar. The dependence of molar uptake selectivity for a sorbent as a function of corresponding gas pressure is depicted in FIG. 10C. It is significant that for any particular sample, the selectivity varies with gas pressure. Of the samples investigated, PPy-600-2 demonstrated highest selectivity of 2.56 at 30 bar.

[0097] FIG. 11A shows a plot of molar CO<sub>2</sub>:CH<sub>4</sub> uptake ratio as a function of the surface area (S<sub>BET</sub>) for all the PC adsorbents measured. For low surface area samples, there is an increase in selectivity with increased surface area. However, as with uptake, further increase in surface area above 2000 m<sup>2</sup>g<sup>-1</sup> does not appear to improve selectivity. In a similar manner, increased total pore volume (V<sub>p</sub>) does facilitate increased selectivity, but only to a pore volume of 1.00 cm<sup>3</sup>g<sup>-1</sup>. No improvement in performance is shown above the aforementioned value (FIG. 11B).

[0098] The series PPy-T-2 (T=500-800° C.) allows for the direct comparison of homologous materials. In this case, it appears that the values of 2,000 m<sup>2</sup>g<sup>-1</sup> and 1.00 cm<sup>3</sup>g<sup>-1</sup> for the surface area and total pore volume (FIG. 12) represent maxima rather than thresholds. It is possible that for any homologous series similar maxima are observed. However, the thresholds observed in FIG. 11 are useful indicators.

[0099] From Table 2, it can be seen that an activation temperature of 600° C. is a minimum for good selectivity. However, from FIG. 12C, it may be seen that for the series PPy-T-2 (T=500-800° C.), this value is actually an optimum. Such results may vary with a particular class of material. However, a lower activation temperature is required to create a material with good selectivity as compared to optimum CO<sub>2</sub> uptake (FIG. 12D), suggesting that the best attainable sorbent material will have to combine a wise trade off of selectivity and CO<sub>2</sub> capture capacity. As may be seen from a comparison of PPy-800-2 and PPy-800-4 (Table 2), increased KOH concentration during the activation step results in greater selectivity.

[0100] The molar CO<sub>2</sub>:CH<sub>4</sub> uptake ratio for NPC samples as a function of their N content is shown in FIG. 13. The selectivity for measurements at 30 bar decreases with N content above 5 wt %. In the case of SPC, there appears to be no effect on selectivity with S content (Tables 1 and 2).

[0101] These results seem to suggest that the presence of neither N nor S correlates in a direct manner with the CO<sub>2</sub>/CH<sub>4</sub> selectivity. This is in line with Applicants' previous proposal. However, in this Example, a higher heteroatom content implies a lower surface area (and total pore volume) of the sorbent materials. Hence, a definite lack of impact of N or S doping on the selectivity performance of PCs cannot be considered a priori. Significantly, as may be seen from the data in Table 2, at lower pressures (10 bar), there is almost no dependence between selectivity and heteroatom content.

[0102] As was observed with the uptake efficiency for CO<sub>2</sub>, the selectivity appears to be more a function of the total heteroatom composition (i.e., Σ(O, N, S) wt %, as presented in FIG. 14 in terms of C wt % (=100-Σ(O, N, S) wt %)). However, based upon the analysis of all the PC, NPC, and SPC materials studied, the 0 wt % seems to be the major contributor. The CO<sub>2</sub>/CH<sub>4</sub> selectivity is at a potential maximum as long as C content is below 90 wt % (i.e., for Σ(O, N, S)>10 wt %). At lower pressure (10 bar), the carbon content is possibly even higher (C<94 wt %).

[0103] A study of a wide range of PC, NPC, and SPC materials under high pressure CO<sub>2</sub> and CH<sub>4</sub> adsorption offers some useful insight into the parameters that may collectively control both the CO<sub>2</sub> uptake efficiency and the CO<sub>2</sub>/CH<sub>4</sub> selectivity. A summary of the proposed key requirements for a PC material with either good CO<sub>2</sub> uptake or good CO<sub>2</sub>/CH<sub>4</sub> selectivity is given in Table 3 based on the results presented herein.

TABLE 3

Summary of proposed parameters required for optimum CO <sub>2</sub> uptake and CO <sub>2</sub> /CH <sub>4</sub> selectivity for PC, NPC, and SPC.		
Parameter	Uptake @ 30 bar	Selectivity @ 30 bar
Surface area (m <sup>2</sup> g <sup>-1</sup> )	>2800	>2000
Total pore volume (cm <sup>3</sup> g <sup>-1</sup> )	>1.35	>1.0
Temperature of activation (° C.)	700-800	600
Carbon content (%)	80-95	<90

[0104] As far as CO<sub>2</sub> uptake is concerned, any porous carbon material with a surface area of more than 2800 m<sup>2</sup>g<sup>-1</sup> at 30 bar is unlikely to be improved (when prepared from the KOH activation of non-nanostructured precursors). A similar threshold appears to be true for the total pore volume of the material (1.35 cm<sup>3</sup>g<sup>-1</sup>). This suggests that seeking synthetic routes to ever higher surface area and/or high pore volume PC-based adsorbents is counterproductive.

[0105] However, it should be understood that if uptake at lower pressures is desired, these threshold values decrease even further. This result is highly important in considering the choice of adsorbent to be used in a large scale unit. The

adsorbent intended for use in a low pressure system needs a lower surface area and pore volume to perform than a potentially more expensive to manufacture material. It also impacts the formation of pelletized materials for adsorbent bed applications, since the formation of the pellet through inclusion of a binder inevitably lowers the surface area and pore volume. Applicants' results suggest that for lower pressure applications, this is not important since the uptake is less dependent on extremely high surface areas and/or pore volumes.

[0106] Given the prior interest in N- and S-doped PC materials, the results show that CO<sub>2</sub> uptake is inversely related to S and N content in SPC and NPC, respectively. However, due to the preparation process used in this Example (KOH activation), there is an intrinsic dependence between heteroatom content and surface area (total pore volume) in all sorbents. In particular, higher surface areas imply lower N or S contents.

[0107] Consequently, the use of KOH activated PCs in industrial scale units must take into account that a higher heteroatom content cannot offset the corresponding drop of CO<sub>2</sub> capture performance due to a decrease of surface area of the materials. In practical terms, it is the Σ(O, N, S) wt % or C wt % (=100-Σ(O, N, S) wt %) that is the defining factor for CO<sub>2</sub> uptake. This is true irrespective of the source of the heteroatom. However, O appears to be the main factor, since a C content of between 80 and 95 wt % offers the potential for high CO<sub>2</sub> uptake. However, at these levels, if the make-up is N or S, the uptake is likely reduced. It should also be observed based upon the source of the heteroatom that if heteroatoms are to be incorporated and "active", they are preferentially included using heterocycle precursors, such as melamine in the case of N, rather than other heteroatom-rich structures.

[0108] It may be assumed that the parameters that makes a good CO<sub>2</sub> adsorbent may be the same as those that make a selective material. However, Applicants' results indicate that the two are only broadly related. The levels of surface area and pore volume can be even lower for good CO<sub>2</sub>/CH<sub>4</sub> selectivity, as compared to CO<sub>2</sub> uptake (Table 3).

[0109] In summary, Applicants demonstrate in this Example that a synthetic goal for PC-based material, for both high CO<sub>2</sub> adsorption and high CO<sub>2</sub>/CH<sub>4</sub> selectivity, would comprise a C content of less than 90%. Given that neither N nor S seem to have a significant effect rather than the O that is present, it is clear that a design C<sub>x</sub>O<sub>1-x</sub> where x<0.9 would possibly make an ideal CO<sub>2</sub> adsorbent material with the best CO<sub>2</sub>/CH<sub>4</sub> selectivity. Furthermore, the goal should be a precursor where oxygen is incorporated into a cyclic moiety.

[0110] Additional experimental results and information are provided in FIGS. 15-23 and Tables 4-6. For instance, the chemical composition of OPC (750) has been thoroughly characterized via XPS, FTIR and Raman spectroscopy (FIG. 23 and Table 6), while textural properties were determined by high resolution scanning electron microscopy (FIGS. 21E-H), transmission electron microscopy (FIGS. 21I-J) and a BET Surface area analyzer (FIG. 16). Moreover, measured values for gas uptakes have been confirmed via volumetric, gravimetric, multiple sample and cycles experiments.

[0111] To the best of Applicants' knowledge, oxygen-rich carbon materials prepared from furfuryl alcohol has never been investigated for high pressure uptake of CO<sub>2</sub> and CH<sub>4</sub>. In fact, there have been no reports of its use as a precursor for oxygen-rich porous carbon materials. In addition, a higher value for the isosteric heat of adsorption of CO<sub>2</sub> (23 kJ·mol<sup>-1</sup>) versus 13 kJ·mol<sup>-1</sup> for CH<sub>4</sub> allows Applicants to scheme a temperature dependent strategy for removing CO<sub>2</sub> from natural gas via selective adsorption and desorption of CH<sub>4</sub> and CO<sub>2</sub> in steps (FIG. 22).

TABLE 4

Survey of different c-feedstock used for the synthesis of various PCs with high CO <sub>2</sub> uptake properties.					
PC sample	Source material for C-precursor	CAS no.	SKU pack size (Sigma Aldrich)	Price	Maximum CO <sub>2</sub> uptake at 30 bar (mmol g <sup>-1</sup> ) (wt %)
SPC (1)	2-Thiophenemethanol	636-72-6	181315-100 G	\$155 for 100 g	18.4 (81)
SPC (2)	Thiophene	110-02-1	T31801-500 G	\$47 for 500 g	—
NPC (1)	Pyrrole	109-97-7	W338605-1 KG	\$315 for 1 kg	—
NPC (2)	Polyacrylonitrile	25014-41-9	181315-100 G	\$190 for 100 g	16.8 (74)
OPC (1)	Furfuryl alcohol	98-00-0	W249106-25 KG	\$60 for 1 kg (\$354 for 25 kg)	26.6 (117)
OPC (2)	Furan	110-00-9	185922-500 ML	\$54 for 500 mL	—

TABLE 5

Survey of gas adsorption properties of various PCs with high CO <sub>2</sub> uptake capacity.					
Sample	Surface area S <sub>BET</sub> (m <sup>2</sup> g <sup>-1</sup> )	Uptake of CO <sub>2</sub> at 30 bar (mmol · g <sup>-1</sup> ) (wt %)	Uptake of CO <sub>3</sub> at 10 bar (mmol · g <sup>-1</sup> ) (wt %)	Uptake of CH <sub>4</sub> at 30 bar (mmol · g <sup>-1</sup> ) (wt %)	Ratio of absorbed CO <sub>2</sub> /CH <sub>4</sub> at 30 bar (molar) (mass)
C-Precursor	48	3.3 (14.5)	1.6 (7.0)	—	—
OPC (500)	1143	17.1 (75.2)	8.6 (37.8)	6.7 (10.7)	2.5 (7.0)
OPC (600)	2116	20.0 (88.1)	12.5 (55.0)	8.3 (13.3)	2.3 (6.3)

TABLE 5-continued

Survey of gas adsorption properties of various PCs with high CO <sub>2</sub> uptake capacity.					
Sample	Surface area S <sub>BET</sub> (m <sup>2</sup> g <sup>-1</sup> )	Uptake of CO <sub>2</sub> at 30 bar (mmol · g <sup>-1</sup> ) (wt %)	Uptake of CO <sub>3</sub> at 10 bar (mmol · g <sup>-1</sup> ) (wt %)	Uptake of CH <sub>4</sub> at 30 bar (mmol · g <sup>-1</sup> ) (wt %)	Ratio of absorbed CO <sub>2</sub> /CH <sub>4</sub> at 30 bar (molar) (mass)
OPC (700)	2610	20.8 (91.5)	12.7 (55.9)	9.1 (14.6)	2.3 (6.2)
OPC (750)	2856	26.6 (117.0)	15.1 (66.4)	9.6 (15.5)	2.75 (7.5)
OPC (750) at 0.5° C.	2856	42.9 (188.9)	18.5 (81.5)	14.6 (23.4)	2.93 (8.0)
OPC (800)	3005	23.0 (101.2)	12.9 (56.7)	9.01 (14.4)	2.5 (7.0)
SPC <sup>a</sup>	2500	18.4 (81.0)	10.0 (44.0)	7.1 (11.3)	2.6 (7.1)
r-NPC <sup>a</sup>	1450	16.8 (74.0)	7.1 (31.2)	7.6 (12.2)	2.2 (6.1)
Act. charcoal	845	8.4 (36.9)	6.3 (27.7)	6.0 (9.6)	1.4 (3.8)

TABLE 6

Elemental composition of various types porous carbon materials as determined by XPS excluding the contribution from elemental H.					
Sample	C (wt %) XPS	O (wt %) XPS	KOH: precursor	Surface area S <sub>BET</sub> (m <sup>2</sup> g <sup>-1</sup> )	Total pore volume V <sub>P</sub> (cm <sup>3</sup> g <sup>-1</sup> )
C-Precursor	69.91	30.09	—	48	0.02
OPC (500)	77.49	22.51	3:1	1143	0.78
OPC (600)	82.04	17.74	3:1	2216	1.19
OPC (700)	85.07	14.93	3:1	2610	1.46
OPC (750)	88.21	11.79	3:1	2856	1.77
OPC (800)	89.28	10.72	3:1	3005	1.92
Act. charcoal	94.10	5.90	3:1	845	0.43

[0112] Without further elaboration, it is believed that one skilled in the art can, using the description herein, utilize the present disclosure to its fullest extent. The embodiments described herein are to be construed as illustrative and not as constraining the remainder of the disclosure in any way whatsoever. While the embodiments have been shown and described, many variations and modifications thereof can be made by one skilled in the art without departing from the spirit and teachings of the invention. Accordingly, the scope of protection is not limited by the description set out above, but is only limited by the claims, including all equivalents of the subject matter of the claims. The disclosures of all patents, patent applications and publications cited herein are hereby incorporated herein by reference, to the extent that they provide procedural or other details consistent with and supplementary to those set forth herein.

What is claimed is:

1. A material for CO<sub>2</sub> adsorption at pressures above 1 bar, said material comprising:  
a porous carbon material with a surface area of at least 2800 m<sup>2</sup>/g, a total pore volume of at least 1.35 cm<sup>3</sup>/g, and a carbon content of between 80% and 95% as measured by X-ray photoelectron spectroscopy,  
wherein the porous carbon material is prepared by heating an organic polymer precursor or biological material in the presence of KOH, and  
wherein the temperature of activation is between 700° C. and 800° C.
2. The material of claim 1, wherein the porous carbon material is prepared by heating an organic polymer precursor.
3. The material of claim 2, wherein the organic polymer precursor comprises oxygen in a functional group.

4. The material of claim 3, wherein the functional group is a furyl.

5. The material of claim 4, wherein the organic polymer precursor polymerizes to form polyfurfuryl alcohol.

6. The material of claim 5, wherein the polyfurfuryl alcohol is prepared by the polymerization of furfuryl alcohol with a catalyst.

7. The material of claim 6, where the catalyst is iron(III) chloride.

8. The material of claim 1, wherein the porous carbon material is prepared by heating a biological material.

9. The material of claim 8, where the biological material is selected from the group consisting of sawdust, coconut husk, and combinations thereof.

10. A material for the separation of CO<sub>2</sub> from natural gas at partial pressures of either component above 1 bar, said material comprising:

a porous carbon material with surface area of at least 2000 m<sup>2</sup>/g, a total pore volume of at least 1.00 cm<sup>3</sup>/g, and a carbon content of greater than 90% as measured by X-ray photoelectron spectroscopy,

wherein the porous carbon material is prepared by heating an organic polymer precursor or biological material in the presence of KOH, and  
wherein the temperature of activation is between 600° C. and 700° C.

11. The material of claim 10, wherein the porous carbon material is prepared by heating an organic polymer precursor.

12. The material of claim 11, wherein the organic polymer precursor contains oxygen in a functional group.

13. The material of claim 12, wherein the functional group is a furyl.

14. The material of claim 13, wherein the organic polymer precursor polymerizes to form polyfurfuryl alcohol.

15. The material of claim 14, wherein the polyfurfuryl alcohol is prepared by the polymerization of furfuryl alcohol with a catalyst.

16. The material of claim 14, wherein the catalyst is iron(III) chloride.

17. The material of claim 10, wherein the porous carbon material is prepared by heating a biological material.

18. The material of claim 17, where the biological material is selected from the group consisting of sawdust, coconut husk, and combinations thereof.

\* \* \* \* \*



US 20180169611A1

(19) United States

(12) Patent Application Publication

Ghosh et al.

(10) Pub. No.: US 2018/0169611 A1

(43) Pub. Date: Jun. 21, 2018

(54) **METHOD, SYNTHESIS, ACTIVATION PROCEDURE AND CHARACTERIZATION OF AN OXYGEN RICH ACTIVATED POROUS CARBON SORBENT FOR SELECTIVE REMOVAL OF CARBON DIOXIDE WITH ULTRA HIGH CAPACITY**

(71) Applicants: **William Marsh Rice University**, Houston, TX (US); **Apache Corporation**, Houston, TX (US)

(72) Inventors: **Saunab Ghosh**, Houston, TX (US); **Andrew R. Barron**, Houston, TX (US); **Jason Ho**, Houston, TX (US)

(73) Assignees: **William Marsh Rice University**, Houston, TX (US); **Apache Corporation**, Houston, TX (US)

(21) Appl. No.: 15/875,471

(22) Filed: Jan. 19, 2018

#### Related U.S. Application Data

- (63) Continuation of application No. 15/631,341, filed on Jun. 23, 2017, which is a continuation-in-part of application No. 15/200,632, filed on Jul. 1, 2016, now abandoned.
- (60) Provisional application No. 62/187,744, filed on Jul. 1, 2015.

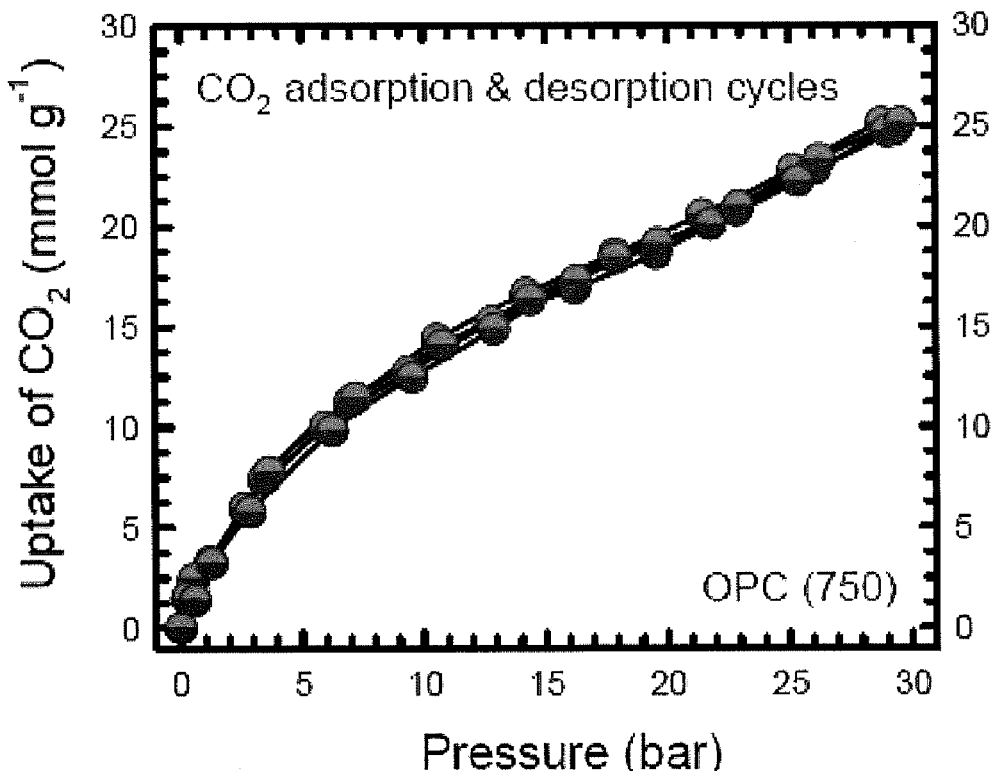
#### Publication Classification

(51) Int. Cl.  
*B01J 20/20* (2006.01)  
*C10L 3/10* (2006.01)  
*B01J 20/30* (2006.01)  
*B01D 53/04* (2006.01)  
*B01J 20/28* (2006.01)

(52) U.S. Cl.  
CPC ..... *B01J 20/20* (2013.01); *C10L 3/104* (2013.01); *B01J 20/28076* (2013.01); *B01D 53/04* (2013.01); *B01J 20/28066* (2013.01); *B01J 20/3078* (2013.01)

#### ABSTRACT

The present disclosure pertains to methods of capturing CO<sub>2</sub> from an environment at pressures above 1 bar by associating the environment with a porous material that has a surface area of at least 2,800 m<sup>2</sup>/g, and a total pore volume of at least 1.35 cm<sup>3</sup>/g, where a majority of pores of the porous material have diameters of less than 2 nm. The present disclosure also pertains to methods for the separation of CO<sub>2</sub> from natural gas in an environment at partial pressures of either component above 1 bar by associating the environment with a porous material that has a surface area of at least 2,200 m<sup>2</sup>/g, and a total pore volume of at least 1.00 cm<sup>3</sup>/g, where a majority of pores of the porous material have diameters of greater than 1 nm and less than 2 nm.



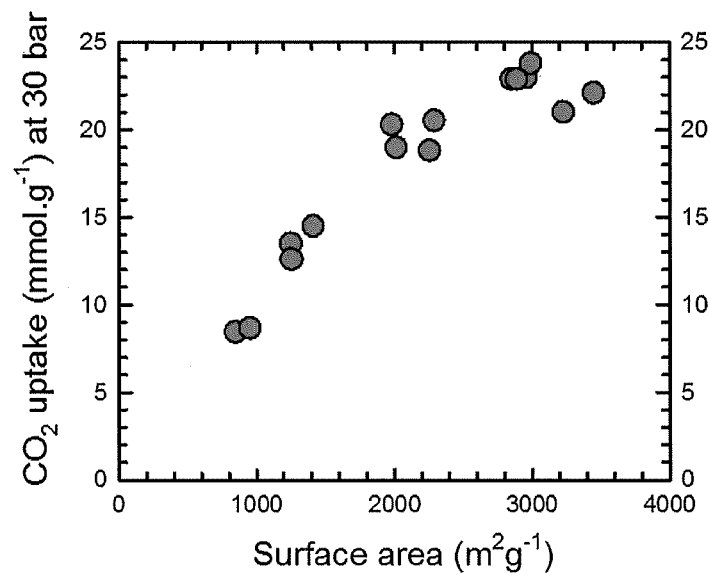


**FIG. 1A**

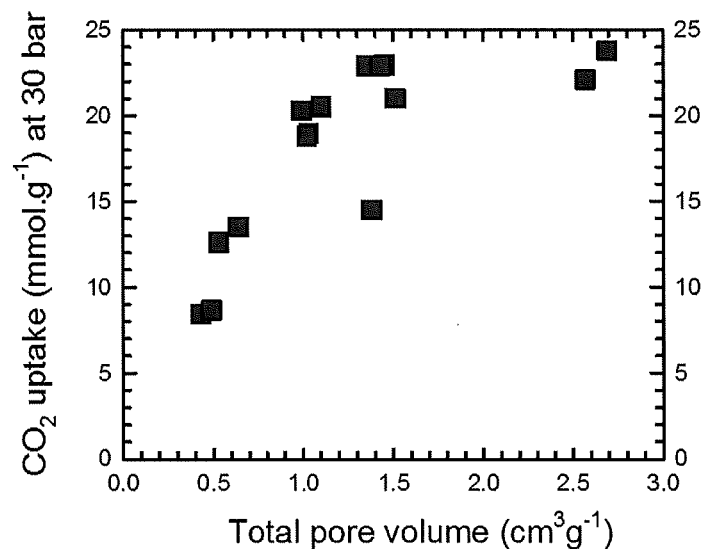


**FIG. 1B**

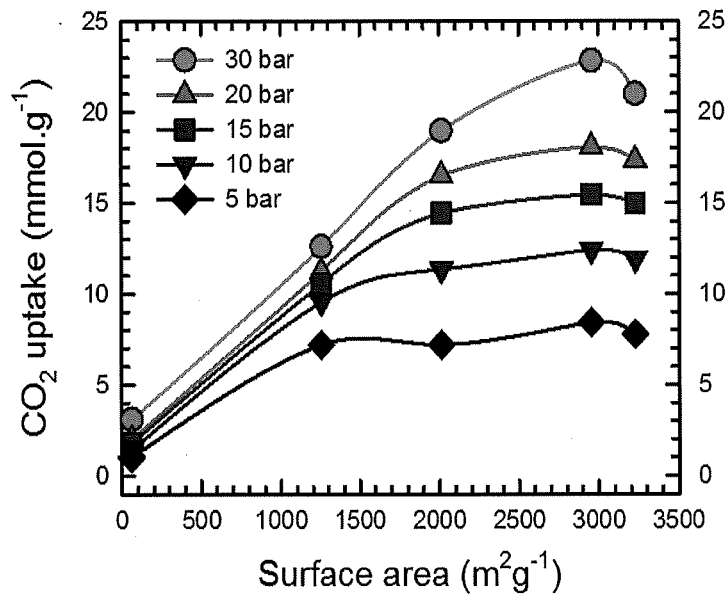


FIG. 1C

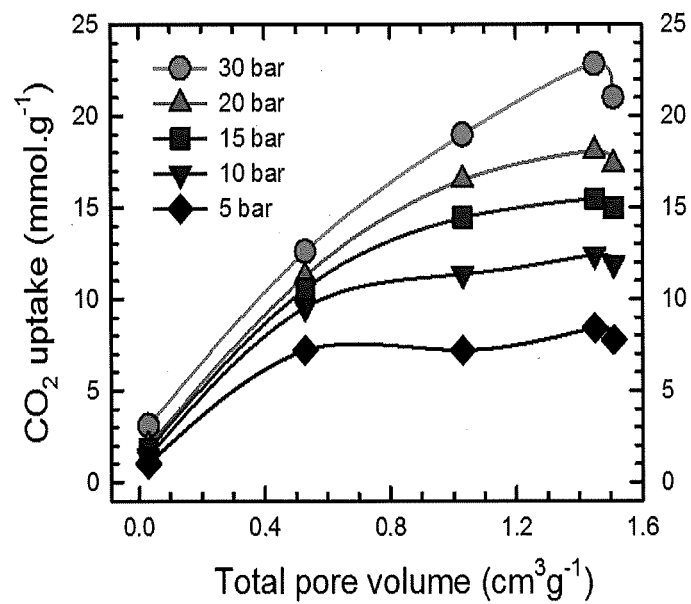


FIG. 1D

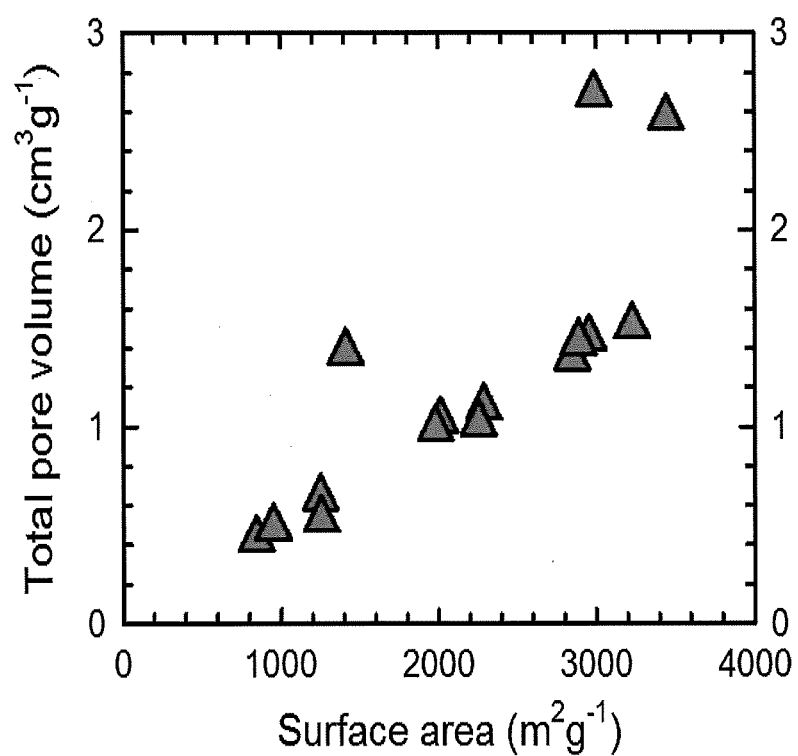


FIG. 1E

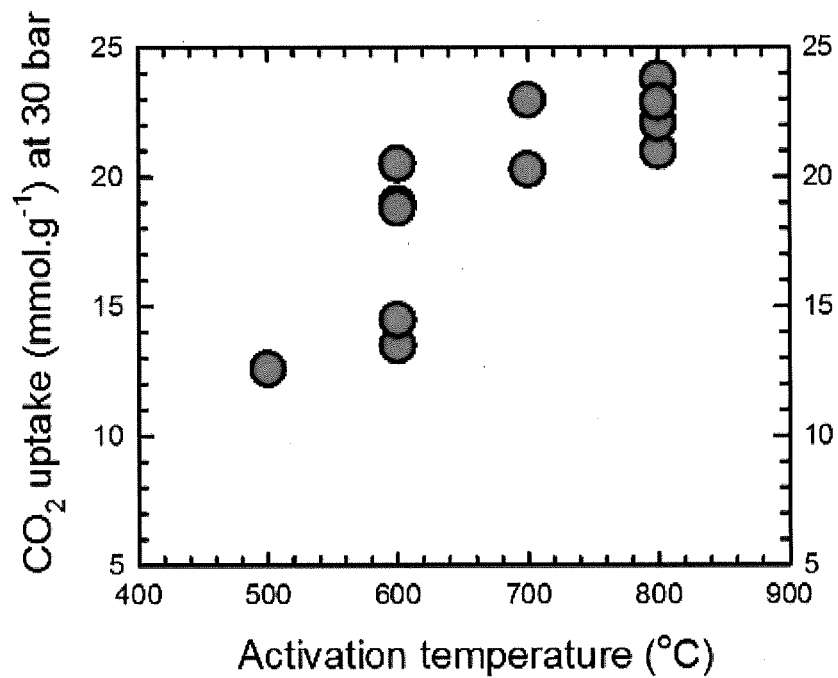
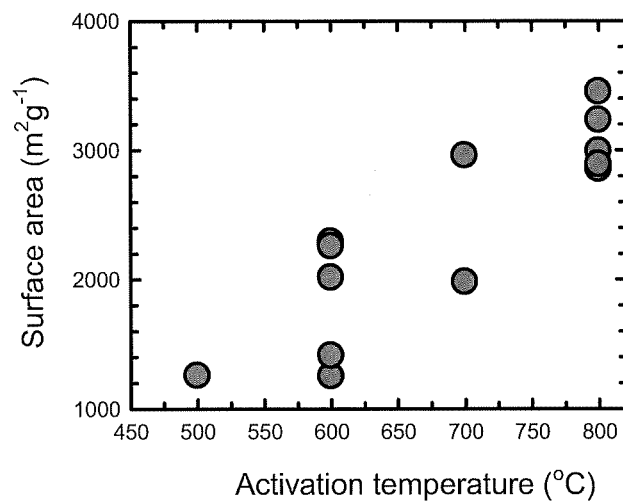
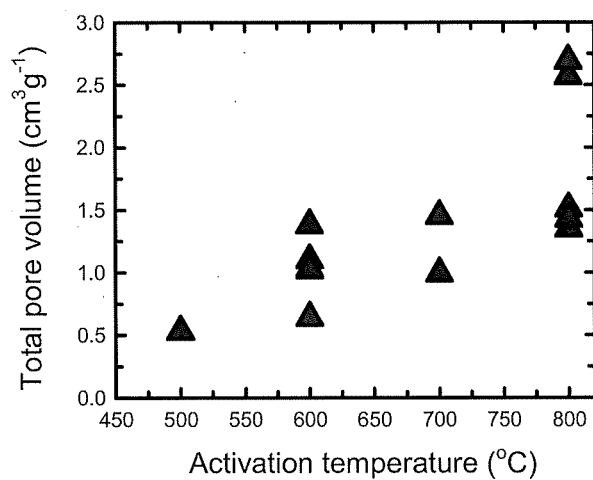


FIG. 2



**FIG. 3A**



**FIG. 3B**

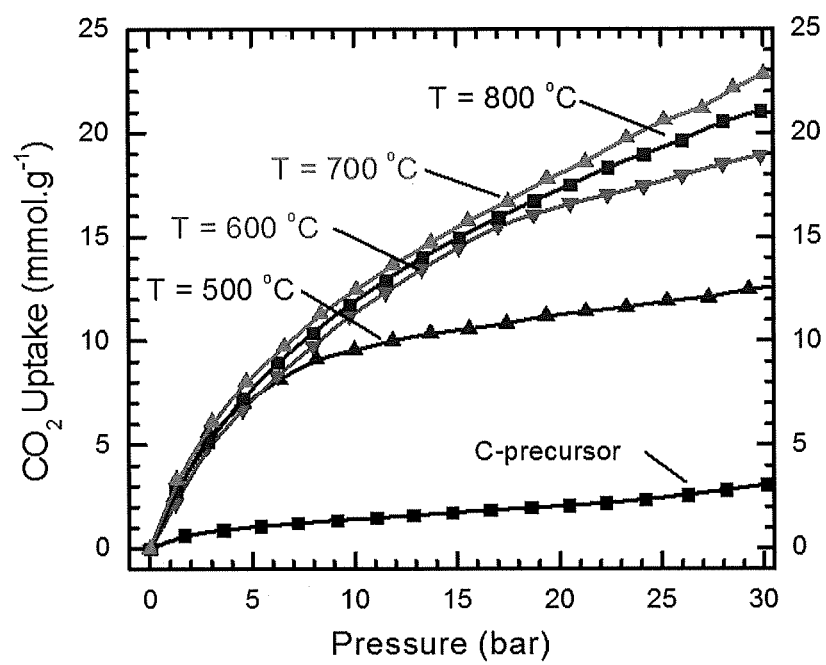


FIG. 4

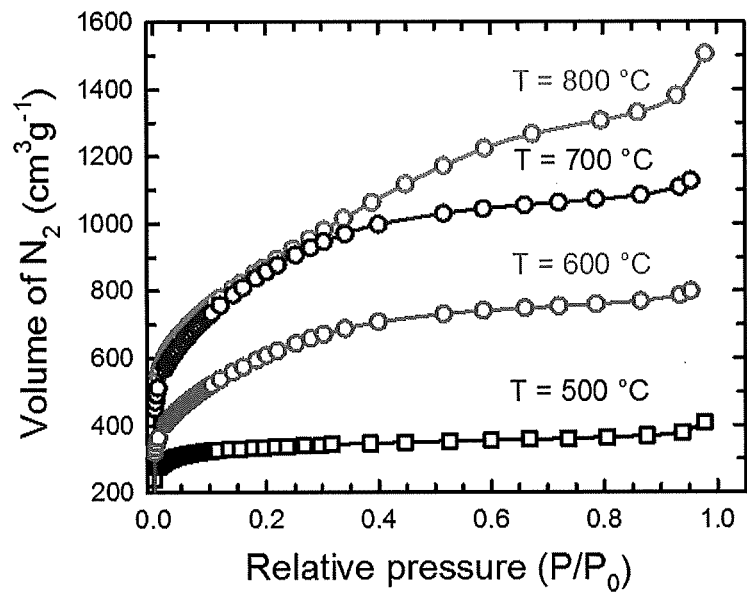


FIG. 5

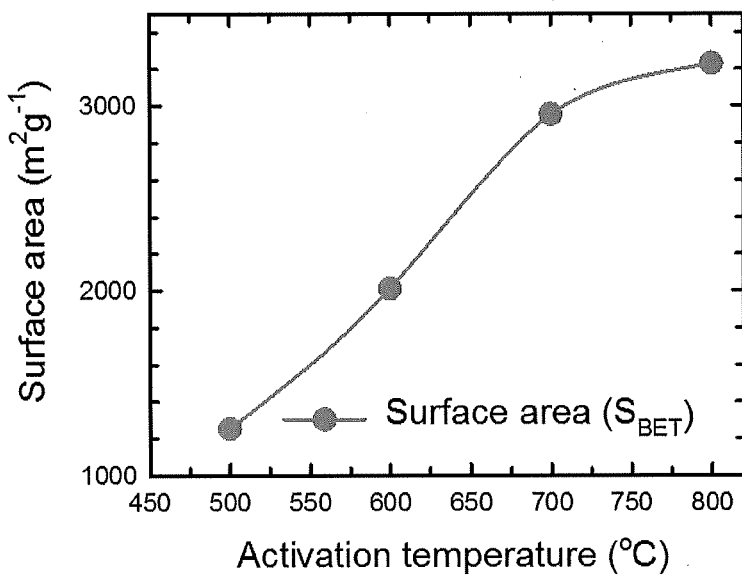


FIG. 6A

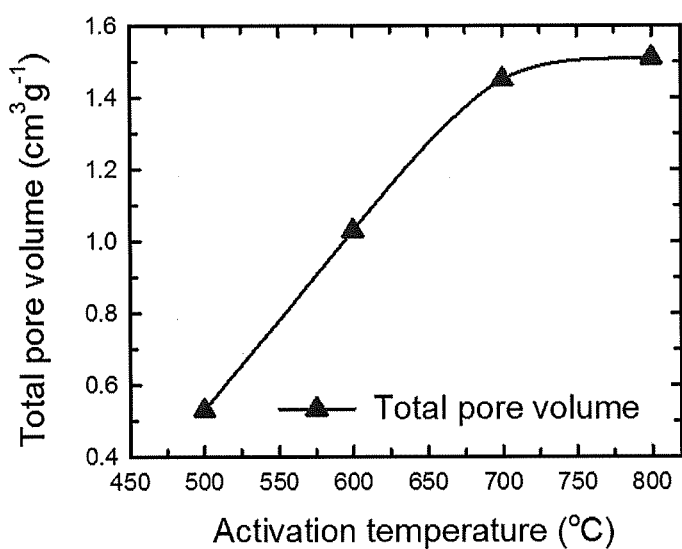


FIG. 6B

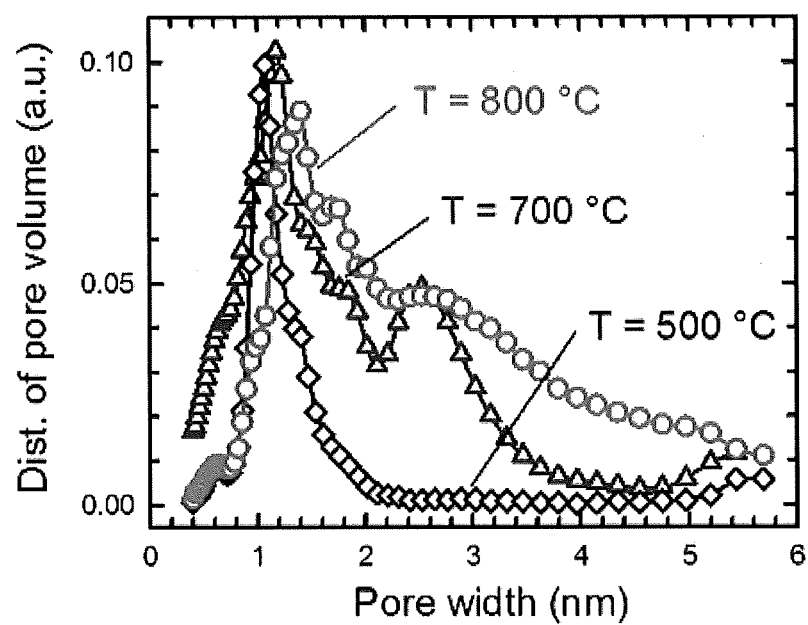


FIG. 7A

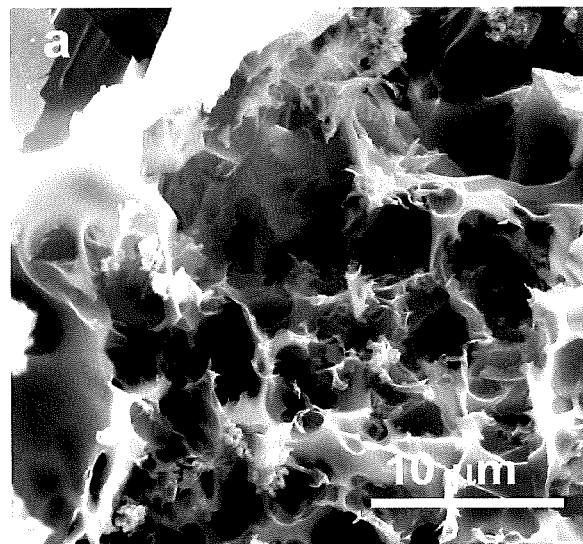


FIG. 7B

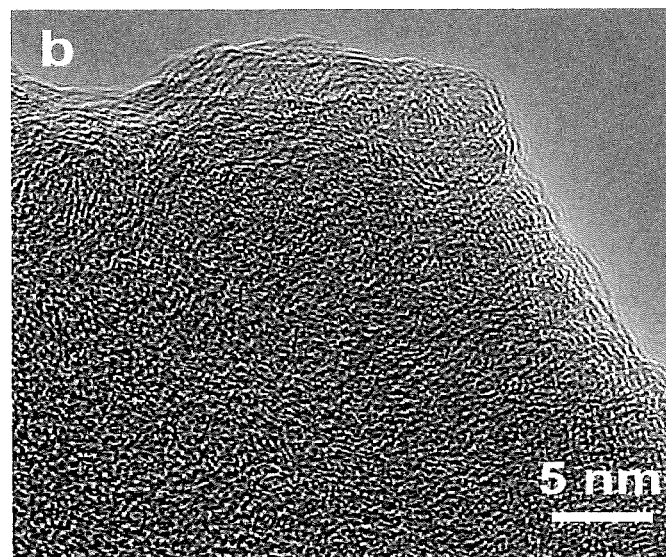


FIG. 7C

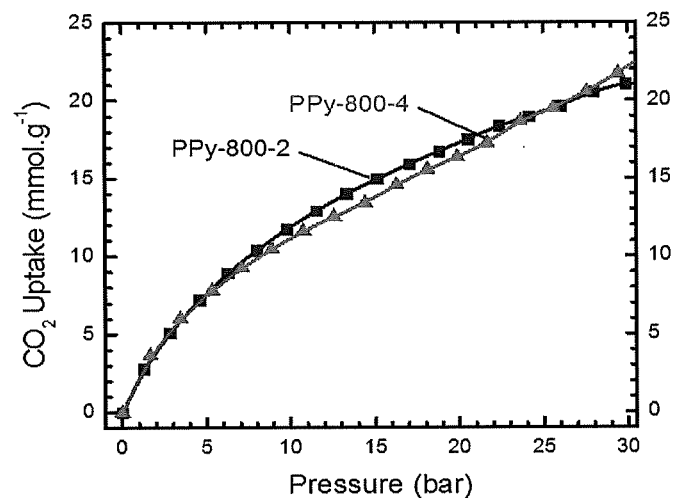


FIG. 7D

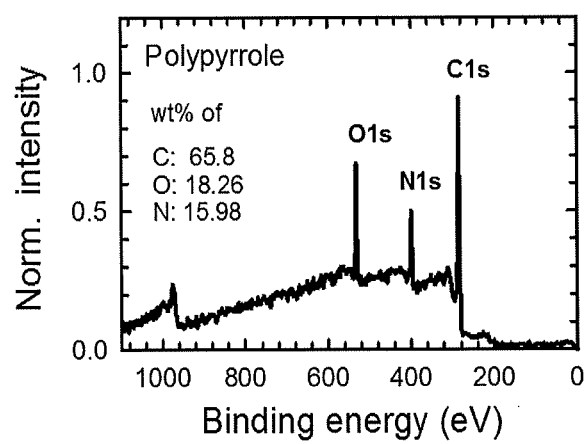
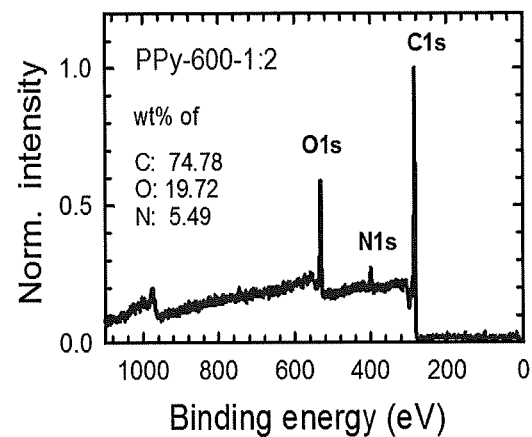
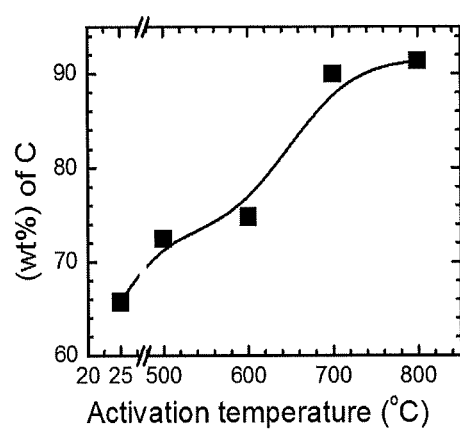


FIG. 7E



**FIG. 7F**



**FIG. 7G**

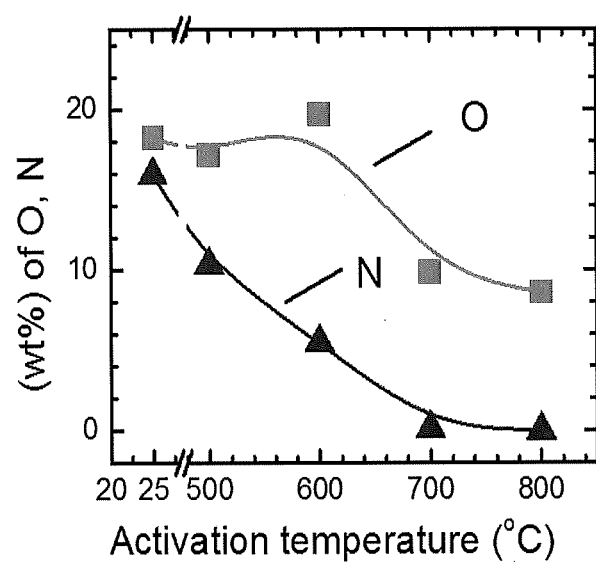


FIG. 7H

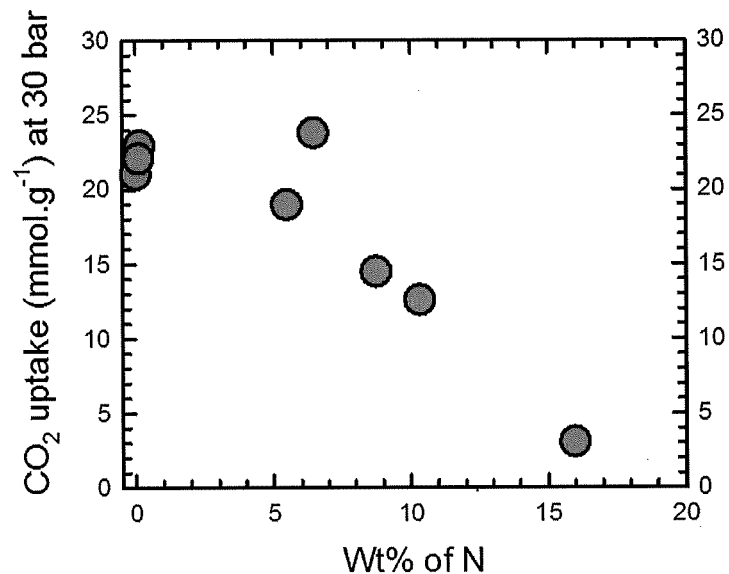


FIG. 8A

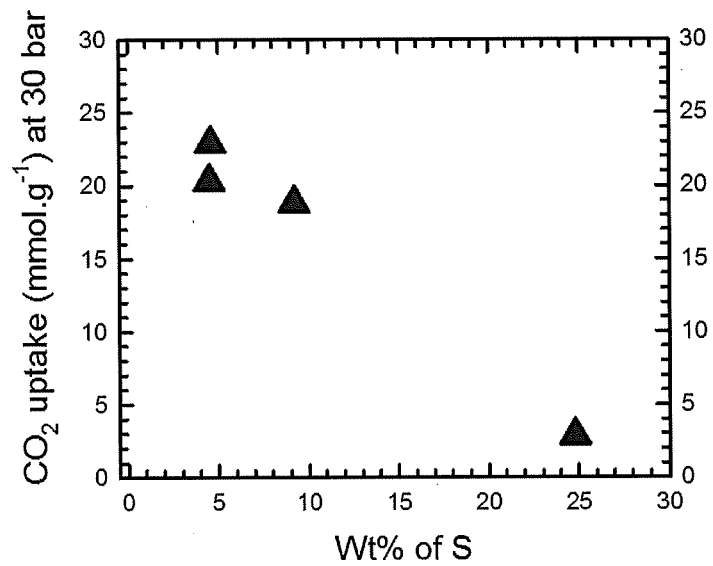
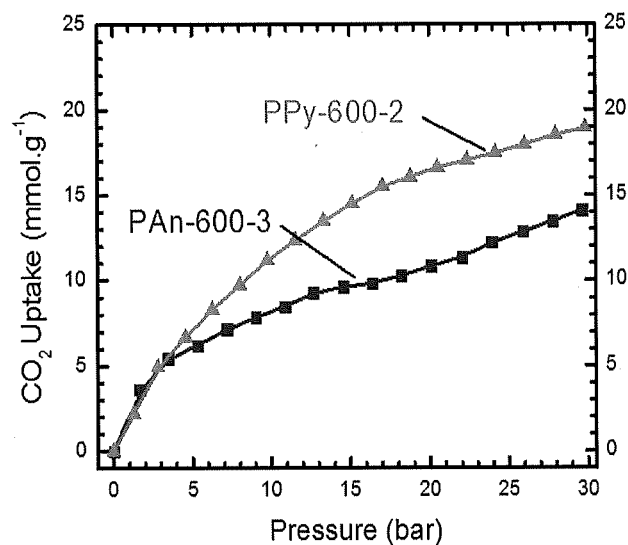
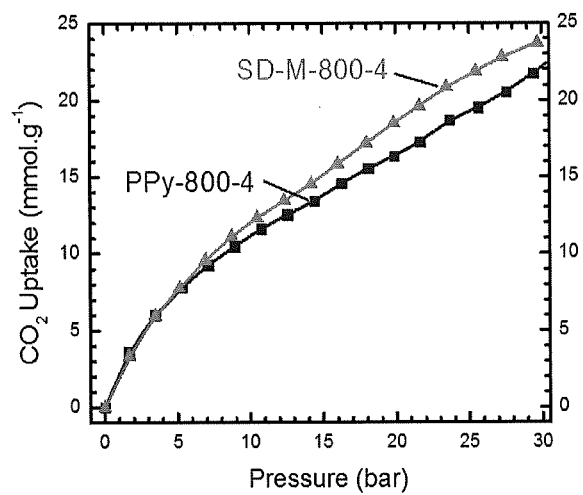


FIG. 8B



**FIG. 8C**



**FIG. 8D**

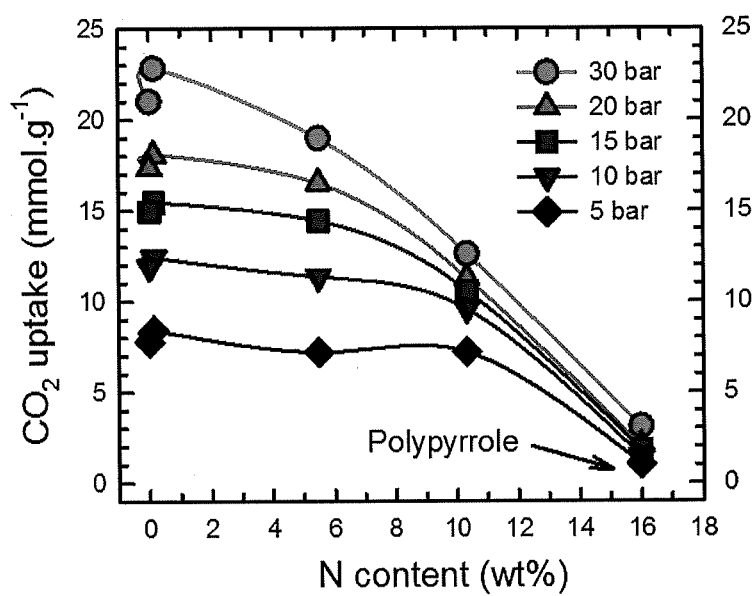


FIG. 8E

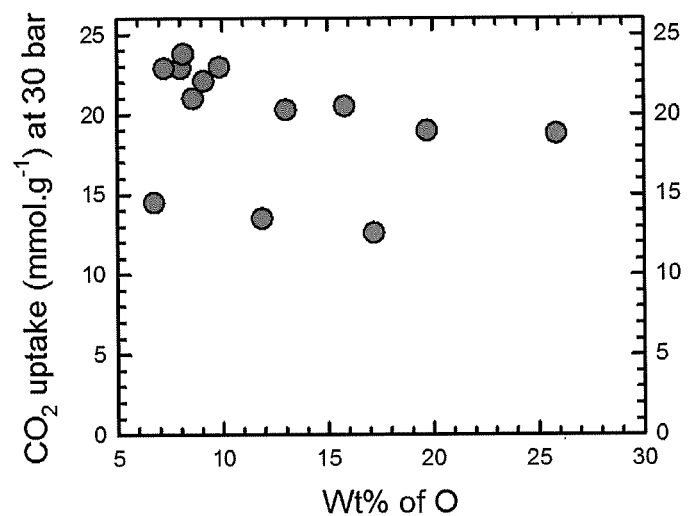


FIG. 9A

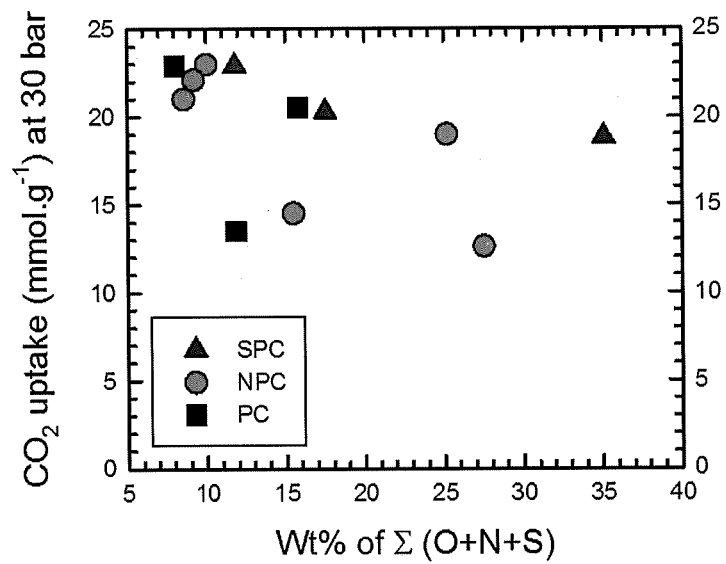
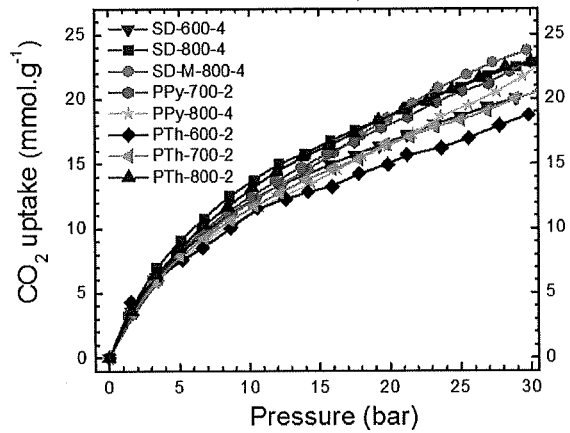
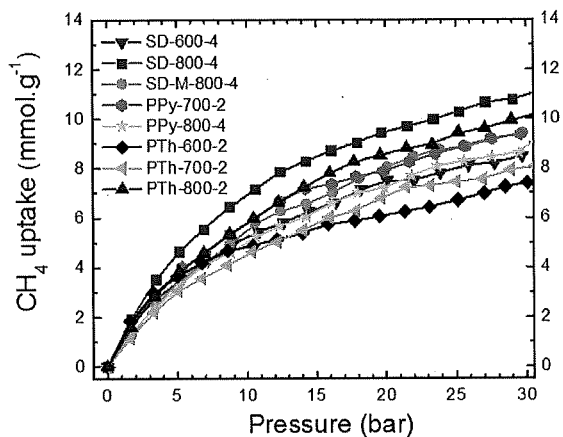


FIG. 9B



**FIG. 10A**



**FIG. 10B**

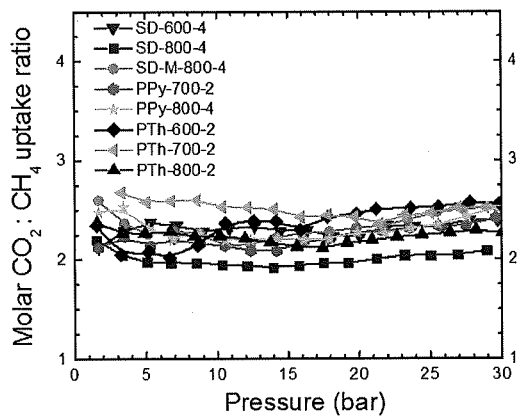


**FIG. 10C**

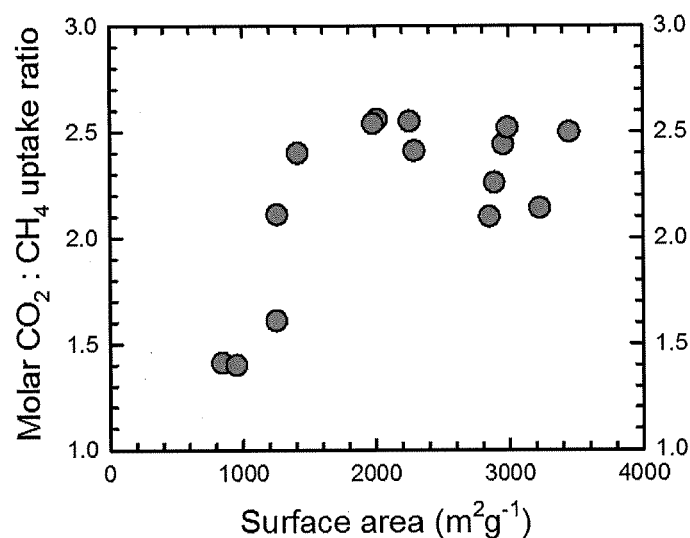


**FIG. 11A**

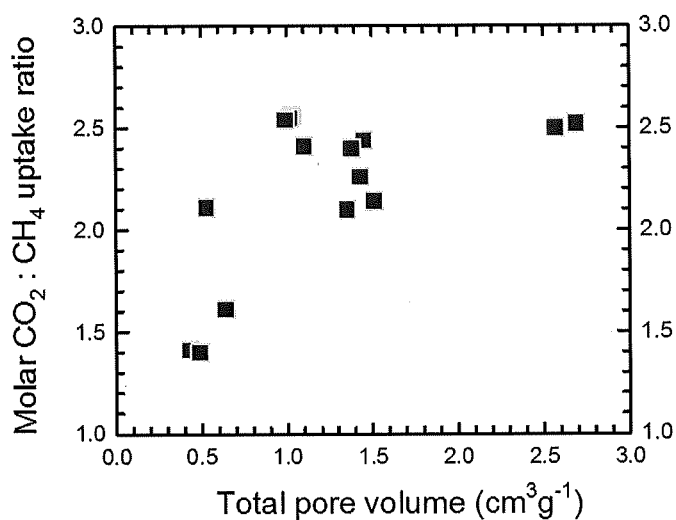


**FIG. 11B**

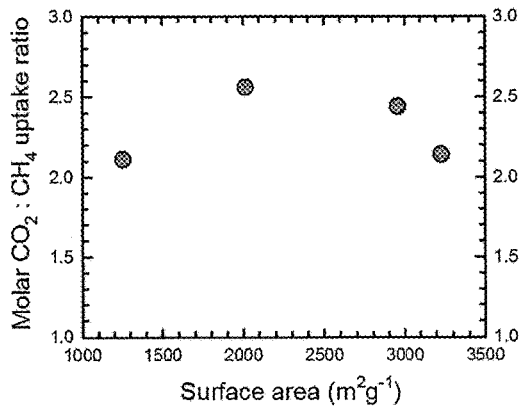


FIG. 12A

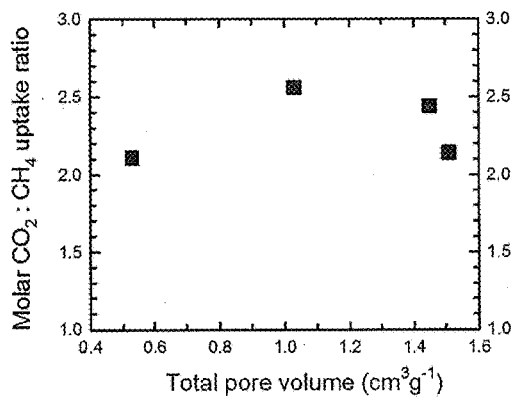


FIG. 12B

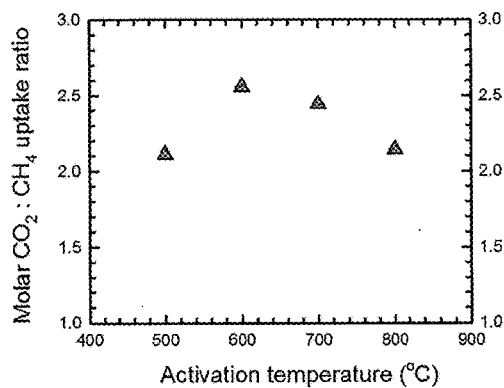


FIG. 12C

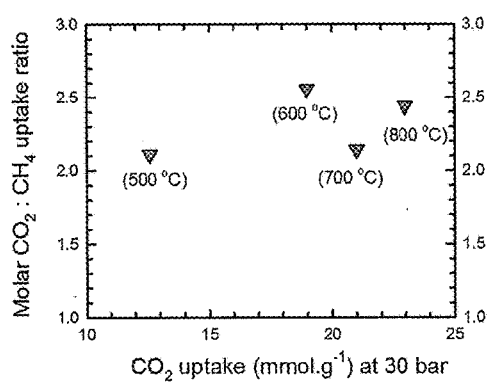


FIG. 12D

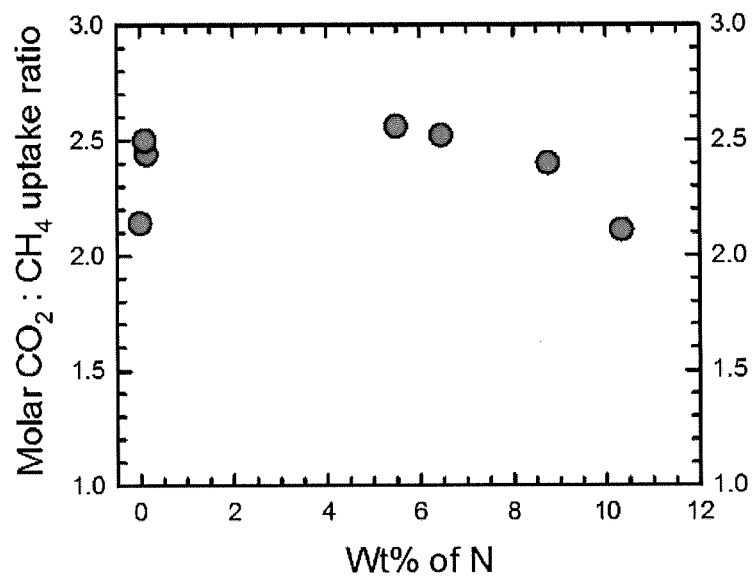


FIG. 13

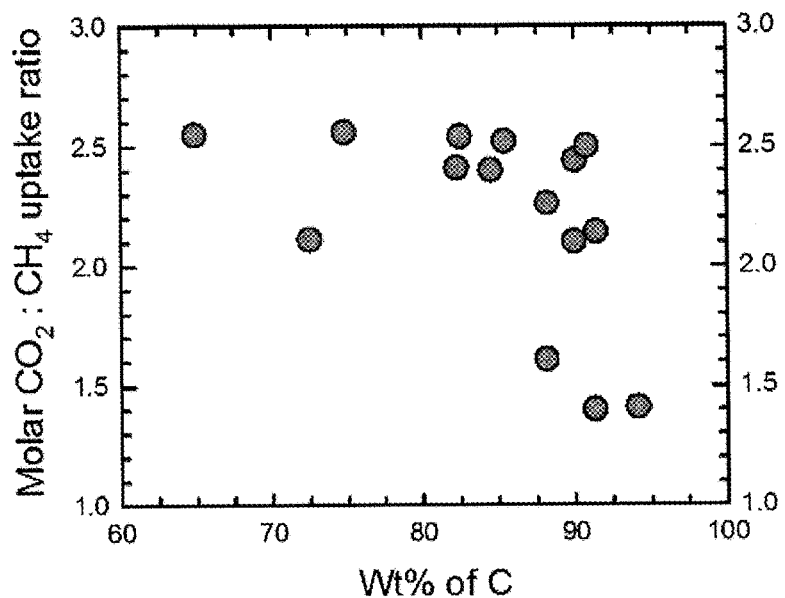


FIG. 14

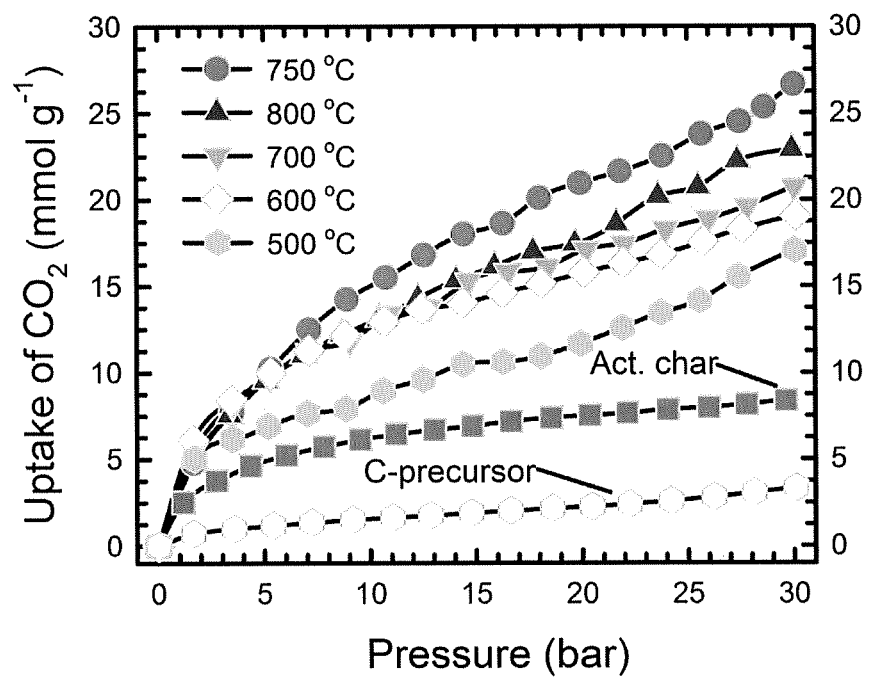


FIG. 15

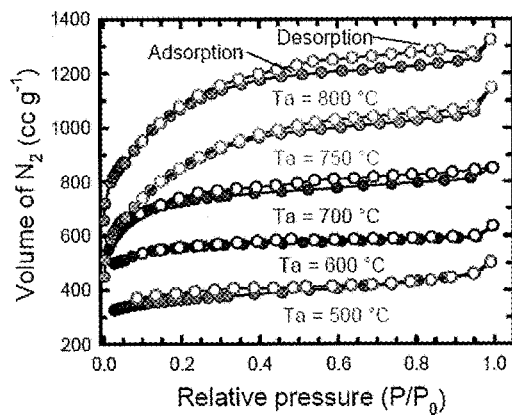


FIG. 16A

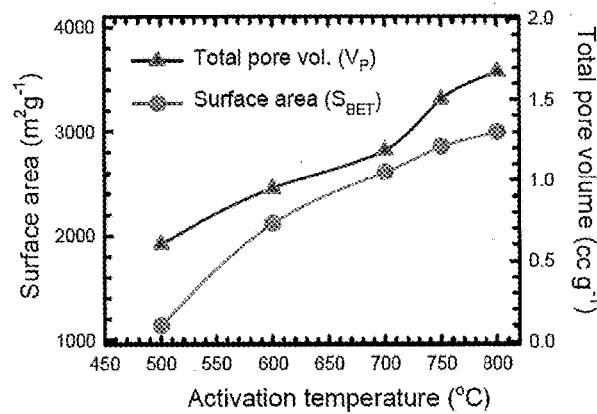


FIG. 16B

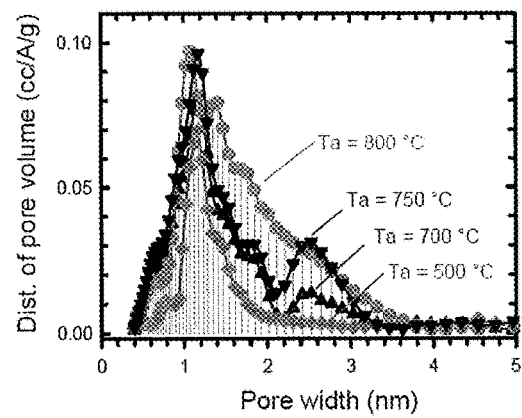


FIG. 16C

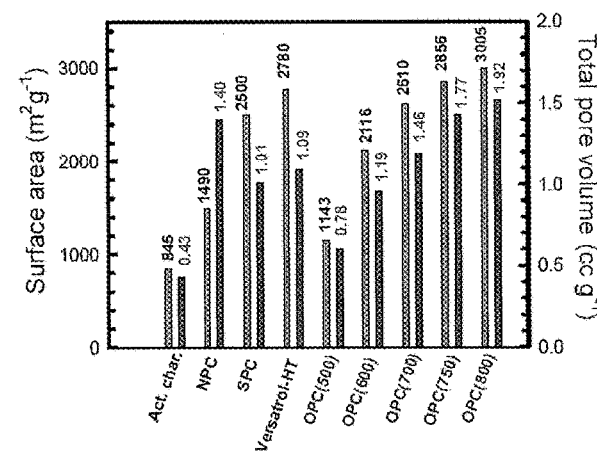


FIG. 16D

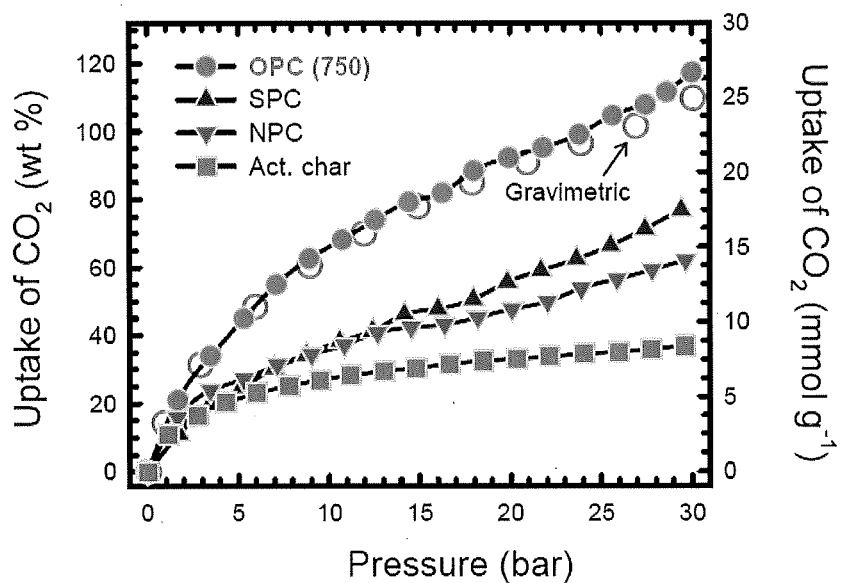


FIG. 17A

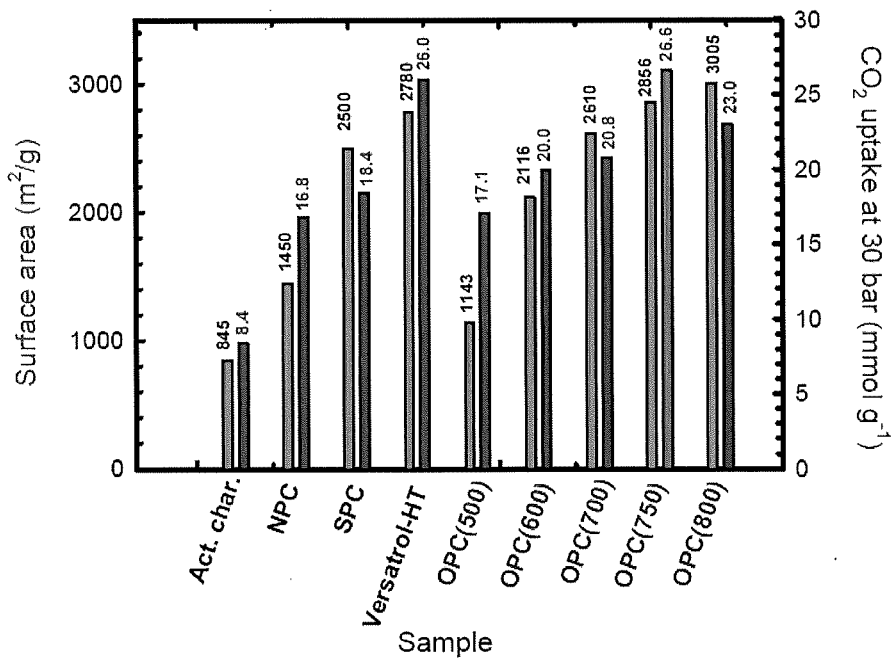


FIG. 17B

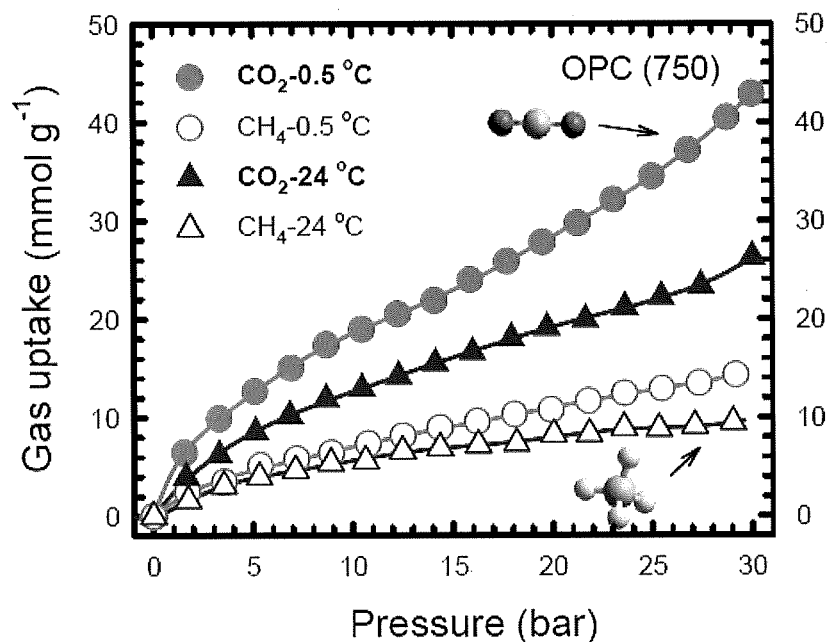


FIG. 18A

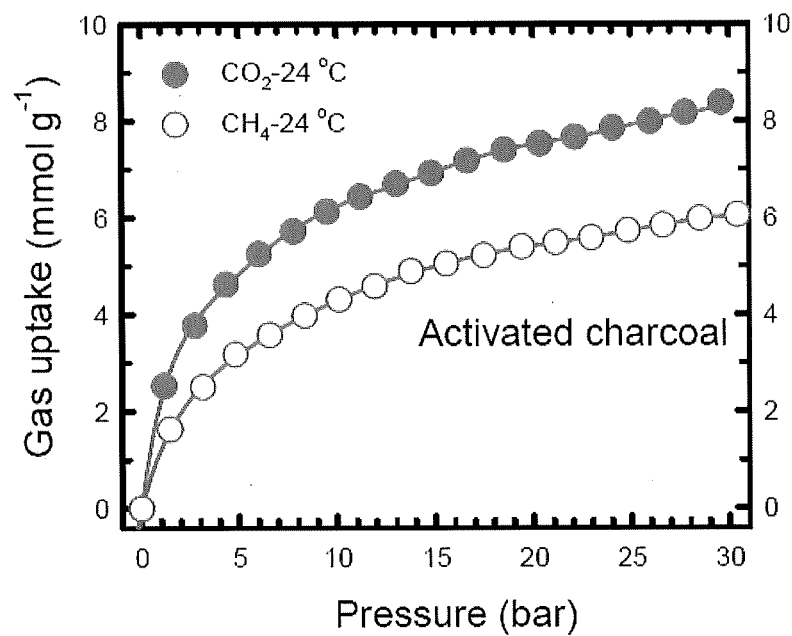


FIG. 18B

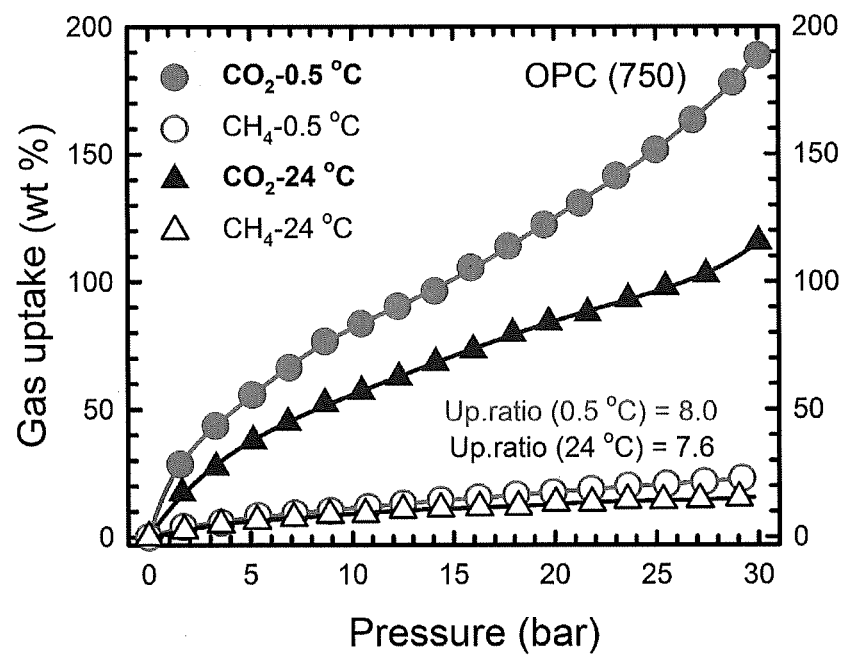
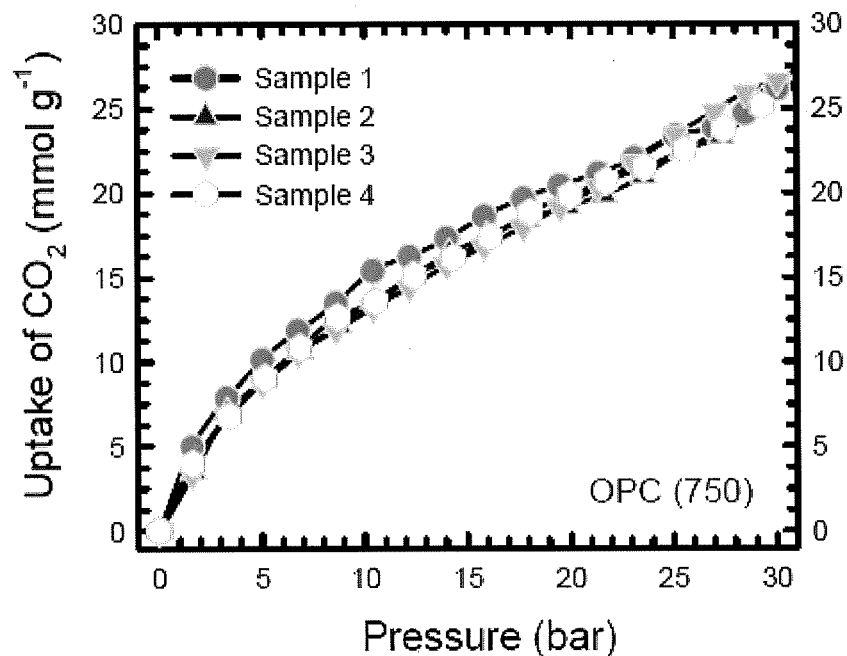
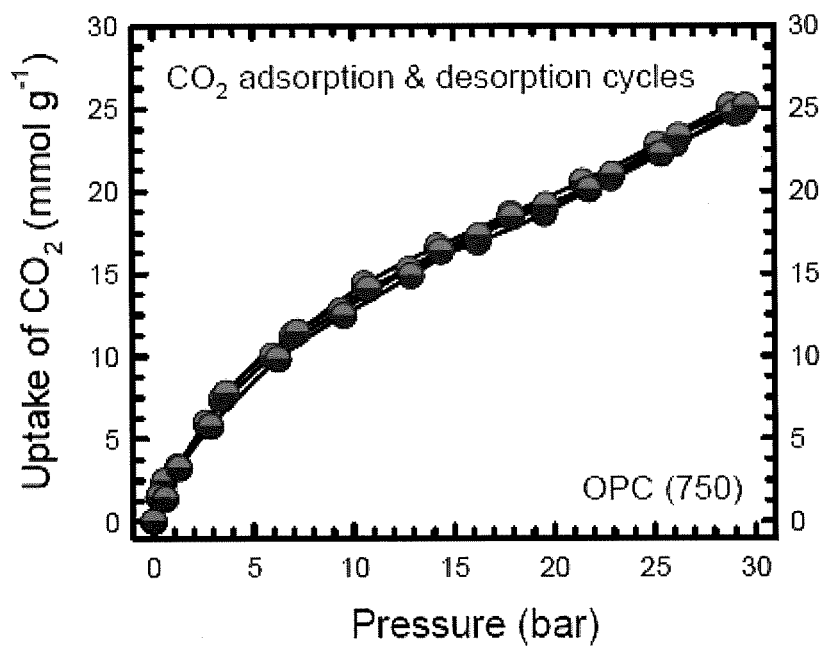


FIG. 19



**FIG. 20A**



**FIG. 20B**

## Synthesis scheme for OPC

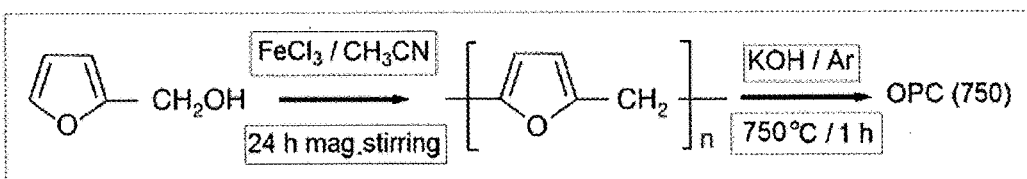
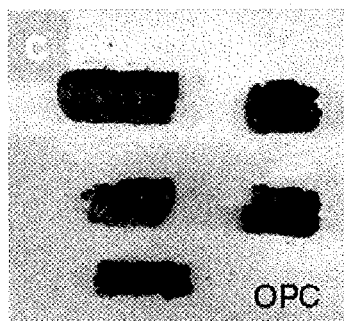


FIG. 21A



A dark, irregularly shaped ink blot on a white background.

FIG. 21B



**FIG. 21C**

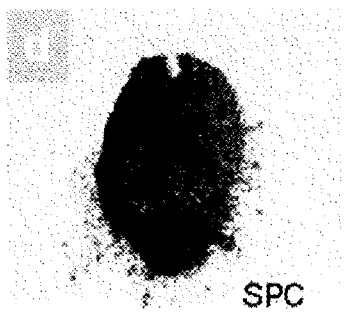


FIG. 21D

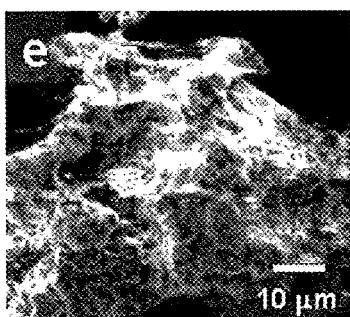


FIG. 21E

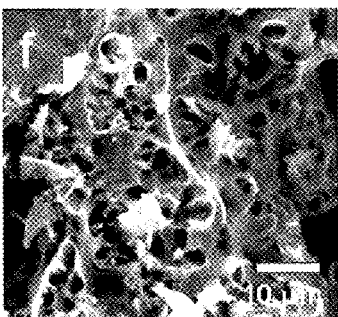


FIG. 21F

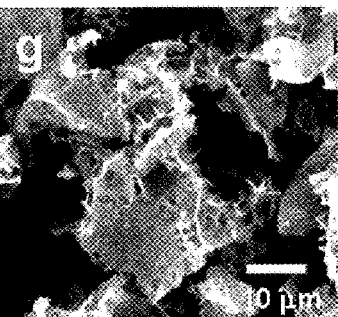


FIG. 21G

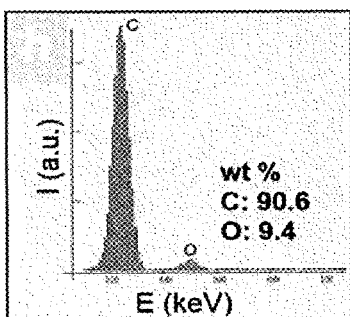


FIG. 21H

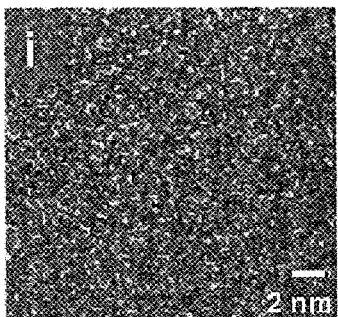


FIG. 21I

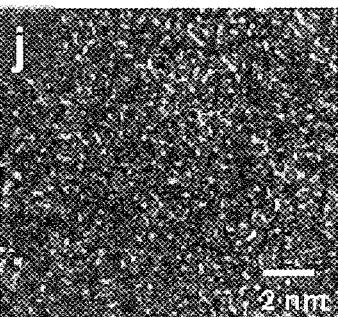


FIG. 21J

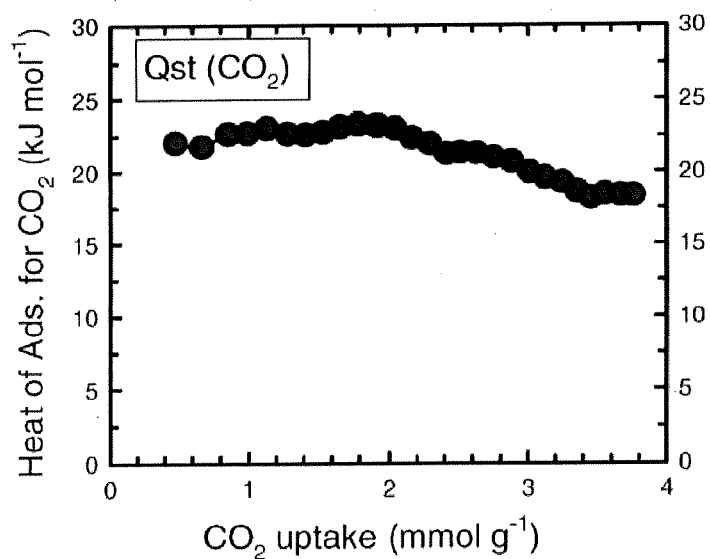


FIG. 22A

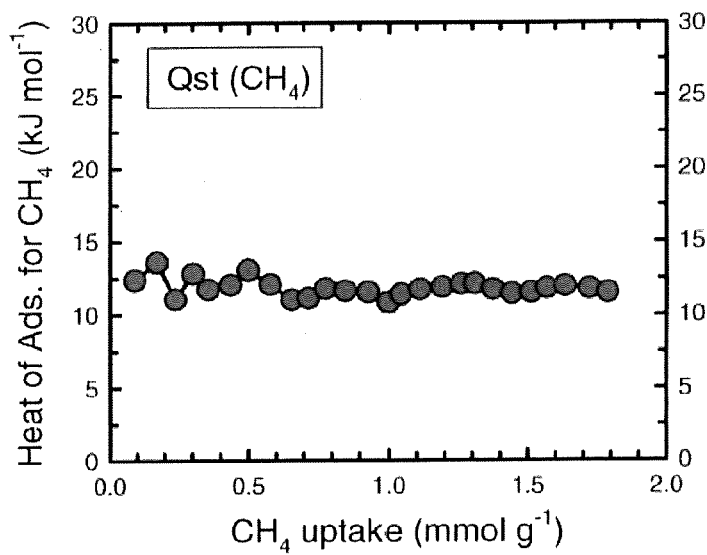


FIG. 22B

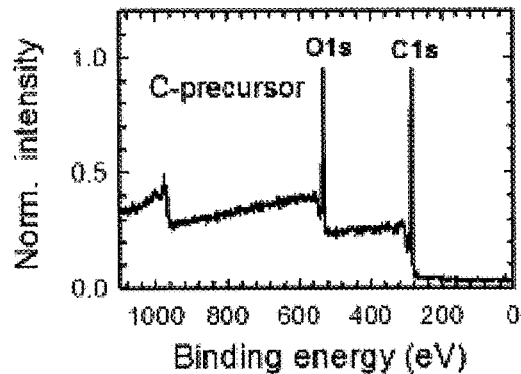


FIG. 23A

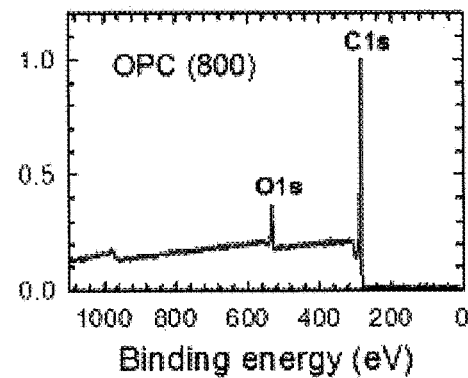


FIG. 23B

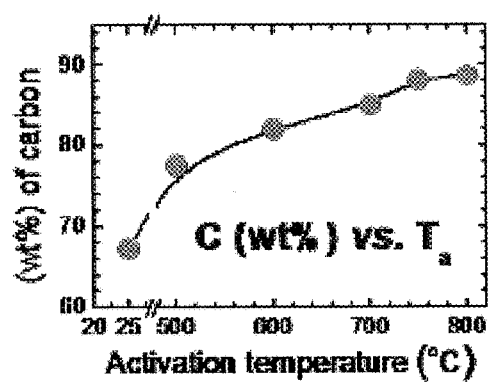


FIG. 23C

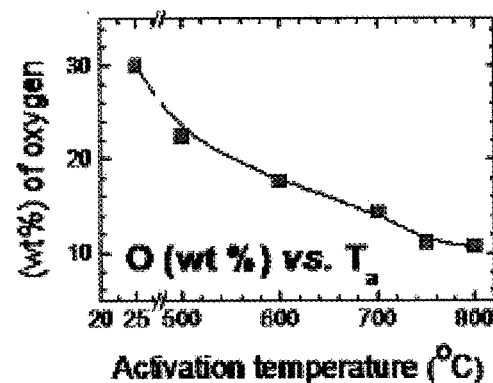


FIG. 23D

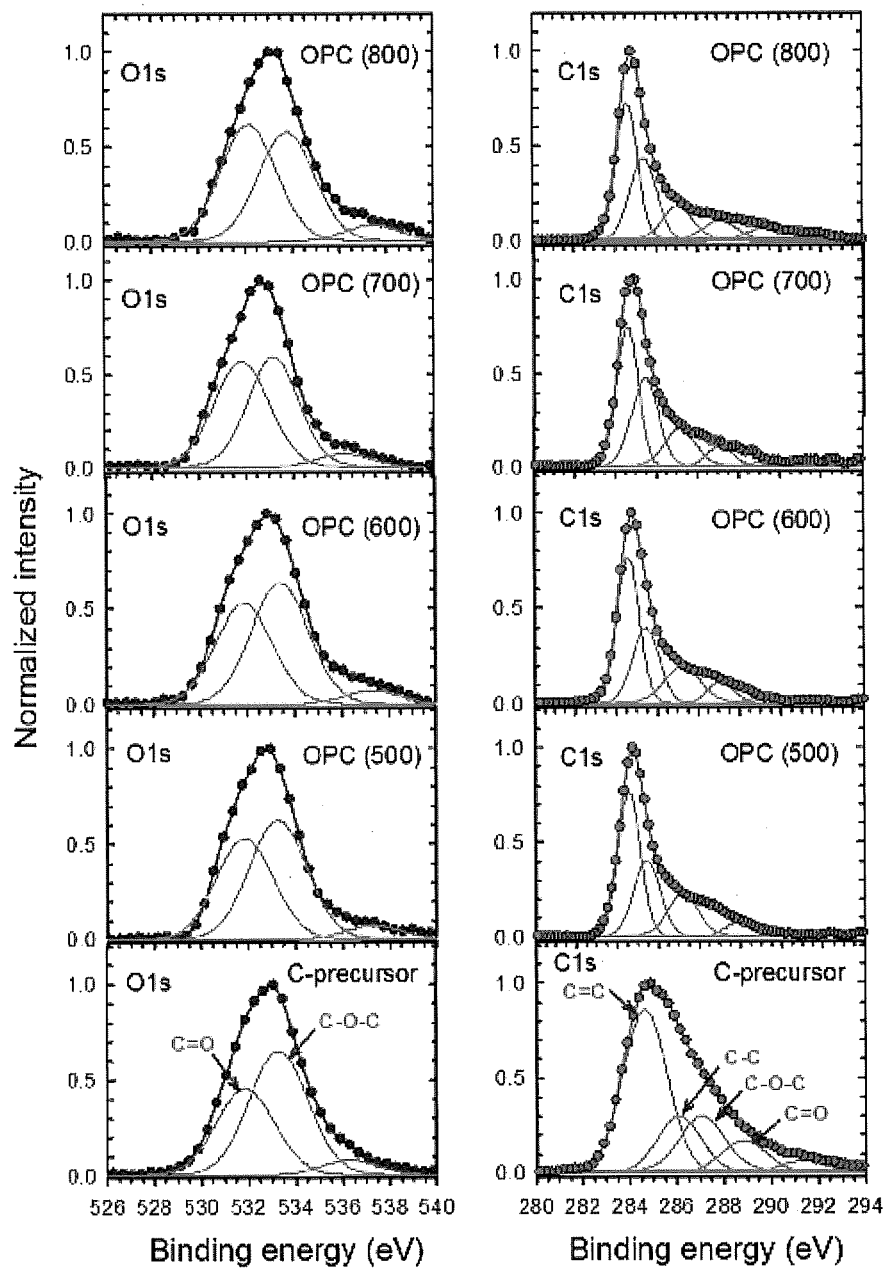


FIG. 23E

FIG. 23F

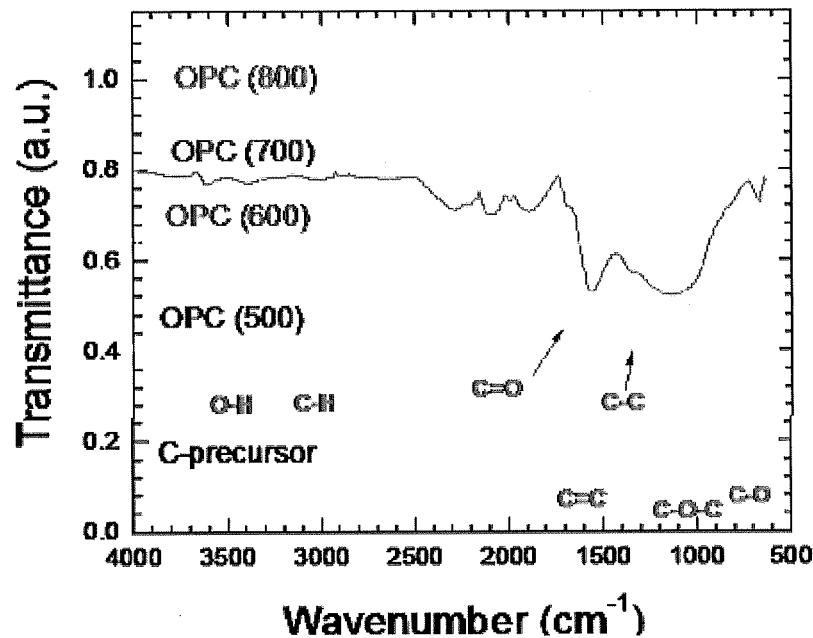


FIG. 23G

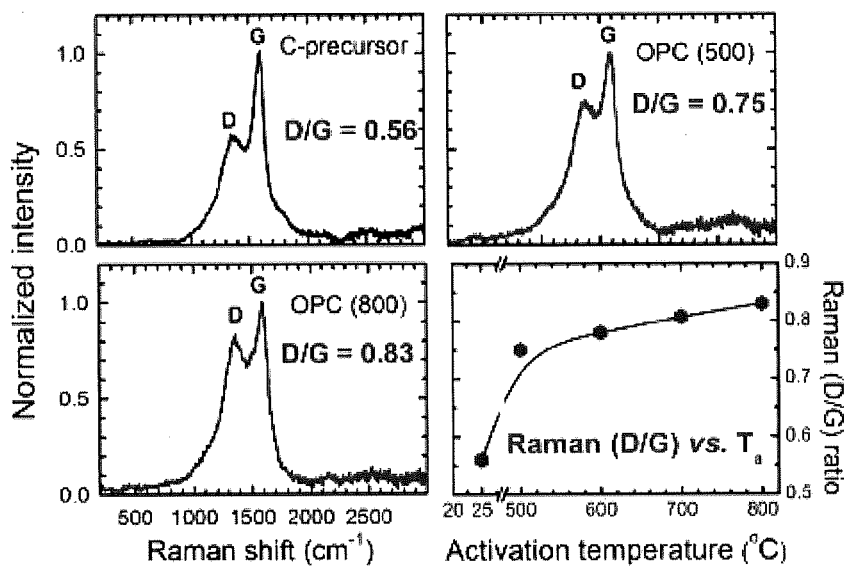


FIG. 23H

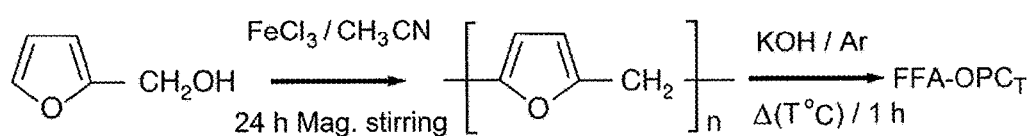


FIG. 24A

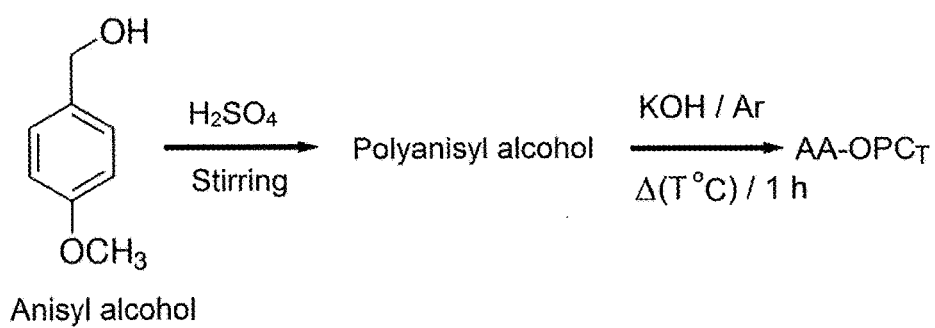
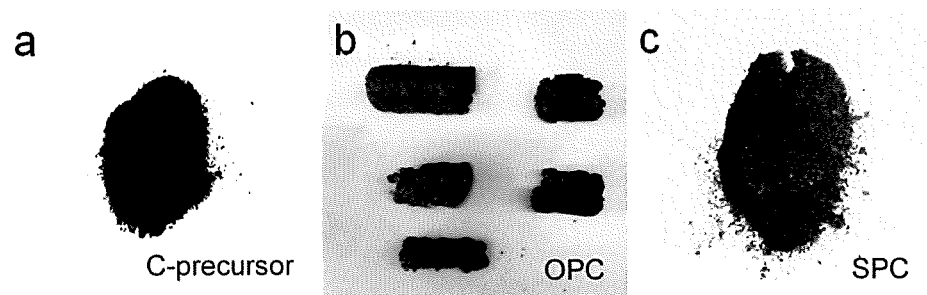


FIG. 24B



**FIG. 25A**

**FIG. 25B**

**FIG. 25C**

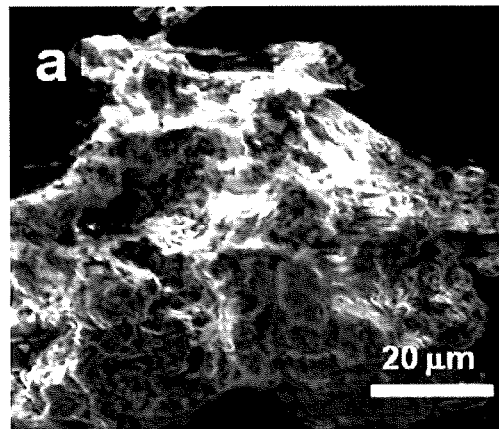


FIG. 26A

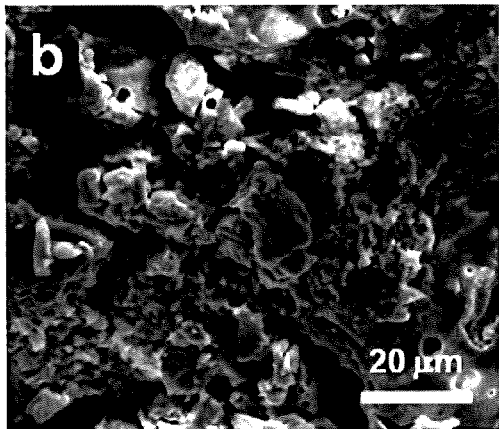


FIG. 26B

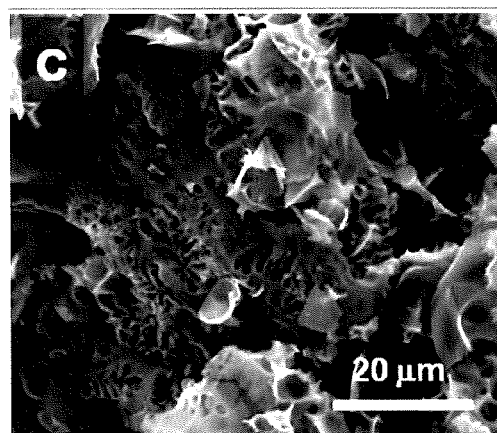


FIG. 26C

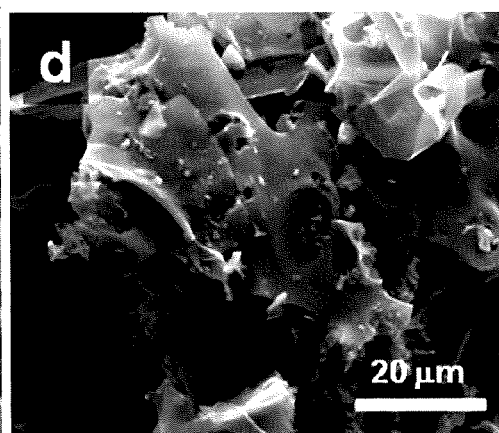
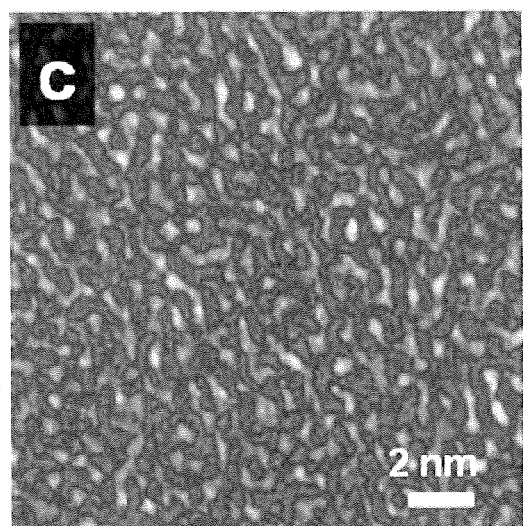
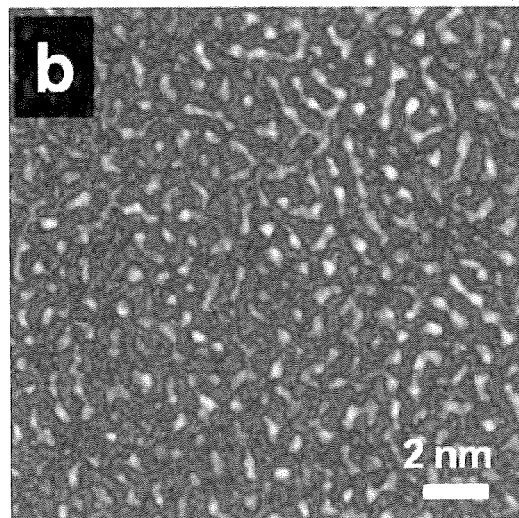
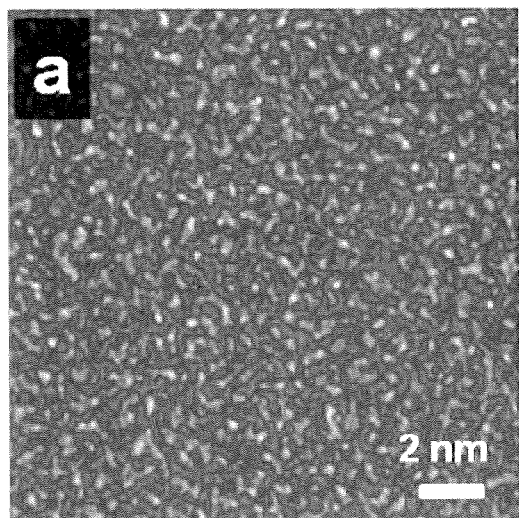


FIG. 26D



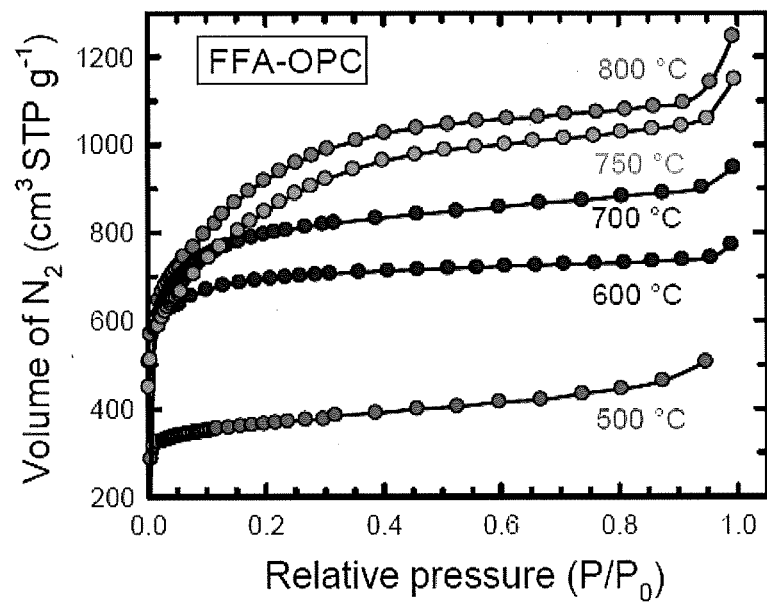


FIG. 28A

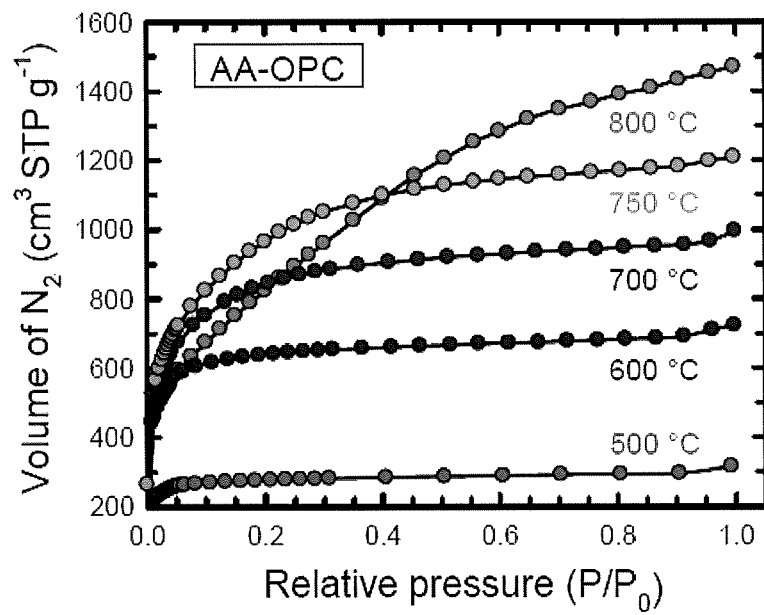


FIG. 28B

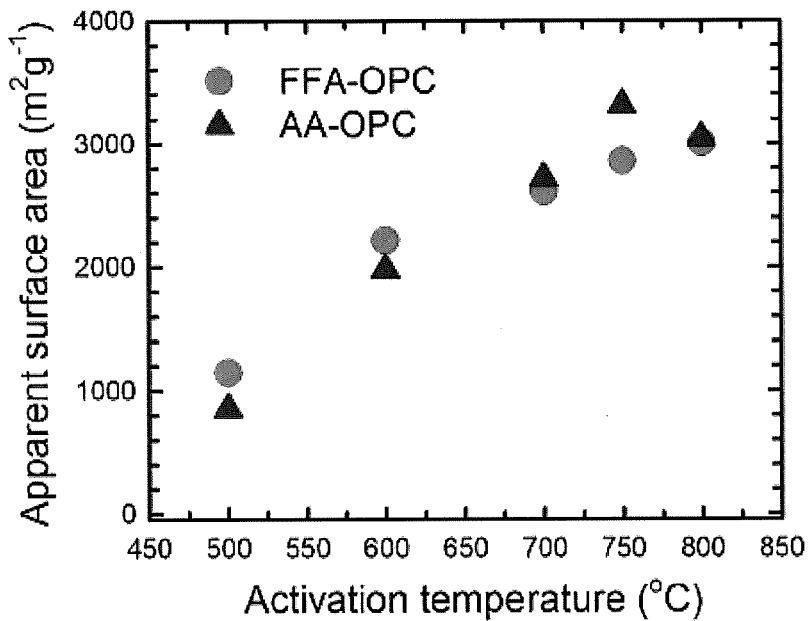


FIG. 29A

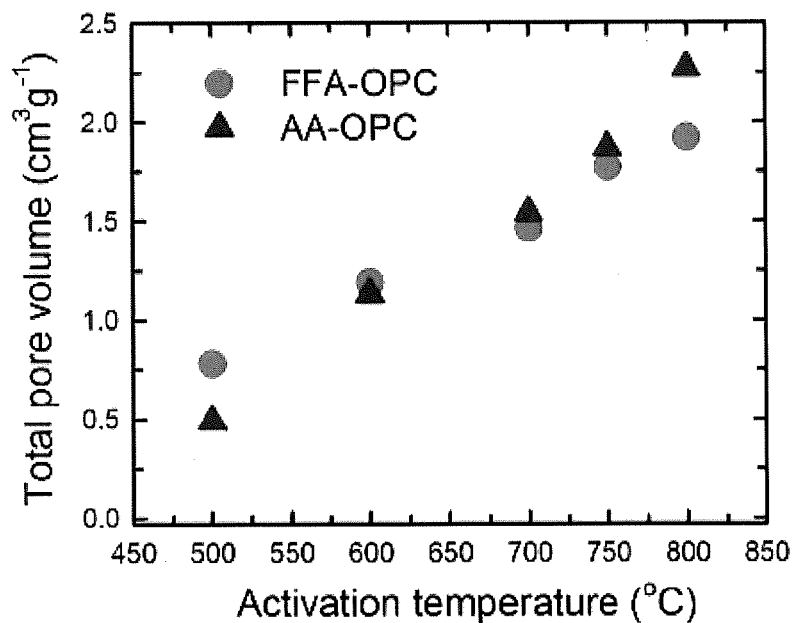


FIG. 29B

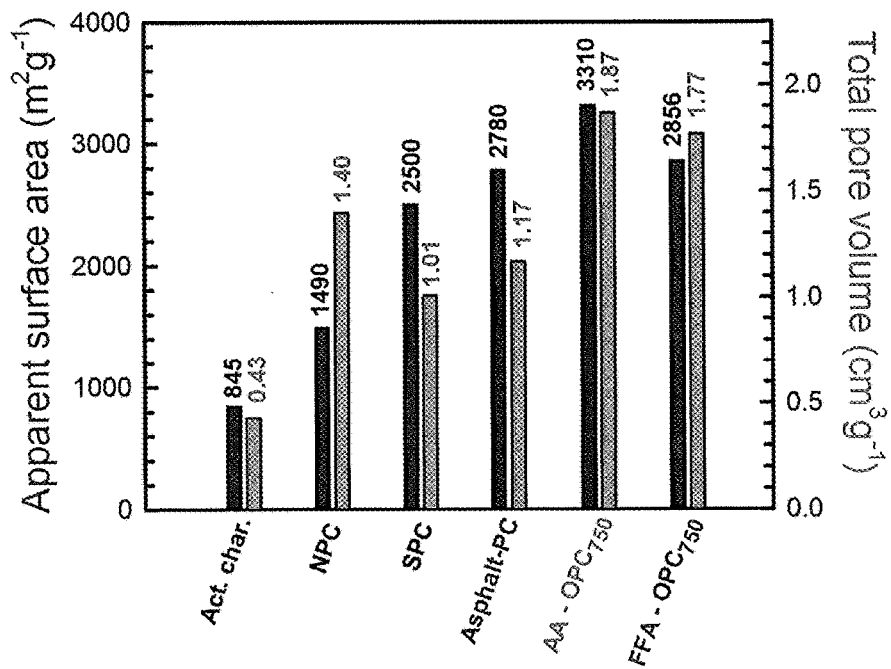


FIG. 30

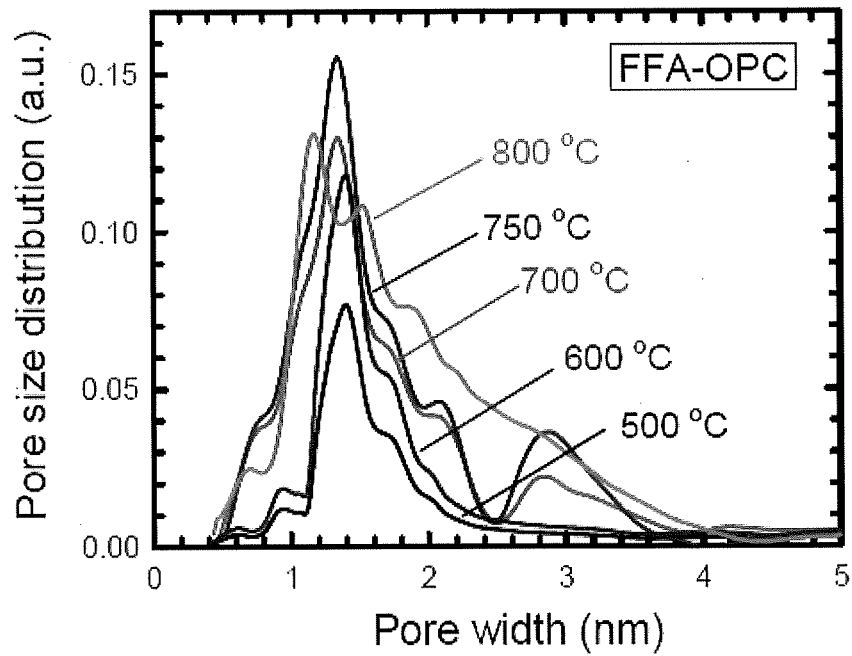


FIG. 31A

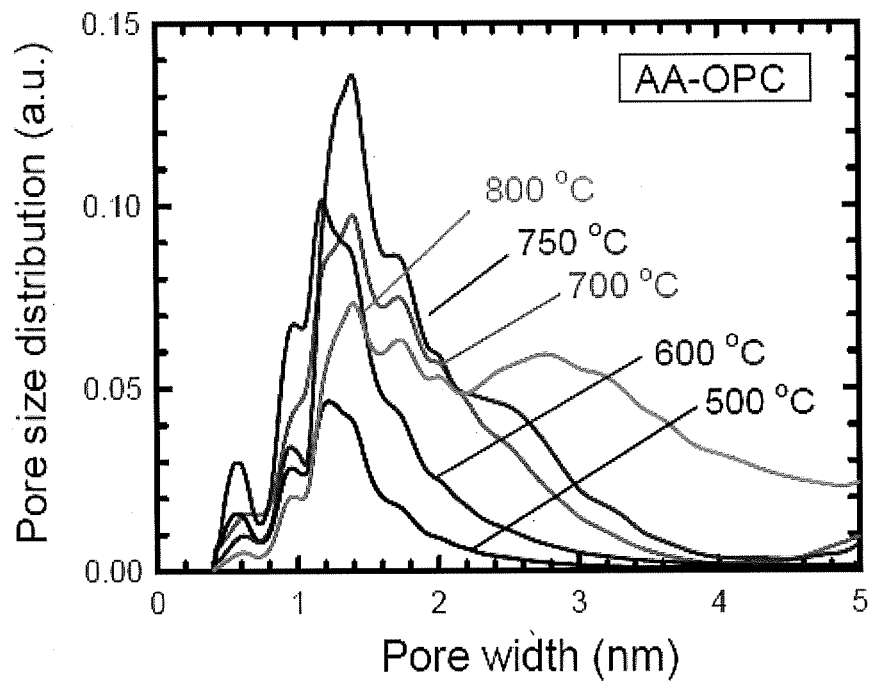


FIG. 31B

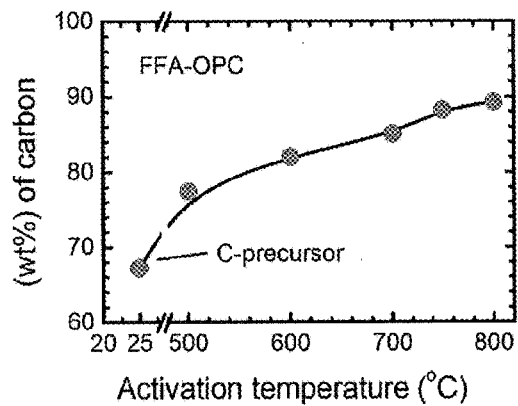


FIG. 32A

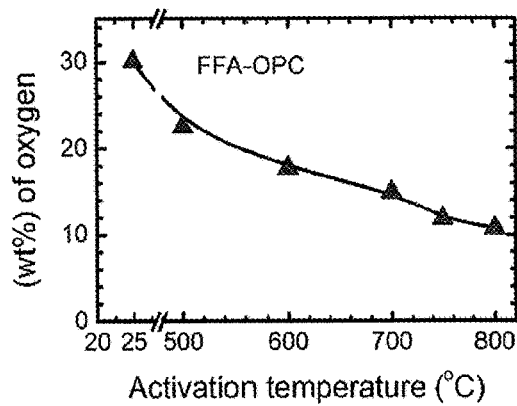


FIG. 32B

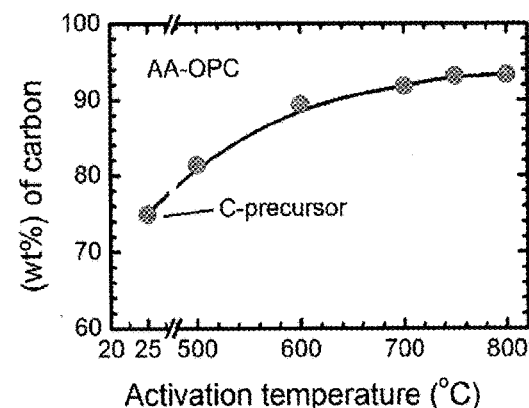


FIG. 32C

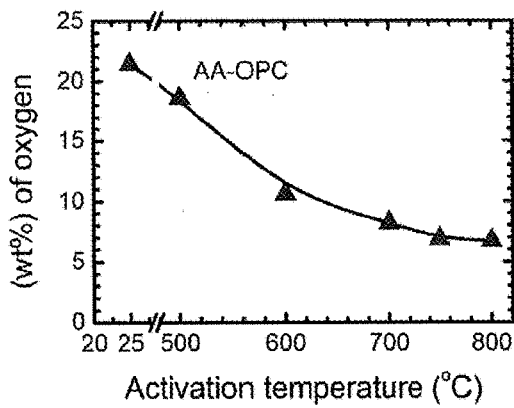


FIG. 32D

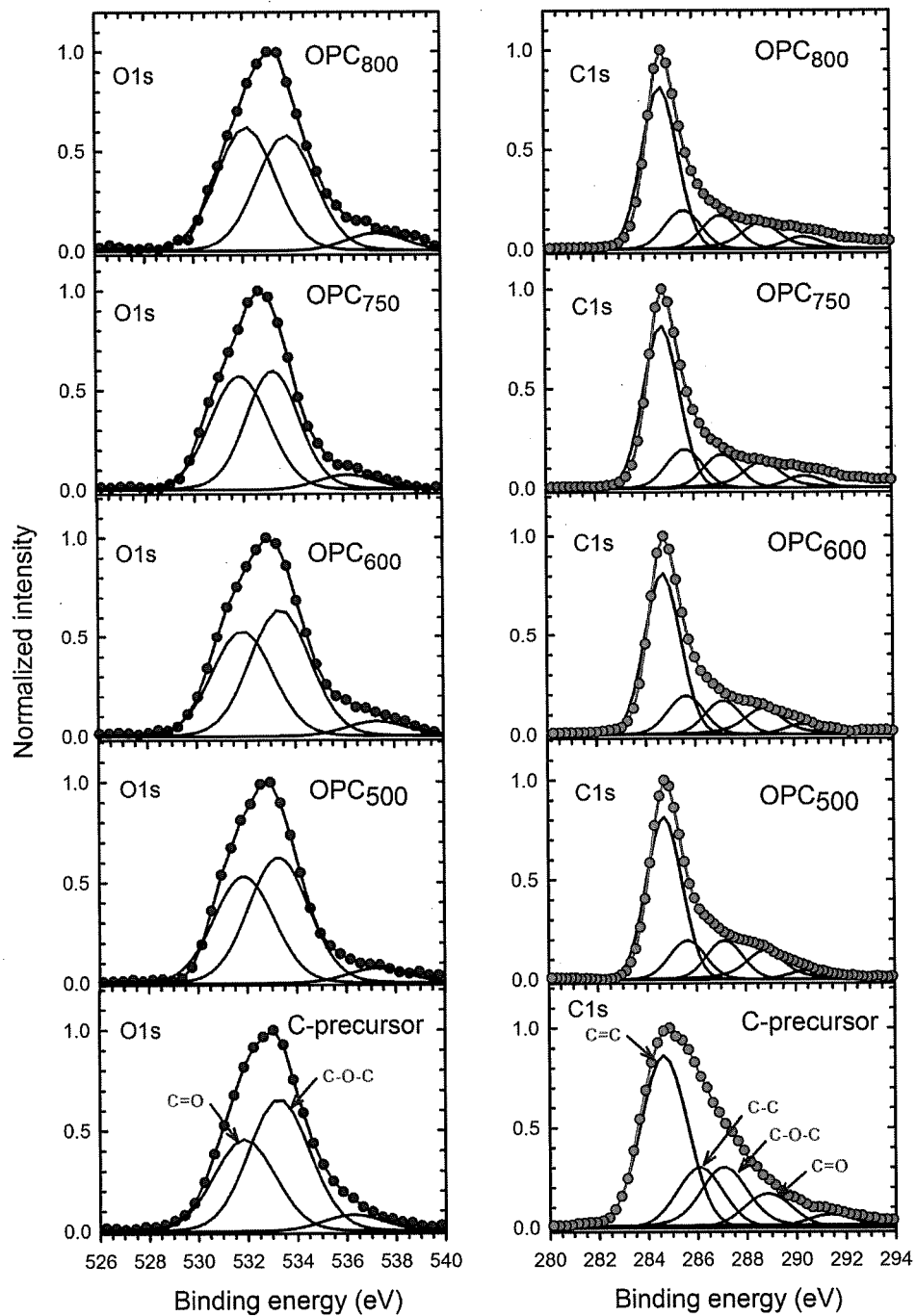


FIG. 33A

FIG. 33B

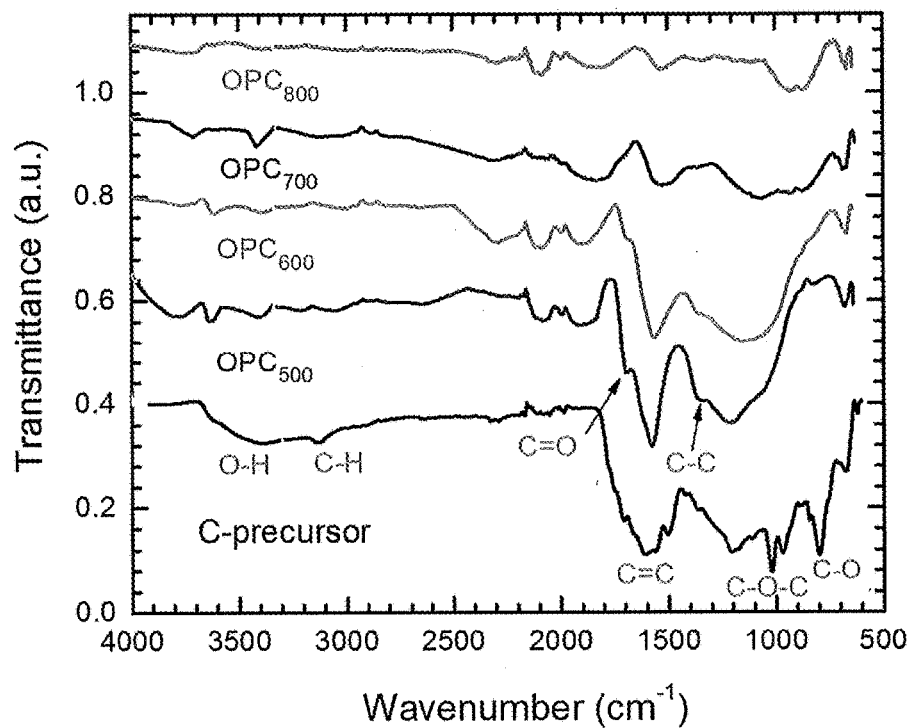


FIG. 34

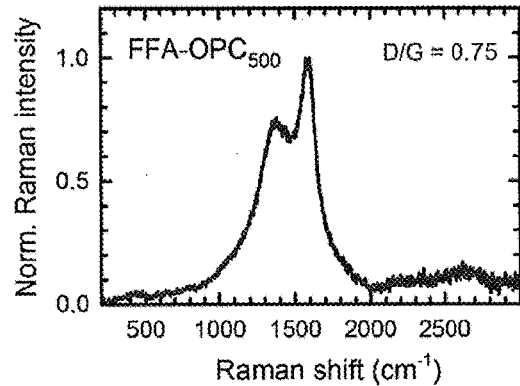
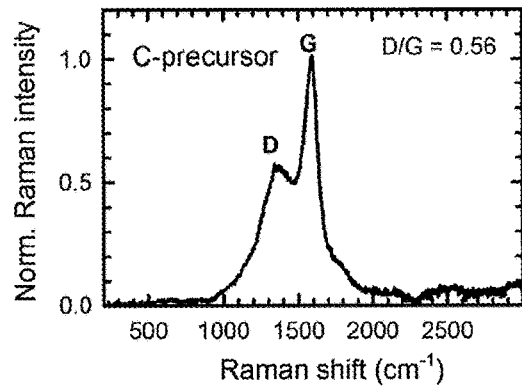


FIG. 35A

FIG. 35B

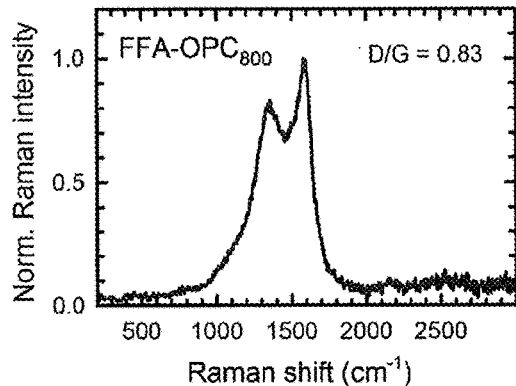


FIG. 35C

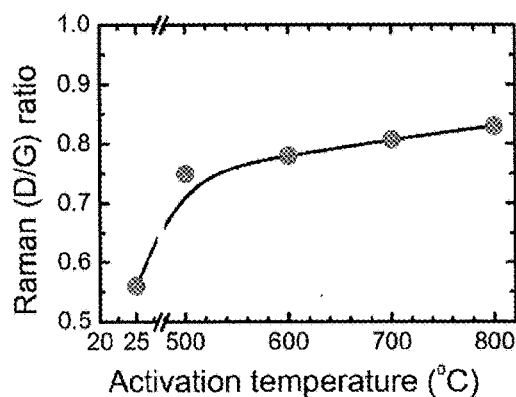


FIG. 35D

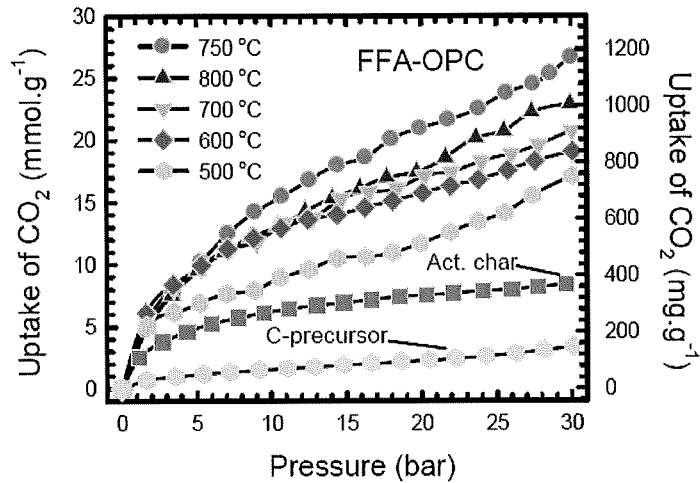


FIG. 36A

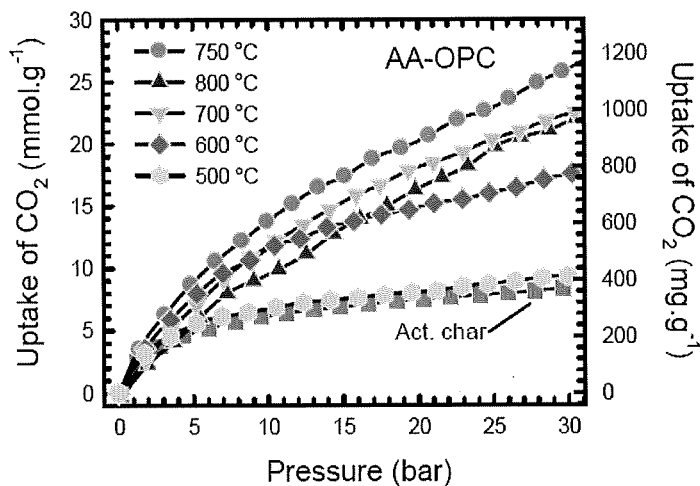


FIG. 36B

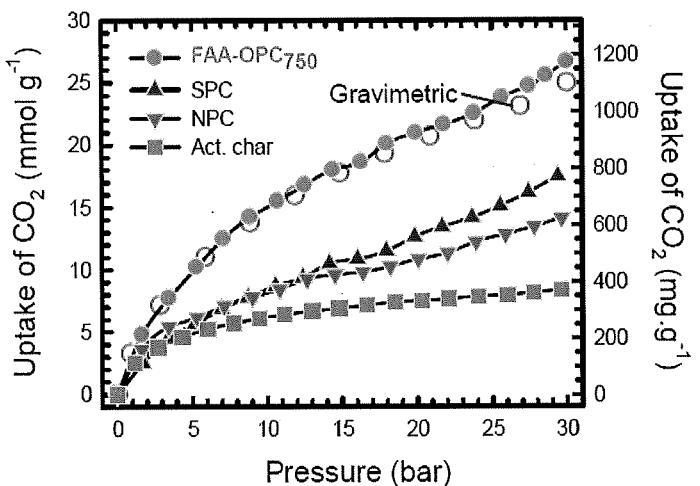


FIG. 36C

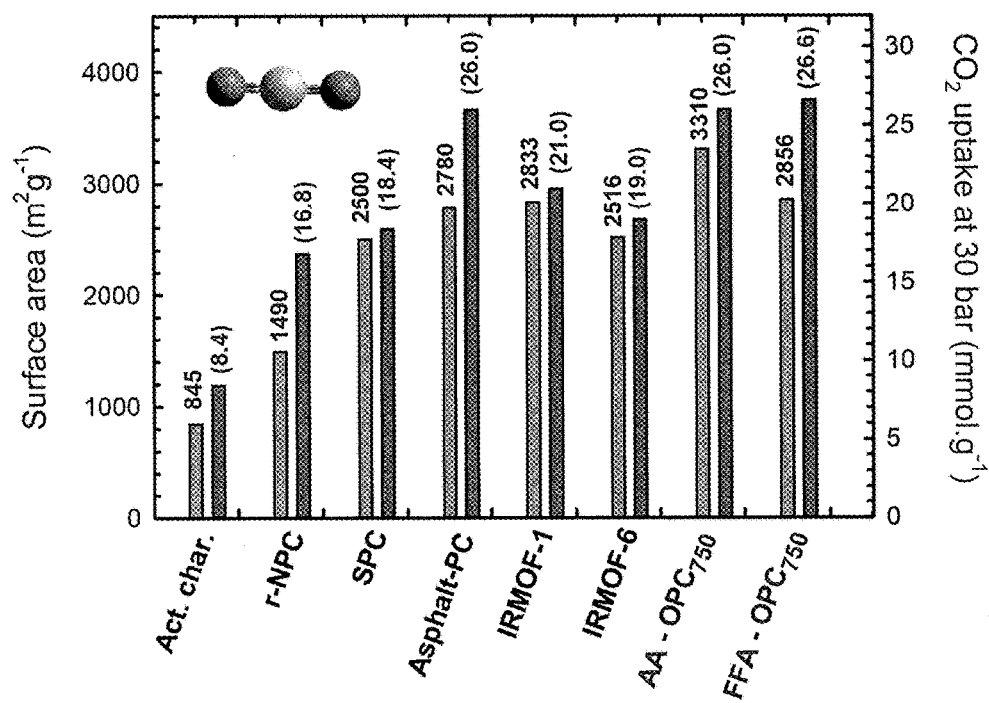


FIG. 37

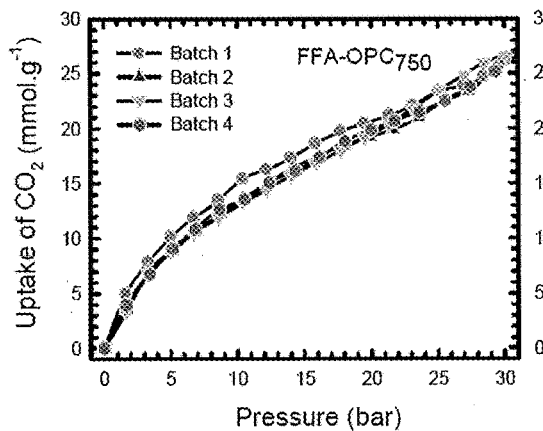


FIG. 38A

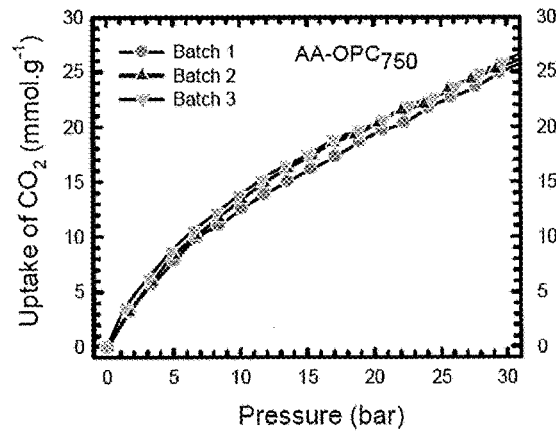


FIG. 38B

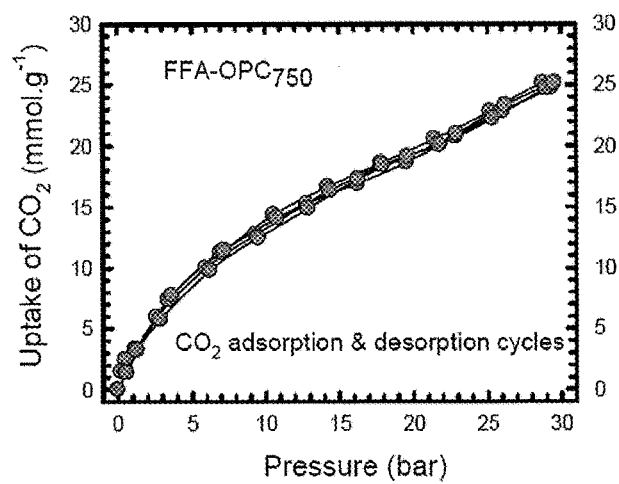


FIG. 38C

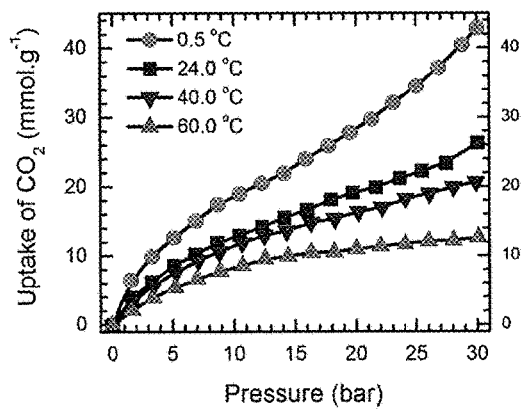


FIG. 39A

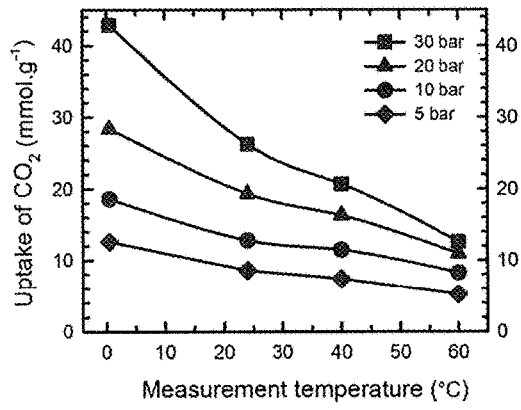


FIG. 39B

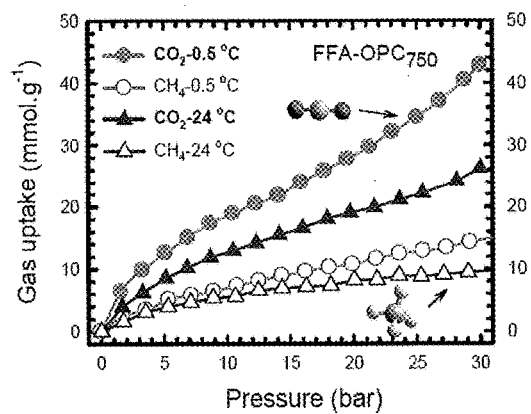


FIG. 40A

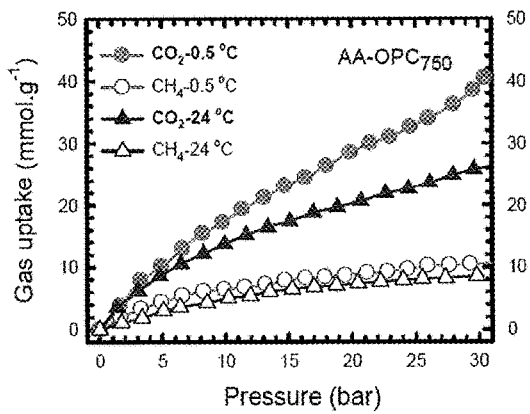


FIG. 40B

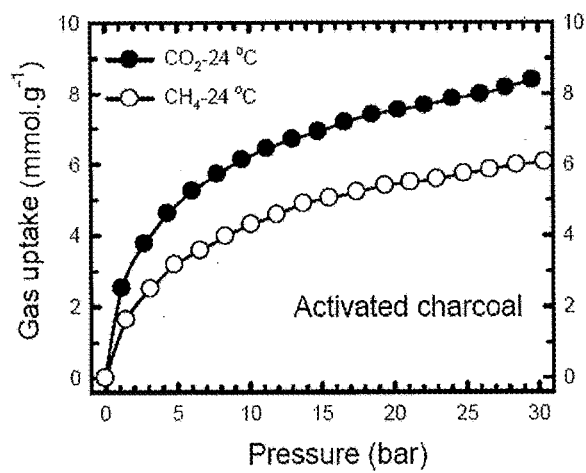


FIG. 40C

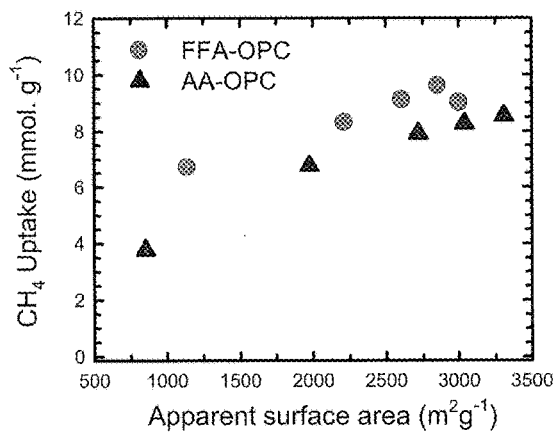


FIG. 41A

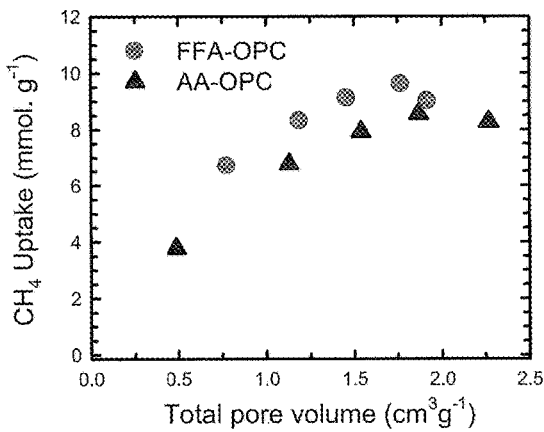


FIG. 41B

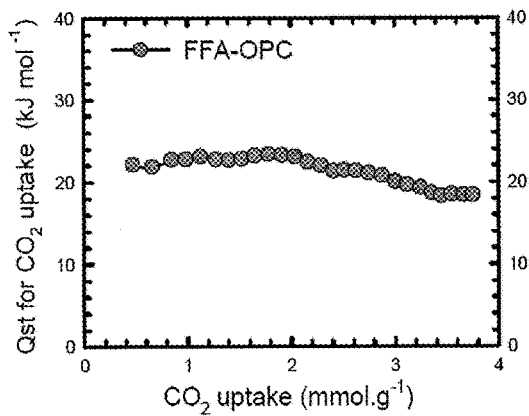


FIG. 42A

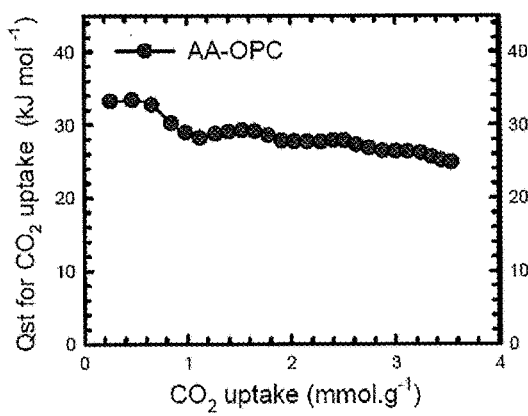


FIG. 42B

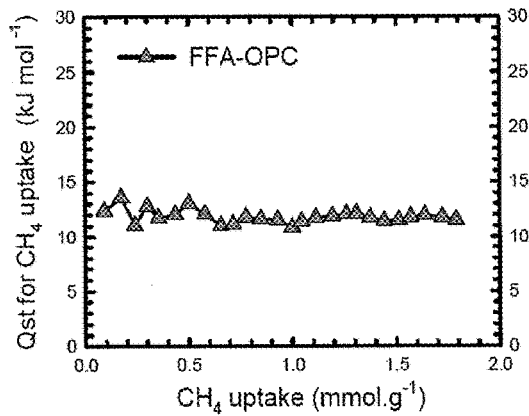


FIG. 42C

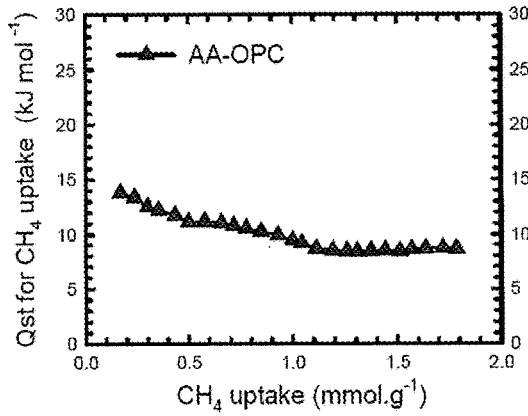


FIG. 42D

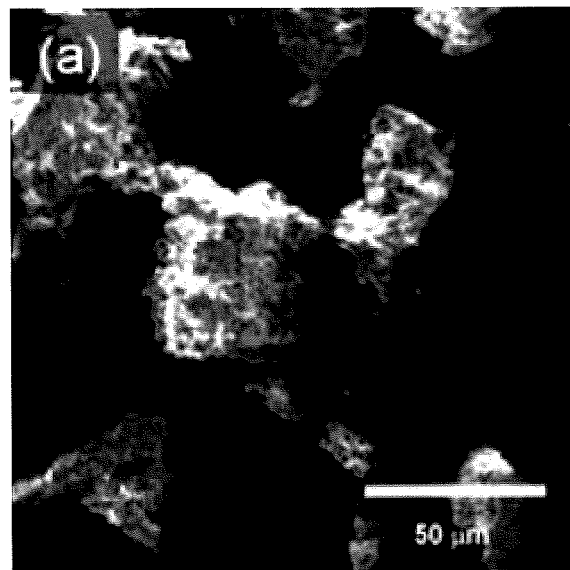


FIG. 43A

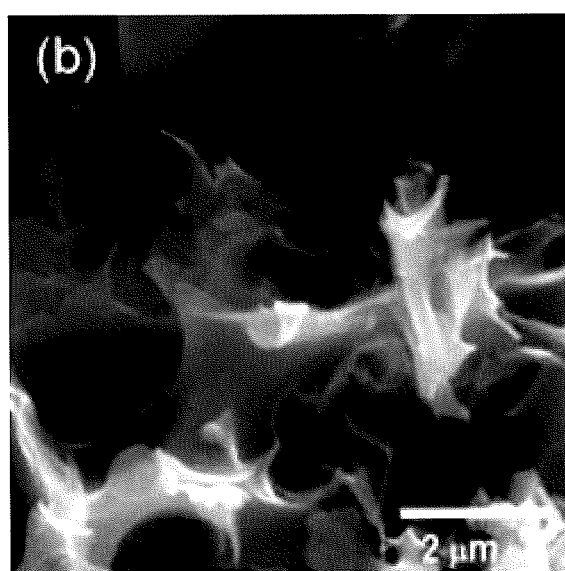


FIG. 43B

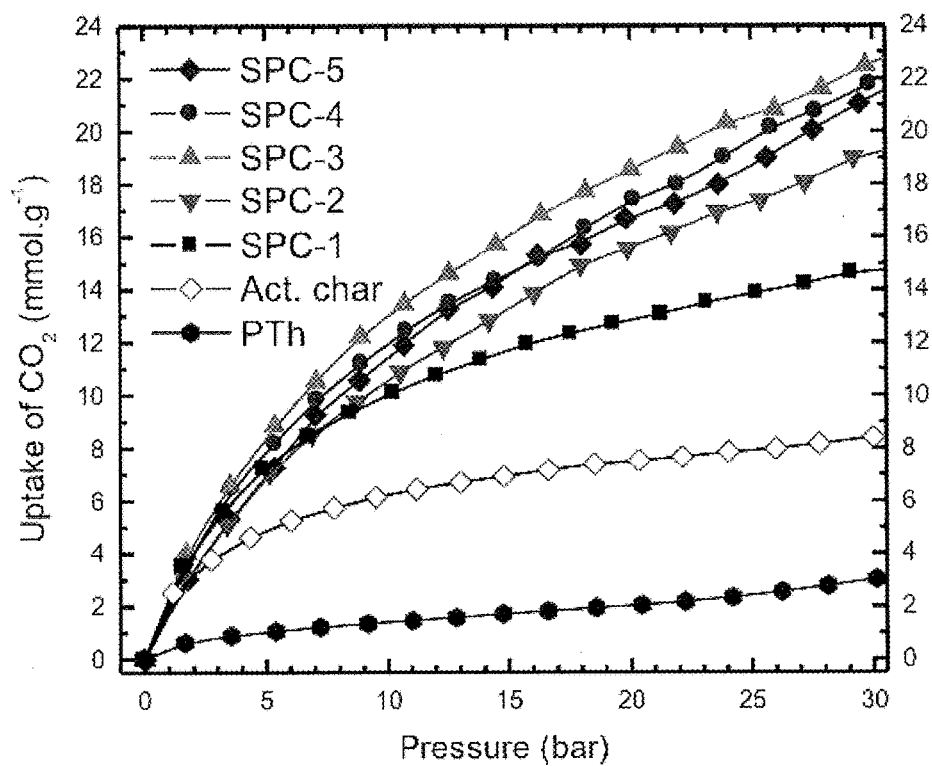


FIG. 44

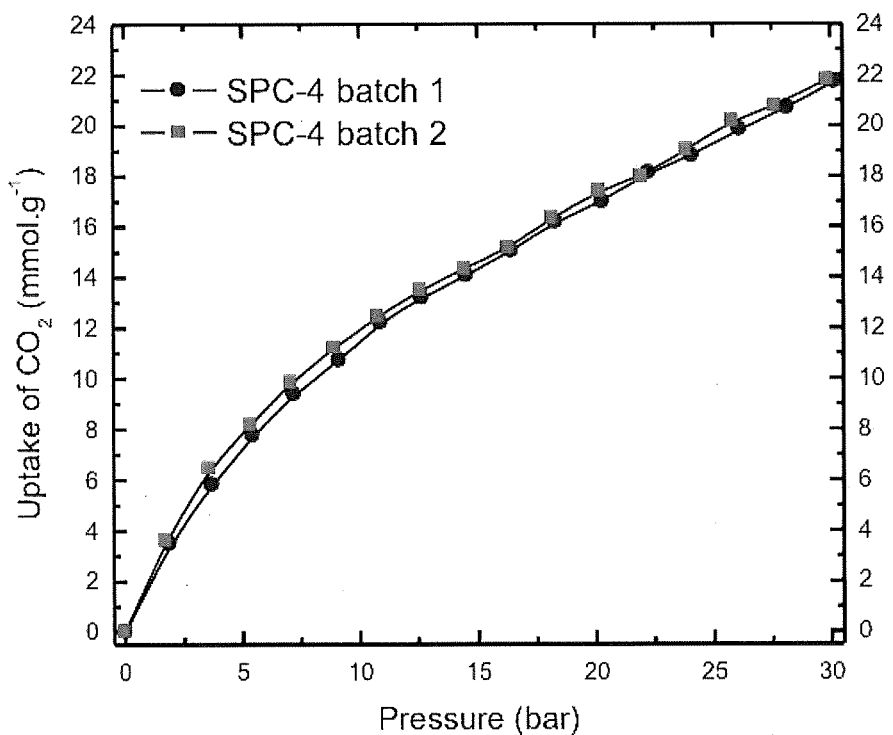


FIG. 45

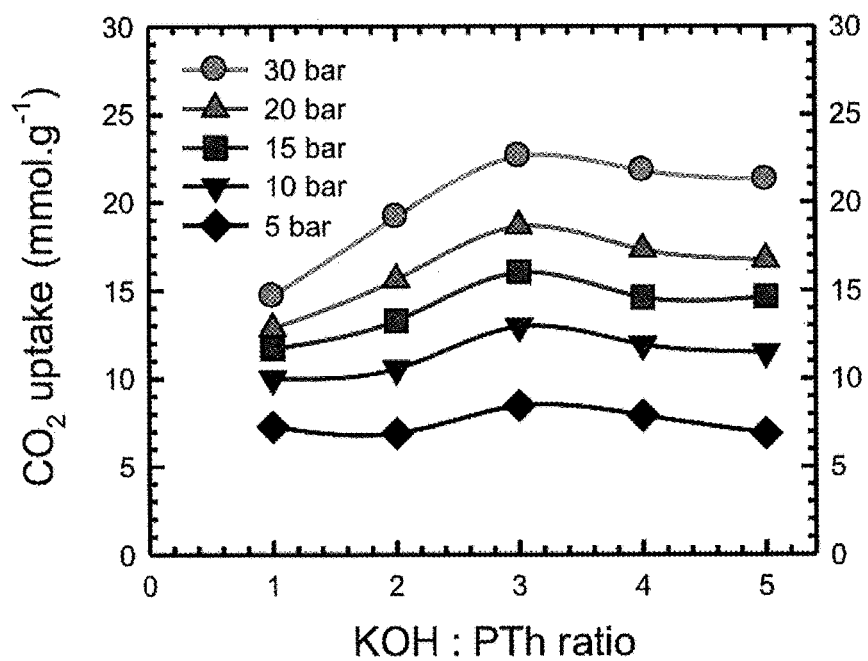


FIG. 46

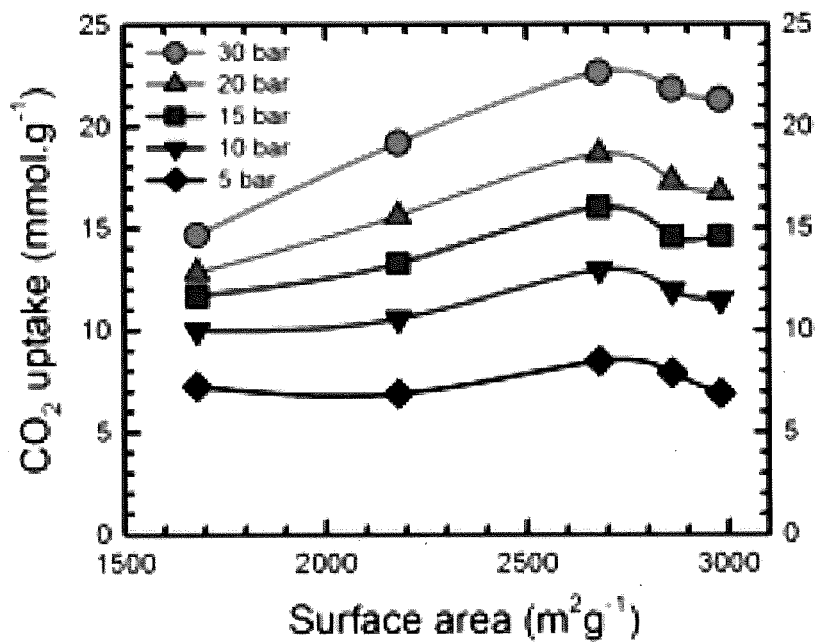


FIG. 47A

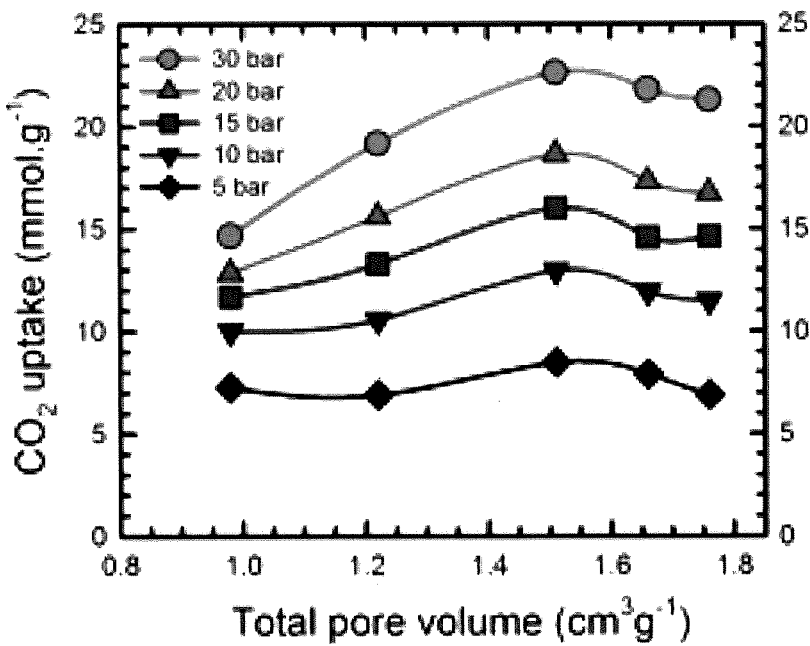


FIG. 47B

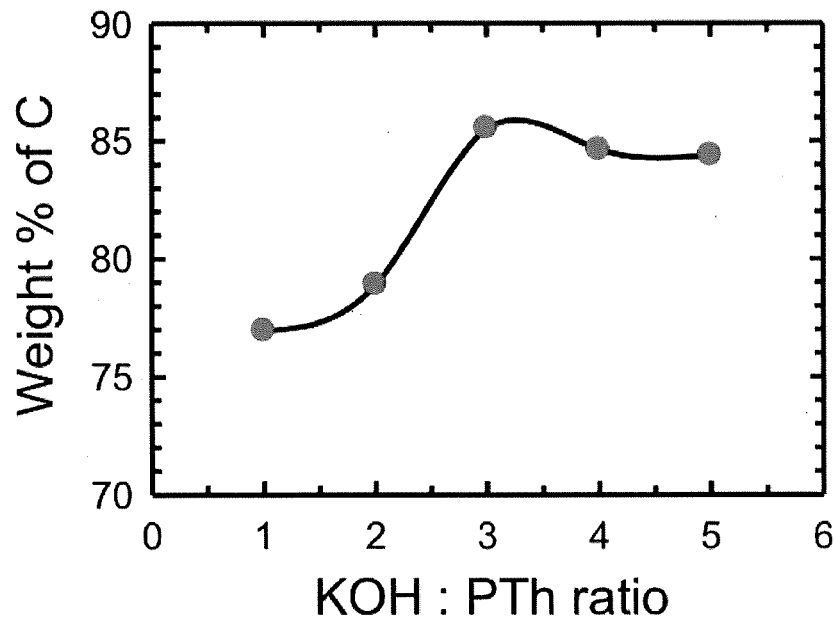


FIG. 48A

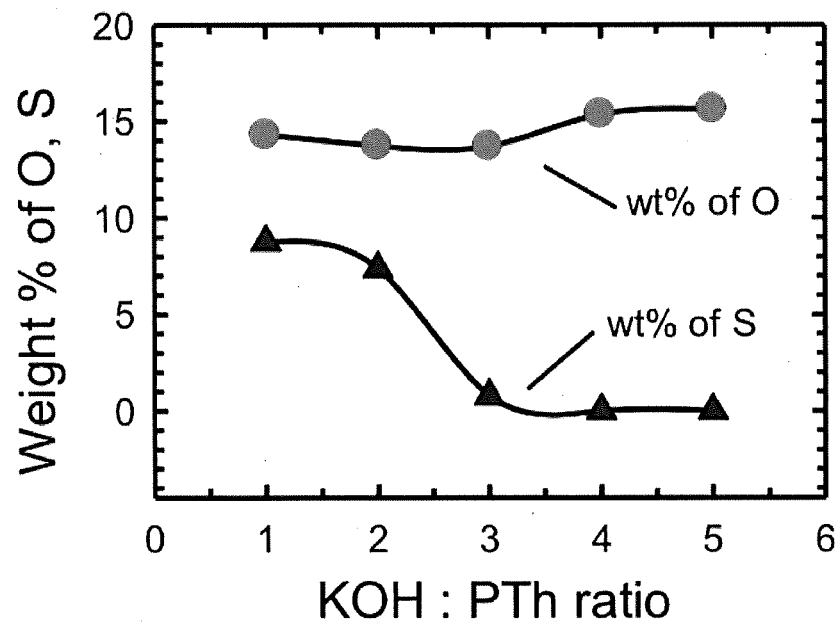


FIG. 48B

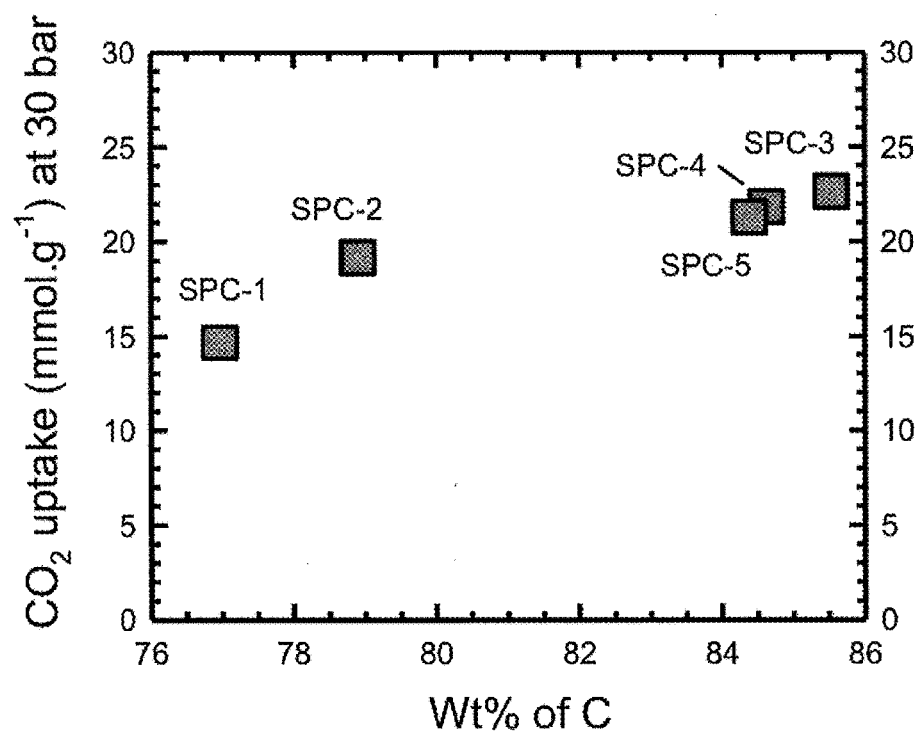


FIG. 49

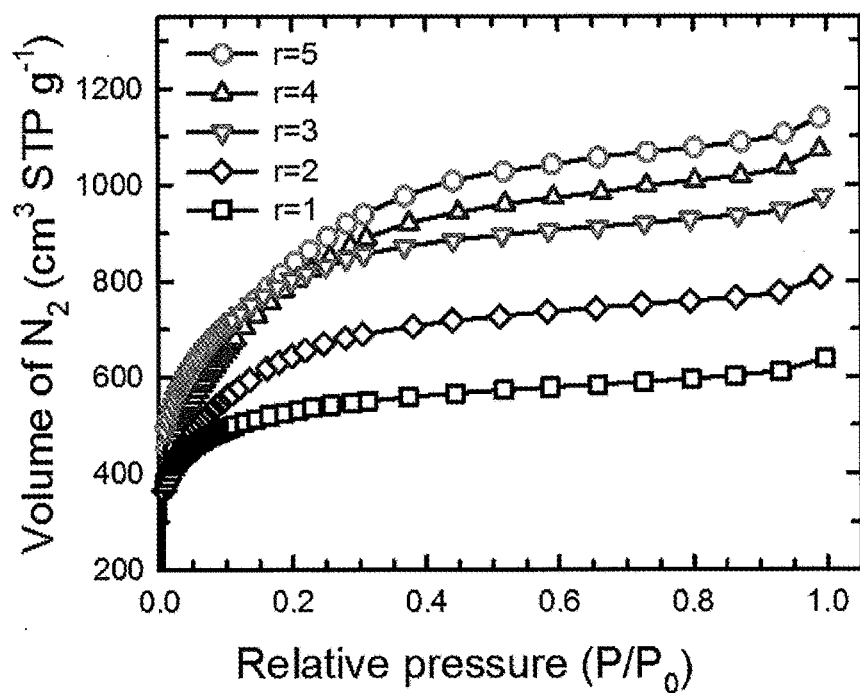
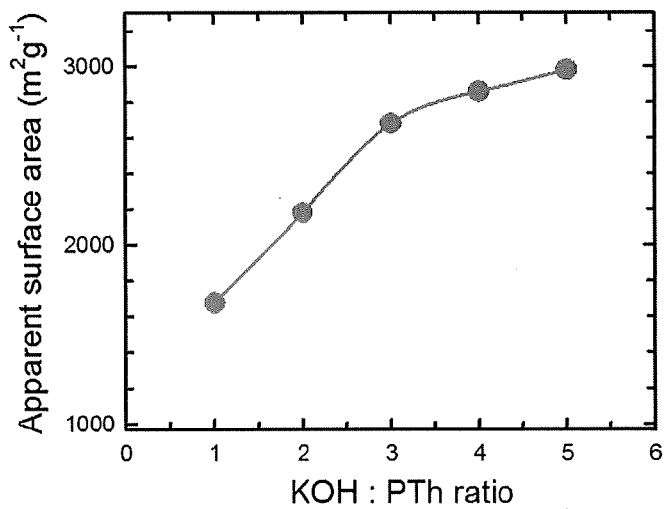
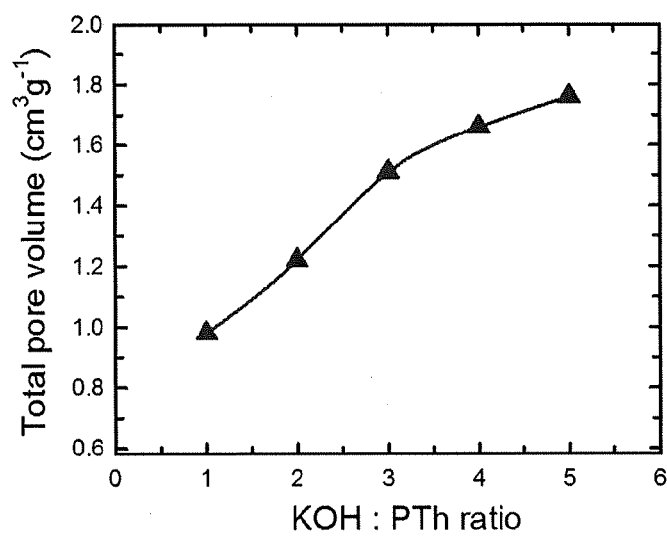


FIG. 50



**FIG. 51A**



**FIG. 51B**

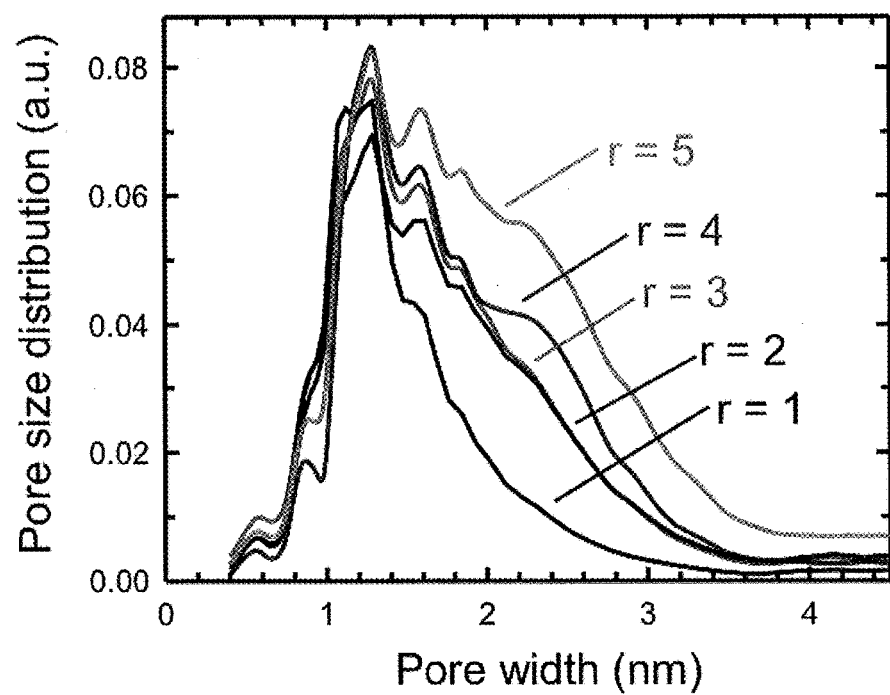


FIG. 52

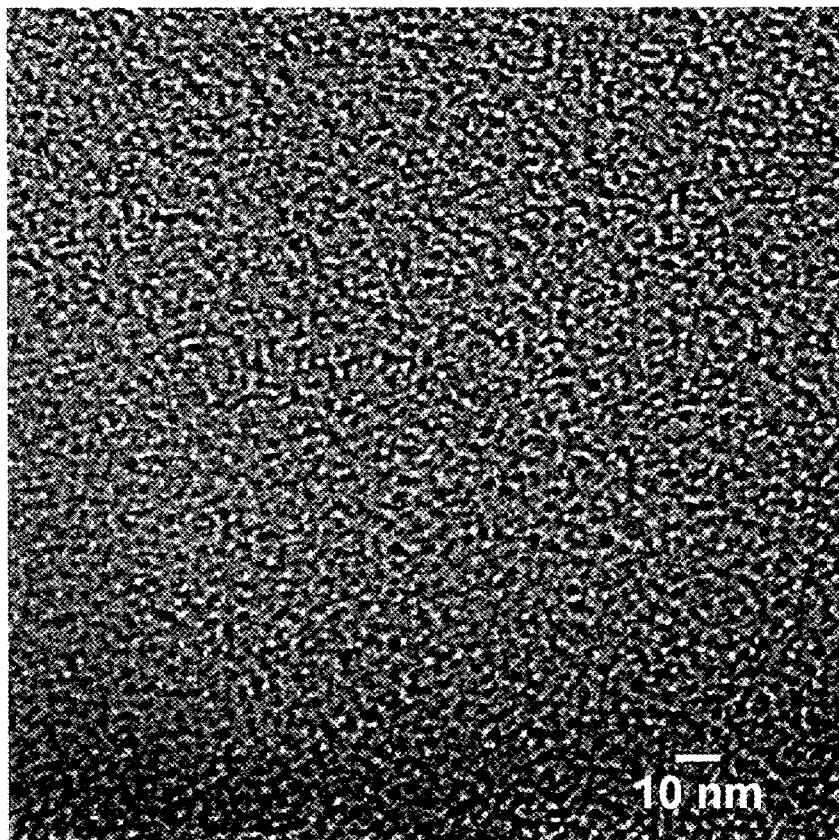
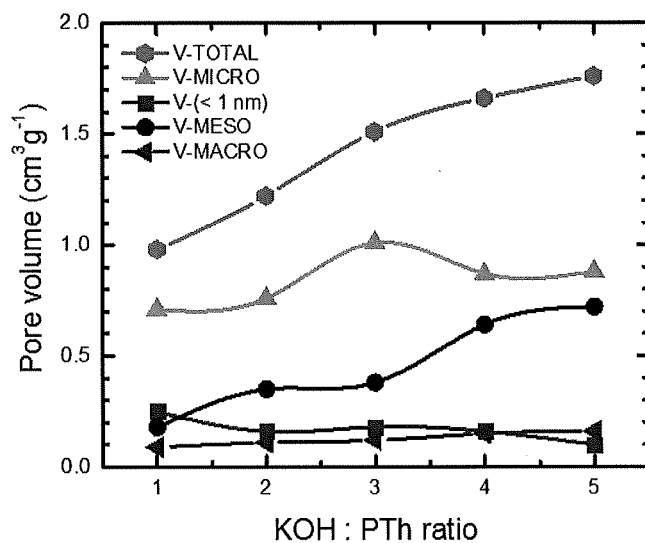
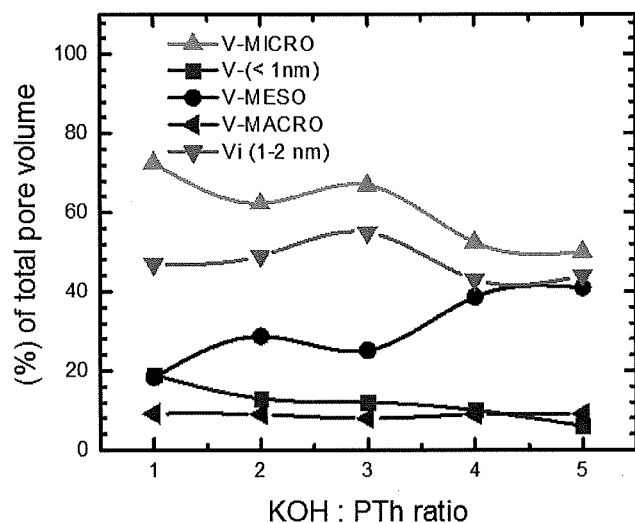


FIG. 53



**FIG. 54A**



**FIG. 54B**

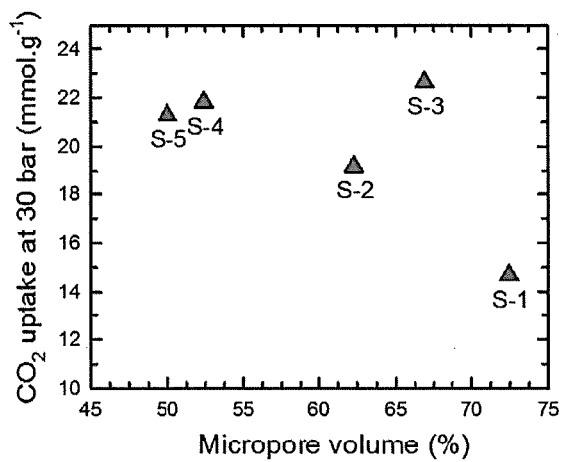


**FIG. 55A**

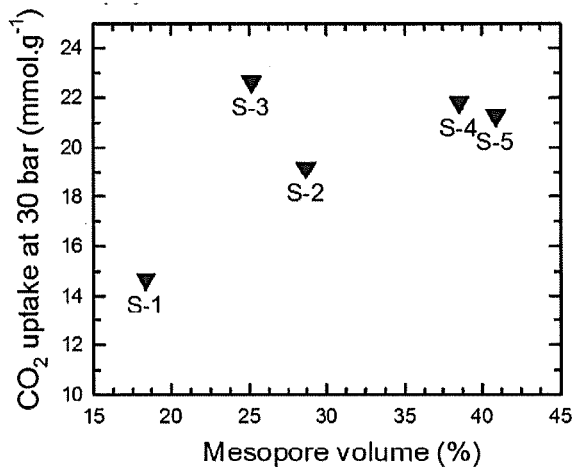


**FIG. 55B**

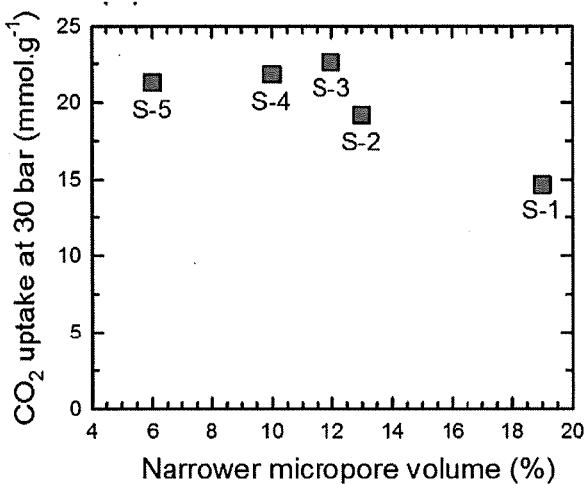


**FIG. 55C**

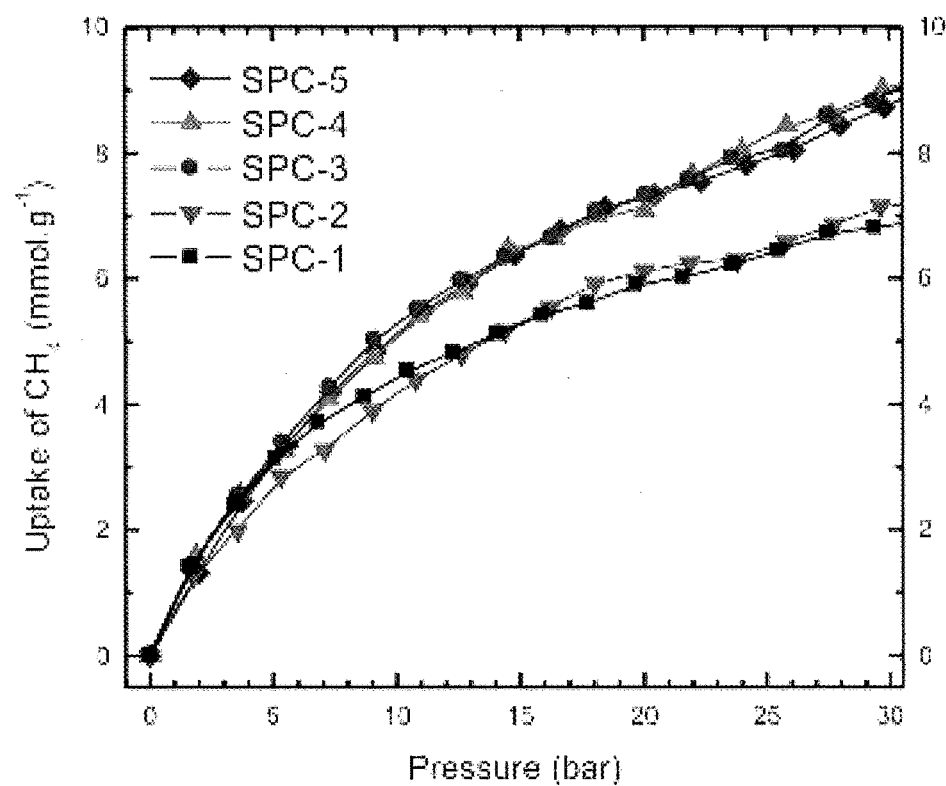


FIG. 56

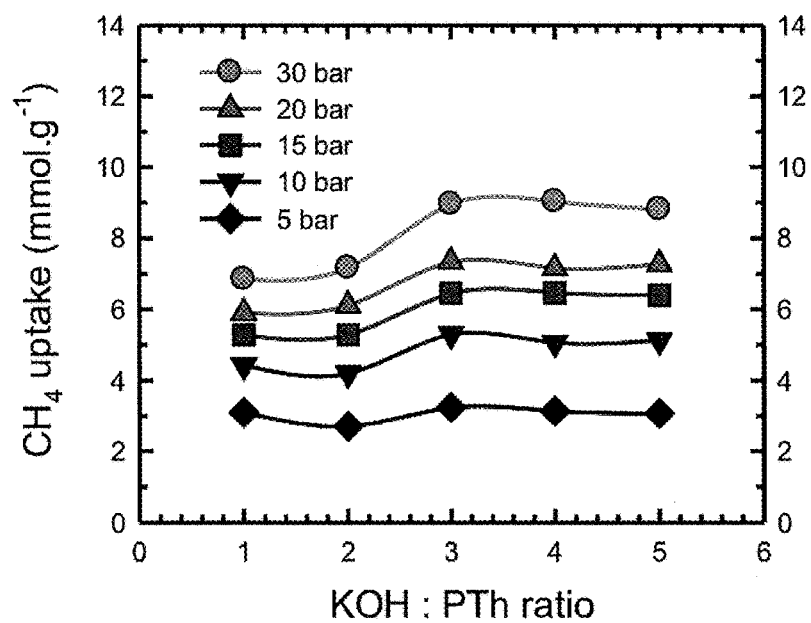
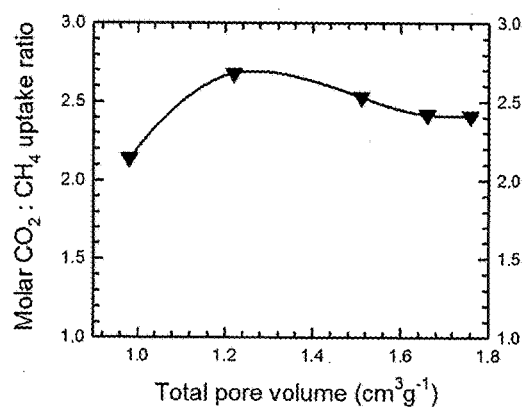
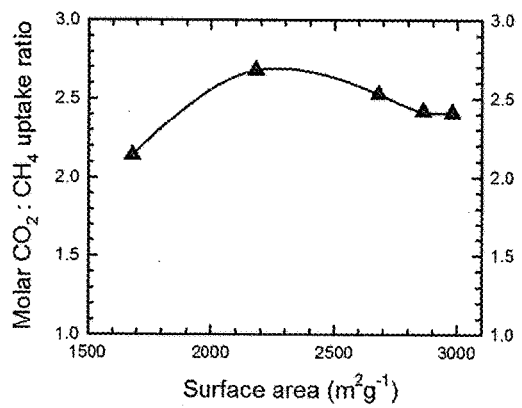
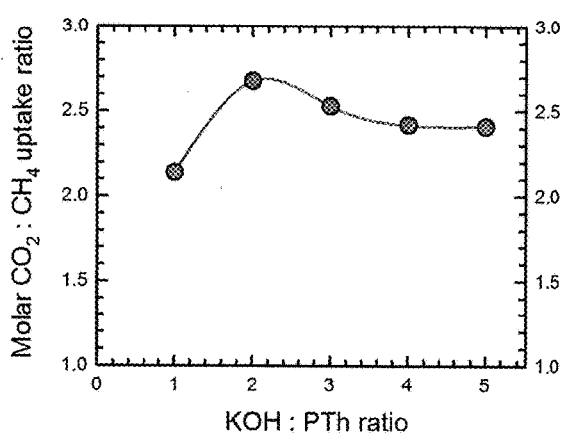
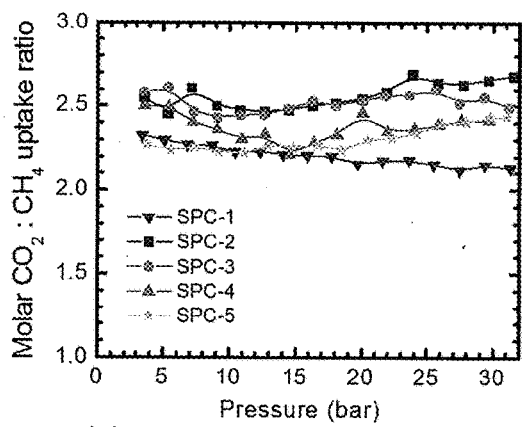


FIG. 57



**METHOD, SYNTHESIS, ACTIVATION  
PROCEDURE AND CHARACTERIZATION  
OF AN OXYGEN RICH ACTIVATED POROUS  
CARBON SORBENT FOR SELECTIVE  
REMOVAL OF CARBON DIOXIDE WITH  
ULTRA HIGH CAPACITY**

**CROSS-REFERENCE TO RELATED  
APPLICATIONS**

[0001] This application is a continuation of U.S. patent application Ser. No. 15/631,341, filed on Jun. 23, 2017, which is a continuation-in-part application of U.S. patent application Ser. No. 15/200,632, filed on Jul. 1, 2016, which claims priority to U.S. Provisional Patent Application No. 62/187,744, filed on Jul. 1, 2015. The entirety of each of the aforementioned applications is incorporated herein by reference.

**STATEMENT REGARDING FEDERALLY  
SPONSORED RESEARCH**

[0002] Not applicable.

**BACKGROUND**

[0003] Current materials for capturing carbon dioxide ( $\text{CO}_2$ ) suffer from numerous limitations, including limited  $\text{CO}_2$  sorption capacity and selectivity. Various embodiments of the present disclosure address these limitations.

**SUMMARY**

[0004] In some embodiments, the present disclosure pertains to materials for  $\text{CO}_2$  adsorption at pressures above 1 bar. In some embodiments, the materials include a porous material with a surface area of at least  $2,800 \text{ m}^2/\text{g}$ , and a total pore volume of at least  $1.35 \text{ cm}^3/\text{g}$ . In some embodiments, a majority of pores of the porous materials have diameters of less than 2 nm as measured from  $\text{N}_2$  sorption isotherms using the BET (Brunauer-Emmett-Teller) method.

[0005] In some embodiments, the present disclosure pertains to materials for the separation of  $\text{CO}_2$  from natural gas at partial pressures of either component above 1 bar. In some embodiments, the materials include a porous material with a surface area of at least  $2,200 \text{ m}^2/\text{g}$ , and a total pore volume of at least  $1.00 \text{ cm}^3/\text{g}$ . In some embodiments, a majority of pores of the porous materials have diameters of greater than 1 nm and less than 2 nm as measured from  $\text{N}_2$  sorption isotherms using the BET (Brunauer-Emmett-Teller) method.

[0006] In some embodiments, the porous materials of the present disclosure include a porous carbon material with a carbon content of between 80% and 95% as measured by X-ray photoelectron spectroscopy. In some embodiments, the porous materials of the present disclosure include a porous carbon material with a surface area of at least  $2,800 \text{ m}^2/\text{g}$ , a total pore volume of at least  $1.35 \text{ cm}^3/\text{g}$ , and a carbon content of between 80% and 95% as measured by X-ray photoelectron spectroscopy.

[0007] In additional embodiments, the present disclosure pertains to materials for the separation of  $\text{CO}_2$  from natural gas at partial pressures of either component above 1 bar. In some embodiments, the materials include a porous carbon material with a surface area of at least  $2,000 \text{ m}^2/\text{g}$ , a total pore volume of at least  $1.00 \text{ cm}^3/\text{g}$ , and a carbon content of greater than 90% as measured by X-ray photoelectron spectroscopy.

[0008] In some embodiments, the porous carbon materials of the present disclosure are prepared by heating an organic polymer precursor or biological material in the presence of potassium hydroxide (KOH). In some embodiments, the temperature of activation is between  $700^\circ \text{ C}$ . and  $800^\circ \text{ C}$ . In some embodiments, the temperature of activation is between  $600^\circ \text{ C}$ . and  $700^\circ \text{ C}$ .

[0009] In some embodiments, the porous carbon materials of the present disclosure are prepared by heating an organic polymer precursor. In some embodiments, the organic polymer precursor includes oxygen in a functional group. In some embodiments, the functional group is a furyl. In some embodiments, the organic polymer precursor is furfuryl alcohol. In some embodiments, the organic polymer precursor polymerizes to form polyfurfuryl alcohol (PFFA). In some embodiments, PFFA is prepared by the polymerization of furfuryl alcohol with a catalyst. In some embodiments, the catalyst is iron(III) chloride.

[0010] In some embodiments, the functional group is an anisyl. In some embodiments, the organic polymer precursor is anisyl alcohol (AA). In some embodiments, the organic polymer precursor polymerizes to form polyanisyl alcohol (PAA). In some embodiments, PAA is prepared by the polymerization of AA with a catalyst. In some embodiments, the catalyst is a protic acid.

[0011] In some embodiments, the porous carbon materials of the present disclosure are prepared by heating a biological material. In some embodiments, the biological material includes, without limitation, sawdust, coconut husk, and combinations thereof. In some embodiments, the biological material is chosen from at least one of the following: sawdust and coconut husk.

[0012] Additional embodiments pertain to methods of making the materials of the present disclosure. Further embodiments pertain to utilizing the materials of the present disclosure for the capture of  $\text{CO}_2$  from various environments.

**DESCRIPTION OF THE FIGURES**

[0013] FIGS. 1A-1B provide data relating to high pressure  $\text{CO}_2$  uptake (at 30 bar and  $24^\circ \text{ C}$ .) as a function of the surface area (FIG. 1A) and total pore volume (FIG. 1B) for a range of porous carbons (PCs), including N-containing PCs (NPCs) and S-containing PCs (SPCs). Also shown are data relating to high pressure  $\text{CO}_2$  uptake at different pressures as a function of surface area (FIG. 1C) and total pore volume (FIG. 1D). A comparison of the total pore volume as a function of surface area for a range of PCs, NPCs and SPCs is also shown (FIG. 1E).

[0014] FIG. 2 provides a plot of  $\text{CO}_2$  uptake at 30 bar and  $24^\circ \text{ C}$ . as a function of activation temperature for PC, NPC, and SPC samples.

[0015] FIGS. 3A-3B provide estimated surface area (FIG. 3A) and total pore volume (FIG. 3B) as a function of activation temperature for PC, NPC and SPC samples.

[0016] FIG. 4 provides comparative data relating to  $\text{CO}_2$  uptake as a function of  $\text{CO}_2$  pressure on N-containing polymer polypyrrole (PPy) precursors and PPy precursors activated at different temperatures (PPy-T-2). Sorption measurements were performed at  $24^\circ \text{ C}$ .

[0017] FIG. 5 provides  $\text{N}_2$  adsorption isotherms for four different NPC samples of PPy-T-2 prepared from polypyrrole and activated at the labelled temperature (T). Sorption measurements were performed at  $24^\circ \text{ C}$ .

[0018] FIGS. 6A-6B provide data relating to the determination of pore structures by N<sub>2</sub> physisorption isotherms of PPy-T-2 samples activated at different temperatures by N<sub>2</sub> physisorption isotherms. Shown are the estimated surface area (FIG. 6A) and total pore volume (FIG. 6B) versus activation temperature.

[0019] FIGS. 7A-7H show additional related data for PPy-T-2 samples. FIG. 7A shows the pore size distributions of PPy-T-2 samples prepared at the three activation temperatures shown, as determined by the non-local density functional theory (NLDFT) method. FIG. 7B shows a scanning electron microscope (SEM) image of a PPy-600-2 sample. FIG. 7C shows high resolution transmission electron microscope (HRTEM) images of the PPy-600-2 sample. FIG. 7D summarizes high pressure volumetric CO<sub>2</sub> adsorption uptake measurements on PPy-800-2 and PPy-800-4, showing the effect of the KOH:precursor ratio. Sorption measurements were performed at 24° C. Also shown are typical X-ray photoelectron spectroscopy (XPS) survey scans for the polypyrrole precursor (FIG. 7E) and PPy-600-2 NPC samples (FIG. 7F). Also shown are the wt % determined by XPS of elemental carbon (FIG. 7G) and oxygen and nitrogen versus activation temperature (FIG. 7H) for the PPy precursor and PPy-T-2 samples.

[0020] FIGS. 8A-8B show high pressure (30 bar) CO<sub>2</sub> uptake as a function of N wt % (FIG. 8A) and S wt % (FIG. 8B) in NPC and SPC samples, respectively. Also shown are high pressure CO<sub>2</sub> adsorption uptake for PAn-600-3 compared with PPy-600-2 (FIG. 8C) and SD-M-800-4 compared with PPy-800-4 (FIG. 8D). FIG. 8E shows the dependence of volumetric CO<sub>2</sub> uptake on N content for PPy-T-2 samples in comparison to the PPy precursor measured at different CO<sub>2</sub> pressures. Sorption measurements were performed at 24° C.

[0021] FIGS. 9A-9B show high pressure (30 bar) CO<sub>2</sub> uptake as a function of 0 wt % (FIG. 9A) and Σ(O,N,S) wt % (FIG. 9B) in PC, NPC and SPC samples. Sorption measurements were performed at 24° C.

[0022] FIGS. 10A-10B show room temperature volumetric CO<sub>2</sub> (FIG. 10A) and methane (CH<sub>4</sub>) (FIG. 10B) adsorption isotherms for PC, NPC, and SPC samples. FIG. 10C shows the molar CO<sub>2</sub>:CH<sub>4</sub> uptake ratio as a function of gas pressure for PC, NPC, and SPC samples.

[0023] FIGS. 11A-11B show plots of molar CO<sub>2</sub>:CH<sub>4</sub> uptake ratio (@ 30 bar) as a function of the surface area (FIG. 11A) and total pore volume (FIG. 11B) for a range of PC, NPC and SPC samples. Sorption measurements were performed at 24° C.

[0024] FIGS. 12A-12D show plots of molar CO<sub>2</sub>:CH<sub>4</sub> uptake ratio (@ 30 bar) as a function of the surface area (FIG. 12A), total pore volume (FIG. 12B), activation temperature (FIG. 12C), and CO<sub>2</sub> uptake (FIG. 12D) for PPy-T-2 (T=500, 600, 700 and 800° C.) NPC samples. Sorption measurements were performed at 24° C.

[0025] FIG. 13 shows high pressure (30 bar) molar CO<sub>2</sub>:CH<sub>4</sub> uptake ratio as a function of N wt % in NPC samples. Sorption measurements were performed at 24° C.

[0026] FIG. 14 shows the high pressure (30 bar) molar CO<sub>2</sub>:CH<sub>4</sub> uptake ratio as a function of C wt % in PC, NPC, and SPC samples. Sorption measurements were performed at 24° C.

[0027] FIG. 15 shows volumetric CO<sub>2</sub> uptake of different OPCs activated at increasing temperature, activated carbon and carbon precursor.

[0028] FIGS. 16A-16D provide an analysis of the porous structure of OPC samples activated at different temperatures. FIG. 16A shows N<sub>2</sub> adsorption and desorption isotherms for a PC (800) sample. FIG. 16B shows estimated surface area and total pore-volume vs. activation temperature. FIG. 16C shows the distribution of pore volumes as a function of activation temperature as estimated by NLDFT. FIG. 16D shows the surface area (blue bars) and total pore volume (purple) for activated charcoal and eight different PC samples known for high CO<sub>2</sub> uptakes (>14 mmol g<sup>-1</sup> at 30 bar).

[0029] FIGS. 17A-17B provide additional data relating to the CO<sub>2</sub> uptake of porous carbons. FIG. 17A shows the volumetric CO<sub>2</sub> uptake of various porous carbons prepared from different carbon precursors, including O-rich PC (OPC), N-rich PC (NPC) and S-rich PC (SPC). Measurements were performed in a PCTPRO instrument at 24° C. FIG. 17B shows the graphical representation of surface areas and maximum CO<sub>2</sub> uptake capacities at 30 bar for nine different porous carbon sorbents. The highest CO<sub>2</sub> uptake property (26.6 mmol g<sup>-1</sup>) is demonstrated by Applicants' newly discovered OPC (750) sample (second bar to the right).

[0030] FIGS. 18A-18B provide a demonstration of optimal gas uptake selectivity of OPC samples for CO<sub>2</sub> over CH<sub>4</sub>. FIG. 18A shows volumetric CO<sub>2</sub> and CH<sub>4</sub> uptake measurements on OPC (750) sorbents up to a pressure range of 30 bar at 0.5 and 24° C. FIG. 18B shows volumetric CO<sub>2</sub> and CH<sub>4</sub> uptake measurements on commercially available activated charcoal. The molar uptake ratios (CO<sub>2</sub>/CH<sub>4</sub>) at 30 bar for OPC (750) and activated charcoal are 2.74 and 1.4, respectively.

[0031] FIG. 19 provides a demonstration of optimal gas uptake selectivity of OPC samples for CO<sub>2</sub> over CH<sub>4</sub>. Volumetric CO<sub>2</sub> and CH<sub>4</sub> uptake measurements on OPC (750) sorbents up to a pressure range of 30 bar at 0.5° C. and 24° C. are shown. The mass uptake ratios (CO<sub>2</sub>/CH<sub>4</sub>) at 30 bar for OPC (750) are 8.0 and 7.6, respectively.

[0032] FIGS. 20A-20B provide a demonstration of the reproducibility of sample preparation and gas uptake properties of OPCs. FIG. 20A shows volumetric CO<sub>2</sub> uptake measurements on four different OPC (750) samples synthesized and activated the same way. FIG. 20B shows two successive CO<sub>2</sub> adsorption and desorption cycles.

[0033] FIGS. 21A-21J provide various schemes and data relating to the synthesis and characterization of OPCs. FIG. 21A provides a synthesis scheme for OPC. Photographs of carbon precursor (FIG. 21B), as-synthesized OPC (FIG. 21C), and as-synthesized SPC samples (FIG. 21D) are also shown. OPC samples are pellet like compared to SPC and other PC materials. Scanning electron microscopy (SEM) images of carbon precursor (FIG. 21E), OPC (600) (FIG. 21F) and OPC (800) samples (FIG. 21G) are also shown. FIG. 21H shows an energy-dispersive X-ray spectroscopy (EDS) elemental scan for OPC (800). Also shown are high resolution transmission electron microscopy (TEM) images of OPC (600) (FIG. 21I) and OPC (800) samples (FIG. 21J) showing nm sized micro porous structures.

[0034] FIGS. 22A-22B show the isosteric heat of absorption of CO<sub>2</sub> (FIG. 22A) and CH<sub>4</sub> (FIG. 22B) as a function of molar gas uptakes.

[0035] FIGS. 23A-23H show the characterization of chemical compositions of carbon precursor and porous carbon samples activated at increasing temperatures. Shown

are X-ray photoelectron spectroscopy (XPS) survey scans for C-precursor (FIG. 23A) and OPC (800) (FIG. 23B). Also shown are the wt % of elemental carbon (FIG. 23C) and oxygen (FIG. 23D) vs. activation temperature. XPS elemental scanning for carbon C1s (FIG. 23E) and oxygen O1s (FIG. 23F) are also shown. FIG. 23G shows the Fourier transform infrared spectroscopy (FTIR) spectra of C-precursor and activated OPCs. FIG. 23H shows the Raman spectra and Raman disorder (D) to graphene (G) band intensity ratio vs. activation temperature. The KOH:Polymer weight ratio is 3 in all cases. IR spectra are base line corrected and vertically offset for clarity.

[0036] FIGS. 24A-24B provide schemes for the synthesis of various porous carbon materials. FIG. 24A provides a synthetic reaction scheme for the synthesis of furfuryl alcohol-OPC (FFA-OPC) ( $\text{FeCl}_3:\text{FA}=10$ , KOH:PFFA=3, and  $T=500\text{-}800^\circ \text{C}$ ). FIG. 24B provides a synthetic reaction scheme for the synthesis of anisyl alcohol (AA)-OPC (AA-OPC) (KOH:PAA=3, and  $T=500\text{-}800^\circ \text{C}$ ).

[0037] FIGS. 25A-25C show photographs of PFFA precursors (FIG. 25A), as-synthesized OPC (FIG. 25B), and as-synthesized SPC samples (FIG. 25C).

[0038] FIGS. 26A-26D show SEM images of PFFA (FIG. 26A), precursors and the associated OPCs (FIG. 26B), FFA-OPC<sub>750</sub> (FIG. 26C), and AA-OPC<sub>750</sub> (FIG. 26D).

[0039] FIGS. 27A-27C show representative high-resolution TEM images of FFA-OPC<sub>500</sub> (FIG. 27A), FFA-OPC<sub>800</sub> (FIG. 27B), and AA-OPC<sub>800</sub> (FIG. 27C) samples showing nanometer sized micro porous structures.

[0040] FIGS. 28A-28B show N<sub>2</sub> adsorption isotherms for FFA-OPCs (FIG. 28A) and AA-OPCs (FIG. 28B) measured at liquid N<sub>2</sub> temperature (77K).

[0041] FIGS. 29A-29B show estimated apparent surface area (FIG. 29A) and total pore volumes versus activation temperature (FIG. 29B) for FFA-OPC and AA-OPC.

[0042] FIG. 30 shows apparent surface area (blue/dark bars) and total pore volumes (purple/light bars) for activated charcoal and PC samples with high CO<sub>2</sub> uptake properties at 30 bar ( $>12 \text{ mmol}\cdot\text{g}^{-1}$ ).

[0043] FIGS. 31A-31B show distribution of pore sizes as a function of pore width for five activation temperatures as determined by the nonlocal DFT method for FFA-OPC (FIG. 31A) and AA-OPC (FIG. 31B).

[0044] FIGS. 32A-32D show the wt % of elemental carbon (FIGS. 32A and 32C) and oxygen (FIGS. 32B and 32D) as determined by XPS versus activation temperature for FFA-OPC (FIGS. 32A and 32B) and AA-OPC (FIGS. 32C and 32D).

[0045] FIGS. 33A-33B show XPS elemental scanning for oxygen O1s (FIG. 33A) and carbon C1s (FIG. 33B) for PFFA precursor and FFA-OPC.

[0046] FIG. 34 shows FTIR spectra of PFFA precursor and activated FFA-OPCs. Spectra are base line corrected and vertically offset for clarity (KOH:PFFA=3 in all cases).

[0047] FIGS. 35A-35D show Raman spectra and Raman disorder (D) to graphene (G) band intensity ratio versus activation temperature (KOH:PFFA=3 in all cases).

[0048] FIGS. 36A-36B show volumetric CO<sub>2</sub> uptakes of FFA-OPC (FIG. 36A) and AA-OPC (FIG. 36B) samples activated at different temperatures. FIG. 36C shows the volumetric CO<sub>2</sub> uptakes of FFA-OPC<sub>750</sub>, NPC, SPC, and activated charcoal up to a pressure limit of 30 bar. Measurements were performed in a PCTPRO instrument at 24° C.

[0049] FIG. 37 shows graphical representation of surface areas and maximum CO<sub>2</sub> uptake capacities at 30 bar for activated charcoal and different sorbent samples with high CO<sub>2</sub> uptake properties at 30 bar ( $>12 \text{ mmol}\cdot\text{g}^{-1}$ ).

[0050] FIGS. 38A-38B show demonstration of reproducibility of sample preparation and gas uptake properties. Volumetric CO<sub>2</sub> uptake measurements are shown on four different batches of FFA-OPC<sub>750</sub> (FIG. 38A) and AA-OPC<sub>750</sub> (FIG. 38B) that were synthesized and activated the same way. FIG. 38C shows successive CO<sub>2</sub> adsorption and desorption cycle measurements on an individual FFA-OPC<sub>750</sub> sample.

[0051] FIGS. 39A-39B show a demonstration of ultrahigh CO<sub>2</sub> uptake capability of an FFA-OPC<sub>750</sub> sample at low temperature. FIG. 39A shows volumetric CO<sub>2</sub> uptake measurements on an FFA-OPC<sub>750</sub> sample at four different temperatures. At 0.5° C. and 30 bar pressure, sorbent adsorbed an ultrahigh amount of CO<sub>2</sub> that maxed to 43 mmol·g<sup>-1</sup> (189 wt %). FIG. 39B shows CO<sub>2</sub> uptakes at four different (labelled) pressures as a function of experiment temperatures.

[0052] FIGS. 40A-40B show volumetric CO<sub>2</sub> and CH<sub>4</sub> uptakes measurements on FFA-OPC<sub>750</sub> (FIG. 40A) and AA-OPC<sub>750</sub> (FIG. 40B) sorbents up to a pressure range of 30 bar at 0.5 and 24° C. FIG. 40C shows volumetric CO<sub>2</sub> and CH<sub>4</sub> uptake measurements on activated charcoal.

[0053] FIGS. 41A-41B show a plot of CH<sub>4</sub> uptake at 30 bar as a function of surface area (FIG. 41A) and total pore volume (FIG. 41B) for FFA-OPC and AA-OPC.

[0054] FIGS. 42A-42D show isosteric heat of gas adsorption of CO<sub>2</sub> (FIGS. 42A-B) and CH<sub>4</sub> (FIGS. 42C-D) as a function molar gas uptake for FFA-OPC<sub>750</sub> (FIGS. 42A and 42C) and AA-OPC<sub>750</sub> (FIGS. 42B and 42D).

[0055] FIGS. 43A-43B show SEM images of the polymer precursor (PTh) (FIG. 43A) and a SPC-2 sample (FIG. 43B).

[0056] FIG. 44 shows high pressure volumetric CO<sub>2</sub> uptake as a function of CO<sub>2</sub> pressure on PTh, activated charcoal and activated SPC-700-R samples activated at 700° C. with increasing KOH:PTh weight ratio (r) where r varies from 1 to 5. Experiments were performed at 24° C.

[0057] FIG. 45 shows high pressure volumetric CO<sub>2</sub> uptake as a function of CO<sub>2</sub> pressure for two batches of SPC-4 activated at 700° C. Uptake measurements were performed at 24° C.

[0058] FIG. 46 shows dependence of CO<sub>2</sub> uptake at the labelled pressure on the KOH:PTh ratio for activated SPC-r samples activated at 700° C. Experiments were performed at 24° C.

[0059] FIGS. 47A-47B show dependence of CO<sub>2</sub> uptake at the labelled pressure on surface area (FIG. 47A) and total pore volume (FIG. 47B). SPC samples were synthesized from PTh by activating at 700° C. with different KOH amounts. Experiments were performed at 24° C.

[0060] FIGS. 48A-48B show chemical composition of the activated SPC samples by XPS spectroscopy showing the wt % of elemental carbon (FIG. 48A) and oxygen and sulfur (FIG. 48B) versus KOH:PTh ratio.

[0061] FIG. 49 shows dependence of CO<sub>2</sub> uptake at the activated SPC samples as a function of carbon composition as determined XPS spectroscopy.

[0062] FIG. 50 shows N<sub>2</sub> adsorption isotherms (measured at 77 K) for five different SPC samples activated at 700° C. with KOH:PTh ratios varied from 1 to 5.

[0063] FIGS. 51A-51B show estimated surface area (FIG. 51A) and total pore volume (FIG. 51B) versus KOH:PTh ratio for five different SPC samples activated at 700° C.

[0064] FIG. 52 shows pore size distributions for the samples in FIGS. 51A-51B.

[0065] FIG. 53 shows a high resolution transmission microscope (HRTEM) image of a SPC-2 sample. Scale bar=10 nm.

[0066] FIGS. 54A-54B show the total pore volume, volume of macropores (>50 nm), mesopores (>2 nm), micropores (<2 nm), and narrower micropores (<1 nm) as a function of KOH:PTh ratio (FIG. 54A), and percentages of total pore volumes for micropores, narrower micropores and mesopores versus KOH:PTh ratio (FIG. 54B).

[0067] FIGS. 55A-55C show percentages of pore volumes for micropores, narrower micropores and mesopores versus CO<sub>2</sub> uptake.

[0068] FIG. 56 shows high pressure volumetric CH<sub>4</sub> uptake as a function of CH<sub>4</sub> pressure on activated SPC-700-R samples activated at 700° C. with increasing KOH: PTh ratio (r) where r varies from 1 to 5. Experiments were performed at 24° C.

[0069] FIG. 57 shows dependence of CH<sub>4</sub> uptake at labeled pressure on KOH:PTh ratios for activated SPC samples. Experiments were performed at 24° C.

[0070] FIGS. 58A-58D show various data related to SPC samples. FIG. 58A shows the molar CO<sub>2</sub>:CH<sub>4</sub> uptake ratio as a function of a gas pressure for SPC sorbents activated with different KOH:PTh ratio. Also shown are plots of molar CO<sub>2</sub>:CH<sub>4</sub> uptake ratios at 30 bar as a function of KOH:PTh ratio (FIG. 58B), surface area (FIG. 58C), and total pore volume (FIG. 58D). Experiments were performed at 24° C.

#### DETAILED DESCRIPTION

[0071] It is to be understood that both the foregoing general description and the following detailed description are illustrative and explanatory, and are not restrictive of the subject matter, as claimed. In this application, the use of the singular includes the plural, the word "a" or "an" means "at least one", and the use of "or" means "and/or", unless specifically stated otherwise. Furthermore, the use of the term "including", as well as other forms, such as "includes" and "included", is not limiting. Also, terms such as "element" or "component" encompass both elements or components comprising one unit and elements or components that comprise more than one unit unless specifically stated otherwise.

[0072] The section headings used herein are for organizational purposes and are not to be construed as limiting the subject matter described. All documents, or portions of documents, cited in this application, including, but not limited to, patents, patent applications, articles, books, and treatises, are hereby expressly incorporated herein by reference in their entirety for any purpose. In the event that one or more of the incorporated literature and similar materials defines a term in a manner that contradicts the definition of that term in this application, this application controls.

[0073] There are generally two classes of materials employed for carbon dioxide (CO<sub>2</sub>) separation: reactants and adsorbents. The former includes amine and other reactive species such as ionic liquids and alkali-metal-based oxides. At present, monoethanolamine (MEA) is the industry standard. However, regeneration, degradation and cor-

rosion, together with health and environmental issues, still affect its large scale implementation.

[0074] Impregnation of CO<sub>2</sub> capture materials onto supports has been investigated, but it is only recently that the regeneration temperature has been lowered by their combination with carbon nanomaterials. Ionic liquids, suitable for high pressure capture, are expensive and toxic, while cheap alkali metal oxides suffer from severe deactivation upon cycling.

[0075] Although the aforementioned materials show optimal selectivity between CO<sub>2</sub> and methane (CH<sub>4</sub>), their myriad drawbacks have meant that much effort has been invested into the study of solid porous sorbents, such as porous carbons (PC), metal-organic frameworks (MOFs), microporous zeolites, and porous silica-based sorbents with high surface area.

[0076] MOFs outperform zeolites in terms of maximum capacity at high pressure, but are expensive since they require complex multistep synthesis procedures. In addition, their gas adsorption capacity degrades after several cycles of usage. Carbonaceous materials, such as activated carbon and charcoal, are cheaper and less sensitive to moisture than zeolites and MOFs, but their adsorption capacity generally increases with loss of selectivity at high pressure.

[0077] Chemically activated porous carbon adsorbents have large surface areas and pore volumes associated with micro- and meso-porous structure. As a result, such materials show significantly improved CO<sub>2</sub> capturing capacity as compared to traditional carbonaceous materials.

[0078] It has been suggested that the presence of nitrogen or sulfur dopants is responsible for improved CO<sub>2</sub> uptake in porous carbon materials (e.g., *Nat Commun.*, 2014, 5, 3961 and U.S. Pat. Pub. No. 2015/0111024). These studies were undertaken at 30 bar (1 bar=100,000, Pa=750.06 mmHg) using compounds previously reported to show improved results over activated carbon at 1 bar (e.g., *Adv. Funct. Mater.*, 2011, 21, 2781-2787; and *Microporous Mesoporous Mater.*, 2012, 158, 318-323). The improved high pressure results were proposed to be due to the S or N centers acting as a Lewis base to facilitate the ambient polymerization of the CO<sub>2</sub>. However, previous investigations of the role of N-doping in CO<sub>2</sub> capture by PCs up to 1 bar pressure shows no correlation (e.g., *ACS Appl. Mater. Interfaces*, 2013, 5, 6360-6368).

[0079] The conventional goal in synthesizing a porous carbon material with optimal CO<sub>2</sub> adsorption is to focus on increased surface area and pore volume (e.g., U.S. Pat. Pub. No. 2016/0136613). The same approach is presumed to also work for the separation of CO<sub>2</sub> from natural gas.

[0080] However, the present disclosure demonstrates that increasing the surface area and pore volume of a carbon material do not guarantee the best adsorbent. Instead, a combination of factors is involved in defining the ideal porous carbon adsorbent material.

[0081] In some embodiments, the present disclosure pertains to novel materials for CO<sub>2</sub> capture. In additional embodiments, the present disclosure pertains to methods of making the materials of the present disclosure. In further embodiments, the present disclosure pertains to methods of utilizing the materials of the present disclosure for the capture of CO<sub>2</sub> from various environments. As set forth in more detail herein, the present disclosure can have various embodiments.

**[0082]** Materials for CO<sub>2</sub> Capture

**[0083]** In some embodiments, the present disclosure pertains to materials for CO<sub>2</sub> adsorption at pressures above 1 bar. In some embodiments, the materials include a porous material with a surface area of at least 2,800 m<sup>2</sup>/g, and a total pore volume of at least 1.35 cm<sup>3</sup>/g. In some embodiments, a majority of pores of the porous material have diameters of less than 2 nm as measured from N<sub>2</sub> sorption isotherms using the BET (Brunauer-Emmett-Teller) method.

**[0084]** In some embodiments, more than about 50% of pores of the porous material have diameters of less than 2 nm. In some embodiments, more than about 60% of pores of the porous material have diameters of less than 2 nm. In some embodiments, more than about 70% of pores of the porous material have diameters of less than 2 nm. In some embodiments, more than about 80% of pores of the porous material have diameters of less than 2 nm. In some embodiments, between about 50% to about 90% of pores of the porous material have diameters of less than 2 nm.

**[0085]** In some embodiments, the present disclosure pertains to materials for the separation of CO<sub>2</sub> from natural gas at partial pressures of either component above 1 bar. In some embodiments, the materials include a porous material with a surface area of at least 2,200 m<sup>2</sup>/g, and a total pore volume of at least 1.00 cm<sup>3</sup>/g. In some embodiments, a majority of pores of the porous material have diameters of greater than 1 nm and less than 2 nm as measured from N<sub>2</sub> sorption isotherms using the BET (Brunauer-Emmett-Teller) method.

**[0086]** In some embodiments, more than about 50% of pores of the porous material have diameters of greater than 1 nm and less than 2 nm. In some embodiments, more than about 60% of pores of the porous material have diameters of greater than 1 nm and less than 2 nm. In some embodiments, more than about 70% of pores of the porous material have diameters of greater than 1 nm and less than 2 nm. In some embodiments, more than about 80% of pores of the porous material have diameters of greater than 1 nm and less than 2 nm. In some embodiments, between about 50% to about 90% of pores of the porous material have diameters of greater than 1 nm and less than 2 nm.

**[0087]** In some embodiments, the porous materials of the present disclosure include a porous carbon material. In some embodiments, the porous carbon material has a carbon content of between 80% and 95% as measured by X-ray photoelectron spectroscopy. In some embodiments, the porous materials include a porous carbon material with a surface area of at least 2,800 m<sup>2</sup>/g, a total pore volume of at least 1.35 cm<sup>3</sup>/g, and a carbon content of between 80% and 95% as measured by X-ray photoelectron spectroscopy. In some embodiments, the materials include a porous carbon material with a surface area of at least 2,000 m<sup>2</sup>/g, a total pore volume of at least 1.00 cm<sup>3</sup>/g, and a carbon content of greater than 90% as measured by X-ray photoelectron spectroscopy.

**[0088]** The porous carbon materials of the present disclosure may be prepared in various manners. For instance, in some embodiments, the porous carbon material is prepared by heating an organic polymer precursor or biological material in the presence of potassium hydroxide (KOH). In some embodiments, the temperature of activation is between 700° C. and 800° C. In some embodiments, the temperature of activation is between 600° C. and 700° C.

**[0089]** The materials of the present disclosure can have various chemical components. For instance, in some

embodiments, the materials of the present disclosure are rich in oxygen. As such, in some embodiments, the materials of the present disclosure are referred to as oxygen rich activated porous carbons (OPCs). In some embodiments, the materials of the present disclosure have an oxygen content of more than about 10 wt %. In some embodiments, the materials of the present disclosure have an oxygen content between about 10 wt % and about 25 wt %.

**[0090]** In some embodiments, the materials of the present disclosure may lack other heteroatoms, such as nitrogen or sulfur. For instance, in some embodiments, the total heteroatom content of the materials of the present disclosure may range from about 0 wt % to about 1 wt %. In some embodiments, the total heteroatom content of the materials of the present disclosure may be less than about 1 wt %.

**[0091]** The materials of the present disclosure can have various advantageous properties. For instance, in some embodiments, the materials of the present disclosure have high surface areas. In some embodiments, the materials of the present disclosure have surface areas of more than about 1,000 m<sup>2</sup>/g. In some embodiments, the materials of the present disclosure have surface areas that range from about 1,000 m<sup>2</sup>/g to about 5000 m<sup>2</sup>/g (e.g., Table 5). In some embodiments, the materials of the present disclosure have surface areas of about 3005 m<sup>2</sup>/g (e.g., in OPC samples chemically activated at 800° C.) (e.g., FIG. 16D).

**[0092]** In some embodiments, the materials of the present disclosure have high CO<sub>2</sub> adsorption capacities. In some embodiments, the materials of the present disclosure have a CO<sub>2</sub> adsorption capacity of more than about 100 wt %. In some embodiments, the materials of the present disclosure have CO<sub>2</sub> adsorption capacities between about 117 wt % and about 189 wt %.

**[0093]** In some embodiments, the materials of the present disclosure have a CO<sub>2</sub> adsorption capacity of up to 117 wt % (26.6 mmol/g) at a pressure of 30 bar, a number that is higher than any reported uptake values for activated porous carbon (PC) adsorbents (e.g., FIGS. 17A-17B and Table 5). In some embodiments, the materials of the present disclosure capture CO<sub>2</sub> from a natural gas containing environment that is rich in CH<sub>4</sub> at a maximum molar uptake ratio of 2.75 (7.5 by mass ratio) at a pressure of 30 bar (e.g., FIGS. 18A-18B and FIG. 19).

**[0094]** In some embodiments, the materials of the present disclosure (e.g., OPCs that are activated at 750° C., referred to herein as OPC (750)) outperform most of the existing porous carbons for high pressure uptake of CO<sub>2</sub> (e.g., 26.6 mmol/g; 117 wt % at 30 bar) and demonstrate optimal selectivity for CO<sub>2</sub> capture over CH<sub>4</sub> uptake (e.g., V<sub>CO<sub>2</sub></sub>:N<sub>CH<sub>4</sub></sub> ratio ~2.7 (molar) and ~7.5 (by wt) at 30 bar) at room temperature. Additionally, OPC (750) demonstrates ultrahigh CO<sub>2</sub> uptake (43 mmol g<sup>-1</sup>; 189 wt %) at 0.5° C., a value that was never reported previously (e.g., FIG. 18A).

**[0095]** In some embodiments, the materials of the present disclosure exhibit remarkable thermal stability and reproducible gas uptake properties for many cycles (e.g., FIGS. 20A-20B). Unlike other fine powder type activated porous carbon materials, the materials of the present disclosure can be clumpy and pelletized in some embodiments. Such properties can in turn make the materials of the present disclosure better candidates for preparing solid pellet-like adsorbents (e.g., FIG. 21C).

[0096] Formation of Materials

[0097] The materials of the present disclosure can be prepared in various manners. Additional embodiments of the present disclosure pertain to methods of making the materials of the present disclosure.

[0098] In some embodiments, a carbon precursor is first synthesized. Next, the carbon precursor is activated to form porous carbon materials. Various methods may be utilized to optimize sample preparation to synthesize activated porous carbon materials with very high CO<sub>2</sub> uptake.

[0099] In some embodiments, a carbon precursor is activated by chemical activation. In some embodiments, the chemical activation includes heating the carbon precursor in a mixture. In some embodiments, the carbon precursor is heated in a mixture that contains a base, such as KOH. In some embodiments, the heating temperature ranges from about 500° C. to about 800° C. (FIG. 15). In some embodiments, the activation temperature is about 750° C.

[0100] In some embodiments, the carbon precursor is synthesized by polymerizing a carbon source. In some embodiments, the polymerization occurs by exposing the carbon source to an oxidant, such as iron (III) chloride (FeCl<sub>3</sub>) in the presence of acetonitrile (CH<sub>3</sub>CN).

[0101] In some embodiments, the materials of the present disclosure are prepared from affordable and readily available carbon sources. In some embodiments, the carbon sources include oxygen-containing carbons. In some embodiments, the oxygen containing carbon sources are rich in alcohol. In some embodiments, the carbon sources lack heteroatoms such as nitrogen, sulfur, and combinations thereof. As such, in some embodiments, the formed materials of the present disclosure also lack such heteroatoms.

[0102] In some embodiments, the materials of the present disclosure are prepared by heating a biological material. In some embodiments, the biological material includes, without limitation, sawdust, coconut husk, and combinations thereof. In some embodiments, the biological material is chosen from at least one of the following: sawdust and coconut husk.

[0103] In some embodiments, the carbon source that is utilized to make the materials of the present disclosure is furfuryl alcohol (FFA) (e.g., purchasable from Sigma Aldrich at a price of \$354 for 25 kg with purity >98%) (e.g., Table 4). In some embodiments where the carbon source is FFA, the formed carbon precursor is polyfurfuryl alcohol (PFFA).

[0104] In some embodiments, the materials of the present disclosure are prepared by heating an organic polymer precursor or biological material. In some embodiments, the organic polymer precursor or biological material includes oxygen in a functional group. In some embodiments, the functional group is a furyl. In some embodiments, the organic polymer precursor is FFA. In some embodiments, the organic polymer precursor polymerizes to form polyfurfuryl alcohol (PFFA). In some embodiments, PFFA is prepared by the polymerization of furfuryl alcohol with a catalyst. In some embodiments, the catalyst is FeCl<sub>3</sub>.

[0105] In some embodiments, the functional group is an anisyl. In some embodiments, the organic polymer precursor polymerizes to form polyanisyl alcohol (PAA). In some embodiments, PAA is prepared by the polymerization of anisyl alcohol with a catalyst. In some embodiments, the catalyst is a protic acid.

[0106] A more specific method of making the materials of the present disclosure is illustrated in FIG. 21A. In this illustration, the FFA is polymerized by using FeCl<sub>3</sub> as the oxidant. In a typical synthesis, a solution of FeCl<sub>3</sub> is prepared by solubilizing FeCl<sub>3</sub> in CH<sub>3</sub>CN. FFA is then mixed with CH<sub>3</sub>CN and slowly added to the FeCl<sub>3</sub> solution. The mixture is then magnetically stirred for 24 hours at room temperature. The polymerized product, brown colored PFFA, is then separated by filtration over a sintered glass funnel, washed thoroughly with abundant distilled water, and then with acetone. This is followed by drying at 40° C. for 12 hours. The yield of the final product was ~98%.

[0107] Next, the porous carbon was chemically activated by heating a PFFA-KOH mixture (KOH/PFFA at a weight ratio of 3) in inert atmosphere. The mixture was then placed inside a quartz tube/tube furnace setup and heated for 1 hour at a fixed temperature in the 500-800° C. range, under a flow of Ar. The activated OPC sample was then thoroughly washed several times with diluted HCl and distilled water and dried on a hot plate at 70° C. for 12 hours.

[0108] In some embodiments, the KOH/PFFA ratio can be varied. In some embodiments, the activation temperatures and the PFFA-KOH mixing procedure can be varied.

#### [0109] Use of Materials for Gas Capture

[0110] The materials of the present disclosure can be utilized to capture and selectively remove various gases (e.g., CO<sub>2</sub>, CH<sub>4</sub>, and combinations thereof) from various environments. Additional embodiments of the present disclosure pertain to methods of utilizing the materials of the present disclosure for the separation of a mixture of gases by preferential adsorption and selective desorption. Further embodiments of the present disclosure pertain to methods of utilizing the materials of the present disclosure for the capture of CO<sub>2</sub> from various environments. In some embodiments, the environments include an atmosphere or an environment that contains a mixture of gases. In some embodiments, the methods of the present disclosure pertain to processes for separating CO<sub>2</sub> from natural gas by exposing the natural gas to the materials of the present disclosure.

[0111] In some embodiments, the methods of the present disclosure utilize the materials of the present disclosure in a process in which selectivity and separation of two gases (such as CH<sub>4</sub> and CO<sub>2</sub>) is accomplished by a combination of an adsorption process that favors one of the components (e.g., selectivity of CO<sub>2</sub> over CH<sub>4</sub>). Thereafter, the desorption of the two components from the carbon materials can be significantly different by control over various parameters, such as temperature, pressure, and combinations thereof. In some embodiments, such control allows for the specific desorption of one of the components prior to the other (e.g., CH<sub>4</sub> over CO<sub>2</sub>). In some embodiments, the overall process allows for the selective separation of at least two gaseous components.

[0112] In some embodiments, the materials of the present disclosure differentiate between CH<sub>4</sub> and CO<sub>2</sub> adsorption as well as desorption. In some embodiments, the selectivity of adsorption is further enhanced since the pressure/temperature dependencies of the desorption of CH<sub>4</sub> and the desorption of CO<sub>2</sub> are distinct from each other such that they may be used to improve separation. Thus, in some embodiments, a mixture of adsorbed CH<sub>4</sub> and CO<sub>2</sub> will desorb under different conditions: the CH<sub>4</sub> first and the CO<sub>2</sub> second. In

some embodiments, this difference means that the overall adsorption/desorption selectivity of CH<sub>4</sub> and CO<sub>2</sub> is higher than prior materials.

[0113] In some embodiments, the materials of the present disclosure can be used for the selective capture of CO<sub>2</sub> from various environments. In some embodiments, the materials of the present disclosure can be utilized for the selective capture of CO<sub>2</sub> over hydrocarbons in the environment (e.g., CH<sub>4</sub>). In some embodiments, the adsorption of CO<sub>2</sub>/CH<sub>4</sub> mixtures and measurement of the desorption selectivity can be varied.

#### [0114] Applications and Advantages

[0115] The methods and materials of the present disclosure can provide numerous advantages. For instance, in some embodiments, the methods and materials of the present disclosure can be utilized for the selective removal of CO<sub>2</sub> from natural gas (e.g., methane) that contains various amounts of CO<sub>2</sub> (e.g., 10-20 mol % of CO<sub>2</sub>). Such an application is an important goal in the field of oil and natural gas, since contaminant CO<sub>2</sub> decreases its power efficiency. For an ideal gas adsorbing material, the major requirements are as follows: it should be cheap, simple to synthesize, demonstrate reproducible and high gas uptake property, and complete desorption of CO<sub>2</sub> at low pressure. In various embodiments, the materials of the present disclosure possess all of these properties.

[0116] In some embodiments, the methods and materials of the present disclosure can be utilized for the separation of CO<sub>2</sub> from natural gas at a source where low to medium levels of CO<sub>2</sub> are present. In some embodiments, the methods and materials of the present disclosure can be used as a secondary recovery method for treating CH<sub>4</sub>/CO<sub>2</sub> mixtures in which CO<sub>2</sub> is the major component. In some embodiments, such mixtures include high-pressure samples that are the result of an initial CH<sub>4</sub>/CO<sub>2</sub> separation using traditional methods.

[0117] The materials of the present disclosure can also provide numerous advantages. In particular, among the most efficient solid sorbents for capturing CO<sub>2</sub> from natural gas or atmosphere, MOFs and KOH aided chemically activated PC materials with large surface areas and micro pores have been investigated for decades. PC composites demonstrate remarkable thermal stability and repeatability for selective gas uptake measurements.

[0118] However, to date, most of the researchers have synthesized porous carbons from carbon rich precursors that contain heteroatoms, such as nitrogen or sulfur. For sulfur rich precursors, the most common feedstock for synthesizing PCs are polythiophene or poly(2-thiophenemethanol), whereas, pyrrole or acrylonitrile are being utilized for the production of nitrogen containing PCs.

[0119] Unfortunately, the high cost of both chemicals hinders the industrial scale use of PCs produced from these materials. Based upon an analysis of the best PC materials in terms of selectivity and CO<sub>2</sub> uptake, Applicants have noted that the common link is not the presence of strong Lewis base species such as N or S, but the presence of oxygen. Thus, Applicants envision that oxygen is an important component for selectivity and high adsorption of gases (e.g., CO<sub>2</sub> and/or CH<sub>4</sub>) in the materials of the present disclosure.

#### Additional Embodiments

[0120] Reference will now be made to more specific embodiments of the present disclosure and experimental results that provide support for such embodiments. However, Applicants note that the disclosure below is for illustrative purposes only and is not intended to limit the scope of the claimed subject matter in any way.

#### Example 1. Preparation of Porous Carbon Materials

[0121] This Example provides processes for the preparation of various porous carbon materials.

##### Example 1.1. Synthesis of Activated Porous Carbon (PC) from Coconut Shell

[0122] Pieces of dry coconut shell were placed inside a quartz tube/tube furnace setup and carbonized for 1 hour at 450° C., under a flow of Ar (flow rate 500 sccm). The carbonized product (500 mg) was thoroughly mixed with potassium hydroxide (KOH) powder (1.0 g). The mixture was then placed inside a quartz tube/tube furnace setup, dried for 20 minutes and then heated for 1 hour at a fixed temperature of 600° C. under continuous flow of Argon (flow rate of about 600 sccm), washed with distilled water (ca. 4 L) and then with acetone (ca. 1 L) and dried at 80° C. for 12 hours.

##### Example 1.2. Synthesis of Nitrogen-Containing Porous Carbon (NPC) from Polypyrrole

[0123] The polymerized carbon precursor polypyrrole was synthesized using FeCl<sub>3</sub> as a catalyst following a modification of Applicants' previous methods. In a typical synthesis, a solution of FeCl<sub>3</sub> (50 g) in CH<sub>3</sub>CN (200 mL) was prepared. Next, a solution of pyrrole (5.0 g) in CH<sub>3</sub>CN (50 mL) was slowly added to the previous solution. The mixture was stirred for 24 hours. The polymerized product was then separated by filtration, washed thoroughly with distilled water (ca. 4 L) and then with acetone (ca. 1 L) and dried at 80° C. for 12 hours. The yield of the final product was ~98%. The polypyrrole was chemically activated by heating with an excess (2 or 4 fold by weight) of KOH in inert atmosphere. In a typical activation process, polypyrrole (500 mg) was thoroughly mixed with KOH (1.0 g) that had been crushed to a fine powder in a mortar. The mixture was then placed inside a quartz tube within a tube furnace, dried for 20 minutes and then heated for 1 hour at a fixed temperature in the 500-800° C. range, under a flow of Ar (flow rate 600 sccm). The activated samples were then thoroughly washed with diluted HCl (1.4 M, 100 mL) and several times with distilled water until the filtrate attained neutral pH 7. Finally, the activated PC was dried on a hot plate at 70° C. for 12 hours.

##### Example 1.3. Synthesis of Polyfurfuryl Alcohol (PFFA)

[0124] In a typical synthesis, a solution was prepared by dissolving FeCl<sub>3</sub> (50 g) in CH<sub>3</sub>CN (200 mL). To this a solution of furfuryl alcohol (5 g, Sigma Aldrich, 98%) mixed with CH<sub>3</sub>CN (50 mL) was slowly added. The mixture was stirred for 24 hours under continuous argon purging. The polymerized product, brown colored polyfurfuryl alcohol (PFFA) was separated by filtration, washed thoroughly with

DI water (ca. 4 L) and acetone (500 mL), before being dried at 40° C. for 12 hours under vacuum (Yield=98%).

**Example 1.4. Conversion of PFFA to Oxygenated Porous Carbon (OPC)**

[0125] In a typical activation process, PFFA (500 mg) was thoroughly mixed with KOH powder (1.5 g, crushed previously) in a mortar for 10 minutes. The mixture was then placed inside a quartz tube/tube furnace, dried for 20 minutes and then heated for 1 hour at 500, 600, 700 or 750° C., under a flow of Ar (99.9%, flow rate 600 sccm). The activated samples were then washed with HCl (100 mL, 1.4 M) and DI water until the filtrate attained pH=7. The product was dried at 70° C. for 12 hours under vacuum. The yield of activated PC materials depended on the activation temperature: OPC<sub>500</sub>=55%, OPC<sub>600</sub>=40%, OPC<sub>700</sub>=30%, and OPC<sub>750</sub>=25-27%.

**Example 2. Characterization of the Porous Carbon Materials**

[0126] This example provides various data relating to the characterization of the porous carbon materials in Example 1.

[0127] The volumetric uptake measurements (sorption and desorption) of CO<sub>2</sub> and CH<sub>4</sub> by the porous carbons were performed in an automated Sievert instrument (Setaram PCTPRO). Various PC samples were first crushed into powders and packed in a stainless steel autoclave sample cell. Initial sample pre-treatment was carried out at 130° C. for 1.5 hours under high vacuum. The free volume inside the sample cell was determined by a series of calibration procedures done under helium. Gas uptake experiments were carried out with high purity research grade CO<sub>2</sub> (99.99%) and CH<sub>4</sub> (99.9%) at 24° C.

[0128] FIG. 1A shows a plot of the uptake of CO<sub>2</sub> at 30 bar as a function of the apparent Brunauer-Emmett-Teller (BET) surface area ( $S_{BET}$ ) for all the PC adsorbent measured. As expected, an increase in surface area correlates with an increase in CO<sub>2</sub> uptake. However, any value above 2,800

m<sup>2</sup>g<sup>-1</sup> does not appear to improve adsorption. Thus, continued attempts to create even higher surface area materials may not result in any further improvements in CO<sub>2</sub> uptake. [0129] It is envisioned that increased total pore volume ( $V_p$ ) will facilitate increased CO<sub>2</sub> adsorption. However, as shown in FIG. 1B, it appears that for pore volumes over 1.35 cm<sup>3</sup>g<sup>-1</sup>, there is not a resulting greater uptake.

[0130] The aforementioned trends were for the highest pressures. However, the homologous series PPy-T-2 (T=500, 600, 700, and 800° C.) along with the precursor (PPy) allows for a comparison across a range of pressures.

[0131] FIGS. 1C and 1D show the relationship between CO<sub>2</sub> uptake and BET surface area (FIG. 1C) and total pore volume (FIG. 1D) for different pressures in the range of 5-30 bar. As expected, these plots clearly show a significant effect of pressure on the CO<sub>2</sub> uptake (i.e., higher pressures result in higher uptake). Moreover, the point at which increased surface area (or total pore volume) does not increase CO<sub>2</sub> uptake decreases with decreased pressure. Thus, whereas at 30 bar CO<sub>2</sub> pressure increasing the surface area above 2,800 m<sup>2</sup>g<sup>-1</sup> does not improve adsorption, at 5 bar this value decreases to 1300 m<sup>2</sup>g<sup>-1</sup> (FIG. 1C). This suggests a greater diminution of returns in attempting to create high surface area adsorbents if lower pressures are to be used in the system. The effect is similar for total pore volume, where at 5 bar it appears that any pore volume over 0.5 cm<sup>3</sup>g<sup>-1</sup> does not result in greater uptake.

[0132] Furthermore, a linear trend has been observed between surface area and pore volume for the majority of the samples studied (FIG. 1E). However, many of the samples show a divergence from the trend. The aforementioned results demonstrate a higher pore volume than expected. Furthermore, Applicants note that the aforementioned porous carbons have some of the highest CO<sub>2</sub> uptake performances.

[0133] FIG. 2 shows the relationship between the activation temperature and the CO<sub>2</sub> uptake for the porous carbon samples listed in Table 1. The general trend is increasing uptake with increased activation temperature with a possible maximum between 700 and 800° C.

TABLE 1

Sample <sup>a</sup>	C (wt %) <sup>b</sup>	O (wt %) <sup>b</sup>	N (wt %) <sup>b</sup>	S (wt %) <sup>b</sup>	Surface area $S_{BET}$ (m <sup>2</sup> g <sup>-1</sup> )	Total pore volume (cm <sup>3</sup> g <sup>-1</sup> ) <sup>c</sup>	CO <sub>2</sub> uptake at 30 bar and 24° C. (mmol · g <sup>-1</sup> )	
Activated charcoal	94.10	5.90	0.00	0.00	845	0.43	8.45	
BPL <sup>d</sup>	91.3	8.7	0.00	0.00	951	0.49	8.66	
SD-600-4	82.24	15.80	0.00	0.00	2290	1.10	20.52	
SD-800-4	89.96	8.03	0.00	0.00	2850	1.35	22.90	
CN-600-2	88.13	11.87	0.00	0.00	1250	0.64	13.50	
PPy-500-2	72.47	17.19	10.33	0.00	1255	0.53	12.60	
PPy-600-2	74.78	19.72	5.49	0.00	2013	1.03	18.98	
PPy-700-2	90.01	9.87	0.14	0.00	2956	1.45	22.98	
PPy-800-2	91.39	8.60	0.00	0.00	3230	1.51	21.01	
PPy-800-4	90.78	9.11	0.10	0.00	3450	2.57	22.10	
PAn-600-3	84.50	6.75	8.75	0.00	1410	1.38	14.50	
SD-M-800-4	85.39	8.15	6.46	0.00	2990	2.69	23.80	
PTh-600-2	64.91	25.88	0.00	9.21	2256	1.02	18.81	

TABLE 1-continued

Summary of PC, NPC, and SPC samples studied with their elemental analysis, physical properties and CO<sub>2</sub> uptake.

Sample <sup>a</sup>	C (wt %) <sup>b</sup>	O (wt %) <sup>b</sup>	N (wt %) <sup>b</sup>	S (wt %) <sup>b</sup>	Surface area S <sub>BET</sub> (m <sup>2</sup> g <sup>-1</sup> )	Total pore volume (cm <sup>3</sup> g <sup>-1</sup> ) <sup>c</sup>	CO <sub>2</sub> uptake at 30 bar and 24° C. (mmol · g <sup>-1</sup> )
PTh-700-2	82.47	13.01	0.00	4.51	1980	0.99	20.32
PTh-800-2	88.18	7.24	0.00	4.58	2890	1.43	22.87

<sup>a</sup>Precursor-temperature-KOH:precursor ratio.

<sup>b</sup>Determined by XPS.

<sup>c</sup>Determined at P/P<sub>o</sub> ~0.99.

<sup>d</sup>Purchased from Calgon Carbon Corp.

[0134] Given the relationships between surface area and pore volume with CO<sub>2</sub> uptake, it is not surprising that their relationship with activation temperature is also similar (FIGS. 3A-3B). The analysis of a series of samples prepared from N-containing polymer polypyrrole (PPy) at different activation temperatures (i.e., PPy-T-2), but otherwise under identical conditions, allows for a convenient direct comparison of the effects of temperature.

[0135] The CO<sub>2</sub> uptake plot for each sample as a function of CO<sub>2</sub> pressures is shown in FIG. 4, whereas FIG. 5 shows their corresponding N<sub>2</sub> adsorption isotherms at 77 K. It may be noticed that the shape of these isotherms is dependent on the activation temperature. The isotherm for PPy-800-2 is much steeper than that of PPy-500-2 between relative pressures of 0.4 and 1.0, indicating the variation in mesoporosity and adsorption capacity. For the homologous series of NPC materials, the estimated surface area (S<sub>BET</sub>) and the total pore volume (V<sub>p</sub>) gradually increase with activation temperature (FIGS. 6A-6B), describing the incremental trend for mildly to strongly activated samples. Between 500 and 700° C., the surface area and total pore volume increases systematically, whereas for temperatures above 700° C. no significant increment is noticed.

[0136] Besides the surface area and pore volume, another important characteristic that can be obtained from the N<sub>2</sub> adsorption isotherms is the pore size distribution (PSD) of the porous solid. FIGS. 7A-7H depict the PSDs for three different PPy-based PCs prepared under mild (T=500° C.) to strong (T=800° C.) activation conditions. The distribution plot for T=500° C. indicates that the activated PC mainly consists of micropores in the 1-2 nm range, whereas the plot for PPy-700-2 clearly shows signature of some larger pores in the 2-3.5 nm range. The most strongly activated PC and PPy-800-2 even shows a significant number of mesopores in the 3-6 nm range, in agreement with the steeper adsorption registered for relative pressures of more than 0.4.

[0137] A comparison of the variation in pore size and distribution (FIG. 7A) with the CO<sub>2</sub> uptake for the same samples (FIG. 4 and Table 1) was also made. From 500° C. to 700° C., there is a dramatic increase in the high pressure uptake, which can be associated with the generation of pores in the range of 2-3 nm. However, as may be seen from FIG. 4, there is a slight (but significant) decrease upon further activation to 800° C., even though there is an increase in the presence of larger pores. This suggests that larger pores are not necessarily ideal for a high CO<sub>2</sub> adsorption. The pore size distribution for the other top adsorbents studied shows a similar bi-modal pore structure centered on 1 nm and 1.5-2 nm.

[0138] The structural and textural morphology of the activated PPy-T-2 samples were characterized by scanning electron microscopy (SEM). FIG. 7B shows that the activated NPC contains multiple layers projected vertically upward and surfaces that are full of micron sized holes. In order to image the microporous structure of the activated sample, high resolution transmission electron microscopy (HRTEM) was utilized.

[0139] FIG. 7C displays an image demonstrating randomly distributed micropores with dimensions in the range of 0.5-1 nm for a PPy-600-2 sample. These and the images of the other samples are in agreement with the BET measurements.

[0140] Given the hazardous nature of working with KOH, the amount used in the activation process is of importance with regard to any scalability issues. Applicants have recently shown that KOH provides greater activation than borates. However, based upon the present data set for PPy-800-n (n=2, 4), it is clear that increasing the KOH: precursor ratio from 2 to 4 does not result in a change in the CO<sub>2</sub> uptake profile (FIG. 7D), despite a dramatic (70%) increase in the pore volume (Table 1).

[0141] Applicants note that PPy-800-4 has one of the highest surface areas (3450 m<sup>2</sup>g<sup>-1</sup>) measured for any PC sorbent. However, PPy-800-4 is less efficient than PPy-800-4 between 10-20 bar.

[0142] The CO<sub>2</sub> uptake for NPC and SPC samples as a function of their N or S content is shown in FIGS. 8A-8B. For both NPC (FIG. 8A) and SPC (FIG. 8B) samples, the CO<sub>2</sub> uptake is at a maximum with the heteroatom content of less than 5 wt %. The chemical composition of polypyrrole precursor and activated PPy derived NPC samples were determined by XPS (Table 1). The identity and wt % of the elements present on the sample surface were determined by XPS survey scans (e.g., FIGS. 7E and 7F). These spectra revealed that the precursor polypyrrole and activated NPCs are primarily composed of C, O, and N. It should be noted that the O content of NPCs has been observed, but discounted as significant, except as a potential source as both Lewis acid and base moieties. Applicants note that H content is not provided by XPS data, and so percentage values measured by other techniques will vary.

[0143] As a result of chemical activation and the activation temperature, the wt % of all elements changes (Table 1). The general trend is that the wt % of C increases, whereas that of O and N decreases gradually with increasing activation temperature. The compositional dependence on the activation temperature is demonstrated for the PPy-T-2 samples (FIG. 7G). The first point to note is that the N

content decreases consistently with activation temperature (FIG. 7H). However, there is a distinct step in the O composition between 600 and 700° C. (FIG. 7H), which is mirrored in the C wt % composition (FIG. 7G). However, it is important to note that while at the highest activation temperatures the N content becomes negligible, the O content remains significant.

[0144] An equally interesting variation was observed for SPC samples (Table 1). The C content stays essentially constant between the PTh precursor and the product activated at 600° C., despite the S composition decreasing. The reason for this anomaly is the oxidation of the PC material as measured by the increased O content. As with the N content in the NPC samples, the S composition in the SPC samples decreases to a low value at the highest activation temperatures.

[0145] Based upon these results, it would appear that the presence of neither N nor S correlates in a positive manner with the CO<sub>2</sub> uptake, although in the present case a higher heteroatom content is associated to lower surface area and pore volume, hence the corresponding lower CO<sub>2</sub> uptake. Nonetheless, the limited effect of the presence of heteroatoms on CO<sub>2</sub> uptake is in line with previous results, and Applicants' proposal that the presence of N or S is not responsible for any stabilization of poly-CO<sub>2</sub> that has been proposed to be responsible for high CO<sub>2</sub> adsorption at 30 bar.

[0146] Furthermore, the source of the heteroatom also appears to affect the physical parameters and hence the CO<sub>2</sub> uptake. For example, the use of polyacrylonitrile (I, PAn) instead of polypyrrole (II, PPy) makes a significant difference suggesting the chemical speciation of the N content is important (FIG. 8C). In addition, the use of a poly-N containing heterocycle, melamine, as the N source results in an improvement in the performance (FIG. 8D). However, it is unclear whether this is a cause or effect. If the amount of CO<sub>2</sub> adsorbed is divided by the total pore volume one gets a similar value for both for PPy-800-4 and SD-M-800-4. Thus, the CO<sub>2</sub> uptake is determined by the total pore volume, but the pore volume is clearly a function of the precursor, rather than the process conditions.

[0147] As was noted with the pressure dependence of the CO<sub>2</sub> uptake on the surface area and total pore volume, the uptake appears to be less affected by the N content at lower pressures. Thus, as shown in FIG. 8E, the greatest CO<sub>2</sub> uptake at 30 bar for NPC requires N<2 wt %. However, if measured at 5 bar the uptake is almost independent of N

content at values <10 wt %. This again suggests that the need to create specialty adsorbents diminishes with decreased operating pressure.

[0148] Both NPC and SPC samples contain significant O, as do the PC samples produced from non-heteroatom containing precursors. Given that some of the PC samples perform in a comparable manner to those of NPC or SPC, N and S composition cannot be the sole key to high adsorption. While the presence of more than 5 wt % of either N or S appears to significantly lower the uptake of CO<sub>2</sub>, although this could be related to the lower surface area of the heteroatom-rich samples, the O content is far more effective for the high CO<sub>2</sub> adsorption observed with 3-16 wt % O (FIG. 9A).

[0149] In support of this observation, there are also some significant findings on the CO<sub>2</sub> capture capacity of activated PCs obtained from the carbonization of asphalt with KOH. The reduction with H<sub>2</sub> of asphalt-derived N-doped PCs causes a significant increase of capture capacity up to 26 mmol·g<sup>-1</sup>. The XPS elemental analysis of the sample before and after H<sub>2</sub> treatment shows that the sample with higher CO<sub>2</sub> capacity undergoes a significant increase of O content while the N content and type is only slightly changed. This finding supports Applicants' hypothesis that O plays a major role in establishing the CO<sub>2</sub> capture capacity of PCs. However, what appears to be more important is the combined presence of a heteroatom (i.e., Σ(O,N,S), FIG. 9B). This can be alternatively stated that the C content should be between 80-95 wt %.

[0150] Based upon the forgoing, it is possible to identify the parameters that define a PC material for maximum CO<sub>2</sub> uptake: have a surface area ≥2,800 m<sup>2</sup>g<sup>-1</sup>, a pore volume ≥1.35 cm<sup>3</sup>g<sup>-1</sup>, and a C content between 80-95 wt %. To achieve these performance parameters it is necessary to activate above 700° C. and to ensure full mixing of the KOH with the precursor. It is significant that the first two of these suggest that developing higher and higher surface area materials is unproductive, and that understanding the third may lead to the design of new PC materials. Furthermore, these values offer additional variance when the uptake of CO<sub>2</sub> is required at lower pressures.

[0151] Applicants have also investigated the CO<sub>2</sub>/CH<sub>4</sub> selectivity by measuring CO<sub>2</sub> and CH<sub>4</sub> uptake isotherms up to a high pressure limit of 10, 20 and 30 bar at 24° C. A summary of the data is shown in Table 2.

TABLE 2

Sample <sup>a</sup>	Summary of PC, NPC, and SPC samples studied with their molar gas uptakes and selectivity for CO <sub>2</sub> over CH <sub>4</sub> at different uptake pressures.								
	CO <sub>2</sub> uptake (mmol · g <sup>-1</sup> ) at			CH <sub>4</sub> uptake (mmol · g <sup>-1</sup> ) at			Molar (CO <sub>2</sub> :CH <sub>4</sub> ) uptake ratio		
	10 bar	20 bar	30 bar	10 bar	20 bar	30 bar	10 bar	20 bar	30 bar
Activated charcoal	6.27	7.51	8.45	4.28	5.44	6.03	1.46	1.38	1.41
BPL	6.30	7.87	8.66	3.24	4.96	6.18	1.94	1.59	1.40
SD-600-4	12.06	16.77	20.52	5.23	7.54	8.52	2.31	2.22	2.41
SD-800-4	13.61	18.78	22.90	6.65	9.45	10.92	2.05	1.99	2.10
CN-600-2	10.91	12.65	13.50	5.94	7.24	7.96	1.83	1.74	1.70
PPy-500-2	9.51	11.27	12.60	4.11	5.06	5.98	2.31	2.23	2.11
PPy-600-2	11.37	16.45	18.98	5.39	6.33	7.41	2.11	2.60	2.56
PPy-700-2	12.50	18.12	22.98	5.75	7.92	9.41	2.17	2.29	2.44
PPy-800-2	11.94	17.21	21.01	5.78	8.23	9.82	2.07	2.09	2.14

TABLE 2-continued

Sample <sup>a</sup>	CO <sub>2</sub> uptake (mmol · g <sup>-1</sup> ) at			CH <sub>4</sub> uptake (mmol · g <sup>-1</sup> ) at			Molar (CO <sub>2</sub> :CH <sub>4</sub> ) uptake ratio		
	10 bar	20 bar	30 bar	10 bar	20 bar	30 bar	10 bar	20 bar	30 bar
PPy-800-4	11.18	16.51	22.11	5.10	7.33	8.83	2.19	2.25	2.50
PAn-600-3	8.19	10.84	14.50	4.04	5.26	6.03	2.03	2.06	2.40
SD-M-800-4	12.09	18.70	23.76	5.58	8.12	9.41	2.17	2.30	2.52
PTh-600-2	11.17	15.42	18.81	4.77	6.12	7.37	2.34	2.52	2.55
PTh-700-2	11.51	16.67	20.32	4.62	6.87	8.01	2.49	2.43	2.54
PTh-800-2	13.10	18.80	22.87	5.81	8.55	10.14	2.25	2.20	2.26

<sup>a</sup>Precursor-temperature-KOH:precursor ratio.

[0152] FIG. 10A shows the CO<sub>2</sub> uptake plots along with the corresponding CH<sub>4</sub> uptake results in FIG. 10B. Additionally, the molar uptake selectivity (CO<sub>2</sub>/CH<sub>4</sub>) is defined by the molar ratio of adsorbed CO<sub>2</sub> and CH<sub>4</sub> at a certain pressure, i.e., at 30 bar. The dependence of molar uptake selectivity for a sorbent as a function of corresponding gas pressure is depicted in FIG. 10C. It is significant that for any particular sample, the selectivity varies with gas pressure. Of the samples investigated, PPy-600-2 demonstrated highest selectivity of 2.56 at 30 bar.

[0153] FIG. 11A shows a plot of molar CO<sub>2</sub>:CH<sub>4</sub> uptake ratio as a function of the surface area (S<sub>BET</sub>) for all the PC adsorbents measured. For low surface area samples, there is an increase in selectivity with increased surface area. However, as with uptake, further increase in surface area above 2000 m<sup>2</sup>g<sup>-1</sup> does not appear to improve selectivity. In a similar manner, increased total pore volume (V<sub>p</sub>) does facilitate increased selectivity, but only to a pore volume of 1.00 cm<sup>3</sup>g<sup>-1</sup>. No improvement in performance is shown above the aforementioned value (FIG. 11B).

[0154] The series PPy-T-2 (T=500-800° C.) allows for the direct comparison of homologous materials. In this case, it appears that the values of 2,000 m<sup>2</sup>g<sup>-1</sup> and 1.00 cm<sup>3</sup>g<sup>-1</sup> for the surface area and total pore volume (FIGS. 12A-12D) represent maxima rather than thresholds. It is possible that for any homologous series similar maxima are observed. However, the thresholds observed in FIGS. 11A-11B are useful indicators.

[0155] From Table 2, it can be seen that an activation temperature of 600° C. is a minimum for good selectivity. However, from FIG. 12C, it may be seen that for the series PPy-T-2 (T=500-800° C.), this value is actually an optimum. Such results may vary with a particular class of material. However, a lower activation temperature is required to create a material with good selectivity as compared to optimum CO<sub>2</sub> uptake (FIG. 12D), suggesting that the best attainable sorbent material will have to combine a wise trade off of selectivity and CO<sub>2</sub> capture capacity. As may be seen from a comparison of PPy-800-2 and PPy-800-4 (Table 2), increased KOH concentration during the activation step results in greater selectivity.

[0156] The molar CO<sub>2</sub>:CH<sub>4</sub> uptake ratio for NPC samples as a function of their N content is shown in FIG. 13. The selectivity for measurements at 30 bar decreases with N content above 5 wt %. In the case of SPC, there appears to be no effect on selectivity with S content (Tables 1 and 2).

[0157] These results seem to suggest that the presence of neither N nor S correlates in a direct manner with the CO<sub>2</sub>/CH<sub>4</sub> selectivity. This is in line with Applicants' previ-

ous proposal. However, in this Example, a higher heteroatom content implies a lower surface area (and total pore volume) of the sorbent materials. Hence, a definite lack of impact of N or S doping on the selectivity performance of PCs cannot be considered a priori. Significantly, as may be seen from the data in Table 2, at lower pressures (10 bar), there is almost no dependence between selectivity and heteroatom content.

[0158] As was observed with the uptake efficiency for CO<sub>2</sub>, the selectivity appears to be more a function of the total heteroatom composition (i.e., Σ(O,N,S) wt %, as presented in FIG. 14 in terms of C wt % (=100-Σ(O,N,S) wt %)). However, based upon the analysis of all the PC, NPC, and SPC materials studied, the 0 wt % seems to be the major contributor. The CO<sub>2</sub>/CH<sub>4</sub> selectivity is at a potential maximum as long as C content is below 90 wt % (i.e., for Σ(O,N,S)>10 wt %). At lower pressure (10 bar), the carbon content is possibly even higher (C<94 wt %).

[0159] A study of a wide range of PC, NPC, and SPC materials under high pressure CO<sub>2</sub> and CH<sub>4</sub> adsorption offers some useful insight into the parameters that may collectively control both the CO<sub>2</sub> uptake efficiency and the CO<sub>2</sub>/CH<sub>4</sub> selectivity. A summary of the proposed key requirements for a PC material with either good CO<sub>2</sub> uptake or good CO<sub>2</sub>/CH<sub>4</sub> selectivity is given in Table 3 based on the results presented herein.

TABLE 3

Parameter	Summary of proposed parameters required for optimum CO <sub>2</sub> uptake and CO <sub>2</sub> /CH <sub>4</sub> selectivity for PC, NPC, and SPC.	
	Uptake @ 30 bar	Selectivity @ 30 bar
Surface area (m <sup>2</sup> g <sup>-1</sup> )	>2800	>2000
Total pore volume (cm <sup>3</sup> g <sup>-1</sup> )	>1.35	>1.0
Temperature of activation (° C.)	700-800	600
Carbon content (%)	80-95	<90

[0160] As far as CO<sub>2</sub> uptake is concerned, any porous carbon material with a surface area of more than 2,800 m<sup>2</sup>g<sup>-1</sup> at 30 bar is unlikely to be improved (when prepared from the KOH activation of non-nanostructured precursors). A similar threshold appears to be true for the total pore volume of the material (1.35 cm<sup>3</sup>g<sup>-1</sup>). This suggests that seeking synthetic routes to ever higher surface area and/or high pore volume PC-based adsorbents is counterproductive.

[0161] However, it should be understood that if uptake at lower pressures is desired, these threshold values decrease

even further. This result is highly important in considering the choice of adsorbent to be used in a large scale unit. The adsorbent intended for use in a low pressure system needs a lower surface area and pore volume to perform than a potentially more expensive to manufacture material. It also impacts the formation of pelletized materials for adsorbent bed applications, since the formation of the pellet through inclusion of a binder inevitably lowers the surface area and pore volume. Applicants' results suggest that for lower pressure applications, this is not important since the uptake is less dependent on extremely high surface areas and/or pore volumes.

[0162] Given the prior interest in N- and S-doped PC materials, the results show that CO<sub>2</sub> uptake is inversely related to S and N content in SPC and NPC, respectively. However, due to the preparation process used in this Example (KOH activation), there is an intrinsic dependence between heteroatom content and surface area (total pore volume) in all sorbents. In particular, higher surface areas imply lower N or S contents.

[0163] Consequently, the use of KOH activated PCs in industrial scale units must take into account that a higher heteroatom content cannot offset the corresponding drop of CO<sub>2</sub> capture performance due to a decrease of surface area of the materials. In practical terms, it is the Σ(O,N,S) wt % or C wt % (=100-Σ(O,N,S) wt %) that is the defining factor for CO<sub>2</sub> uptake. This is true irrespective of the source of the heteroatom. However, O appears to be the main factor, since

the O that is present, it is clear that a design C<sub>x</sub>O<sub>1-x</sub> where x<0.9 would possibly make an ideal CO<sub>2</sub> adsorbent material with the best CO<sub>2</sub>/CH<sub>4</sub> selectivity. Furthermore, the goal should be a precursor where oxygen is incorporated into a cyclic moiety.

[0166] Additional experimental results and information are provided in FIGS. 15-23H and Tables 4-6. For instance, the chemical composition of OPC (750) has been thoroughly characterized via XPS, FTIR and Raman spectroscopy (FIGS. 23A-23H and Table 6), while textural properties were determined by high resolution scanning electron microscopy (FIGS. 21E-H), transmission electron microscopy (FIGS. 21I-J) and a BET Surface area analyzer (FIGS. 16A-16D). Moreover, measured values for gas uptakes have been confirmed via volumetric, gravimetric, multiple sample and cycles experiments.

[0167] To the best of Applicants' knowledge, oxygen-rich carbon materials prepared from furfuryl alcohol has never been investigated for high pressure uptake of CO<sub>2</sub> and CH<sub>4</sub>. In fact, there have been no reports of its use as a precursor for oxygen-rich porous carbon materials. In addition, a higher value for the isosteric heat of adsorption of CO<sub>2</sub> (23 kJ·mol<sup>-1</sup>) versus 13 kJ·mol<sup>-1</sup> for CH<sub>4</sub> allows Applicants to scheme a temperature dependent strategy for removing CO<sub>2</sub> from natural gas via selective adsorption and desorption of CH<sub>4</sub> and CO<sub>2</sub> in steps (FIGS. 22A-22B).

TABLE 4

Survey of different c-feedstock used for the synthesis of various PCs with high CO <sub>2</sub> uptake properties.					
PC sample	Source material for C-precursor	CAS no.	SKU pack size (Sigma Aldrich)	Price	Maximum CO <sub>2</sub> uptake at 30 bar (mmol g <sup>-1</sup> ) (wt %)
SPC (1)	2-Thiophenemethanol	636-72-6	181315-100 G	\$155 for 100 g	18.4 (81)
SPC (2)	Thiophene	110-02-1	T31801-500 G	\$47 for 500 g	—
NPC (1)	Pyrole	109-97-7	W338605-1 KG	\$315 for 1 kg	—
NPC (2)	Polyacrylonitrile	25014-41-9	181315-100 G	\$190 for 100 g	16.8 (74)
OPC (1)	Furfuryl alcohol	98-00-0	W249106-25 KG	\$60 for 1 kg (\$354 for 25 kg)	26.6 (117)
OPC (2)	Furan	110-00-9	185922-500 ML	\$54 for 500 mL	—

a C content of between 80 and 95 wt % offers the potential for high CO<sub>2</sub> uptake. However, at these levels, if the make-up is N or S, the uptake is likely reduced. It should also be observed based upon the source of the heteroatom that if heteroatoms are to be incorporated and "active", they are preferentially included using heterocycle precursors, such as melamine in the case of N, rather than other heteroatom-rich structures.

[0164] It may be assumed that the parameters that makes a good CO<sub>2</sub> adsorbent may be the same as those that make a selective material. However, Applicants' results indicate that the two are only broadly related. The levels of surface area and pore volume can be even lower for good CO<sub>2</sub>/CH<sub>4</sub> selectivity, as compared to CO<sub>2</sub> uptake (Table 3).

[0165] In summary, Applicants demonstrate in this Example that a synthetic goal for PC-based material, for both high CO<sub>2</sub> adsorption and high CO<sub>2</sub>/CH<sub>4</sub> selectivity, would comprise a C content of less than 90%. Given that neither N nor S seem to have a significant effect rather than

TABLE 5

Sample	Surface area S <sub>BET</sub> (m <sup>2</sup> g <sup>-1</sup> )	Uptake of CO <sub>2</sub> at 30 bar (mmol · g <sup>-1</sup> ) (wt %)	Uptake of CO <sub>2</sub> at 10 bar (mmol · g <sup>-1</sup> ) (wt %)	Uptake of CH <sub>4</sub> at 30 bar (mmol · g <sup>-1</sup> ) (wt %)	Ratio of CO <sub>2</sub> /CH <sub>4</sub> adsorbed at 30 bar (molar) (mass)
		C-Precursor	48	3.3 (14.5)	1.6 (7.0)
OPC (500)	1143	17.1 (75.2)	8.6 (37.8)	6.7 (10.7)	2.5 (7.0)
OPC (600)	2116	20.0 (88.1)	12.5 (55.0)	8.3 (13.3)	2.3 (6.3)
OPC (700)	2610	20.8 (91.5)	12.7 (55.9)	9.1 (14.6)	2.3 (6.2)
OPC (750)	2856	26.6 (117.0)	15.1 (66.4)	9.6 (15.5)	2.75 (7.5)
OPC (750) at 0.5° C.	2856	42.9 (188.9)	18.5 (81.5)	14.6 (23.4)	2.93 (8.0)
OPC (800)	3005	23.0 (101.2)	12.9 (56.7)	9.01 (14.4)	2.5 (7.0)
SPC <sup>a</sup>	2500	18.4 (81.0)	10.0 (44.0)	7.1 (11.3)	2.6 (7.1)

TABLE 5-continued

Survey of gas adsorption properties of various PCs with high CO <sub>2</sub> uptake capacity.					
Sample	Surface area <i>S<sub>BET</sub></i> (m <sup>2</sup> g <sup>-1</sup> )	Uptake of CO <sub>2</sub> at 30 bar (mmol · g <sup>-1</sup> ) (wt %)	Uptake of CO <sub>2</sub> at 10 bar (mmol · g <sup>-1</sup> ) (wt %)	Uptake of CH <sub>4</sub> adsorbed at 30 bar (mmol · g <sup>-1</sup> ) (wt %)	Ratio of CO <sub>2</sub> /CH <sub>4</sub> (molar) (mass)
r-NPC <sup>a</sup>	1450	16.8 (74.0)	7.1 (31.2)	1.6 (12.2)	2.2 (6.1)
Act. charcoal	845	8.4 (36.9)	6.3 (27.7)	6.0 (9.6)	1.4 (3.8)

TABLE 6

Elemental composition of various types porous carbon materials as determined by XPS excluding the contribution from elemental H.					
Sample	C (wt %) XPS	O (wt %) XPS	KOH:precursor	Surface area <i>S<sub>BET</sub></i> (m <sup>2</sup> g <sup>-1</sup> )	Total pore volume <i>V<sub>P</sub></i> (cm <sup>3</sup> g <sup>-1</sup> )
C-Precursor	69.91	30.09	—	48	0.02
OPC (500)	77.49	22.51	3:1	1143	0.78
OPC (600)	82.04	17.74	3:1	2216	1.19
OPC (700)	85.07	14.93	3:1	2610	1.46
OPC (750)	88.21	11.79	3:1	2856	1.77
OPC (800)	89.28	10.72	3:1	3005	1.92
Act. charcoal	94.10	5.90	3:1	845	0.43

**Example 3. Optimizing Carbon Dioxide Uptake and Carbon Dioxide-Methane Selectivity of Oxygen-Doped Porous Carbon Prepared from Oxygen Containing Polymer Precursors**

[0168] In this Example, Applicants report a reproducible synthesis of oxygen containing PC (OPC) by KOH activation at 500-800° C. of two oxygen containing precursor polymers: polyfurfuryl alcohol (PFFA) and polyanisyl alcohol (PAA), yielding FFA-OPC and AA-OPC, respectively. Both OPCs exhibit remarkable thermal stability and reproducible gas uptake properties for multiple cycles. Unlike other fine powder type activated PC materials, as-synthesized OPC sorbents are large pellet-like, making them a better candidate for preparing binder free solid pellet-like sorbent. The surface area and pore volumes of the OPC are independent of the precursor identity, but controlled by the activation temperature.

[0169] Similarly, the uptake of CO<sub>2</sub> is determined by the physical properties of the OPC: activation at 750° C. results in uptake that equals or out-performs existing PCs for high pressure uptake (30 bar) at 24.0° C. (FFA-OPC<sub>750</sub>: 117 wt %; AA-OPC<sub>750</sub>: 115 wt %). In contrast, while the uptake of CH<sub>4</sub> for both OPCs is greatest for samples activation at 750° C., FFA-OPC<sub>750</sub> shows significantly greater uptake compared to AA-OPC<sub>750</sub>, 15.5 wt % versus 13.7 wt %, respectively. As a consequence, AA-OPC<sub>750</sub> demonstrates optimal selectivity for CO<sub>2</sub> capture over CH<sub>4</sub> uptake (AA-OPC<sub>750</sub>: V<sub>mass</sub>(CO<sub>2</sub>/CH<sub>4</sub>)=8.37 at 30 bar) as compared to other reported PCs. A higher value for the isosteric heat of adsorption of CO<sub>2</sub> (33 kJ mol<sup>-1</sup>) versus CH<sub>4</sub> (14 kJ mol<sup>-1</sup>) suggests a new temperature dependent strategy for removing CO<sub>2</sub> from natural gas via selective adsorption and desorption cycles. The differences in performance for CH<sub>4</sub> uptake between FA-OPC and AA-OPC, prepared under identical

conditions, suggests that the structure of the precursor (heterocyclic versus exocyclic oxygen) is an additional variable in the design of new OPC materials.

[0170] In this Example, Applicants envision that an ideal PC would have a surface area of more than 2,800 m<sup>2</sup>g<sup>-1</sup>, a pore volume of more than 1.35 cm<sup>3</sup>g<sup>-1</sup>, and an oxygen content of between 5-20%. In this regard, Applicants have concentrated research efforts in developing routes to such materials that allow for low cost and reproducible synthesis.

[0171] Furfuryl alcohol (FA) has previously been formed into a highly cross-linked precursor via acid catalysis that can be converted to a PC. However, the process results in only a modest surface area and adsorption not sufficient to reach the performance parameters listed above. In this Example, Applicants report that, through FeCl<sub>3</sub> catalyzed polymerization and activation of polyfurfuryl alcohol (PFFA), an oxygenated PC (OPC) sorbent may be prepared which demonstrated higher room temperature CO<sub>2</sub> uptake as compared to other PC materials.

[0172] Applicants have shown that process conditions (temperature and KOH:precursor ratio) control the formation of micro (<2 nm) versus meso (>2 nm) porosity that is responsible for the highest CO<sub>2</sub> uptake. Although there appeared to be no significant difference in the performance as a function of the precursor, in creating nitrogen-doped PCs (NPCs) it was noted that incorporation of nitrogen into 6 versus a 5-membered cyclic precursor made a significant difference in the performance. Thus, there is interest as to whether using identical process conditions the precursor makes any significant effect. Applicants have therefore investigated a new OPC precursor polyanisyl alcohol (PAA) to compare with PFFA.

[0173] Moreover, if OPC is to be scaled, the cost of the catalyst used for PFFA, and similar polymeric precursors, is an issue to be addressed. Anisyl alcohol (4-methoxybenzyl alcohol), which is used as fragrance and flavourant and thus produced on a large scale, represents a low cost OPC precursor, while the formation of the polymer feedstock for OPC, polyanisyl alcohol (PAA), is synthesized by treating anisyl alcohol with concentrate H<sub>2</sub>SO<sub>4</sub> in a single step.

**Example 3.1. Materials and Methods**

[0174] FeCl<sub>3</sub>, furfuryl alcohol (Sigma Aldrich, 98% purity), anisyl alcohol (Sigma Aldrich, 98% purity), CH<sub>3</sub>CN, powdered KOH, distilled water, acetone, HCl, Ar (99.9% pure), CO<sub>2</sub> (99.99% pure, Matheson TRIGAS) and CH<sub>4</sub> (99.9% pure) were used as supplied. The SPC and NPC samples used as comparison were synthesized from 2-thiophenemethanol and polyacrylonitrile (Sigma Aldrich), respectively, following protocols previously described.

[0175] The chemical composition of the polymer and porous carbon materials were determined by X-ray photo-electron spectroscopy (XPS), Fourier transform infrared spectroscopy (FTIR) and Raman spectroscopy. The XPS measurements were carried out in a PHI Quanta 600 scanning XPS microprobe. The wt % of chemical elements was determined by XPS survey scans with pass energy of 140 eV.

[0176] For detailed elemental analysis high-resolution multi-cycle elemental scans with pass energy 26 eV was performed. Each spectrum was then deconvoluted by appropriate basis functions. Before spectral fitting, each spectrum was corrected for reference binding energy for C1s to 284.8

eV. FTIR spectral measurements were performed in a Nicolet FTIR Infrared Microscope equipped with a liquid N<sub>2</sub> cooled detector. Raman spectra of solid samples were measured in a Renishaw Raman microscope equipped with a 514 nm excitation laser. Scanning electron microscopic images were obtained by a FEI Quanta 400 ESEM FEG high-resolution field emission scanning electron microscope. The high-resolution TEM images of activated OPC's were obtained by a JEOL 2100 field emission gun transmission electron microscope.

[0177] The textural properties: surface areas, distributions of pore volumes and total pore volume of carbonaceous materials were obtained by analyzing N<sub>2</sub> sorption isotherms (measured at 77 K), measured in a Quantachrome Autosorb-3b BET Surface Analyzer.

[0178] The surface area ( $S_{BET}$ ) was calculated by the multipoint BET (Brunauer-Emmett-Teller) method. Before measurements, samples were dried at 140° C. for 12 hours under high vacuum system equipped with a liquid N<sub>2</sub> cold trap. The apparent BET surface area ( $S_{BET}$ ) of the activated PC samples was calculated from the N<sub>2</sub> adsorption isotherm in the partial pressure (P/P<sub>0</sub>) range of 0.05-0.30 and the total pore volume ( $V_P$ ) was estimated from the amount of N<sub>2</sub> adsorbed at P/P<sub>0</sub>=0.99. The distributions of pore volumes were determined by analyzing the data via non-local density functional theory. Selected results are given in Table 7.

#### Example 3.2. Synthesis of Polyfurfuryl Alcohol (PFFA)

[0179] In a typical synthesis, a solution was prepared by dissolving FeCl<sub>3</sub> (50 g) in CH<sub>3</sub>CN (200 mL). To this, a solution of furfuryl alcohol (5 g, Sigma Aldrich, 98%) mixed with CH<sub>3</sub>CN 50 (mL) was slowly added. The mixture was stirred for 24 hours under continuous argon purging. The polymerized product, brown colored polyfurfuryl alcohol (PFFA) was separated by filtration, washed thoroughly with DI water (ca. 4 L) and acetone (500 mL), before being dried at 40° C. for 12 hours under vacuum (Yield=98%).

#### Example 3.3. Synthesis of Polyanisyl Alcohol (PAA)

[0180] In a typical synthesis, concentrated H<sub>2</sub>SO<sub>4</sub> (~6 mL) was slowly added dropwise to a glass beaker containing anisyl alcohol (10 g) in three steps. In each step, H<sub>2</sub>SO<sub>4</sub> (2 mL) was added in drops to the glass beaker, stirred with a

glass stirrer and a purple colored solid polymer of polyanisyl alcohol was formed. The synthesized polymer was separated from the mixture. To avoid over heating of reactants, the glass beaker was kept surrounded by a water/ice mixture. The reaction process continued until all the anisyl alcohol was converted into solid polymer. The synthesized polymer was washed with DI water (4x50 mL) to remove excess acid and then with acetone (200 mL). The solid polymer was then crushed into powder, transferred to a glass beaker and quickly washed with acetone (100 mL) and dried at room temperature for 12 hours under vacuum. The final product was a dark brown colored semi-soft mixture of PAA and trace amount of acetone, which helps mixing of polymer with KOH before chemical activation.

#### Example 3.4. Conversion of Polymer Precursors to Oxygenated Porous Carbon (OPC)

[0181] In a typical activation process, either PFFA or PAA (500 mg) was thoroughly mixed with KOH powder (1.5 g, crushed previously) in a mortar for 10 minutes. The mixture was then placed inside a quartz tube/tube furnace, dried for 20 minutes and then heated for 1 hour (for AA-OPC 30 minutes) at 500, 600, 700, 800 or 750° C., under a flow of Ar (99.9%, flow rate 600 sccm). The activated samples were then washed with HCl (100 mL, 1.4 M) and DI water until the filtrate attained pH=7. The product was dried at 70° C. for 12 hours under vacuum. The yield of activated PC materials depended on the activation temperature (e.g., FFA-OPC<sub>500</sub>=55%, FFA-OPC<sub>600</sub>=40%, FFA-OPC<sub>700</sub>=30%, FFA-OPC<sub>750</sub>=25-27%, and FFA-OPC<sub>800</sub>=15%).

#### Example 3.5. CO<sub>2</sub> and CH<sub>4</sub> Uptake Measurements

[0182] The volumetric uptake measurements (pressure dependent excess isotherms) of CO<sub>2</sub> and CH<sub>4</sub> were performed in an automated Sievert instrument (Setaram PCT-PRO). Various OPC samples were first crushed into powders and packed in a stainless steel autoclave sample cell. Initial sample pre-treatment was carried out at 130° C. for 1.5 hours under high vacuum. The free volume inside the sample cell was determined by a series of calibration procedures done under helium. Gas uptake experiments were carried out with high purity research grade CO<sub>2</sub> (99.99% purity, Matheson TRIGAS) and CH<sub>4</sub> (99.9% purity). The gravimetric uptake measurements were performed in a Rubotherm magnetic suspension balance instrument (Rubotherm, Germany). A summary of selected results is given in Table 7.

TABLE 7

CO<sub>2</sub> and CH<sub>4</sub> uptake properties (@ 24° C.) in comparison with commercial PC samples of OPC samples prepared from polyfurfuryl alcohol (FFA-OPC) and polyanisyl alcohol (AA-OPC).

Sample <sup>a</sup>	Surface area	Total pore	Uptake CO <sub>2</sub>		Uptake CO <sub>2</sub>		Uptake CH <sub>4</sub>		Molar ratio	Mass ratio
	$S_{BET}$	$V_P$	(mmol · g <sup>-1</sup> ) <sup>e</sup>	(wt %)	(mmol · g <sup>-1</sup> )	(wt %)	(mmol · g <sup>-1</sup> )	(wt %)	CO <sub>2</sub> /CH <sub>4</sub>	CO <sub>2</sub> /CH <sub>4</sub>
FFA-OPC <sub>500</sub>	1143	0.78	8.6	37.8	17.1	75.2	6.7	10.7	2.5	7.0
FFA-OPC <sub>600</sub>	2116	1.19	12.5	55.0	20.0	88.1	8.3	13.3	2.4	6.6
FFA-OPC <sub>700</sub>	2610	1.46	12.7	55.9	20.8	91.5	9.1	14.6	2.3	6.3
FFA-OPC <sub>750</sub> <sup>b</sup>	2856	1.77	15.1	66.4	26.6	117.0	9.6	15.5	2.8	7.6
			(18.5)	(81.5)	(42.9)	(188.9)	(14.6)	(23.4)	(2.9)	(8.0)
FFA-OPC <sub>800</sub>	3005	1.92	12.9	56.7	23.0	101.2	9.0	14.4	2.5	7.0
AA-OPC <sub>500</sub>	853	0.49	6.7	29.7	9.5	41.6	3.8	6.1	2.7	7.3
AA-OPC <sub>600</sub>	1980	1.13	11.6	50.9	17.6	77.3	6.8	10.9	2.6	7.1
AA-OPC <sub>700</sub>	2700	1.54	11.9	52.6	22.4	98.5	7.9	12.7	2.8	7.8
AA-OPC <sub>750</sub> <sup>b</sup>	3310	1.87	13.9	61.0	26.0	114.5	8.5	13.7	3.0	8.4
			(17.6)	(77.5)	(39.3)	(172.9)	(10.5)	(16.8)	(3.7)	(10.3)

TABLE 7-continued

CO <sub>2</sub> and CH <sub>4</sub> uptake properties (@ 24° C.) in comparison with commercial PC samples of OPC samples prepared from polyfurfuryl alcohol (FFA-OPC) and polyanisyl alcohol (AA-OPC).										
	Surface area S <sub>BET</sub>	Total pore volume V <sub>P</sub>	Uptake CO <sub>2</sub> @ 10 bar		Uptake CO <sub>2</sub> @30 bar		Uptake CH <sub>4</sub> @30 bar	Molar ratio CO <sub>2</sub> /CH <sub>4</sub>	Mass ratio CO <sub>2</sub> /CH <sub>4</sub>	
Sample <sup>a</sup>	(m <sup>2</sup> g <sup>-1</sup> ) <sup>e</sup>	(cm <sup>3</sup> g <sup>-1</sup> ) <sup>f</sup>	(mmol · g <sup>-1</sup> )	(wt %)	(mmol · g <sup>-1</sup> )	(wt %)	(mmol · g <sup>-1</sup> )	(wt %)	@30 bar	@30 bar
AA-OPC <sub>800</sub>	3040	2.27	9.6	42.2	21.8	96.0	8.3	13.2	2.6	7.2
Act. Charcoal <sup>c</sup>	845	0.47	6.3	27.6	8.5	37.2	6.0	9.7	1.4	3.9
BPL <sup>d</sup>	951	0.53	6.30	27.7	8.7	38.1	6.18	9.9	1.4	3.8

<sup>a</sup> OPC activation temperature.<sup>b</sup> Values in parenthesis performed at 0.5° C.<sup>c</sup> purchased from Mallinckrodt chemical works.<sup>d</sup> Purchased from Calgon carbon corp.<sup>e</sup> Apparent BET surface area estimated in P/P<sub>0</sub> range of 0.05-0.30.<sup>f</sup> Total pore volume measured at P/P<sub>0</sub> ~0.99

### Example 3.6. Results and Discussion

**[0183]** The experimental procedures for the synthesis of the best PC sample using KOH activation with the highest CO<sub>2</sub> uptake property rely on the optimization of two major parameters: the KOH:PFFA ratio and the temperature of activation (T<sub>a</sub>). Earlier reports suggest that the overall porosity and the surface area of a chemically activated PC material increase with KOH concentration, and initial results suggested that KOH:PFFA=3 is best for developing nano-sized micropores (1-2 nm range). Thus, Applicants' procedures were carried out by keeping KOH:PFFA ratio fixed to 3 and by activating premixed KOH-PFFA mixtures at a single temperature in the range of 500-800° C.

**[0184]** A schematic outlining the synthetic protocol for OPC from FA is presented in FIG. 24A. In the first step, a solid powder-like polymer of FA was prepared from liquid FA by the reaction in the presence of a FeCl<sub>3</sub> catalyst in CH<sub>3</sub>CN. The synthesis of polyanisyl alcohol (PAA) is more facile and involves treating anisyl alcohol with concentrate H<sub>2</sub>SO<sub>4</sub> in a single step (FIG. 24B).

**[0185]** The PFFA and PAA were then chemically activated by mixing with pre-ground KOH followed by pyrolysis at a stable temperature in the 500-800° C. range. A significant advantage of the use of the PFFA prepared in this manner, as compared to previous methods, is that it only releases a small amount of volatile product during activation, unlike other PC precursors.

**[0186]** FIGS. 25A-25B show representative images of the PFFA and the resulting FFA-OPC<sub>750</sub>. Both the as prepared OPC has a large pellet-like morphology. In comparison, an image of sulfur containing porous carbon (SPC) sample prepared under identical activation conditions is shown in FIG. 25C. This important structural rigidity makes OPC sorbents more appropriate for practical applications as opposed to other powder like sorbents.

**[0187]** The structural and textural morphology of the as-synthesized polymer and resulting activated OPC samples were determined by scanning electron microscopy (SEM) as represented by FIGS. 26A-26D. The PFFA and PAA precursors have a relatively dense morphology, but after activation with KOH, the resulting OPCs exhibit a texture full of micron size holes, multiple corners and edges that are absent in the precursors.

**[0188]** The related energy dispersive X-ray spectroscopy (EDS) determined elemental composition confirms the OPCs are primarily composed of carbon and oxygen (Table 8).

TABLE 8

Elemental composition of OPC as determined by XPS and EDS.				
Sample	XPS		EDS	
	C (wt %)	O (wt %)	C (wt %)	O (wt %)
PFFA-precursor	69.91	30.09	68.64	31.36
FFA-OPC <sub>500</sub>	77.49	22.51	78.64	18.85
FFA-OPC <sub>600</sub>	82.04	17.74	87.09	12.91
FFA-OPC <sub>700</sub>	85.07	14.93	89.92	10.08
FFA-OPC <sub>750</sub>	88.21	11.79	90.12	8.08
FFA-OPC <sub>800</sub>	89.28	10.72	90.58	9.42
PAA-precursor <sup>b</sup>	74.90	21.41		
AA-OPC <sub>500</sub>	76.66	23.34		
AA-OPC <sub>600</sub>	83.36	13.64		
AA-OPC <sub>700</sub>	89.37	10.63		
AA-OPC <sub>750</sub>	91.01	8.99		
AA-OPC <sub>800</sub>	91.27	8.73		

<sup>a</sup>Contributions from elemental H were excluded.<sup>b</sup>PAA-precursor contained 3.7% S residue from the acid catalyst.

**[0189]** In order to image the microporous structure of activated OPCs, high-resolution transmission electron microscopy (HRTEM) was utilized. FIGS. 27A-27C display a set of images demonstrating randomly distributed micropores with dimension in the range of 1-2 nm for FFA-OPC<sub>600</sub> and slightly larger but evenly distributed micropores for FFA-OPC<sub>800</sub> and AA-OPC<sub>800</sub> samples. These nano-sized micropores play key roles in the ultra high CO<sub>2</sub> uptake at higher pressure.

**[0190]** Further characterization to determine important structural parameters such as surface area, pore size distribution and the total pore volumes of C-precursor and different OPC specimens activated at a fixed temperature in the range of 500-800° C. with a fixed KOH/PFFA ratio of 3 was carried out by measurement of the N<sub>2</sub> adsorption isotherms (at 77 K) using a BET (Brunauer-Emmett-Teller) surface area analyzer.

**[0191]** FIGS. 28A-28B show such set of isotherms for the OPCs activated at labelled temperature. Difference in the shape of these isotherms was noticed depending on the activation temperature. The isotherm for FFA-OPC<sub>800</sub> was much steeper than that of FFA-OPC<sub>500</sub> up to a relative

pressure of 0.4 (FIG. 28A), indicating the variation in microporosity and adsorption capacity. The isotherm for AA-OPC<sub>800</sub> was shallower than that of the other samples, suggesting meso pore generation.

[0192] The estimated surface area ( $S_{BET}$ ) and the total pore volume ( $V_p$ ) gradually increased with activation temperature (FIGS. 29A-29B) describing the incremental trend for mildly to strongly activated samples. Activation between 650° C. and 800° C. the surface area for FFA-OPCs varied smoothly than that for pore volumes (FIG. 29A). In contrast, the surface area for AA-OPCs reaches an apparent maximum at 750° C. (FIG. 29B). Irrespective of these differences, both parameters increase with increasing activation temperature, with activation above 750° C. giving materials with surface area and pore volume above the threshold (i.e.,  $>2,800 \text{ m}^2\text{g}^{-1}$  and  $>1.35 \text{ cm}^3\text{g}^{-1}$ , respectively) to enable maximum CO<sub>2</sub> uptake.

[0193] FIG. 30 provides a comparison with other reported carbon based activated sorbents such as activated charcoal, SPC, NPC and asphalt derived PC specifically, explored for high pressure CO<sub>2</sub> uptakes. The values for AA-OPC<sub>750</sub> are amongst of the highest reported surface area and pore volume values for carbon based PC samples reported to date.

[0194] FIGS. 31A-31B depict the distributions of pore sizes as a function of pore width for activation temperatures (500° C.  $\leq T_a \leq 800^\circ \text{ C.}$ ) to strong ( $T_a=800^\circ \text{ C.}$ ) activation conditions. These plots show that samples activated at temperatures between 500 and 700° C. mainly consisted of micropores in the range of 1-2 nm. In contrast, the distribution plot for FFA-OPC<sub>800</sub> indicates that chemical activation at temperature of about 800° C. created some additional mesopores in the 2.0-3.5 nm range, confirming the findings from HRTEM images discussed earlier (FIG. 27B). Pores larger than 4 nm were practically absent in all samples, except for AA-OPC<sub>800</sub> where the mesopore ( $>2 \text{ nm}$ ) contribution is dominant (FIG. 31B).

[0195] As noted above, the best CO<sub>2</sub> uptake of a PC is observed with a carbon content of 80-95 wt %. The chemical composition of polymer precursors and the subsequent OPCs was determined by X-ray photoelectron spectroscopy (XPS). The identity and wt % of the elements present on the sample surface were determined by XPS survey scans for core level electrons (Table 8). The XPS data further confirms that OPC samples primarily contained C and O (the H contents are not shown in XPS).

[0196] As expected, the C and O content varied from the polymers to the OPCs during chemical activation, and for the OPC samples the general trend was that the wt % of C increased and O decreased gradually with increasing activation temperature (FIGS. 32A-32D). Based upon the analysis, samples activated between 600° C. and 800° C. fall within the range required for maximum CO<sub>2</sub> uptake.

[0197] A set of high resolution XPS elemental scan data for C1s and O1s of PFPA and FFA-OPC samples (FIGS. 33A-33B), de-convoluted by appropriate basis peaks helped Applicants identify the possible functional groups present in the precursor and numerous activated samples. For PFPA, the C1s band could be resolved into four main peaks and labelled according to probable functional groups as in poly-thiophene. Thus, these peaks were assigned to the following functional groups: sp<sup>2</sup> hybridized C=C (284.7 eV), C-C (286.1 eV), C—O—C (287.1 eV) and C=O (288.9 eV). An additional shoulder near 291.3 eV is attributed to  $\pi-\pi^*$  shake-up peak. In contrast to PFPA, the activated sample

exhibited much narrower C=C peak (FWHM: 1.3 eV versus 2.2 eV for PFPA). The resolved basis peaks under O1s spectra were attributable to two main functional groups: the C—O—C group at 533.2 eV (O within the furan ring) and the carbonyl group (C=O) at 531.8 eV. Without being bound by theory, Applicants believe that KOH induced oxidation during chemical activation at higher temperature resulted in formation of more carbonyl groups, though the absence of well resolved band for O1s made it difficult to extract the absolute proportion of these two functionalities. [0198] The nature of carbon and oxygen functional groups present in the as-synthesized PFPA and activated FFA-OPCs were further explored via FTIR spectroscopy. The IR spectrum for PFPA (FIG. 34) exhibited well defined but broad peaks originated from various IR active vibrational stretches identified as: C—O—C asymmetric stretching vibration (1020 cm<sup>-1</sup>), C=C stretching (1358 cm<sup>-1</sup>), and C=C symmetric and asymmetric stretching vibrations in the furan ring (1510 and 1585 cm<sup>-1</sup>, respectively). The frequency shift and broadness of these bands may be attributed to the aggregated phase of the synthesized polymer. In contrast to PFPA, the activated samples exhibited multiple stretching vibrations with gradually decreasing intensity. The intensity of all these peaks decreased systematically with increasing activation temperature as evidenced by the spectra of FFA-OPC<sub>500</sub> and FFA-OPC<sub>800</sub>. For FFA-OPC<sub>500</sub>, in addition to C=C stretching frequencies another shoulder peak was identified near 1710 cm<sup>-1</sup>, which could be assigned to C=O stretching vibrations. Moreover, the C—O—C and O—H functional groups that were present in the C-precursor and mildly activated samples ( $T_a=500^\circ \text{ C.}$ ) slowly removed due to chemical activation at higher temperature.

[0199] The aromatic sp<sup>2</sup> hybridized C=C and amorphous sp<sup>3</sup> hybridized C—C bonds present in PFPA and activated FFA-OPCs were further characterized by Raman spectroscopy. FIGS. 35A-35C represent a set of three normalized spectra depicting spectral changes for two major bands; the sharp graphene (G) band (1590 cm<sup>-1</sup>) and the broad disorder (D) band located (1360 cm<sup>-1</sup>), attributing to the aromatic sp<sup>2</sup> and amorphous sp<sup>3</sup> hybridized carbons, respectively. A more direct dependence for the (D/G) intensity ratio on activation temperature is shown in FIG. 35D, bottom panel. The D/G value varied from 0.56 for PFPA, to 0.75 for FFA-OPC<sub>500</sub> and 0.83 for FFA-OPC<sub>800</sub>, signifying the gradual removal of sp<sup>2</sup> and addition of sp<sup>3</sup> carbons as a result of chemical activation under mild to strong activation conditions.

### Example 3.7. CO<sub>2</sub> Uptake

[0200] Among the various types of solid porous materials that efficiently capture CO<sub>2</sub>, MOFs (metal organic frameworks), zeolites, cross-linked polyethylenimine, and a variety of powder like activated PCs play significant roles over other sorbents and widely utilized for industrial application due to their high surface area, thermal stability, low cost of synthesis, and high gas adsorption capacity with remarkable reproducibility. However, within the category of activated PC materials with high CO<sub>2</sub> uptake capacity, to date, most of the sorbents were investigated for CO<sub>2</sub> uptake performance up to a pressure limit of only 1 bar due to the limitation of available instruments. However, in industrial applications, higher pressures are needed.

[0201] For example, removal of CO<sub>2</sub> from natural gas at the wellhead needs to be optimized between 15-30 bar. Applicants have previously shown that the best PC materials

show a maximum  $\text{CO}_2$  uptake of 20–25  $\text{mmol}\cdot\text{g}^{-1}$  at 30 bar and 24° C. In this context, Applicants have carried out careful volumetric  $\text{CO}_2$  uptake experiments on the OPC sorbents as a function of gas pressure up to a limit of 30 bar and compared the results to previously reported PC samples measured under the same conditions.

[0202] In order to identify the OPC sorbent with the highest  $\text{CO}_2$  uptake capacity, Applicants measured pressure dependent  $\text{CO}_2$  uptake for a set of OPC samples prepared with a fixed KOH:polymer=3 and activated at a fixed temperature in the 500–800° C. range (FIGS. 36A–36C). Clear difference between the shapes of uptake isotherms indicates that uptake varies with activation temperature ( $T_a$ ). In particular, higher values of  $T_a$  correlated with higher uptake values for a specific adsorption pressure.

[0203] The C-precursors adsorbed negligible amount of  $\text{CO}_2$  and the most mildly activated OPC, AA-OPC<sub>500</sub> showed an uptake similar to activated charcoal. The general trend was: OPC that was activated at higher temperature contained more micropores and with larger surface area performed better. Strikingly, both FFA-OPC<sub>750</sub> and AA-OPC<sub>750</sub> captured more  $\text{CO}_2$  than their OPC<sub>800</sub> homologs; while in the case of FFA-OPC<sub>800</sub> it has a higher surface area and pore volume (Table 7).

[0204] A similar observation was reported for low pressure (up to 1 bar) gas uptake of  $\text{CO}_2$  by polypyrrole derived PCs. Applicants believe that the reason for the higher uptake performance of OPC<sub>750</sub> was that OPC<sub>800</sub> contained more mesopores larger than 2 nm. In this context, it is important to note that up to a pressure bar of 5 bar all OPC samples capture similar amount of  $\text{CO}_2$  (except the OPC<sub>500</sub> samples).

[0205] FIG. 36C displays a set of equilibrium volumetric  $\text{CO}_2$  uptakes at room temperature as a function of adsorbate pressure for various PC specimens such as activated charcoal, NPC, SPC, FFA-OPC<sub>750</sub>, and AA-OPC<sub>750</sub>.

[0206] Applicants noticed that among the all activated OPCs, though all of them captured more  $\text{CO}_2$  than previous reported SPC or NPC samples, both FFA-OPC<sub>750</sub> and AA-OPC<sub>750</sub>, demonstrated the highest  $\text{CO}_2$  capture capability. Thus, Applicants subsequently carried out repeated uptake experiments on different batches of both OPC<sub>750</sub>. The  $\text{CO}_2$  uptake result for FFA-OPC<sub>750</sub> was further verified by another gravimetric uptake experiment carried out in a Rubotherm magnetic suspension balance instrument (FIG. 36C, open circles). These uptake plots further established that at a pressure of 30 bar, FFA-OPC<sub>750</sub> exhibited an ultrahigh  $\text{CO}_2$  capture capacity of 26.6  $\text{mmol}\cdot\text{g}^{-1}$  (117 wt %), outperforming other doped PCs by a large margin. Moreover, OPC<sub>750</sub> adsorbed slightly, but repeatedly, more  $\text{CO}_2$  than the recently reported activated PCs made from asphalt Versatrol-HT (26.6 versus 26  $\text{mmol}\cdot\text{g}^{-1}$ ).

[0207] It should be noted that the latter material required multiple activation steps, pretreatment, N-addition and reduction by  $\text{H}_2$  to be capable of adsorbing such quantity of  $\text{CO}_2$ , which is in contrast with the far simpler process described herein. In contrast, OPC<sub>750</sub> is prepared from a simple precursor in a single activation step without N-addition or  $\text{H}_2$  reduction.

[0208] To the best of Applicants' knowledge, among the category of high  $\text{CO}_2$  uptake PC materials, FFA-OPC<sub>750</sub> exhibits remarkable  $\text{CO}_2$  capture properties comparable to expensive MOFs with similar apparent surface area. For example, IRMOF-1 with a surface area of 2833  $\text{m}^2\cdot\text{g}^{-1}$  captures about 21  $\text{mmol}\cdot\text{g}^{-1}$  of  $\text{CO}_2$  at 30 bar. IRMOF-6 with a surface area of 2516  $\text{m}^2\cdot\text{g}^{-1}$  captures about 19  $\text{mmol}\cdot\text{g}^{-1}$  at 30 bar. The overall volumetric  $\text{CO}_2$  uptake results at 30 and 10 bar, for various sorbents are compared in Table 7, while

the maximum amounts of gas uptakes at 30 bar for different PC samples with corresponding surface area is represented by FIG. 37.

[0209] For large scale gas uptake applications, such as removing  $\text{CO}_2$  from natural gas, it is essential for a solid sorbent to exhibit both reproducible gas uptake capability and batch to batch reproducibility. This important requirement was examined via two experiments as shown in FIGS. 18A–18B, which displays a set of pressure dependent  $\text{CO}_2$  uptake plots for different OPC<sub>750</sub> batches synthesized and activated same way. Almost identical gas adsorption characteristics, up to an upper pressure limit of 30 bar, confirmed the applicability of both OPC materials as cheap but very effective sorbent for industrial application. The other necessity for practical usage was further established by multiple cycles of gas adsorption-desorption measurements (2 cycles of adsorption and 2 cycles of desorption) that showed negligible or no hysteresis (FIG. 38C). Applicants' multiple cycle measurements and prolonged exposure to  $\text{CO}_2$  on the same OPC sample satisfied two major requirements for practical application: no degradation in quality and no drop in gas uptake capacity.

[0210] For most of the solid sorbents, the gas uptake capacity increases with decreasing capture temperature. At 0.5° C. and a pressure of 30 bar, FFA-OPC<sub>750</sub> demonstrated an ultrahigh  $\text{CO}_2$  uptake capacity that maxed to 189 wt % (43  $\text{mmol}\cdot\text{g}^{-1}$ ) that is 60% higher than room temperature uptake (FIG. 39A). For any solid porous sorbents with high surface area, the trend of gas uptake is: the higher the gas pressure, the higher the  $\text{CO}_2$  uptake and the uptake is both pressure and temperature dependent.

[0211] This result is further established by a set of plots describing the gas uptake capacity at four different uptake pressures as a function of experiment temperature (FIG. 39B). At a pressure of 5 bar, the  $\text{CO}_2$  uptake varied from 5.2 to 12.6  $\text{mmol}\cdot\text{g}^{-1}$  (increased by 142%) for a temperature change of 60 to 0.5° C.; whereas, at 30 bar, the change was significantly high, uptake varied from 12.6 to 42.9  $\text{mmol}\cdot\text{g}^{-1}$  (increased by 240%). This important result signifies the possibility of selective  $\text{CO}_2$  removal by exploiting the pressure-temperature dependent adsorption and desorption from a  $\text{CO}_2$  rich gas mixture.

### Example 3.8. $\text{CO}_2/\text{CH}_4$ Selectivity

[0212] The selective removal of  $\text{CO}_2$  from natural gas, which essentially contains  $\text{CH}_4$  and higher hydrocarbons along with other gases ( $\text{CO}_2$ ,  $\text{H}_2\text{S}$ , and  $\text{N}_2$ ), is one of the important industrial research goals, because these contaminant gases decrease power efficiency of the natural gas. The capture of  $\text{CO}_2$  from natural gas primarily relies on purification strategies that allow the gas mixture to pass through a column packed with solid porous materials that captures  $\text{CO}_2$  from the  $\text{CH}_4$ -rich environment with minimal  $\text{CH}_4$  uptake. Applicants have previously shown that, unlike total  $\text{CO}_2$  adsorption, the best  $\text{CH}_4:\text{CO}_2$  adsorption ratio requires a PC with a surface area of more than 2000  $\text{m}^2\cdot\text{g}^{-1}$ , a total pore volume of more than 1.0  $\text{cm}^3\cdot\text{g}^{-1}$ , and a carbon content of less than 90 wt %. Based upon the forgoing, both OPC<sub>750</sub> materials meet these requirements. The absolute  $\text{CO}_2:\text{CH}_4$  selectivity test was carried out by measuring volumetric  $\text{CO}_2$  and  $\text{CH}_4$  uptake isotherms up to a high pressure limit of 30 bar at 0.5 and 24.0° C. Applicants' study focused on the selectivity of FFA-OPC<sub>750</sub> and AA-OPC<sub>750</sub>.

[0213] Two sets of volumetric  $\text{CO}_2$  and  $\text{CH}_4$  adsorption uptake measurements performed on each OPC<sub>750</sub> sorbent, at 0.5 and 24.0° C. (FIGS. 40A–40B, respectively). A similar set of room temperature uptake result for activated charcoal

are presented in FIG. 40C. Here, the molar uptake selectivity ( $\eta_{CO_2}/\eta_{CH_4}$ ) is defined by the molar ratio of adsorbed CO<sub>2</sub> and CH<sub>4</sub> at a certain pressure (i.e., at 30 bar).

[0214] Although the surface area and pore volumes and the CO<sub>2</sub> uptake of the two different OPC samples appear to be essentially independent of the choice of precursor (see FIGS. 29A-29B and Table 7), the same is not true of CH<sub>4</sub> uptake. As may be seen from Table 7, the CH<sub>4</sub> uptake for FFA-OPC is greater than that for AA-OPC for any given activation temperature. Given the relationship observed in FIGS. 29A-29B, this trend is also true for surface area and pore volume (FIGS. 41A-41B). Thus, even with similar physical parameters (surface area and pore volume) OPC prepared from PFFA shows greater CH<sub>4</sub> uptake than materials prepared from PAA. Although the differences are about 10%, this results in a comparable difference in CO<sub>2</sub>/CH<sub>4</sub> selectivity, with AA-OPC samples providing better selectivity than FFA-OPC samples across the range of activation temperatures (Table 7).

[0215] Another important parameter that can be determined from FIGS. 42A-42D is the corresponding isosteric heat of adsorption of CO<sub>2</sub> and CH<sub>4</sub> for OPC<sub>750</sub> using the

function of the CO<sub>2</sub>/CH<sub>4</sub> selectivity suggest that Applicants' previous proposal is correct. The greater the relative percentage of pores less than 2 nm, the greater the CO<sub>2</sub> uptake is in line with previous suggestions. However, the comparison of FFA-OPC<sub>750</sub> and AA-OPC<sub>750</sub> provides further insight into Applicants' previous proposal that it was pores in the range of 1-2 nm that are most important in defining CO<sub>2</sub>/CH<sub>4</sub> selectivity.

[0217] In order to recognize the PC sorbent with the highest CO<sub>2</sub>/CH<sub>4</sub> selectivity, Applicants surveyed molar selectivity (at 30 bar) of recently explored PC sorbents such as SPC, NPC and activated charcoal and AA-OPC<sub>750</sub>. The absolute molar (CO<sub>2</sub>/CH<sub>4</sub>) uptake selectivity of OPC<sub>750</sub> (3.05) is greater than values for SPC (2.6), reduced-NPC (2.2) and activated charcoal (1.4) and slightly higher than the recently reported asphalt Versatrol-HT derived PC (3.0). These results clearly established that among the category of activated PC materials for selective CO<sub>2</sub> capture from natural gas, AA-OPC<sub>750</sub> is one of the best absorbents reported so far and much lower cost relative to SPC and NPC prepared from analogous polymers.

TABLE 10

Sample <sup>a</sup>	V <sub>MICRO</sub> (0-2 nm) (cm <sup>3</sup> g <sup>-1</sup> )	V <sub>NARROW</sub> (0-1 nm) (cm <sup>3</sup> g <sup>-1</sup> )	V <sub>i</sub> (1-2 nm) (m <sup>2</sup> g <sup>-1</sup> )	V <sub>MESO</sub> (2-50 nm) (cm <sup>3</sup> g <sup>-1</sup> )	V <sub>MACRO</sub> (>50 nm) (m <sup>2</sup> g <sup>-1</sup> )
FFA-OPC <sub>750</sub>	1.10	0.23 (13%)	0.87 (49%)	0.57 (32%)	0.10 (6%)
AA-OPC <sub>750</sub>	1.24	0.12 (6%)	1.12 (60%)	0.58 (31%)	0.05 (3%)

thermodynamic equations described elsewhere. In thermodynamic point of view, isosteric heat of adsorption of a gas determines the temperature change in a sorbent as a result of adsorption of adsorbate molecules to the sorbent surface and thus, it is one of the key thermodynamic parameters that can be utilized to separate this gas from a mixture of gases. The higher the difference between isosteric heats of adsorption for two gases the better will be the separation. For instance, as shown by FIGS. 42A-42D, there is a higher value for the isosteric heat of adsorption of CO<sub>2</sub> as compared CH<sub>4</sub> (Table 9), which allows Applicants to propose a temperature dependent strategy for removing CO<sub>2</sub> from natural gas via selective adsorption and desorption of CH<sub>4</sub> and CO<sub>2</sub>. The results also suggest that understanding the factors controlling the difference between the values will offer a guide to the design of future adsorbents.

TABLE 9

Isosteric heat of adsorption for CO <sub>2</sub> and CH <sub>4</sub> .		
Sample	CO <sub>2</sub> (kJ mol <sup>-1</sup> )	CH <sub>4</sub> (kJ mol <sup>-1</sup> )
FFA-OPC <sub>750</sub>	23	13
AA-OPC <sub>750</sub>	33	14

[0216] Applicants have previously reported that with regard to CO<sub>2</sub> uptake, the relative distribution of pores within defined ranges defined performance. The micro- and meso-porosity analysis of these samples was determined by the t-plot method and revealed pore volume dependencies on KOH amounts (Table 10). The absolute volumes and percentage of total pore volume for OPC<sub>750</sub> samples as a

[0218] Based upon prior work, it is known that the best CO<sub>2</sub> uptake and CO<sub>2</sub>/CH<sub>4</sub> differentiation is obtained with a defined set of parameters involving surface area, pore volume, and carbon content. The latter has been related to the relative percentage of pores less than 2 nm. These results suggested that the way to prepare an ideal PC adsorbent is to use a pre-formed O-containing precursor, and the formation of both PFFA and PAA meets these needs. Thus, the use of a designed precursor allows for the reproducible formation of an OPC material with the required physical attributes. Furthermore, unlike NPC and SPC materials, the OPC reported herein lends to pellet formation as required for scalable processes.

[0219] In this Example, the structural features of the precursor appear to be irrelevant to the OPC that is formed when considering CO<sub>2</sub> adsorption. However, this is not true for CH<sub>4</sub> adsorption and hence CO<sub>2</sub>/CH<sub>4</sub> selectivity. Based upon the results herein, and without being bound by theory, Applicants suggest that the identity of the precursor and the subsequent control over the pore structure is important for CH<sub>4</sub> adsorption and hence CO<sub>2</sub>/CH<sub>4</sub> selectivity. In conclusion, Applicants propose in this Example that, while CO<sub>2</sub> uptake is optimized by maximization of pores of less than 2 nm, the CO<sub>2</sub>/CH<sub>4</sub> selectivity requires optimization of pores in the 1-2 nm range.

#### Example 4. The Effect of KOH Concentration in Chemical Activation of Porous Carbon Sorbents for Carbon Dioxide Uptake and Carbon Dioxide-Methane Selectivity: The Relative Formation of Micro (<2 nm) Versus Meso (>2 nm) Porosity

[0220] In this Example, Applicants demonstrate that PC sorbents are synthesized from polymer precursors mixed

with a chemical activation reagent and pyrolyzed ( $>500^{\circ}\text{C}$ ). KOH is known to be the best activator for a wide range of precursors, as it creates PCs with a large surface area ( $1200\text{-}4000 \text{ m}^2\text{g}^{-1}$ ). In order to determine the optimum KOH:polymer ratio for both  $\text{CO}_2$  adsorption and  $\text{CO}_2/\text{CH}_4$  selectivity, Applicants prepared a set of five S-containing porous carbon (SPC) samples from polythiophene (PTh) with increasing KOH:PTh ratio (1 to 5), and investigated  $\text{CO}_2$  and  $\text{CH}_4$  uptake measurements on carbonaceous SPC samples up to a pressure limit of 30 bar. The SPCs have been characterized by XPS, SEM, TEM and BET surface area analysis.

[0221] Although the apparent surface area and total pore volume increased with increasing KOH concentration, the maximum  $\text{CO}_2$  uptake (5-30 bar) was demonstrated for samples with KOH:PTh=3. This equates to SPC samples with a surface area and total pore volume of  $\sim 2700 \text{ m}^2\text{g}^{-1}$  and  $1.5 \text{ cm}^3\text{g}^{-1}$ , respectively. Greater values for either parameter do not enhance the  $\text{CO}_2$  uptake, showing that it is not total porosity that is important. SPC samples formed with KOH:PTh=3 show both a maximum C composition (85%), and a maximum fraction of micro ( $<2 \text{ nm}$ ) porosity with a concomitant decrease in meso-pores ( $>2 \text{ nm}$ ). KOH:PTh=3 is also the synthetic conditions to maximize  $\text{CH}_4$  uptake (5-30 bar). However, the optimum  $\text{CO}_2/\text{CH}_4$  selectivity occurred with KOH:PTh=2. This correlates with different surface area ( $2,200 \text{ m}^2\text{g}^{-1}$ ) and total pore volume ( $1.2 \text{ cm}^3\text{g}^{-1}$ ) that required for optimum  $\text{CO}_2$  uptake.

[0222] These results suggest that process conditions that lead to high relative micro porosity need to be considered rather than total surface area or pore volume. These results also suggest that, besides surface area and total pore volume of a particular sample, the relative composition of meso and micro porosity is the defining structural feature for optimizing  $\text{CO}_2$  uptake.

electron microscopy (HRTEM) and BET surface area analysis. The XPS measurements were carried out in a PHI Quantera scanning XPS microprobe. The wt % of chemical elements was determined by XPS survey scans with pass energy of 140 eV. For detailed elemental analysis, high-resolution multi-cycle elemental scans with pass energy 26 eV was performed. Each spectrum was then deconvoluted by appropriate basis functions. Before spectral fitting, each spectrum was corrected for reference binding energy for C1s to 284.8 eV. FTIR spectral measurements were performed in a Nicolet FTIR Infrared Microscope equipped with a liquid  $\text{N}_2$  cooled detector. Scanning electron microscopic images were obtained by a FEI Quanta 400 ESEM FEG high-resolution field emission scanning electron microscope. The high-resolution TEM images of activated SPCs were obtained by a JEOL 2100 field emission gun transmission electron microscope.

[0224] The textural properties (i.e., surface areas, distributions of pore volumes and total pore volume) of carbonaceous materials were obtained by analyzing  $\text{N}_2$  sorption isotherms (measured at 77 K), measured in a Quantachrome Autosorb-3b BET Surface Analyzer. Before measurements, samples were dried at  $130^{\circ}\text{C}$ . for 6 hours under high vacuum system equipped with a liquid  $\text{N}_2$  cold trap. The apparent BET surface area (SBET) was calculated from  $\text{N}_2$  adsorption isotherms in the partial pressure ( $P/P_0$ ) range of 0.05-0.30 by the multipoint BET (Brunauer-Emmett-Teller) method. The total pore volume was estimated from the amount of adsorbed  $\text{N}_2$  at  $P/P_0=0.99$ . The distributions of pore volumes were determined by analyzing the data via non-local density functional theory. Pore volumes and surface area of micropores were determined by analyzing  $\text{N}_2$  isotherms by t-plot method. Results are given in Table 11.

TABLE 11

Summary of PC and SPC samples studied with their elemental analysis, physical properties, and  $\text{CO}_2$  uptakes.

Sample <sup>a</sup>	C (wt %) <sup>b</sup>	O (wt %) <sup>b</sup>	S (wt %) <sup>b</sup>	Surface area $S_{BET}$ ( $\text{m}^2\text{g}^{-1}$ )	Total pore volume $V_P$ ( $\text{cm}^3\text{g}^{-1}$ )	$\text{CO}_2$ uptake at 30 bar (mmol · g <sup>-1</sup> )	$\text{CO}_2$ uptake at 30 bar (mg · g <sup>-1</sup> )
Act. charcoal <sup>c</sup>	94.10	5.90	0.00	845	0.47	8.45	372
BPL <sup>d</sup>	91.30	8.70	0.00	951	0.53	8.66	381
SPC-1	76.96	14.30	8.74	1680	0.98	14.68	646
SPC-2	78.89	13.73	7.37	2180	1.22	19.18	844
SPC-3	85.53	13.70	0.77	2675	1.51	22.64	996
SPC-4	84.63	15.37	0.00	2860	1.66	21.82	960
SPC-5	84.38	15.62	0.00	2980	1.76	21.29	937
PTh	61.45	5.39	29.49	40	0.02	2.40	106

<sup>a</sup>PC-KOH:precursor ratio. All SPC samples were activated at  $700^{\circ}\text{C}$ .

<sup>b</sup>Determined by XPS.

<sup>c</sup>Purchased from Mallinckrodt chemical works.

<sup>d</sup>Purchased from Calgon carbon corp. Total pore volumes are measured at  $P/P_0 \sim 0.99$ .

#### Example 4.1. Materials and Methods

[0223]  $\text{FeCl}_3$ , 2-thiophenemethanol (purchased from Sigma Aldrich, 98% purity),  $\text{CH}_3\text{CN}$ , powdered KOH, distilled water, acetone, HCl, Ar (99.9% pure),  $\text{CO}_2$  (99.99% pure, Matheson TRIGAS) and  $\text{CH}_4$  (99.9% pure) were used as supplied. Polymer precursors and SPC materials were characterized by X-ray photoelectron spectroscopy (XPS), Fourier transform infrared spectroscopy (FTIR), scanning electron microscopy (SEM), high resolution transmission

#### Example 4.2. Synthesis of S-Containing Polymer Precursor (PTh)

[0225] The polymer precursor was prepared by a modification of previously reported protocols. A solution of 2-thiophenemethanol (5 g, Sigma Aldrich, 98% purity) mixed with  $\text{CH}_3\text{CN}$  (20 mL) was slowly added to a solution of  $\text{FeCl}_3$  (25 g) in  $\text{CH}_3\text{CN}$  (200 mL). The mixture was stirred for 2 hours under continuous Ar purging. The brown polythiophene (PTh) was separated by filtration, washed with DI water (4

L) and acetone (1 L), and dried at 60° C. for 12 hours under vacuum (Yield=98%).

#### Example 4.3. Conversion of PTh to S-Containing Porous Carbon (SPC)

[0226] In a typical activation process, PTh (500 mg) was thoroughly mixed with KOH powder (crushed previously, with KOH:PTh weight ratio varying from 1 to 5) in a mortar for 10 minutes. The mixture was then placed inside a quartz tube/tube furnace, dried for 10 minutes and then heated for 1 hour at a stable temperature of 700° C., under a flow of Ar (99.9%, flow rate 600 sccm). The activated samples were then washed with DI water, HCl (100 mL, 1.4 M) to remove excess inorganic salt residue and DI water until the filtrate attained pH=7. The product was dried at 80° C. for 12 hours under vacuum.

#### Example 4.4. CO<sub>2</sub> and CH<sub>4</sub> Uptake Measurements

[0227] The volumetric uptake measurements (pressure dependent excess isotherms) of CO<sub>2</sub> and CH<sub>4</sub> were performed in an automated Sievert instrument (Setaram PCT-PRO). Various OPC samples were first crushed into powders and packed in a stainless steel autoclave sample cell. Initial sample pre-treatment was carried out at 130° C. for 1.5 hours under high vacuum. The free volume inside the sample cell was determined by a series of calibration procedures done under helium. Gas uptake experiments were carried out with high purity research grade CO<sub>2</sub> (99.99% purity, Matheson TRIGAS) and CH<sub>4</sub> (99.9% purity). A summary of selected results is given in Table 11.

#### Example 4.5. Results and Discussion

[0228] The polymer precursor Applicants selected for the synthesis of activated sulfur containing porous carbon (SPC) sorbents is poly[2-thiophenemethanol] (PTh) synthesized by reacting with FeCl<sub>3</sub> following the protocol reported elsewhere. This polymer was further activated by a strong oxidant, KOH, at a fixed temperature under inert atmosphere.

[0229] In general, the optimization procedure for synthesis of a PC sorbent with high surface area, from a polymer precursor activated by KOH, depends on two major parameters: finding the right KOH to PTh weight ratio; and the identification of the correct temperature of activation that gave satisfactory porosity and yield. Earlier reports suggest that the porosity of a SPC sorbent increased with activation temperature. However, a final yield of the activated product decreased significantly with activation temperature above 700° C. Additionally, previous reports suggest that the overall porosity and the surface area of a chemically activated PC material increase with KOH concentration.

[0230] Therefore, Applicants synthesized a set of SPC samples activated at a fixed activation temperature with gradually increasing KOH:PTh ratio r, where r varies from 1 to 5. These samples are labelled by SPC-r (Table 11).

[0231] The structural and textural morphology of synthesized PTh and activated SPC samples were characterized by scanning electron microscopy (SEM). The precursor demonstrated more rigid rock like blunt texture (FIG. 43A), while the SEM image of a SPC-2 sample (FIG. 43B) exhibits a texture full of micron size holes, multiple corners and edges that are absent in the precursor. The energy

dispersive X-ray spectroscopy (EDS) confirmed that the SPCs are primarily composed of carbon, oxygen and sulfur.

#### Example 4.6. CO<sub>2</sub> Uptake

[0232] The volumetric CO<sub>2</sub> excess uptake (mmol of adsorbed CO<sub>2</sub> per g of sample) measurements for the SPC sorbent specimens activated at 700° C. with different KOH: PTh weight ratio are shown in FIG. 44 as a function of adsorbate pressure for the labelled SPC specimens, PTh and commercial charcoal powders (Mallinckrodt Chemical Works). In this set of isotherms, the C-precursor PTh adsorbed the least amount of CO<sub>2</sub> and the SPC-1 specimen demonstrated twice as much CO<sub>2</sub> adsorption as activated charcoal at 30 bar.

[0233] The difference in the shape of uptake isotherms confirms that gas uptake strongly depends on the KOH:PTh weight ratio (r). In particular, higher values of r correlate with higher uptake amounts for a specific adsorbate pressure (>12 bar up to r=3). Moreover, the SPC-4 and SPC-5 samples captured less CO<sub>2</sub> than SPC-3. The reproducibility of both the synthesis and the measurements is shown by a comparison of the volumetric CO<sub>2</sub> excess uptake of two batches of SPC-4 (FIG. 45).

[0234] Additional information for the dependence of gas uptake amounts at a specific pressure on the KOH:PTh weight ratio is presented by FIG. 46. The CO<sub>2</sub> capturing capacity increased from r=1 to 3 and then decreased again at higher r values. Previous low pressure studies (1 bar) results for KOH activation of petroleum coke show that KOH ratio of 3 and 4 show similar results.

[0235] Decreased uptake for SPC-4 and SPC-5 would have been expected to be a consequence of decreased surface area and/or pore volume. However, as seen from FIGS. 47A-47B, such expectation is not true. Instead, above a surface area value of 2675 m<sup>2</sup>g<sup>-1</sup> and total pore volume of 1.51 cm<sup>3</sup>g<sup>-1</sup>, the gas uptake began to drop. This indicates that there are other factors besides surface area and pore volume that influence the CO<sub>2</sub> uptake capacity of a specific SPC sample.

[0236] The chemical composition of the SPCs activated with different amounts of KOH was determined by X-ray photoelectron spectroscopy (XPS) and compared with PTh and commercial activated carbons. Applicants note that XPS only provides surface (and near surface) chemical composition that may differ from bulk chemical composition. However, surface composition is what matters in a surface adsorption process.

[0237] It should also be noted that the H content is not provided by XPS data. Therefore, percentage values measured by other techniques will vary. The wt % of elements present as determined by XPS survey scans is presented in Table 11. The PTh and consequently the SPC-r samples were primarily composed of C, O, and S and chemical activation by increasing amount KOH gradually changed wt % of all three elements. FIGS. 48A-48B depict these changes.

[0238] Applicants have previously determined that for a wide range of PCs, the maximum CO<sub>2</sub> uptake occurs when the C composition (as determined by XPS) is in the range 80-95 wt %. In this Example, this range may be further specified as being more than 85%. However, the most important observation is that the trend observed in FIGS. 48A-48B is essentially the same as in FIG. 46. In particular, as indicated in FIG. 49, the CO<sub>2</sub> uptake increases with

percentage of carbon content rather than the expected relationship with surface area or pore volume.

[0239] By consideration of the change in S content with increasing KOH:PTh ratio, it is clear that the loss of the majority of S correlates with the formation of PC samples with the highest CO<sub>2</sub> uptake (e.g., comparison between FIGS. 46 and 48B). However, replacement of S with O (at high KOH:PTh ratios) decreases the CO<sub>2</sub> uptake. Clearly, there is some significant physical change that occurs in these two regimes. In order to determine if there are distinct structural features that are associated with the C % and hence CO<sub>2</sub> uptake, Applicants have determined the pore structure changes that occur with KOH:PTh ratio.

[0240] The surface area, total pore volume and pore size distribution of SPC samples activated with different KOH:PTh ratios were determined by measuring low temperature (77 K) N<sub>2</sub> adsorption isotherms in a BET (Brunauer-Emmett-Teller) surface area analyzer. FIG. 50 shows such set of isotherms for five SPC-r samples activated at 700° C. Here, KOH:PTh ratio dependent differences in the shape of these isotherms was noticed. The isotherms for SPC-3 to SPC-5 are much steeper than SPC-1 or SPC-2 in the relative pressure range 0.05-0.3, defining rapid increase of surface area and adsorption capacity with higher amount of KOH.

[0241] The estimated surface area (S<sub>BET</sub>) and the total pore volume (V<sub>p</sub>) gradually increased with activation temperature (FIGS. 51A and 51B, respectively), describing the

contrast, the distribution plots for SPC-4 and SPC-5 indicate that chemical activation with large amounts of KOH created some additional mesopores in the 3-4.5 nm range. The SPC-5 sample even contained pores larger than 4 nm. Confirmation of the pore sizes is obtained from high resolution transmission electron microscopy (HRTEM). For example, FIG. 53 displays an image of SPC-2, demonstrating randomly distributed micropores with dimension in the range of 1-2 nm.

[0244] It is clear from FIG. 51B that total pore volumes (sum of pore volumes of narrower micro (<1 nm), micro, meso and macro-sized pores) systematically increase with KOH:PTh ratio. In addition, volume change behaves differently for different sizes of pores. The micro- and mesoporosity analysis of these samples was determined by the t-plot method and revealed pore volume dependencies on KOH amounts (Table 12).

[0245] FIGS. 54A-54B depict absolute volumes and percentage of total pore volume for a set of five SPC samples as a function of the KOH:PTh ratio. In contrast to total pore volumes (FIG. 51B), the relative pore composition of micropores (defined as <2 nm) shows a marked increase with increased KOH:PTh ratio until SPC-3, above which the fraction of the total pore volume associated with these size regimes decreases (FIG. 54A). The mesopore composition shows the obverse trend. Interestingly, the micropore volumes show the strongest dependence on KOH.

TABLE 12

Sample <sup>a</sup>	Summary of meso (>2 nm), micro (<2 nm), and narrower micropore (<1 nm) volume (V) for PC and SPC samples studied . . .				
	V <sub>MICRO</sub> (0-2 nm) (cm <sup>3</sup> g <sup>-1</sup> )	V <sub>NARROW</sub> (0-1 nm) (cm <sup>3</sup> g <sup>-1</sup> )	V <sub>i</sub> (1-2 nm) (m <sup>2</sup> g <sup>-1</sup> )	V <sub>MESO</sub> (2-50 nm) (cm <sup>3</sup> g <sup>-1</sup> )	V <sub>MACRO</sub> (>50 nm) (m <sup>2</sup> g <sup>-1</sup> )
Act. Charcoal <sup>b</sup>	0.32	0.11 (23%)	0.21 (45%)	0.11 (24%)	0.04 (8%)
BPL <sup>c</sup>	0.38	0.13 (25%)	0.25 (47%)	0.12 (23%)	0.03 (5%)
SPC-1	0.71	0.19 (19%)	0.52 (54%)	0.18 (18%)	0.09 (9%)
SPC-2	0.76	0.16 (13%)	0.60 (49%)	0.35 (29%)	0.11 (9%)
SPC-3	1.01	0.18 (12%)	0.83 (55%)	0.38 (25%)	0.12 (8%)
SPC-4	0.87	0.16 (10%)	0.71 (43%)	0.64 (38%)	0.15 (9%)
SPC-5	0.88	0.10 (6%)	0.78 (44%)	0.72 (41%)	0.16 (9%)

<sup>a</sup>PC-KOH:precursor ratio. All SPC samples were activated at 700° C.

<sup>b</sup>Purchased from Mallinckrodt chemical works.

<sup>c</sup>Purchased from Calgon carbon corp. Micropore volumes are determined by t-plot method. Micropores include pores between 0.4 to 2 nm. Within parentheses, % of total pore volumes is shown.

incremental trend for mildly to strongly activation conditions. As expected, the surface area increases with increased KOH:PTh ratio, although there is a change in the relationship above KOH:PTh=3. A similar trend is observed for the total pore volume (FIG. 51B), and the two show a near linear relationship. These demonstrate the strong influence of KOH on the porous properties of activated samples.

[0242] One key piece of information that can be obtained from the BET surface area analysis is the pore size distributions as a function of pore sizes of a specific porous solid. FIG. 52 plots pore size distribution as a function of pore size for a set of five SPCs activated with mild (KOH:PTh=1) to strong (KOH:PTh=5) activation conditions. These plots show that SPC-1 sample primarily contains pores narrower than ~2 nm. As the KOH amount increases, wider pores began to form as evidenced by the PSD plot for SPC-2.

[0243] Samples activated with minimal amount of KOH (i.e., SPC-1) contained pores in the range of 1-3 nm. In

[0246] The relationship between relative composition of the various pore sizes and the CO<sub>2</sub> uptake is shown in FIGS. 55A-55C. This clearly shows that, in order to maximize CO<sub>2</sub> uptake, activation conditions (in this case KOH:PTh ratio) should be chosen to maximize the relative narrower micro and micro pores (especially those between 1-2 nm) rather than requiring solely on ever increasing surface area or pore volume.

[0247] A comparison of FIG. 54B with FIG. 48A suggests that narrower micropore formation is associated with the increased C content. However, mesopore formation appears to be controlled by increased O content. Previous work with carbide-derived carbons (CDCs) and PCs (at 1 bar) suggests that it is the pore volume less than 1 nm that is important. In contrast, it has also been suggested that mesopores (>2 nm) are the most important. There has also been a proposal that the important sizes depend on the pressure used. Applicants' results clearly show that, at higher pressures (>10 bar) it is a larger set (1-2 nm) that is controlling CO<sub>2</sub> uptake.

#### Example 4.7. CO<sub>2</sub>/CH<sub>4</sub> Selectivity

**[0248]** The selective removal of CO<sub>2</sub> from natural gas, which essentially contains CH<sub>4</sub> and other gases such as CO<sub>2</sub>, H<sub>2</sub>S, and N<sub>2</sub>, is one of the important industrial research goals, because these contaminant gases decrease power efficiency of the natural gas. Thus, Applicants have been directed to explore selective CO<sub>2</sub> capture capacity of different carbon-based porous sorbents at different gas pressure and temperature. For an ideal sorbent for selective removal of CO<sub>2</sub> from natural gas, the sorbent should demonstrate significantly lower CH<sub>4</sub> uptake than CO<sub>2</sub>. In order to compare high pressure CH<sub>4</sub> uptake capacities of five SPC samples with their CO<sub>2</sub> uptakes, Applicants measured room temperature volumetric CH<sub>4</sub> uptake of same set of samples under similar condition.

**[0249]** FIG. 56 represents a set of such uptake isotherms. In contrast to CO<sub>2</sub> uptake isotherms, Applicants see two distinct sets of isotherms. One set comprises SPC-1 and SPC-2 and the other for SPC-3, 4, and 5. This feature is further demonstrated by a set of plots showing dependence of CH<sub>4</sub> uptake on the KOH:PTh weight ratio of the corresponding sorbent at a specific capture pressure (FIG. 57). For example, at 30 bar, there was negligible difference in CH<sub>4</sub> uptakes of all three samples SPC-3 to 5 (~9 mmol·g<sup>-1</sup>), suggesting that the amount of KOH had much weaker effect on the CH<sub>4</sub> uptake property relative to than CO<sub>2</sub> uptake, though surface area and porosity had changed significantly.

**[0250]** The molar uptake selectivity (molar CO<sub>2</sub>:CH<sub>4</sub> uptake ratio) for the SPC samples as a function of gas pressure is shown in FIG. 58A. The selectivity traces for SPC-1 to SPC-3 varied smoothly between 10 to 30 bar. The dependence of high pressure selectivity at 30 bar on the KOH:PTh ratios, surface area and total pore volume of the corresponding SPCs are presented in FIGS. 58B-58D, respectively. Surprisingly, the SPC-2 sample (with surface area=2180 m<sup>2</sup>·g<sup>-1</sup> and total pore volume=1.22 cm<sup>3</sup>·g<sup>-1</sup>) demonstrated highest molar selectivity (2.68) at 30 bar, though SPC-3 exhibited the highest CO<sub>2</sub> uptake.

**[0251]** The shift from KOH:PTh ratio of 3 to 2 for optimum selectivity as opposed to uptake for both CO<sub>2</sub> and CH<sub>4</sub> is due to the relative shape of the uptake as a function of reagent ratios (e.g., comparison of FIGS. 46 and 57). While the CO<sub>2</sub> uptake increased uniformly with KOH:PTh ratio from 1 to 3, that for CH<sub>4</sub> is a step function. This suggests that, in determining optimum selectivity, it is important to understand the variations between CO<sub>2</sub> and CH<sub>4</sub> adsorption rather than the maximum for both.

**[0252]** Applicants' prior work has demonstrated that the best CO<sub>2</sub> uptake and CO<sub>2</sub>/CH<sub>4</sub> differentiation is obtained with a defined set of parameters involving surface area, pore volume, and carbon content which are in turn a function of the polymer precursor and the process activation temperature. In this Example, Applicants extend this work and demonstrate that there is an optimum KOH:PTh ratio for activation of the SPC. The ratio for optimum CO<sub>2</sub> (and CH<sub>4</sub> uptake) is 3, which equates to SPC samples with a surface area and total pore volume of 2700 m<sup>2</sup>·g<sup>-1</sup> and 1.5 cm<sup>3</sup>·g<sup>-1</sup>, respectively. In contrast, the ratio is 2 for the best CO<sub>2</sub>/CH<sub>4</sub> differentiation, which produces a surface area of 2,200 m<sup>2</sup>·g<sup>-1</sup> and total pore volume of 1.2 cm<sup>3</sup>·g<sup>-1</sup>.

**[0253]** Moreover, in this Example, Applicants demonstrate that the optimum CO<sub>2</sub> uptake is not for a material with the highest pore volume or surface area, but for the material with S<sub>BET</sub>>2000 m<sup>2</sup>·g<sup>-1</sup> and the highest percentage of a

maximum fraction of narrower micro (<1 nm) and micro (<2 nm) porosity as compared to meso-pores (>2 nm). Increasing in the latter type of pores does increase both the surface area and pore volume, but not the CO<sub>2</sub> uptake.

**[0254]** Without further elaboration, it is believed that one skilled in the art can, using the description herein, utilize the present disclosure to its fullest extent. The embodiments described herein are to be construed as illustrative and not as constraining the remainder of the disclosure in any way whatsoever. While the embodiments have been shown and described, many variations and modifications thereof can be made by one skilled in the art without departing from the spirit and teachings of the invention. Accordingly, the scope of protection is not limited by the description set out above, but is only limited by the claims, including all equivalents of the subject matter of the claims. The disclosures of all patents, patent applications and publications cited herein are hereby incorporated herein by reference, to the extent that they provide procedural or other details consistent with and supplementary to those set forth herein.

What is claimed is:

1. A method of capturing CO<sub>2</sub> from an environment at pressures above 1 bar, the method comprising:  
associating the environment with a porous material,  
wherein the porous material comprises a surface area of at least 2,800 m<sup>2</sup>/g, and a total pore volume of at least 1.35 cm<sup>3</sup>/g,  
wherein a majority of pores of the porous material have diameters of less than 2 nm as measured from N<sub>2</sub> sorption isotherms using the BET (Brunauer-Emmett-Teller) method, and  
wherein the associating results in CO<sub>2</sub> capture from the environment by the porous material.
2. The method of claim 1, wherein more than about 60% of pores of the porous material have diameters of less than 2 nm.
3. The method of claim 1, wherein the porous material has an oxygen content of more than about 7 wt % as measured by X-ray photoelectron spectroscopy.
4. The method of claim 1, wherein the porous material has an oxygen content between about 7 wt % and about 18 wt % as measured by X-ray photoelectron spectroscopy.
5. The method of claim 1, wherein the environment is a natural gas containing environment, an environment containing a mixture of gases, or combinations thereof.
6. The method of claim 1, wherein the CO<sub>2</sub> capture occurs by adsorption of the CO<sub>2</sub> to the porous material.
7. The method of claim 1, wherein the CO<sub>2</sub> capture occurs selectively over hydrocarbons in the environment.
8. The method of claim 1, wherein the porous material has a molar CO<sub>2</sub>/CH<sub>4</sub> selectivity of at least about 2.5.
9. The method of claim 1, wherein the porous material has a CO<sub>2</sub> sorption capacity of at least about 100 wt % at 30 bar.
10. The method of claim 1, wherein the porous material comprises a porous carbon material with a carbon content of between 80% and 95% as measured by X-ray photoelectron spectroscopy.
11. The method of claim 10, further comprising a step of preparing the porous carbon material prior to the step of associating the porous material with the environment.
12. The method of claim 11, wherein the porous carbon material is prepared by heating an organic polymer precursor or biological material in the presence of an activating agent, wherein the activating agent optionally comprises

KOH or steam, and wherein the temperature of activation is between 700° C. and 800° C.

**13.** The method of claim **12**, wherein the organic polymer precursor or biological material comprises oxygen in a functional group.

**14.** The method of claim **13**, wherein the functional group comprises a furyl, and wherein the organic polymer precursor polymerizes to form polyfurfuryl alcohol.

**15.** The method of claim **13**, wherein the functional group comprises an anisyl, and wherein the organic polymer precursor polymerizes to form polyanisyl alcohol.

**16.** The method of claim **15**, wherein the polyanisyl alcohol is prepared by the polymerization of anisyl alcohol with a catalyst, wherein the catalyst optionally comprises a protic acid.

**17.** A method for the separation of CO<sub>2</sub> from natural gas in an environment at partial pressures of either component above 1 bar, the method comprising:

associating the environment with a porous material, wherein the porous material comprises a surface area of at least 2,200 m<sup>2</sup>/g, and a total pore volume of at least 1.00 cm<sup>3</sup>/g, wherein a majority of pores of the porous material have diameters of greater than 1 nm and less than 2 nm as measured from N<sub>2</sub> sorption isotherms using the BET (Brunauer-Emmett-Teller) method, and

wherein the associating results in CO<sub>2</sub> capture from the environment by the porous material.

**18.** The method of claim **17**, wherein the porous material has an oxygen content of more than about 7 wt % as measured by X-ray photoelectron spectroscopy.

**19.** The method of claim **17**, wherein the porous material has an oxygen content between about 7 wt % and about 18 wt % as measured by X-ray photoelectron spectroscopy.

**20.** The method of claim **17**, wherein the environment is a natural gas containing environment, an environment containing a mixture of gases, or combinations thereof.

**21.** The method of claim **17**, wherein the CO<sub>2</sub> capture occurs by adsorption of the CO<sub>2</sub> to the porous material.

**22.** The method of claim **17**, wherein the CO<sub>2</sub> capture occurs selectively over hydrocarbons in the environment.

**23.** The method of claim **17**, wherein the porous material has a molar CO<sub>2</sub>/CH<sub>4</sub> selectivity of at least about 2.5.

**24.** The method of claim **17**, wherein the porous material has a CO<sub>2</sub> sorption capacity of at least about 100 wt % at 30 bar.

**25.** The method of claim **17**, wherein the porous material comprises a porous carbon material with a carbon content of between 80% and 95% as measured by X-ray photoelectron spectroscopy.

**26.** The method of claim **25**, further comprising a step of preparing the porous carbon material prior to the step of associating the porous material with the environment.

**27.** The method of claim **26**, wherein the porous carbon material is prepared by heating an organic polymer precursor or biological material in the presence of an activating agent, wherein the activating agent optionally comprises KOH or steam, and wherein the temperature of activation is between 700° C. and 800° C.

**28.** The method of claim **27**, wherein the organic polymer precursor comprises oxygen in a functional group.

**29.** The method of claim **28**, wherein the functional group comprises a furyl, and wherein the organic polymer precursor polymerizes to form polyfurfuryl alcohol.

**30.** The method of claim **28**, wherein the functional group comprises an anisyl, and wherein the organic polymer precursor polymerizes to form polyanisyl alcohol.

\* \* \* \* \*



US 20180318789A1

(19) United States

(12) Patent Application Publication (10) Pub. No.: US 2018/0318789 A1  
STABLER et al. (43) Pub. Date: Nov. 8, 2018(54) HIGH PERFORMANCE SORPTION BINDER  
FOR GAS PHASE STORAGE DEVICES

(71) Applicant: Arkema Inc., King of Prussia, PA (US)

(72) Inventors: Sean M. STABLER, Pottstown, PA (US); Azaz A. VAHORA, Eagleville, PA (US); Denis KATO DE ALMEIDA, Philadelphia, PA (US); Florence MEHLMANN, Berwyn, PA (US); Ramin AMIN-SANAYEI, Malvern, PA (US)

(21) Appl. No.: 16/032,682

(22) Filed: Jul. 11, 2018

## Related U.S. Application Data

(63) Continuation-in-part of application No. 15/768,682, filed on Apr. 16, 2018, filed as application No. PCT/US2016/047445 on Aug. 18, 2016.

(60) Provisional application No. 62/207,401, filed on Aug. 20, 2015.

## Publication Classification

## (51) Int. Cl.

*B01J 20/20* (2006.01)  
*B01J 20/26* (2006.01)  
*B01J 20/28* (2006.01)  
*B01J 20/30* (2006.01)  
*B01D 53/02* (2006.01)

## (52) U.S. Cl.

CPC ..... *B01J 20/20* (2013.01); *B01J 20/261* (2013.01); *B01J 20/28007* (2013.01); *B01J 20/2803* (2013.01); *B01J 20/28064* (2013.01); *B01J 20/28066* (2013.01); *B01D 2253/102* (2013.01); *B01J 20/28083* (2013.01); *B01J 20/28088* (2013.01); *B01J 20/3042* (2013.01); *B01J 20/3007* (2013.01); *B01D 53/02* (2013.01); *B01J 20/28073* (2013.01)

## (57) ABSTRACT

The invention relates to the use of a high performance thermoplastic polymer binder material for immobilizing adsorptive materials, such as activated carbon, in gas storage devices. The use of these binders, especially polyamide binders, polytetrafluoroethylene binders, or polyvinylidene fluoride binders such as Kyblock® resin, provides for high sorbent packing density, low fouling solid structure that maximizes the volume of gas to the volume of the storage space.

## HIGH PERFORMANCE SORPTION BINDER FOR GAS PHASE STORAGE DEVICES

[0001] This application is a continuation-in-part of copending U.S. application Ser. No. 15/768,682, filed Apr. 16, 2018, from which priority is claimed. This application also claims benefit, under U.S.C. §119(e) of US Provisional Application No. 62/207,401, filed Aug. 20, 2015 and PCT/US16/47445 filed Aug. 18, 2016. The cited references are incorporated herein by reference.

### FIELD OF THE INVENTION

[0002] The invention relates to the use of high performance thermoplastic polymer binder materials for immobilizing adsorptive materials for gas storage devices. The use of these new binders, especially fluoropolymers or polyamide binders, provides a porous solid having a high sorbent packing density, low binder fouling of sorbent, and maximizes the volume of gas to the volume of the storage space.

### BACKGROUND OF THE INVENTION

[0003] Adsorbed gas storage provides an advancement in the temporary storage of gaseous materials that overcome obstacles related to high pressure systems commercially used today to compress gases.

[0004] Gases such as noble gases, O<sub>2</sub>, N<sub>2</sub>, hydrocarbons, and other small gas molecules are used in many markets including, but not limited to, industrial, automotive, pharmaceutical, food, beverage, electronics, etc. Specific applications include concentrated medical oxygen, industrial desiccants, portable and residential liquefied petroleum gas (LPG), stranded gas flares, kerosene burners, cook stoves, compressed natural gas (CNG), and many others.

[0005] The storage and transport of said gases are typically in vessels where high pressures are used to condense or even liquefy the gas to utilize the greatest concentration safely possible within an occupied volume. The pressurization process results in unwanted and excessive costs due to the energy and infrastructure requirements. In addition, there is a limitation in storage containment geometry to safely store and transport the gas; resulting in limitations of storage designs. The use of sorbents to store gases at lower pressures is known to solve some of these issues.

[0006] The technology to convert low bulk density sorbent powder into an immobilized higher density block using a thermoplastic binder is well known for filtration applications. It is also widely believed that high surface area sorption materials formed into high density compacted structures can achieve the economic storage volume needed for gases.

[0007] U.S. Pat. No. 7,708,815 describes the unique needs and challenges for the storage of hydrogen, achieved by a hydriding/dehydriding process in the presence of non-porous metal compounds, which are in the form of a fine powder of less than 30 microns. A thermoplastic binder is used to minimize packing of the metal compounds during hydriding/dehydriding cycles. The patent fails to address the needs and challenges to bind other active particles, such as carbons and molecular sieve sorbent, which have significant porosity (>40%), and larger particle sizes (>100 microns), especially those with a BET surface area greater than 1,400 m<sup>2</sup>/g. Porosity is defined as the ratio of void space in a volume to the total volume. Surprisingly in these cases, we found that the role of the binder is not to minimize packing

of active particles, but actually to maximize such packing. The patent also fails to teach an appropriate range for the binder particle sizes to allow for maximizing packing and good mechanical integrity of the composite hydrogen storage material, as the binder particle size of <0.1 microns is too small to effectively bind activated carbon and molecular sieve particles.

[0008] U.S. Pat. No. 4,999,330 describes the needs and challenges for the high-density sorbent used in ANG systems. High surface area activated carbon is the sorbent typically used in high density sorbent structures. However loose carbon particles have the drawbacks of low packing density, and the ability to move sorbent with the gas stream and cause potential contamination.

[0009] The U.S. Pat. No. 4,999,330 reference solves the above limitations by forming a methyl cellulose or polyvinyl alcohol binder solvent solution, coating high surface area carbon particles with the binder solution, followed by removing the solvent and compressing the binder-coated particles to cause a bulk volume reduction of 50 to 200%. The '330 system suffers from its complexity and many steps. It also involves coating the entire activated carbon particles with polymer solution—which ultimately blocks many of the micropores—this fouling reducing the amount of surface area available for adsorption. Some of the pores can be pre-filled with solvent which can later be removed by heat to unblock many of the pores, however the net effect of a full coating is a large reduction in active surface area.

[0010] US2017/0007982 uses a water soluble cellulosic binder to coat active carbon particles and form a monolith. The monolith also suffers from a complicated manufacturing process, and significant fouling of the activated carbon pores due to the binder coating. In addition, the monolith requires the incorporation of a scaffold material, to achieve good mechanical integrity. Scaffold materials include natural or synthetic fibers, such as polyester and polypropylene fibers.

[0011] Carbon block targeted for filtration applications are described in U.S. Pat. No. 5,019,311, U.S. Pat. No. 5,147,722, and U.S. Pat. No. 5,331,037, uses an extrusion process to produce a porous article containing bound active particles, such as activated carbon, bound together by a thermoplastic binder. The carbon block filter is designed to remove contaminants from a fluid stream—such as in the purification of water. The polymer binder, which is generally a polyethylene, is needed at a high level.

[0012] U.S. Pat. No. 6,395,190 describes carbon filters and a method for making them having a 15 to 25 weight percent of a thermoplastic binder. The problem with polyethylene and other typical binders is that high loading percentages are required to adequately hold the sorbent materials together. Poor fouling resistance is also a problem.

[0013] Poly(vinylidene fluoride) as a binder for carbon block filters, has been found to improve the carbon block article performance by providing effective binding at lower loading—which in turn provides greater efficiency by reducing the pressure drop when the fluid passes through the block.

[0014] Examples of such carbon block filters, as well as methods for producing them, are described for example in WO 2014/055473 and WO 2014/182861, the entire disclosures of each of which are incorporated herein by reference for all purposes. These articles use polyvinylidene fluoride or polyamide binders, rather than the polyethylene binders previously used for carbon block filtration articles. There is

no mention of the use of such systems for small molecules storage, or with sorbent of high BET specific surface area greater than 1,000 m<sup>2</sup>/g.

[0015] In the area of gas storage, there is a need to improve the volume of gas that can be stored in a given volume of container space (v/v<sub>o</sub>), to improve the economics of this technology. The activated carbons used in filtration systems have high ball hardness and moderate BET surface area, in order to minimize the pressure drop when a fluid passes through the system. In contrast, activated carbons with low ball hardness and high BET surface areas are needed to effectively store gases, and pose different challenges when it comes to combine them with a binder. In this case, the binder needs to maximize packing of the carbon particles, instead of minimizing it in the case of filtration systems.

[0016] Surprisingly it has now been found that a high v/v<sub>o</sub> can be obtained in a gas storage article using low levels of polyvinylidene fluoride, polytetrafluoroethylene, or polyamide binders of moderate particle sizes, with suitable activated carbon. The low levels of binder have little negative effect on the ratio of activated sorbent volume to container volume. Moderate binder particle size is needed for efficient packing of the activated carbon particles, if the binder particles are too large (>1 micron), they allow for some carbon particles to remain loose, if the binder particles are too small (<0.1 micron) they can't reach multiple carbon particles which lead to ineffective binding. In addition to providing a solid adsorption article having a high density packing, low level of binder volume, the solid porous sorbent structure of the invention also show excellent resistance to fouling of the sorbent. In some cases, fouling is further reduced by processing the article of the invention at temperature equal or below the melting point of the binder. Lastly, polyvinylidene fluoride, polytetrafluoroethylene or polyamide binders also provide excellent chemical resistance to the gas storage environment. Additionally, the high relative thermal index of these polymers is useful for the temperature range an adsorptive storage monolith would encounter during the product life cycle.

#### SUMMARY OF THE INVENTION

[0017] The invention relates to a gas storage article comprising a solid, dense, porous sorbent media bound together by 0.5 to 30 weight percent of thermoplastic binder particles, wherein said binder particles have a discrete particle size of between 5 and 1000 nanometers, aspect ratio of 1 to 1000, and/or agglomerates between 1 and 150 micrometers

[0018] The invention also relates to a sealed container containing the gas storage block article, having at least one valve opening for charging and discharging of a gas, the container capable of holding a pressurized gas.

[0019] The invention also relates to a gas storage container, holding the solid sorbent and containing natural gas (methane).

[0020] The invention also relates to a method for making a gas storage article.

#### DETAILED DESCRIPTION OF THE INVENTION

[0021] All references listed in this application are incorporated herein by reference. All percentages in a composition are weight percent, unless otherwise indicated, and all molecular weights are given as weight average molecular

weight, unless stated otherwise. Combinations of different elements described herein are also considered as part of the invention.

[0022] "Interconnectivity", as used herein means that the active particles or fibers are permanently bonded together by the polymer binder particles without completely coating the active primary and secondary particles or functional particles or fibers. The binder adheres the sorbent at specific discrete points to produce an organized, porous structure. The porous structure allows a gas to pass through the interconnected particles or fibers, and the gas is exposed directly to the surface(s) of the sorbent particles or fibers, favoring the adsorption of the gas onto the sorbent material. Since the polymer binder adheres to the sorbent particles in only discrete points, less binder is used for complete interconnectivity compared to a binder that is coated onto the sorbent.

[0023] The invention relates to a solid porous gas storage article made of activated carbon or other gas sorbent, the sorbent material being bound together by small discrete thermoplastic polymer binder particles to provide interconnectivity. The solid porous article is generally present within a closed container, capable of holding a pressurized gas. The sorbent and binder are combined under pressure to produce a dense porous solid gas-sorbent structure.

#### Binder

[0024] The polymer particles of the composite of the invention are thermoplastic, elastomeric, thermoplastic vulcanized (TPV), or thermoplastic elastomer (TPE) polymer particles with discrete particle sizes in the sub-micrometer range. The average discrete particle size is less than 1 micrometer, preferably less than 500 nm, preferably less than 400 nm, and more preferably less than 300 nm, with an aspect ratio of 1 to 1000. The average discrete particle size is generally at least 20 nm and preferably is higher for lower aspect ratio, i.e. at least 50 nm, most preferably at least 100nm for aspect ratio of about 1.

[0025] Useful polymers include, but are not limited to fluoropolymers, styrene-butadiene rubbers (SBR), ethylene vinyl acetate (EVAc), ethylene vinyl alcohol (EVA), acrylic polymers such as polymethyl methacrylate polymer and copolymers, polyurethanes, styrenic polymers, polyamides, polyolefins, including polyethylene, and polypropylene and the copolymers thereof, polyester including polyethylene terephthalate, polyvinyl chlorides, polycarbonate and thermoplastic polyurethane (TPU). In order to obtain the small polymer particle size useful in the invention, it is preferred that the thermoplastic polymers are made by emulsion (or inverse emulsion) polymerization.

[0026] Preferred polymers are polyamides, and fluoropolymers such as PVDF, PTFE, PETFE, FEP, PFA, FKM, FFKM, with homopolymers and copolymers of polyvinylidene fluoride and of polytetrafluoroethylene being especially useful.

[0027] Preferably, the binder is a fluoropolymer. Useful fluoropolymers are thermoplastic homopolymers and copolymers having greater than 50 weight percent of fluoromonomer units by weight, preferably more than 65 weight percent, more preferably greater than 75 weight percent and most preferably greater than 90 weight percent of one or more fluoromonomers. Useful fluoromonomers for forming the fluoropolymer include but are not limited to: vinylidene fluoride (VDF or VF<sub>2</sub>), tetrafluoroethylene (TFE), trifluo-

roethylene (TrFE), chlorotrifluoroethylene (CITE), hexafluoropropene (HFP), vinyl fluoride (VF), hexafluoroisobutylene (HFIB), perfluorobutylethylene (PFBE), pentafluoropropene, 3,3,3-trifluoro-1-propene, 2-trifluorotethyl-3,3,3-trifluoropropene, fluorinated vinyl ethers including perfluoromethyl ether (PMVE), perfluoroethylvinyl ether (PEVE), perfluoropropylvinyl ether (PPVE), perfluorobutylvinyl ether (PBVE), longer chain perfluorinated vinyl ethers, fluorinated dioxoles, partially- or per-fluorinated alpha olefins of C<sub>4</sub> and higher, partially- or per-fluorinated cyclic alkenes of C<sub>3</sub> and higher, and combinations thereof.

[0028] Especially preferred fluoropolymers are polyvinylidene fluoride (PVDF) homopolymers, and copolymers, polytetrafluoroethylene (PTFE) homopolymers and copolymers, and poly(vinylidene fluoride-hexafluoropropylene-tetrafluoroethylene) terpolymers. While the invention applies to all thermoplastic polymers, and in particular all fluoropolymers and copolymers, and polyamides, vinylidene fluoride and tetrafluoroethylene polymers will be used to illustrate the invention, and are the preferred polymer. One of ordinary skill in the art will understand and be able to apply the specific references to PVDF, P(VDF-HFP), and PTFE to these other thermoplastic polymers, which are considered to be within the realm of, and embodied in the invention.

[0029] In one embodiment, vinylidene fluoride or tetrafluoroethylene fluoride copolymers are preferred, due to their lower crystallinity (or no crystallinity), making them more flexible than the more crystalline homopolymers. Flexibility of the binder allows it to better withstand the manufacturing process, as well as increased pull-through strength and better adhesion properties.

[0030] Preferred VDF copolymers include those containing at least 50 mole percent, preferably at least 75 mole %, more preferably at least 80 mole %, and even more preferably at least 85 mole % of vinylidene fluoride copolymerized with one or more comonomers selected from the group consisting of tetrafluoroethylene, trifluoroethylene, chlorotrifluoroethylene, hexafluoropropene, vinyl fluoride, pentafluoropropene, tetrafluoropropene, trifluoropropene, perfluoromethyl vinyl ether, perfluoropropyl vinyl ether and any other monomer that would readily copolymerize with vinylidene fluoride.

[0031] In one embodiment, up to 30%, preferably up to 25%, and more preferably up to 15% by weight of hexafluoropropene (HFP) units and 70% or greater, preferably 75% or greater, more preferably 85% or greater by weight or more of VDF units are present in the vinylidene fluoride polymer. It is desired that the HFP units be distributed as homogeneously as possible to provide PVDF-HFP copolymer with excellent dimensional stability in the end-use environment.

[0032] The PVDF used in the invention is generally prepared by means known in the art, using aqueous free-radical emulsion polymerization—although suspension, solution and supercritical CO<sub>2</sub> polymerization processes may also be used. In a general emulsion polymerization process, a reactor is charged with deionized water, water-soluble surfactant capable of emulsifying the reactant mass during polymerization and optional paraffin wax antifoulant. The mixture is stirred and deoxygenated. A predetermined amount of chain transfer agent, CTA, is then introduced into the reactor, the reactor temperature raised to the desired level and vinylidene fluoride (and possibly one or more comonomers)

are fed into the reactor. Once the initial charge of vinylidene fluoride is introduced and the pressure in the reactor has reached the desired level, an initiator emulsion or solution is introduced to start the polymerization reaction. The temperature of the reaction can vary depending on the characteristics of the initiator used and one of skill in the art will know how to do so. Typically the temperature will be from about 30° to 150° C., preferably from about 60° to 120° C. Once the desired amount of polymer has been reached in the reactor, the monomer feed will be stopped, but initiator feed is optionally continued to consume residual monomer. Residual gases (containing unreacted monomers) are vented and the latex recovered from the reactor.

[0033] The surfactant used in the polymerization can be any surfactant known in the art to be useful in PVDF emulsion polymerization, including perfluorinated, partially fluorinated, and non-fluorinated surfactants. Preferably the PVDF emulsion of the invention is fluorosurfactant-free, with no fluorosurfactants being used in any part of the polymerization. Non-fluorinated surfactants useful in the PVDF polymerization could be both ionic and non-ionic in nature including, but are not limited to, 3-allyloxy-2-hydroxy-1-propane sulfonic acid salt, polyvinylphosphonic acid, polyacrylic acids, polyvinyl sulfonic acid, and salts thereof, polyethylene glycol and/or polypropylene glycol and the block copolymers thereof, alkyl phosphonates and siloxane-based surfactants.

[0034] The PVDF polymerization results in a latex generally having a solids level of 10 to 60 percent by weight, preferably 10 to 50 percent.

[0035] The PTFE homopolymers or copolymers used in the invention are generally prepared by means known in the art, using aqueous free-radical emulsion or suspension polymerization, although other polymerization processes may also be used. The molecular weight of the polymer is not especially limited, however a high weight average molecular weight may be beneficial due to the ability of the polymer to undergo fibrillation when used as a binder.

[0036] The surfactant used in the emulsion polymerization can be any surfactant known in the art to be useful in PTFE emulsion polymerization, including perfluorinated, partially fluorinated, and non-fluorinated surfactants.

[0037] The latex binder is generally reduced to a powder form by spray drying, coagulation, or other known process, to produce a dry powder. The powder shape and particle size may be modified by any known process, such as milling. The polymer may be exposed to thermal or radiation treatments to control the molecular weight of the powder.

[0038] Binder particles are generally from 5 to 700 nm in size, preferably from 50 to 500 nm, and more preferably from 100-300 nm as an average particle size. In some cases, polymer particles may agglomerate into 1 to 150 micrometer groupings, 3 -50 micrometers, 5-15 micrometers, and preferably 6-8 micrometer agglomerates, but it has been found that these agglomerates can break into individual particles or fibrils during processing to form an article. Some of the binder particles are discrete particles, and remain as discrete particles in the formed solid porous sorbent article. During processing into articles, the particles adjoin sorbent material together and provide interconnectivity.

[0039] It is important that as little binder is used as necessary to hold the sorbent materials together, as this allows more of the surface area to be exposed and be active in gas absorption. One advantage of PVDF and PTFE

binders is that they have a very high specific gravity of at least about 1.75 g/cc, preferably at least about 1.77 g/cc. Thus the low weight percent of binder needed represents an even lower volume percent.

[0040] The particle size of the binder plays a role in the lower weight % loadings needed to make a solid immobilized porous media block. Further the rheology of PVDF resin based on the higher molecular weights of preferably 200,000 to 5,000,000 g/mole, and preferably 300,000-900,000 g/mole, assists in the binder not flowing into the carbon and fouling the high surface area of the activated carbon sorption media.

#### Sorbent

[0041] The sorbents of the invention are those capable of adsorbing and desorbing specific gas molecules. In one important embodiment of the invention, activated carbon is used to adsorb natural gas (methane), however, other sorbents with adsorption specificity for other gases are also contemplated by this invention. Activated carbon, carbon fibers and molecular sieves are especially useful sorbents of the invention. Activated carbon having a large level of surface area and pore volume is especially preferred, as are nano carbon fibers. Activated carbon having a high pore volume is also preferred. Activated carbon having pore sizes suitable for the adsorption of gases are especially preferred, containing micropores (less than 20 Å) and/or mesopores (20 to 500 Å). Literature supports that gas adsorption is most effective in pores that have space for one to three layers of gas molecules, for instance with the size of gas molecules being typically between 3 and 5 Å (H<sub>2</sub> 3 Å, N<sub>2</sub> 3.5 Å, alkanes 4.5 Å), it is desirable that the sorbent has a least 30%, preferably at least 50% of pores in the range from 6 to 30 Å, and especially 6 to 18 Å, or 7 to 21 Å, or 9 to 27 Å, or 10 to 30 Å. Other useful sorbents include, but are not limited to: carbon molecular sieves, molecular sieves, silica gel, metal organic framework, etc. have special affinity to specific gas adsorption.

[0042] The sorbent particles of the invention are generally in the size range of 0.1 to 3,000 microns, preferably from 1 to 500 microns, and most preferably from 5 to 100 microns in diameter. In certain embodiments, sorbent particles have a multimodal particle size distribution, for instance with some particles having an average particle size of less than 100 microns, and some particles having an average particle size of more than 200 microns. Sorbent particles can also be in the form of fibers of 0.1 to 250 microns in diameter of essentially unlimited length to width ratio. Fibers are preferably chopped to no more than 5 mm in length.

[0043] Sorbent fibers or powders should have sufficient thermal conductivity to allow heating of the powder mixtures. In addition, in an extrusion process, the particles and fibers must have melting points sufficiently above the melting point of the fluoropolymer binder resin to prevent both substances from melting and producing a continuous melted phase rather than the usually desired multi-phase system.

[0044] There are many sources of activated carbon and various techniques to differentiate the performance of each activated carbon per application. Sources of activated carbon include, but are not limited to, coconut shell, bitumen, coal, grass, organic polymers, hard wood, and soft wood. Each product has their own characteristics which can affect gas sorption and desorption performance. It is known that for gas sorption onto activated carbon it is dependent on the

close proximity to surface area contact coupled with Van der Waal's forces to attract gas molecules and temporarily store them until desorption occurs. Key characteristics of the activated carbon which impacts the volume of gas sorption is the macro-, micro-, meso-porosity of the carbon surface area. The porosity is further characterized by the BET surface area curves. In general, high BET surface area of at least 1,400 m<sup>2</sup>/g is preferred, of at least 2,000 m<sup>2</sup>/g is especially preferred.

[0045] It has been found that a hard carbon with low BET surface area is preferred to economically manufacture densified block with known state of the art manufacturing. However the hard carbons having a low BET surface area are not preferred for gas sorption performance, but a soft carbon with high BET surface area is preferred. A soft carbon cannot be highly densified or manufactured at an economical rate using solid state extrusion or compression molding. Surprisingly, it has been discovered that unique blends of soft carbon and hard carbon can achieve both an economic manufacturing process and also achieve high performance gas sorption characteristics.

[0046] For the solid state extrusion process, a minimum of 5 percent by weight, preferably 10 weight percent, and preferably in the range of 10-60 weight percent of hard carbon is used to resist the pressure of the extruder and extrude a block structure. A higher level of the hard carbon, up to 100 weight percent will produce a well-formed solid state extruded block, however, the higher cost, and lower BET surface area of the hard carbon reduce performance and economics. Blocks prepared containing entirely soft carbons are possible, but the extrusion speed may be limited due to their compressibility. Blocks containing entirely soft carbons can be more efficiently produced by a compression molding process.

[0047] Hard carbons are considered those with a ball pan hardness per ASTM D 3802 to be greater than 80% and soft carbons are considered when measured by the same method as being less than or equal to 80%. Low BET surface area is considered less than 1400 m<sup>2</sup>/g, while high 2 BET surface area is considered greater than or equal to 1400 m<sup>2</sup>/g. The pore sizes of porous materials are categorized by International Union of Pure and Applied Chemistry (IUPAC) as follows. Pores with size of less than 2 nm in diameters are micropores, pores with size of between 2 nm and 50 nm are mesopores, and pores with size of more than 50 nm are macropores.

#### Process

[0048] The binder and sorbent particles may be blended and processed by several methods. The binder particles are generally in a powder form, which can be dry blended with the sorbent materials. Solvent or aqueous blends may also be formed by known means. Preferably 0.3 to 30, preferably 0.5 to 25, and more preferably 1 to 16 weight percent of binder is used for each 84 to 99.5 weight percent of sorbent material. Preferably the level of binder is from 4 to 12 weight percent, and even more preferably from about 5 to 10 weight percent.

[0049] There are generally three methods to form a solid porous sorbent article from a homogeneous mixture of the sorbent and binder: 1) dry powder homogeneous blends which are compression molded, 2) dry powder homogeneous blends which are extruded, and 3) solvent or aqueous blends which are cast and dried. Because a very dense solid

sorbent article is desired, compression molding and extrusion processing at higher pressures can be used. The compression molding and extrusion processes are practiced in a manner that causes a softening of the polymer binder particles, but does not cause them to melt and flow to the point that they contact other polymer particles and form agglomerates or a continuous layer. To be effective in the contemplated end-uses, the polymer binder remains as discreet polymer particles that bind the sorbent materials into an interconnected web, for good permeability. In a solvent system, individual polymer particles no longer exist, as they are dissolved and form a continuous coating over the sorbent particles. The continuous coating reduces the amount of activated surface area available for adsorption on the particles, and can reduce their overall effectiveness.

[0050] The most economical solution for high quality and high output capacity is utilizing the extrusion process which makes uniform and highly packed immobilized porous media.

[0051] An advantage of the extrusion is that the sorbent density is fairly constant across the article, while a compression molded article tends to show a density gradient. It is increasingly difficult to have a uniform packing density gradient on a compression molded article especially as the aspect ratio (length/diameter ratio) increases. An advantage of a compression molded process is that a large variety of shapes are available.

[0052] The polymer binder particles can be formed into a porous block article in an extrusion process, such as that described in U.S. Pat. No. 5,331,037. The polymer binder/sorbent material composite of the invention is wet or dry-blended, optionally with other additives, such as processing aids, and extruded, molded or formed into articles. Continuous extrusion under heat, pressure and shear can produce an infinite length 3-dimensional multi-phase profile structure. In order to form the continuous web of forced-point bonding of binder to the sorbent materials, a critical combination of applied pressure, temperature and shear is used.

[0053] The extrusion process can produce a continuous block structure at any diameter and length desired. Lengths of 1 cm to hundreds of meters are possible with the right manufacturing equipment. The continuous solid block can then be cut into desired final lengths. Typical diameters of the solid blocks would be 15 cm or less, and more preferably 15 cm or less—though with the proper size die(s) larger diameter structures up to 1.5 meters and larger could be produced.

[0054] An alternative to a single, solid structure, is forming two or more structures—a solid rod, and one or more hollow block cylinders designed to nest together to form the larger structure.

[0055] Once each annular or rod-shaped block component is formed, the components can be nested together to create a larger structure. This process can provide several advantages over the extrusion of a single large structure. The blocks with smaller cross-sectional diameter can be produced at a faster rate than producing a large, solid, single-pass block. The cooling profile can be better controlled for each of the smaller-cross sectional pieces. A further advantage of this concept may be reduced gas diffusion path lengths through the monoliths as the spacing between concentric blocks could serve as channels for rapid flow of gas.

## Properties

[0056] Articles formed by the invention are high density, porous, solid articles that maximize the volume of sorbent to volume of the container ratio.

[0057] The articles formed are used within a closed container capable of holding a pressurized gas of up to 5000 psi. The sorbent composite article should fit with a narrow tolerance inside the container, to maximize the amount of sorbent per container volume. The container will have an inlet which will be used to fill the container with gas and will have a discharge end where the gas can leave the container. The sorbent material does not settle or move during use, such as to power a vehicle, as it is interconnected by the binder particles. Gas is provided into the container under pressure, and is adsorbed and stored by the sorbent material. When the pressure is released, and the container open to a lower pressure environment, the gas will desorb from the sorbent material, and be used in the application.

[0058] The gas storage article has an immobilized density greater than 1.1 times, preferable greater than 1.3 times, and most preferably greater than 1.5 times that of the apparent density of the sorption media. Densification permits more storage capacity per unit volume, thus increasing the possible v/v<sub>o</sub> in a given gas storage article.

[0059] The gas storage article has a percent fouling of the sorbent of less than 15%, preferably less than 10%, more preferably less than 5%.

[0060] The gas storage article is combined with one or more gases selected from, but not limited to, noble gases, hydrocarbons, hydrogen-based gases, methane, natural gas, CO<sub>2</sub>, CO, O<sub>2</sub>, N<sub>2</sub>, fluorinated gases, halogenated gases, silanes, phosphine, phosgene, boron trihalides, ammonia, hydrogen halide, sulfide, and cyanide. In one embodiment, the gas is natural gas. In another embodiment, the gas is not hydrogen H<sub>2</sub>.

[0061] In one embodiment, the container holding the composite solid sorbent article, is used to power a vehicle. Other embodiments, the container holding the composite is for storage purposes to supply fuel to grill and stove burners, refrigerators, freezers, furnaces, generators, emergency equipment, etc.

## EXAMPLES

### Test Methods

[0062] Particle size of activated carbon is measured using a TYLER RX-29 sieve shaker. The data is reported either as a weight average particle size, or as a nominal "m x n" size where at least 90 wt % particles are larger than "n" mesh and at least 90 wt % particles are smaller than "m" mesh.

[0063] Particle size of polymeric powder is measured using a Malvern Masturizer 2000 particle size analyzer. The data is reported as weight-average particle size (diameter)

[0064] Powder/latex average discrete particle size is measured using a NICOMP<sup>®</sup> 380 submicron particle sizer. The data is reported as weight-average particle size (diameter).

[0065] BET specific surface area, pore volume, and pore size distribution of materials are determined using a QUANTACHROME NOVA-E gas sorption instrument. Nitrogen adsorption and desorption isotherms are generated at 77K. The multi-point Brunauer-Emmett-Teller (BET) nitrogen adsorption method is used to characterize the specific surface area. A Nonlocal Density Functional Theory (NLDFT,

N2, 77k, slit pore model) is used to characterize the pore volume and pore size distribution.

[0066] Bulk density measurement of materials or blocks are made by measuring the weight of material or block contained in a known volume, after the material or block has been dried at 110 C under vacuum for 8 hours

[0067] The Percent fouling of the sorbent is calculated as [1-(BET specific surface area of block\*100)/(BET specific area of sorbent\*wt. % sorbent in block)]\*100.

#### Example 1

[0068] Dry powder blends are formed by dry blending 15 wt % of Kyblock FG-81 polyvinylidene fluoride homopolymer binder from Arkema and 85 wt % of Oxbow 8325CAW/70 coconut shell activated carbon. The Kyblock® FG-81 has a weight average particle size of 9 microns, and a discrete weight average particle size of 220 nm. The activated carbon is a nominally 80x325 mesh carbon, but also includes particles smaller than 325 mesh (44 micrometers) and greater than 80 (177 micrometers) mesh with a particle size distribution designed to maximize the particle packing density. The two dry, powdery materials are mixed in a high shear mixer or a planetary centrifugal mixer, until they are a homogeneous blend. The blend is then forced into a die which is heated to a minimum of 180° C. under pressures greater than 100 psi, forming a self-supporting, porous structure with good mechanical integrity. The structure is then cooled to room temperature. The bulk density of the activated carbon is initially 0.49 g/cc and this density is increased to 0.71 g/cc when combined with the binder and extruded. Under higher packing pressure loadings the density can be increased even further. The pure carbon powder has a specific surface area BET (m<sup>2</sup>/g) of 1150. The 15 wt % Kyblock® FG-81 block has a specific surface area BET (m<sup>2</sup>/g) 973. After normalizing by weight percent of sorbent, the Kyblock® FG-81 is responsible for 0.4% fouling of the activated carbon surface, which is less than 10% fouling, and even less than 5% fouling.

#### Example 2 (Comparative)

[0069] The same activated carbon used in Example 1 is combined with 15 wt % of MICROTHENE FN510-00 (LyondellBassell) linear low density polyethylene (PE) binder. A block of the same bulk density is prepared by a comparable solid state extrusion process. The Microthene FN510-00 powder has a weight average particle size of 22 microns, and the particles are not made of discrete smaller particles. The pure carbon powder has a specific surface area BET (m<sup>2</sup>/g) of 1150. The 15 wt % FN510-00 block has a specific surface area BET (m<sup>2</sup>/g) 674. After normalizing by weight percent of sorbent, the FN510-00 is responsible for 30% fouling of the activated carbon surface. The Kyblock®-based block prepared in Example 1 is greater than 80x more fouling resistant than the PE sample of Example 2. Due to its high particle size, the polyethylene binder leads to a high level of fouling of the sorbent.

#### Example 3

[0070] A dry powder blend of 14 wt. % KYBLOCK® FG-42 polyvinylidene fluoride copolymer and 86 wt. % of the same activated carbon in EXAMPLE 1 is prepared in a low shear mixer. The Kyblock® FG-42 has a weight average particle size of 12 microns, and a discrete weight average

particle size of 220 nm. The powder blend is filled into a 10" tall steel annular mold with an outside diameter of 2.5" and an inside diameter of 1.25". The mold containing powder is heated to 400° F. for one hour, and compressed with a hydraulic ram to achieve a block bulk density of 0.7 g/cc. The pure carbon powder has a specific surface area BET (m<sup>2</sup>/g) of 1150. The 14 wt % Kyblock® FG-42 block has a specific surface area BET (m<sup>2</sup>/g) 953 m<sup>2</sup>/g.

#### Example 4 (Comparative)

[0071] A dry powder blend of 30 wt % Microthene FN510-00 used in Example 2, and 70 wt % of the same activated carbon in EXAMPLE 1 is prepared in a low shear mixer and compression molded into an annular monolith of the same dimensions and density as in EXAMPLE 3. Due to its high particle size, a higher level of Microthene FN510-00 binder is required to produce a block with adequate strength by compression molding. The pure carbon powder has a specific surface area BET (m<sup>2</sup>/g) of 1150. The 30 wt % FN510-00 block has a specific surface area BET (m<sup>2</sup>/g) 600 m<sup>2</sup>/g. For blocks of examples 3 and 4 produced by compression molding, the binder weight percent loading is much higher for FN510-00 than for Kyblock® FG-42, to achieve similar mechanical strength. This leads to further reduction of BET specific area of the activated carbon when using FN510-00 as the binder.

#### Example 5

[0072] An extruded annular monolith is produced by first preparing a dry powder blend containing 20 wt. % FX1184 (Jacobi Carbons) wood based carbon with BET specific surface area of 1400 m<sup>2</sup>/g ground and sieved to 120x625 mesh, 70 wt. % of the 80x325 mesh carbon described in EXAMPLE 1, and 10 wt. % Kyblock® FG-81 binder, in a low shear mixer. A 1.9" outside diameter by 1.19" inside diameter annulus is extruded using a processing temperature of 230 ° C. at a rate of 2 cm/min. The bulk density of the resulting block is 0.62 g/cc. The BET specific surface area of the extruded block is 1176 m<sup>2</sup>/g.

#### Example 6

[0073] A dry powder blend is formed by dry blending 10 wt % of Kyblock FG-81 polyvinylidene fluoride homopolymer binder from Arkema and 90 wt % of Ingevity Nuchar SA-1500 activated carbon. The activated carbon has a bulk density of less than 0.4 g/cc, a weight average particle size of about 50 micron, a BET specific surface area of 2,010 m<sup>2</sup>/g, a total pore volume of 1.28 cc/g, a volume of 6-18 Å pores of 0.50 cc/g, a volume of 7-21 Å pores of 0.56 cc/g, and a volume of 9-27 Å pores of 0.68 cc/g. The Kyblock® FG-81 powder has a specific gravity of 1.78 g/cc, a weight average particle size of 9 microns, and a discrete weight average particle size of 220 nm. The two dry, powdery materials are mixed in a low shear mixer or a planetary centrifugal mixer until they are a homogeneous blend. SEM analysis shows good dispersion of discrete binder particles on the surface of carbon particles. The blend is heated in an oven at 240° C., then compression molded under 15,000 psi pressure to produce a block. The resulting block has good mechanical integrity, a bulk density of 0.50 g/cc, a BET specific surface area of 1,750 m<sup>2</sup>/g, a total pore volume of 1.06 cc/g, a volume of 6-18 Å pores of 0.48 cc/g, a volume of 7-21 Å pores of 0.56 cc/g, and a volume of 9-27 Å pores

of 0.61 cc/g. Under higher packing pressure loadings, the bulk density can be increased even further.

#### Example 7

**[0074]** The same materials and process as in example 6 are used, except that the weight percent binder is 25 wt %. The resulting block has excellent mechanical integrity, and a bulk density of 0.58, a BET specific surface area of 1,380 m<sup>2</sup>/g, a total pore volume of 0.80 cc/g, a volume of 6-18 Å pores of 0.40 cc/g, a volume of 7-21 Å pores of 0.45 cc/g, and a volume of 9-27 Å pores of 0.58 cc/g.

#### Example 8

**[0075]** The same materials and process as in example 6 are used, except that the weight percent binder is 5 wt %. The resulting block has average mechanical integrity, and a bulk density of 0.51.

#### Example 9

**[0076]** The same materials and process as in example 6 are used, except that the discrete particle size of the binder is 150 nm, and the binder loading is 5 wt %. The resulting block has improved mechanical integrity over the block of example 6.

#### Example 10

**[0077]** The same materials and process as in example 6 are used, except that the discrete particle size of the binder is 90 nm, and the binder loading is 5 wt %. The resulting block has poor to average mechanical integrity.

#### Example 11

**[0078]** The same materials and process as in example 6 are used, except that the Kyblock FG-81 binder is used in a latex form and mixed with the activated carbon in a low shear mixer. The blend contains about 40-60 wt % water, and is subsequently dried in an oven at 110° C. for 8 hours, prior to heating and compression molding steps. The resulting block has good mechanical integrity.

#### Example 12

**[0079]** A powder blend is formed by blending Dyneon TF5060GZ polytetrafluoroethylene 60 wt % aqueous solution and the same activated carbon used in example 1, in a high shear mixer. The TF5060GZ has a specific gravity of 2.16, a discrete weight average particle size of 220 nm. The blend contains 40-60 wt % water and a weight percent ratio of solid PTFE to activated carbon of 10 to 90, and is subsequently dried in an oven at 110° C. for 8 hours. The blend is heated in an oven at 220° C., then compression molded under 15,000 psi pressure to produce a block. The resulting block has good mechanical integrity, and a bulk 0.43 g/cc. Under higher packing pressure loadings, the bulk density can be increased even further.

#### Example 13

**[0080]** The same materials and process as in example 10 are used, except that the weight percent of solid PTFE binder is reduced from 10 wt % to 5 wt %. The resulting block has good mechanical integrity, and a bulk density of 0.41 g/cc.

#### Example 14

**[0081]** A powder blend is formed by blending Dyneon TF5060GZ polytetrafluoroethylene 60 wt % aqueous solution, Arkema Kyblock® FG-81 polyvinylidene fluoride homopolymer, and the same activated carbon used in example 1, in a low shear mixer. The blend contains 40-60 wt % water and a weight percent ratio of solid PTFE to solid PVDF to activated carbon of 5 to 5 to 90, and is subsequently dried in an oven at 110° C. for 8 hours. The blend is heated in an oven at 240° C., then compression molded under 15,000 psi pressure to produce a block with good mechanical integrity.

#### Example 15

**[0082]** The same materials and process as in example 6 are used, except that the activated carbon has a bimodal particle size to improve packing density, and the binder is used at 25 wt % loading. The activated carbon consists of 33 wt % of Ingevity Nuchar SA-1500 with weight average particle size of 50 micron, and 67 wt % of Ingevity Nuchar WVA-1500 which has been ground and sieved to 50×625 mesh. WVA-1500 has similar BET surface area, pore volume and pore size distribution as SA-1500, as described in example 6. The resulting block has good mechanical integrity, and a bulk density of 0.66 g/cc.

**[0083]** Within this specification embodiments have been described in a way which enables a clear and concise specification to be written, but it is intended and will be appreciated that embodiments may be variously combined or separated without parting from the invention. For example, it will be appreciated that all preferred features described herein are applicable to all aspects of the invention described herein.

1. A gas storage article comprising a solid, dense, porous sorbent media bound together by 0.3 to 30 weight percent of thermoplastic binder particles, wherein said binder particles have an average discrete particle size of between 5 nm and 1,000 nm, and may optionally exist as agglomerates between 1 and 50 microns.

2. The gas storage article of claim 1, wherein said thermoplastic binder is selected from the group consisting of fluoropolymers, styrene-butadiene rubbers (SBR), ethylene vinyl acetate (EVA), acrylic polymers, polymethyl methacrylate polymers and copolymers, polyurethanes, styrenic polymers, polyamides, polyolefins, polyethylene and copolymers thereof, polypropylene and copolymers thereof, polyethylene oxide, polyesters, polyethylene terephthalate, polyvinyl chlorides, polycarbonate, polyether ketone ketone (PEKK), polyether ether ketone (PEEK), and thermoplastic polyurethane (TPU).

3. The gas storage article of claim 1, wherein said binder particles have an average discrete particle size of from 100 to 500 nm

4. The gas storage article of claim 2, wherein said thermoplastic binder comprises a fluoropolymer, said fluoropolymer comprising one or more monomers selected from the group consisting of vinylidene fluoride (VDF), tetrafluoroethylene (TFE), trifluoroethylene (TrFE), chlorotrifluoroethylene (CTFE), hexafluoropropene (HFP), vinyl fluoride (VF), hexafluoroisobutylene (HFIB), perfluorobutylethylene (PFBE), pentafluoropropen 3,3,3-trifluoro-1-propene, 2-trifluoromethyl-3,3,3-trifluoropropene, fluorinated vinyl ethers including perfluoromethyl ether (PMVE), perfluoroethylvi-

nyl ether (PEVE), perfluoropropylvinyl ether (PPVE), per-fluorobutylvinyl ether (PBVE), longer chain perfluorinated vinyl ethers, fluorinated dioxoles, partially- or per-fluorinated alpha olefins of  $C_4$  and higher, partially- or per-fluorinated cyclic alkenes of  $C_3$  and higher, and combinations thereof.

**5.** The gas storage article of claim **2**, wherein said thermoplastic binder is selected from one or more of the group consisting of polyvinylidene fluoride homopolymer and copolymer, polytetrafluoroethylene homopolymers and copolymers, and polyamides.

**6.** The gas storage article of claim **1**, wherein said sorbent is selected from the group consisting of activated carbon, carbon fibers, molecular sieves, carbon molecular sieves, molecular sieves, silica gel, and metal organic framework.

**7.** The gas storage article of claim **6**, wherein said sorbent is activated carbon or carbon fibers.

**8.** The gas storage article of claim **6**, wherein said sorbent has a BET specific surface area greater than 1,000  $m^2/g$ .

**9.** The gas storage article of claim **6**, wherein said sorbent has a BET specific surface area greater than 1,400  $m^2/g$ .

**10.** The gas storage article of claim **6**, wherein said sorbent has a pore volume of at least 0.7 cc/g, and/or more than 30% of pore volume with pore sizes in the range of 6 to 30 Å.

**11.** The gas storage article of claim **6**, wherein said sorbent has a porosity higher than 40%

**12.** The gas storage article of claim **6**, wherein said sorbent has an average particle size of 20 to 1000 microns

**13.** The gas storage article of claim **6**, wherein said sorbent has a multimodal particle size distribution

**14.** The gas storage article of claim **1** wherein said gas storage device further comprises at least one adsorbed gas selected from the group consisting of noble gases, hydrocarbons, hydrogen-based gases, methane, natural gas, CO<sub>2</sub>, CO, O<sub>2</sub>, N<sub>2</sub>, fluorinated gases, halogenated gases, silanes, phosphine, phosgene, boron trihalides, ammonia, hydrogen halide, sulfide, and cyanide.

**15.** The gas storage article of claim **1** having an immobilized bulk density greater than 1.1 times that of the bulk density of the sorbent.

**16.** The gas storage article of claim **1** having a percent fouling of the sorbent of less than 15%.

**17.** The gas storage article of claim **1**, wherein said gas storage article is present within a container capable of holding a pressurized gas at pressures up to 5000 psi.

**18.** A solid block article comprising an activated carbon media bound together by 0.3 to 30 weight percent of thermoplastic binder particles, wherein said binder particles have a discrete particle size of between 5 nm and 1,000 nm, and may optionally exist as agglomerates between 1 and 50 microns, wherein said article comprises two or more concentric nesting annuli produced by either solid state extrusion or compression molding.

**19.** A method for producing a gas storage article, the method comprising the steps of:

- a) blending a sorbent and thermoplastic binder, wherein said blend comprises 0.3 to 30 weight percent binder,
- b) optionally heating blend
- c) processing by extrusion or compression molding, to form a gas storage article.

**20.** The method of claim **19**, wherein said blending step comprises a dry powder blending of said sorbent and said thermoplastic binder.

**21.** The method of claim **19**, wherein said blending step comprises an aqueous or solvent blend of said sorbent and said thermoplastic binder.

**22.** The method of claim **19**, further comprising the step of forming the thermoplastic binder by an emulsion or suspension process, prior to the step of blending with said sorbent.

**23.** The method of claim **19**, wherein said heating, compression, and/or extrusion step occurs at a temperature at or below the melting point of said binder.

\* \* \* \* \*

(12) INTERNATIONAL APPLICATION PUBLISHED UNDER THE PATENT COOPERATION TREATY (PCT)

(19) World Intellectual Property Organization

International Bureau



(10) International Publication Number

WO 2014/210295 A2

(43) International Publication Date  
31 December 2014 (31.12.2014)

WIPO | PCT

(51) International Patent Classification:  
*B01D 53/04* (2006.01)    *B01J 20/28* (2006.01)  
*B01J 20/20* (2006.01)    *B01J 20/24* (2006.01)

(74) Agent: AMINI, Farhang; Winstead PC, P.O.Box 131851, Dallas, TX 75313 (US).

(21) International Application Number:  
PCT/US2014/044315

(81) Designated States (unless otherwise indicated, for every kind of national protection available): AE, AG, AL, AM, AO, AT, AU, AZ, BA, BB, BG, BH, BN, BR, BW, BY, BZ, CA, CH, CL, CN, CO, CR, CU, CZ, DE, DK, DM, DO, DZ, EC, EE, EG, ES, FI, GB, GD, GE, GH, GM, GT, HN, HR, HU, ID, IL, IN, IR, IS, JP, KE, KG, KN, KP, KR, KZ, LA, LC, LK, LR, LS, LT, LU, LY, MA, MD, ME, MG, MK, MN, MW, MX, MY, MZ, NA, NG, NI, NO, NZ, OM, PA, PE, PG, PH, PL, PT, QA, RO, RS, RU, RW, SA, SC, SD, SE, SG, SK, SL, SM, ST, SV, SY, TH, TJ, TM, TN, TR, TT, TZ, UA, UG, US, UZ, VC, VN, ZA, ZM, ZW.

(22) International Filing Date:  
26 June 2014 (26.06.2014)

(84) Designated States (unless otherwise indicated, for every kind of regional protection available): ARIPO (BW, GH, GM, KE, LR, LS, MW, MZ, NA, RW, SD, SL, SZ, TZ, UG, ZM, ZW), Eurasian (AM, AZ, BY, KG, KZ, RU, TJ, TM), European (AL, AT, BE, BG, CH, CY, CZ, DE, DK, EE, ES, FI, FR, GB, GR, HR, HU, IE, IS, IT, LT, LU, LV, MC, MK, MT, NL, NO, PL, PT, RO, RS, SE, SI, SK, SM,

(25) Filing Language: English

(26) Publication Language: English

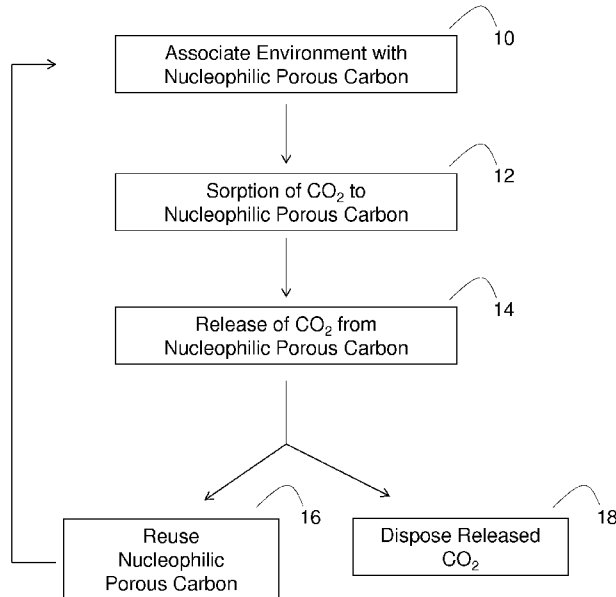
(30) Priority Data:  
61/839,567    26 June 2013 (26.06.2013)    US

(71) Applicant: WILLIAM MARSH RICE UNIVERSITY [US/US]; 6100 Main Street, Houston, TX 77005 (US).

(72) Inventors: TOUR, James, M.; 4625 Spruce St., Bellaire, TX 77401 (US). HWANG, Chih-chau; 1414 Richmond Ave., Apt. 2007, Houston, TX 77006 (US). TOUR, Josiah; 4625 Spruce St., Bellaire, TX 77401 (US).

[Continued on next page]

(54) Title: NUCLEOPHILIC POROUS CARBON MATERIALS FOR REVERSIBLE CO<sub>2</sub> CAPTURE



(57) Abstract: In some embodiments, the present disclosure pertains to methods of capturing CO<sub>2</sub> from an environment by associating the environment (e.g., a pressurized environment) with a porous carbon material that comprises a plurality of pores and a plurality of nucleophilic moieties. In some embodiments, the associating results in sorption of CO<sub>2</sub> to the porous carbon materials. In some embodiments, the sorption of CO<sub>2</sub> to the porous carbon materials occurs selectively over hydrocarbons in the environment. In some embodiments, the methods of the present disclosure also include a step of releasing captured CO<sub>2</sub> from porous carbon materials. In some embodiments, the releasing occurs without any heating steps by decreasing environmental pressure. In some embodiments, the methods of the present disclosure also include a step of disposing released CO<sub>2</sub> and reusing porous carbon materials. Additional embodiments of the present disclosure pertain to porous carbon materials that are used for CO<sub>2</sub> capture.

FIG. 1



TR), OAPI (BF, BJ, CF, CG, CI, CM, GA, GN, GQ, GW,  
KM, ML, MR, NE, SN, TD, TG).

**Published:**

— *without international search report and to be republished  
upon receipt of that report (Rule 48.2(g))*

**TITLE****NUCLEOPHILIC POROUS CARBON MATERIALS FOR REVERSIBLE CO<sub>2</sub> CAPTURE****CROSS-REFERENCE TO RELATED APPLICATIONS**

[0001] This application claims priority to U.S. Provisional Patent Application No. 61/839,567, filed on June 26, 2013. The entirety of the aforementioned application is incorporated herein by reference.

**STATEMENT REGARDING FEDERALLY SPONSORED RESEARCH**

[0002] Not applicable.

**BACKGROUND**

[0003] Current methods and materials for capturing CO<sub>2</sub> from an environment suffer from numerous limitations, including low CO<sub>2</sub> selectivity, limited CO<sub>2</sub> sorption capacity, and the need for stringent reaction conditions. The CO<sub>2</sub> sorbents and CO<sub>2</sub> capture methods of the present disclosure address these needs.

**SUMMARY**

[0004] In some embodiments, the present disclosure pertains to methods of capturing CO<sub>2</sub> from an environment. In some embodiments, the methods comprise a step of associating the environment with a porous carbon material. In some embodiments, the porous carbon material comprises a plurality of pores and a plurality of nucleophilic moieties. In some embodiments, the associating results in sorption of the CO<sub>2</sub> to the porous carbon material.

[0005] The methods of the present disclosure may be utilized to capture CO<sub>2</sub> from various environments. In some embodiments, the environments include, without limitation, industrial

gas streams, natural gas streams, natural gas wells, industrial gas wells, oil and gas fields, and combinations thereof. In some embodiments, the environment is a pressurized environment with a total pressure that is higher than atmospheric pressure (e.g., 5 bar to 500 bar).

[0006] In some embodiments, porous carbon materials are associated with an environment by placing the porous carbon materials at or near the environment. In some embodiments, porous carbon materials are associated with an environment by flowing the environment through a structure that contains the porous carbon materials.

[0007] In some embodiments, the sorption of the CO<sub>2</sub> to the porous carbon materials occurs above atmospheric pressure (e.g., 5 bar to 500 bar). In some embodiments, the sorption of the CO<sub>2</sub> to the porous carbon materials occurs at a partial CO<sub>2</sub> pressure of about 0.1 bar to about 100 bar. In some embodiments, the sorption of the CO<sub>2</sub> to the porous carbon materials occurs at ambient temperature without any heating steps. In some embodiments, the sorption of the CO<sub>2</sub> to the porous carbon materials occurs selectively over hydrocarbons in the environment. In some embodiments, the CO<sub>2</sub> is converted to poly(CO<sub>2</sub>) within the pores of the porous carbon materials.

[0008] In some embodiments, the methods of the present disclosure also include a step of releasing the captured CO<sub>2</sub> from the porous carbon materials. In some embodiments, the releasing occurs by decreasing the pressure of the environment. In some embodiments, the releasing occurs by placing the porous carbon materials in a second environment that has a lower pressure than the environment where CO<sub>2</sub> capture occurred. In some embodiments, the releasing occurs at pressures ranging from about 0 bar to about 100 bar. In some embodiments, the releasing occurs at ambient temperature or the same temperature at which CO<sub>2</sub> sorption occurred. In some embodiments, the releasing occurs without heating the porous carbon materials. In some embodiments, the releasing occurs through depolymerization of formed poly(CO<sub>2</sub>).

[0009] In some embodiments, the methods of the present disclosure also include a step of disposing the released CO<sub>2</sub>. In some embodiments, the methods of the present disclosure also

include a step of reusing the porous carbon material after the releasing step to capture additional CO<sub>2</sub> from an environment.

[0010] The methods of the present disclosure can utilize various porous carbon materials. Additional embodiments of the present disclosure pertain to such porous carbon materials for CO<sub>2</sub> capture. Generally, such porous carbon materials comprise a plurality of pores and a plurality of nucleophilic moieties.

[0011] In some embodiments, the porous carbon materials include, without limitation, nucleophilic polymers, polypeptides, proteins, waste materials, nitrogen-containing porous carbon materials, sulfur-containing porous carbon materials, metal-containing porous carbon materials, metal oxide-containing porous carbon materials, metal sulfide-containing porous carbon materials, phosphorous-containing porous carbon materials, and combinations thereof. In some embodiments, the porous carbon materials include a nucleophilic polymer. In some embodiments, the nucleophilic polymer includes, without limitation, nitrogen-containing polymers, sulfur-containing polymers, polythiophene (PTH), polythiophene-methanol (also called 2-(hydroxymethyl)thiophene), polyacrylonitrile (PAN), polypyrrole, and combinations thereof. In some embodiments, the nucleophilic polymer is carbonized. In some embodiments the nucleophilic carbon polymer is carbonized and reduced.

[0012] In some embodiments, the nucleophilic moieties are part of the porous carbon materials. In some embodiments, the nucleophilic moieties are embedded within the pores of the porous carbon materials. In some embodiments, the nucleophilic moieties include, without limitation, primary nucleophiles, secondary nucleophiles, tertiary nucleophiles and combinations thereof. In some embodiments, the nucleophilic moieties include, without limitation, oxygen-containing moieties, sulfur-containing moieties, metal-containing moieties, metal oxide-containing moieties, metal sulfide-containing moieties, phosphorous-containing moieties, nitrogen-containing moieties, and combinations thereof.

[0013] The porous carbon materials of the present disclosure may have various properties. For instance, in some embodiments, the porous carbon materials of the present disclosure have surface areas ranging from about 1,000 m<sup>2</sup>/g to about 3,000 m<sup>2</sup>/g. In some embodiments, the pores in the porous carbon materials have diameters ranging from about 5 nm to about 100 nm. In some embodiments, the pores in the porous carbon materials have volumes ranging from about 1 cm<sup>3</sup>/g to about 10 cm<sup>3</sup>/g. In some embodiments, the porous carbon materials have densities ranging from about 0.3 g/cm<sup>3</sup> to about 4 g/cm<sup>3</sup>. In some embodiments, the porous carbon materials have CO<sub>2</sub> sorption capacities ranging from about 10% to about 200% of the porous carbon material weight. In some embodiments, the porous carbon materials have CO<sub>2</sub> sorption capacities of about 55% to about 90% of the porous carbon material weight.

### **DESCRIPTION OF THE FIGURES**

[0014] **FIGURE 1** provides a scheme of a method of capturing carbon dioxide (CO<sub>2</sub>) from an environment.

[0015] **FIGURE 2** provides synthetic schemes and micrographic images of various porous carbon materials. **FIG. 2A** provides a scheme for the synthesis of sulfur-containing porous carbon (SPC) or nitrogen containing porous carbon (NPC) by treating poly[(2-hydroxymethyl)thiophene] or poly(acrylonitrile) with KOH at 600 °C and then washing with dilute HCl and water until the extracts are neutral. The NPC is further reduced using 10% H<sub>2</sub> at 600 °C to form reduced NPC (R-NPC). The synthetic details are described in Example 1. **FIG. 2B** provides a scanning electron microscopy (SEM) image of NPCs at a scale bar of 100 μm. **FIG. 2C** provides an SEM image of SPCs at a scale bar of 500 nm. **FIG. 2D** provides a transmission electron microscopy (TEM) image of the SPCs in **FIG. 2B** at a scale bar of 25 nm.

[0016] **FIGURE 3** provides x-ray photoelectron spectroscopy (XPS) of SPCs (left panel) and NPCs (right panel). The XPS indicates 13.3 atomic % of S in the SPC precursor and 22.4 atomic % of N in the NPC precursor. The resulting SPC and NPC then had 8.1 atomic % of S content and 6.2 atomic % of N content, respectively. The S<sub>2p</sub> and N<sub>1s</sub> XPS peaks were taken from the

SPC and NPC. The S<sub>2p</sub> core splits into two main peaks of 163.7 (2p<sub>3/2</sub>) and 164.8 eV (2p<sub>1/2</sub>), which correspond to thiophenic sulfur atoms incorporated into the porous carbon framework via the formation of C-S-C bond. The N<sub>1s</sub> reflects two different chemical environments: pyridinic nitrogen (N-6) and pyrrolic nitrogen (N-5) atoms.

[0017] **FIGURE 4** provides data relating to CO<sub>2</sub> uptake measurements for SPCs. **FIG. 4A** provides volumetric and gravimetric uptake of CO<sub>2</sub> on SPC at different temperatures and pressures. Data designated with (\*) were recorded volumetrically at Rice University. Data designated with (§) were performed volumetrically at the National Institute of Standards and Technology (NIST). Data designated with (+) were measured gravimetrically at NIST. All gravimetric measurements were corrected for buoyancy. **FIGS. 4B-D** provide three consecutive CO<sub>2</sub> sorption-desorption cycles on the SPC over a pressure range from 0 to 30 bar at 30 °C. All solid circles indicate CO<sub>2</sub> sorption, while the open circles designate the desorption process. **FIG. 4E** provides volumetric SPC CO<sub>2</sub> sorption isotherms at 23 °C and 50 °C over a pressure range from 0 to 1 bar.

[0018] **FIGURE 5** provides pictorial descriptions of excess and absolute CO<sub>2</sub> uptake. **FIG. 5A** is adapted from *Chem. Sci.* **5**, 32-51 (2014). The blue dashed line indicates the Gibbs dividing surface. It divides the free volume into two regions in which gas molecules are either in an adsorbed or bulk state. **FIG. 5B** shows a depiction of total uptake, which can be used as an approximation for absolute uptake for microporous materials with negligible external surface areas.

[0019] **FIGURE 6** shows CO<sub>2</sub> uptake on the SPC. Comparison of absolute uptake and excess uptake at 22 °C and 50 °C exemplifies the small differences over this pressure and temperature range.

[0020] **FIGURE 7** shows spectral changes before and after sorption-desorption at 23 °C and the proposed polymerization mechanism. Attenuated total reflectance infrared spectroscopy (ATR-IR) (**FIGS. 7A-B**), Raman spectroscopy (**FIG. 7C**) and 50.3 MHz <sup>13</sup>C MAS NMR spectra (**FIG.**

**7D)** are shown before and after CO<sub>2</sub> sorption at 10 bar and room temperature. All spectra were recorded at the elapsed times indicated on the graphs after the SPC sorbent was returned to ambient pressure. In the NMR experiments, the rotor containing the SPC was tightly capped during the analyses. For the third NMR experiment (top), the same material was left under ambient conditions for 19 h before being repacked in the rotor to obtain the final spectrum. Each NMR spectrum took 80 min to record. Example 1 provides more details. **FIGS. 7E-F** show proposed mechanisms that illustrate the poly(CO<sub>2</sub>) formation in SPC or NPC, respectively, in a higher pressure CO<sub>2</sub> environment. With the assistance of the nucleophile, such as S or N, the CO<sub>2</sub> polymerization reaction is initiated under pressure, and the polymer is further likely stabilized by the van der Waals interactions with the carbon surfaces in the pores.

[0021] **FIGURE 8** shows ATR-IR (**FIG. 8A**) and Raman (**FIG. 8B**) spectra for the ZIF-8 before and after CO<sub>2</sub> sorption at 10 bar. All spectra were recorded 3 and 20 minutes after the ZIF-8 sorbent was returned to ambient pressure at room temperature.

[0022] **FIGURE 9** shows ATR-IR (**FIG. 9A**) and Raman (**FIG. 9B**) spectra for the activated carbon before and after CO<sub>2</sub> sorption at 10 bar. Spectra were taken 3 min and 20 min after the activated carbon was returned to ambient pressure at room temperature.

[0023] **FIGURE 10** provides volumetric gas uptake data. **FIG. 10A** provides data relating to volumetric CO<sub>2</sub> uptake performance at 30 °C of SPC, NPC, R-NPC and the following traditional sorbents: activated carbon, ZIF-8, and zeolite 5A. Aluminum foil was used as a reference to ensure no CO<sub>2</sub> condensation was occurring in the system at this temperature and pressure. Volumetric CO<sub>2</sub> and CH<sub>4</sub> uptake tests at 23 °C on SPC (**FIG. 10B**), activated carbon (**FIG. 10C**) and ZIF-8 sorbents (**FIG. 10D**) are also shown.

[0024] **FIGURE 11** shows various mass spectrometry (MS) data. **FIG. 11A** shows MS data that was taken while the system was being pressurized with a premixed gas of CO<sub>2</sub> in natural gas during the uptake process. **FIG. 11B** shows MS data that was recorded while the premixed gas-filled SPC was desorbing from 30 bar. The mixed gas was purchased from Applied Gas Inc.

[0025] **FIGURE 12** provides comparative data relating to the CO<sub>2</sub> uptake capacities of various carbon sources.

## **DETAILED DESCRIPTION**

[0026] It is to be understood that both the foregoing general description and the following detailed description are illustrative and explanatory, and are not restrictive of the subject matter, as claimed. In this application, the use of the singular includes the plural, the word “a” or “an” means “at least one”, and the use of “or” means “and/or”, unless specifically stated otherwise. Furthermore, the use of the term “including”, as well as other forms, such as “includes” and “included”, is not limiting. Also, terms such as “element” or “component” encompass both elements or components comprising one unit and elements or components that comprise more than one unit unless specifically stated otherwise.

[0027] The section headings used herein are for organizational purposes and are not to be construed as limiting the subject matter described. All documents, or portions of documents, cited in this application, including, but not limited to, patents, patent applications, articles, books, and treatises, are hereby expressly incorporated herein by reference in their entirety for any purpose. In the event that one or more of the incorporated literature and similar materials defines a term in a manner that contradicts the definition of that term in this application, this application controls.

[0028] Traditional solid CO<sub>2</sub> sorbents, such as activated carbons and zeolites, show moderate CO<sub>2</sub> sorption capacity due to their high surface area. Moreover, the selectivity of such sorbents to CO<sub>2</sub> is very low, thereby limiting their application in oil and gas fields where CO<sub>2</sub> is present in the presence of hydrocarbon gases and other small organic and inorganic gases.

[0029] Although amine polymer modified silica show good CO<sub>2</sub> selectivity and uptake capacity, they require much more energy for regeneration. For instance, amine polymer modified silica may typically be heated to temperatures above 100 °C in order to be regenerated.

[0030] Aqueous sorbents (e.g., aqueous amine scrubbers) are also used to remove CO<sub>2</sub> from natural gas. However, many aqueous sorbents such as aqueous amines are corrosive. Moreover,

CO<sub>2</sub>-containing liquids require stringent heating (e.g., heating at temperatures between 125-140 °C) to liberate the CO<sub>2</sub> from the aqueous sorbent (e.g., amine carbonate).

[0031] Other materials for CO<sub>2</sub> capture include metal oxide frameworks (MOFs), zeolites, ionic liquids, cryogenic distillation, membranes and metal oxides. However, many of such materials have hydrolytic instabilities or low densities that lead to low volumetric efficiencies or poor selectivity relative to methane or other hydrocarbons. Moreover, synthesis constraints or energy costs associated with these materials lessen their suitability for on-site CO<sub>2</sub> capture from various environments, such as environments containing natural gas streams.

[0032] As such, a need exists for improved CO<sub>2</sub> sorbents and CO<sub>2</sub> capture methods that can be used to capture CO<sub>2</sub> more effectively and selectively without requiring stringent conditions, such as temperature swings. The present disclosure addresses these needs.

[0033] In some embodiments, the present disclosure pertains to methods of capturing CO<sub>2</sub> from an environment by utilizing various porous carbon materials that include a plurality of pores and a plurality of nucleophilic moieties (also referred to as nucleophilic porous carbons). In some embodiments illustrated in **FIG. 1**, the CO<sub>2</sub> capture methods of the present disclosure include a step of associating the environment with the porous carbon material (step 10), such as a nitrogen-containing or a sulfur-containing porous carbon material. In some embodiments, the associating results in the sorption of the CO<sub>2</sub> to the porous carbon material (step 12). In some embodiments, the sorption occurs selectively in a pressurized environment, such as a subsurface oil and gas well.

[0034] In some embodiments, the methods of the present disclosure also include a step of releasing the captured CO<sub>2</sub> from the porous carbon material (step 14). In some embodiments, the releasing occurs by decreasing environmental pressure in the absence of a heating step.

[0035] In additional embodiments, the methods of the present disclosure also include a step of reusing the porous carbon material after the releasing step for additional CO<sub>2</sub> capture (step 16).

In some embodiments, the methods of the present disclosure also include a step of disposing the released CO<sub>2</sub> (step 18). Further embodiments of the present disclosure pertain to the porous carbon materials that are utilized for CO<sub>2</sub> capture.

[0036] As set forth in more detail herein, the CO<sub>2</sub> capture methods and the porous carbon materials of the present disclosure have numerous embodiments. For instance, various methods may be utilized to associate various types of porous carbon materials with various environments to result in the capture of various amounts of CO<sub>2</sub> from the environment. Moreover, the captured CO<sub>2</sub> may be released from the porous carbon materials in various manners.

**[0037] Environments**

[0038] The methods of the present disclosure may be utilized to capture CO<sub>2</sub> from various environments. In some embodiments, the environment includes, without limitation, industrial gas streams, natural gas streams, natural gas wells, industrial gas wells, oil and gas fields, and combinations thereof. In some embodiments, the environment is a subsurface oil and gas field. In more specific embodiments, the methods of the present disclosure may be utilized to capture CO<sub>2</sub> from an environment that contains natural gas, such as an oil well.

[0039] In some embodiments, the environment is a pressurized environment. For instance, in some embodiments, the environment has a total pressure higher than atmospheric pressure.

[0040] In some embodiments, the environment has a total pressure of about 0.1 bar to about 500 bar. In some embodiments, the environment has a total pressure of about 5 bar to about 100 bar. In some embodiments, the environment has a total pressure of about 25 bar to about 30 bar. In some embodiments, the environment has a total pressure of about 100 bar to about 200 bar. In some embodiments, the environment has a total pressure of about 200 bar to about 300 bar.

**[0041] Association of Porous Carbon Materials with an Environment**

**[0042]** Various methods may be utilized to associate porous carbon materials of the present disclosure with an environment. In some embodiments, the association occurs by incubating the porous carbon materials with the environment (e.g., a pressurized environment). In some embodiments, the association of porous carbon materials with an environment occurs by flowing the environment through a structure that contains the porous carbon materials. In some embodiments, the structure may be a column or a sheet that contains immobilized porous carbon materials. In some embodiments, the structure may be a floating bed that contains porous carbon materials.

**[0043]** In some embodiments, the porous carbon materials are suspended in a solvent while being associated with an environment. In more specific embodiments, the solvent may include water or alcohol. In some embodiments, the porous carbon materials are associated with an environmental in pelletized form. In some embodiments, the pelletization can be used to assist flow of the gases through the porous carbon materials.

**[0044]** In some embodiments, the associating occurs by placing the porous carbon material at or near the environment. In some embodiments, such placement occurs by various methods that include, without limitation, adhesion, immobilization, clamping, and embedding. Additional methods by which to associate porous carbon materials with an environment can also be envisioned.

**[0045] CO<sub>2</sub> Sorption to Porous Carbon Materials**

**[0046]** The sorption of CO<sub>2</sub> to porous carbon materials of the present disclosure can occur at various environmental pressures. For instance, in some embodiments, the sorption of CO<sub>2</sub> to porous carbon materials occurs above atmospheric pressure. In some embodiments, the sorption of CO<sub>2</sub> to porous carbon materials occurs at total pressures ranging from about 0.1 bar to about 500 bar. In some embodiments, the sorption of CO<sub>2</sub> to porous carbon materials occurs at total

pressures ranging from about 5 bar to about 500 bar. In some embodiments, the sorption of CO<sub>2</sub> to porous carbon materials occurs at total pressures ranging from about 5 bar to about 100 bar. In some embodiments, the sorption of CO<sub>2</sub> to porous carbon materials occurs at total pressures ranging from about 25 bar to about 30 bar. In some embodiments, the sorption of CO<sub>2</sub> to porous carbon materials occurs at total pressures ranging from about 100 bar to about 500 bar. In some embodiments, the sorption of CO<sub>2</sub> to porous carbon materials occurs at total pressures ranging from about 100 bar to about 300 bar. In some embodiments, the sorption of CO<sub>2</sub> to porous carbon materials occurs at total pressures ranging from about 100 bar to about 200 bar.

[0047] In some embodiments, the sorption of CO<sub>2</sub> to porous carbon materials occurs at a partial CO<sub>2</sub> pressure of about 0.1 bar to about 100 bar. In some embodiments, the sorption of CO<sub>2</sub> to porous carbon materials occurs at a partial CO<sub>2</sub> pressure of about 5 bar to about 30 bar. In some embodiments, the sorption of CO<sub>2</sub> to porous carbon materials occurs at a partial CO<sub>2</sub> pressure of about 30 bar.

[0048] The sorption of CO<sub>2</sub> to porous carbon materials can also occur at various temperatures. For instance, in some embodiments, the sorption of CO<sub>2</sub> to porous carbon materials occurs at temperatures that range from about 0 °C (e.g., a sea floor temperature where a wellhead may reside) to about 100 °C (e.g., a temperature where machinery may reside). In more specific embodiments, the sorption of CO<sub>2</sub> to porous carbon materials occurs at ambient temperature (e.g., temperatures ranging from about 20-25 °C, such as 23 °C). In some embodiments, the sorption of CO<sub>2</sub> to porous carbon materials occurs below ambient temperature. In some embodiments, the sorption of CO<sub>2</sub> to porous carbon materials occurs above ambient temperature. In some embodiments, the sorption of CO<sub>2</sub> to porous carbon materials occurs without the heating of the porous carbon materials.

[0049] Without being bound by theory, it is envisioned that the sorption of CO<sub>2</sub> to porous carbon materials occurs by various molecular mechanisms. For instance, in some embodiments, the sorption of CO<sub>2</sub> to porous carbon materials occurs by at least one of absorption, adsorption, ionic

interactions, physisorption, chemisorption, covalent bonding, non-covalent bonding, hydrogen bonding, van der Waals interactions, and combinations of such mechanisms. In some embodiments, the sorption includes an absorption interaction between the CO<sub>2</sub> in an environment and the porous carbon materials. In some embodiments, the sorption includes an ionic interaction between the CO<sub>2</sub> in an environment and the porous carbon materials. In some embodiments, the sorption includes an adsorption interaction between the CO<sub>2</sub> in an environment and the porous carbon materials. In some embodiments, the sorption includes a physisorption interaction between the CO<sub>2</sub> in an environment and the porous carbon materials. In some embodiments, the sorption includes a chemisorption interaction between the CO<sub>2</sub> in an environment and the porous carbon materials. In some embodiments, the sorption includes a covalent bonding interaction between the CO<sub>2</sub> in an environment and the porous carbon materials. In some embodiments, the sorption includes a non-covalent bonding interaction between the CO<sub>2</sub> in an environment and the porous carbon materials. In some embodiments, the sorption includes a hydrogen bonding interaction between the CO<sub>2</sub> in an environment and the porous carbon materials. In some embodiments, the sorption includes a van der Waals interaction between the CO<sub>2</sub> in an environment and the porous carbon materials. In some embodiments, the sorption of CO<sub>2</sub> to porous carbon materials occurs by adsorption and absorption.

[0050] Without being bound by theory, it is envisioned that CO<sub>2</sub> sorption may be facilitated by various chemical reactions. For instance, in some embodiments, the sorbed CO<sub>2</sub> is converted to poly(CO<sub>2</sub>) within the pores of the porous carbon materials. In some embodiments, the poly(CO<sub>2</sub>) comprises the following formula: -(O-C(=O))<sub>n</sub>-, where n is equal to or greater than 2. In some embodiments, n is between 2 to 10,000. In some embodiments, the formed poly(CO<sub>2</sub>) may be further stabilized by van der Waals interactions with the carbon surfaces in the pores of the carbon materials. In some embodiments, the formed poly(CO<sub>2</sub>) may be in solid form.

[0051] In some embodiments, the sorption of CO<sub>2</sub> to the porous carbon materials occurs selectively. For instance, in some embodiments, the sorption of CO<sub>2</sub> to the porous carbon

materials occurs selectively over hydrocarbons in the environment (e.g., ethane, propane, butane, pentane, methane, and combinations thereof). In further embodiments, the molecular ratio of sorbed CO<sub>2</sub> to sorbed hydrocarbons in the porous carbon materials is greater than about 2. In additional embodiments, the molecular ratio of sorbed CO<sub>2</sub> to sorbed hydrocarbons in the porous carbon materials ranges from about 2 to about 3. In additional embodiments, the molecular ratio of sorbed CO<sub>2</sub> to sorbed hydrocarbons in the porous carbon materials is about 2.6.

[0052] In more specific embodiments, the sorption of CO<sub>2</sub> to porous carbon materials occurs selectively over the CH<sub>4</sub> in the environment. In further embodiments, the molecular ratio of sorbed CO<sub>2</sub> to sorbed CH<sub>4</sub> (n<sub>CO<sub>2</sub></sub> / n<sub>CH<sub>4</sub></sub>) in the porous carbon materials is greater than about 2. In additional embodiments, n<sub>CO<sub>2</sub></sub>/n<sub>CH<sub>4</sub></sub> in the porous carbon materials ranges from about 2 to about 3. In more specific embodiments, n<sub>CO<sub>2</sub></sub>/n<sub>CH<sub>4</sub></sub> in the porous carbon materials is about 2.6.

[0053] In some embodiments, sorption of CO<sub>2</sub> to porous carbon materials occurs selectively through poly(CO<sub>2</sub>) formation within the pores of the porous carbon materials. Without being bound by theory, it is envisioned that poly(CO<sub>2</sub>) formation within the pores of the porous carbon materials can displace other gases associated with the porous carbon materials, including any physisorbed gases and hydrocarbons (e.g., methane, propane, and butane). Without being bound by further theory, it is also envisioned that the displacement of other gases from the porous carbon materials creates a continual CO<sub>2</sub> selectivity that far exceeds various CO<sub>2</sub> selectively ranges, including the CO<sub>2</sub> selectivity ranges noted above.

[0054] In some embodiments, the covalent bond nature of poly(CO<sub>2</sub>) within the pores of the porous carbon materials can be 100 times stronger than that of other physisorbed entities, including physisorbed gases within the pores of the porous carbon materials. Therefore, such strong covalent bonds can contribute to the displacement of the physisorbed gases (e.g., methane, propane and butane).

**[0055] Release of Captured CO<sub>2</sub>**

**[0056]** In some embodiments, the methods of the present disclosure also include a step of releasing captured CO<sub>2</sub> from porous carbon materials. Various methods may be utilized to release CO<sub>2</sub> from porous carbon materials. For instance, in some embodiments, the releasing occurs by decreasing the pressure of the environment. In some embodiments, the pressure of the environment is reduced to atmospheric pressure or below atmospheric pressure. In some embodiments, the releasing occurs by placing the porous carbon material in a second environment that has a lower pressure than the environment where CO<sub>2</sub> capture occurred. In some embodiments, the second environment may be at or below atmospheric pressure. In some embodiments, the releasing occurs spontaneously as the environmental pressure decreases.

**[0057]** The release of captured CO<sub>2</sub> from porous carbon materials can occur at various pressures. For instance, in some embodiments, the release occurs at or below atmospheric pressure. In some embodiments, the release occurs at total pressures ranging from about 0 bar to about 100 bar. In some embodiments, the release occurs at total pressures ranging from about 0.1 bar to about 50 bar. In some embodiments, the release occurs at total pressures ranging from about 0.1 bar to about 30 bar. In some embodiments, the release occurs at total pressures ranging from about 0.1 bar to about 10 bar.

**[0058]** Without being bound by theory, it is envisioned that the release of captured CO<sub>2</sub> from porous carbon materials can occur by various mechanisms. For instance, in some embodiments, the release of captured CO<sub>2</sub> can occur through a depolymerization of the formed poly(CO<sub>2</sub>) within the pores of the porous carbon materials. In some embodiments, the depolymerization can be facilitated by a decrease in environmental pressure.

**[0059]** The release of captured CO<sub>2</sub> from porous carbon materials can also occur at various temperatures. In some embodiments, the release occurs at ambient temperature. In some embodiments, the release occurs at the same temperature at which CO<sub>2</sub> sorption occurred. In some embodiments, the releasing occurs without heating the porous carbon materials. Therefore,

in some embodiments, a temperature swing is not required to release captured CO<sub>2</sub> from porous carbon materials.

[0060] In some embodiments, the release occurs at temperatures ranging from about 30 °C to about 200 °C. In some embodiments, the release is facilitated by also lowering the pressure.

[0061] In some embodiments, heat for release of CO<sub>2</sub> from porous carbon materials can be supplied from various sources. For instance, in some embodiments, the heat for the release of CO<sub>2</sub> from a porous carbon material-containing vessel can be provided by an adjacent vessel whose heat is being generated during a CO<sub>2</sub> sorption step.

**[0062] Disposal of the Released CO<sub>2</sub>**

[0063] In some embodiments, the methods of the present disclosure also include a step of disposing the released CO<sub>2</sub>. For instance, in some embodiments, the released CO<sub>2</sub> can be off-loaded into a container. In some embodiments, the released CO<sub>2</sub> can be pumped downhole for long-term storage. In some embodiments, the released CO<sub>2</sub> can be vented to the atmosphere. Additional methods by which to dispose the released CO<sub>2</sub> can also be envisioned.

**[0064] Reuse of the Porous Carbon Material**

[0065] In some embodiments, the methods of the present disclosure also include a step of reusing the porous carbon materials after CO<sub>2</sub> release to capture more CO<sub>2</sub> from an environment. In some embodiments, the porous carbon materials of the present disclosure may be reused over 100 times without substantially affecting their CO<sub>2</sub> sorption capacities. In some embodiments, the porous carbon materials of the present disclosure may be reused over 1000 times without substantially affecting their CO<sub>2</sub> sorption capacities. In some embodiments, the porous carbon materials of the present disclosure may be reused over 10,000 times without substantially affecting their CO<sub>2</sub> sorption capacities.

[0066] In some embodiments, the porous carbon materials of the present disclosure may retain 100% of their CO<sub>2</sub> sorption capacities after being used multiple times (e.g., 100 times, 1,000 times or 10,000 times). In some embodiments, the porous carbon materials of the present disclosure may retain at least 98% of their CO<sub>2</sub> sorption capacities after being used multiple times (e.g., 100 times, 1,000 times or 10,000 times). In some embodiments, the porous carbon materials of the present disclosure may retain at least 95% of their CO<sub>2</sub> sorption capacities after being used multiple times (e.g., 100 times, 1,000 times or 10,000 times). In some embodiments, the porous carbon materials of the present disclosure may retain at least 90% of their CO<sub>2</sub> sorption capacities after being used multiple times (e.g., 100 times, 1,000 times or 10,000 times). In some embodiments, the porous carbon materials of the present disclosure may retain at least 80% of their CO<sub>2</sub> sorption capacities after being used multiple times (e.g., 100 times, 1,000 times or 10,000 times).

#### [0067] Porous carbon materials

[0068] The methods of the present disclosure can utilize various types of porous carbon materials for CO<sub>2</sub> capture. Further embodiments of the present disclosure pertain to such porous carbon materials. In general, the porous carbon materials of the present disclosure include a plurality of pores and a plurality of nucleophilic moieties. As set forth in more detail herein, various porous carbon materials with various porosities and nucleophilic moieties may be utilized. Furthermore, the porous carbon materials of the present disclosure may have various surface areas, pore diameters, pore volumes, densities, and CO<sub>2</sub> sorption capacities.

#### [0069] Carbon Materials

[0070] The porous carbon materials of the present disclosure may be derived from various carbon materials. For instance, in some embodiments, the porous carbon materials of the present disclosure may include, without limitation, nucleophilic polymers, polypeptides, proteins, waste materials, nitrogen-containing porous carbon materials, sulfur-containing porous carbon materials, metal-containing porous carbon materials, metal oxide-containing porous carbon

materials, metal sulfide-containing porous carbon materials, phosphorous-containing porous carbon materials, and combinations thereof. In some embodiments, the porous carbon materials of the present disclosure may include whey proteins. In some embodiments, the porous carbon materials of the present disclosure may include rice proteins. In some embodiments, the porous carbon materials of the present disclosure may include food waste. In some embodiments, the porous carbon material is carbonized. In some embodiments, the porous carbon material is reduced. In some embodiments, the porous carbon material is reduced and carbonized.

[0071] In more specific embodiments, the porous carbon materials of the present disclosure include a nucleophilic polymer. In some embodiments, the nucleophilic polymer includes, without limitation, nitrogen-containing polymers, sulfur-containing polymers, polythiophene (PTH), polythiophene-methanol (also called 2-(hydroxymethyl)thiophene), polyacrylonitrile (PAN), polypyrrole, and combinations thereof. In some embodiments, the nucleophilic polymer is carbonized. In some embodiments, the nucleophilic polymer is reduced. In some embodiments, the nucleophilic polymer is reduced and carbonized. In some embodiments, the nucleophilic polymer is reduced with hydrogen (H<sub>2</sub>) treatment.

[0072] In additional embodiments, the porous carbon materials of the present disclosure include nitrogen containing porous carbons. In some embodiments, the nitrogen groups in the nitrogen containing porous carbons include at least one of pyridinic nitrogen (N-6), pyrrolic nitrogen (N-5), nitrogen oxides, and combinations thereof. In more specific embodiments, the nitrogen groups in the nitrogen containing porous carbons include nitrogen oxides, such as N-oxides. In some embodiments, the nitrogen containing porous carbons may include a nitrogen containing polymer, such as polyacrylonitrile. In some embodiments, the nitrogen containing porous carbons include carbonized polyacrylonitrile, such as reduced and carbonized polyacrylonitrile.

[0073] In some embodiments, the porous carbons of the present disclosure include sulfur containing porous carbons. In more specific embodiments, the sulfur containing porous carbons include a polythiophene, such as poly[(2-hydroxymethyl)thiophene]. In further embodiments,

the porous carbons of the present disclosure include polymer-derived nitrogen containing porous carbons with primary amines, secondary amines, tertiary amines, or nitrogen oxides. In some embodiments, the porous carbons of the present disclosure include polymer-derived sulfur containing porous carbons with primary sulfur groups (e.g., thiol), secondary sulfur groups, or sulfur oxides.

[0074] The porous carbon materials of the present disclosure may be fabricated by various methods. For instance, in some embodiments where porous carbon materials include nucleophilic polymers, nucleophilic polymer precursors may be polymerized to form the porous carbon materials. In some embodiments, the nucleophilic polymer precursors may be polymerized through treatment with a base, such as potassium hydroxide (KOH), sodium hydroxide (NaOH) or lithium hydroxide (LiOH). In some embodiments, the formed nucleophilic polymer materials may also be carbonized. In some embodiments, the formed nucleophilic polymers may also be reduced. In some embodiments, the formed nucleophilic polymers may be carbonized and reduced.

#### [0075] Nucleophilic Moieties

[0076] The porous carbon materials of the present disclosure may contain various arrangements of nucleophilic moieties. In some embodiments, the nucleophilic moieties are part of the porous carbon material. For instance, in some embodiments, the nucleophilic moieties are embedded within the porous carbon materials. In some embodiments, the nucleophilic moieties are homogenously distributed throughout the porous carbon material framework. In some embodiments, the nucleophilic moieties are embedded within the plurality of the pores of the porous carbon materials.

[0077] The porous carbon materials of the present disclosure may also contain various types of nucleophilic moieties. For instance, in some embodiments, the nucleophilic moieties include, without limitation, primary nucleophiles, secondary nucleophiles, tertiary nucleophiles and combinations thereof. In more specific embodiments, the nucleophilic moieties include, without

limitation, oxygen-containing moieties, sulfur-containing moieties, metal-containing moieties, nitrogen-containing moieties, metal oxide-containing moieties, metal sulfide-containing moieties, phosphorous-containing moieties, and combinations thereof.

[0078] In more specific embodiments, the nucleophilic moieties include phosphorous-containing moieties. In some embodiments, the phosphorous containing moieties include, without limitation, phosphines, phosphites, phosphine oxides, and combinations thereof.

[0079] In more specific embodiments, the nucleophilic moieties of the present disclosure may include metal-containing moieties, such as metal oxide-containing moieties or metal sulfide containing moieties. In some embodiments, the metal-containing moieties may include metal centers. In some embodiments, the metal-containing moieties may include, without limitation, iron oxide, iron sulfide, aluminum oxide, silicon oxide, titanium oxide, and combinations thereof. In more specific embodiments, the metal-containing moieties of the present disclosure include iron oxide. In more specific embodiments, the metal-containing moieties of the present disclosure include iron sulfide.

[0080] In additional embodiments, the nucleophilic moieties of the present disclosure include nitrogen-containing moieties. In some embodiments where the porous carbon materials include nitrogen containing porous carbons, the nitrogen-containing moieties include the nitrogen groups within the porous carbons. In some embodiments, the nitrogen-containing moieties include, without limitation, primary amines, secondary amines, tertiary amines, nitrogen oxides, and combinations thereof. In some embodiments, the nitrogen-containing moieties include secondary amines. In some embodiments, the nitrogen-containing moieties include at least one of pyridinic nitrogen (N-6), pyrrolic nitrogen (N-5), nitrogen oxides, and combinations thereof. In more specific embodiments, the nitrogen containing moieties include nitrogen oxides, such as N-oxides.

[0081] In further embodiments, the nucleophilic moieties of the present disclosure include sulfur-containing moieties. In some embodiments where the porous carbon materials include

sulfur-containing porous carbons, the sulfur-containing moieties include the sulfur groups within the porous carbons. In some embodiments, the sulfur-containing moieties include, without limitation, primary sulfurs, secondary sulfurs, sulfur-oxides, and combinations thereof. In some embodiments, the sulfur-containing moieties include secondary sulfurs. In more specific embodiments, the sulfur-containing moieties include thiophene groups. In some embodiments, the thiophene groups include thiophenic sulfur atoms that are incorporated into the porous carbon material framework through the formation of C-S-C bonds.

**[0082] Surface Areas**

**[0083]** The porous carbon materials of the present disclosure may have various surface areas. For instance, in some embodiments, the porous carbon materials of the present disclosure have surface areas that range from about 1,000 m<sup>2</sup>/g to about 3,000 m<sup>2</sup>/g. In some embodiments, the porous carbon materials of the present disclosure have surface areas that range from about 1,000 m<sup>2</sup>/g to about 2,000 m<sup>2</sup>/g. In some embodiments, the porous carbon materials of the present disclosure have surface areas that range from about 1,400 m<sup>2</sup>/g to about 2,500 m<sup>2</sup>/g. In more specific embodiments, the porous carbon materials of the present disclosure have surface areas that include at least one of 1450 m<sup>2</sup> g<sup>-1</sup>, 1,500 m<sup>2</sup>/g, 1,700 m<sup>2</sup>/g, 1,900 m<sup>2</sup>/g, or 2500 m<sup>2</sup> g<sup>-1</sup>.

**[0084] Porosities**

**[0085]** The porous carbon materials of the present disclosure may have various porosities. For instance, in some embodiments, the pores in the porous carbon materials include diameters between about 1 nanometer to about 5 micrometers. In some embodiments, the pores include macropores with diameters of at least about 50 nm. In some embodiments, the pores include macropores with diameters between about 50 nanometers to about 3 micrometers. In some embodiments, the pores include macropores with diameters between about 500 nanometers to about 2 micrometers. In some embodiments, the pores include mesopores with diameters of less than about 50 nm. In some embodiments, the pores include micropores with diameters of less

than about 2 nm. In some embodiments, the pores include diameters that range from about 5 nm to about 100 nm.

[0086] The pores of the porous carbon materials of the present disclosure may also have various volumes. For instance, in some embodiments, the pores in the porous carbon materials have volumes ranging from about 1 cm<sup>3</sup>/g to about 10 cm<sup>3</sup>/g. In some embodiments, the pores in the porous carbon materials have volumes ranging from about 1 cm<sup>3</sup>/g to about 5 cm<sup>3</sup>/g. In some embodiments, the pores in the porous carbon materials have volumes ranging from about 1 cm<sup>3</sup>/g to about 3 cm<sup>3</sup>/g. In more specific embodiments, the plurality of pores in the porous carbon materials have volumes of about 1.5 cm<sup>3</sup>/g or about 1.43 cm<sup>3</sup>/g.

#### [0087] Densities

[0088] The porous carbon materials of the present disclosure may also have various densities. For instance, in some embodiments, the porous carbon materials of the present disclosure have densities that range from about 0.3 g/cm<sup>3</sup> to about 10 g/cm<sup>3</sup>. In some embodiments, the porous carbon materials of the present disclosure have densities that range from about 0.3 g/cm<sup>3</sup> to about 4 g/cm<sup>3</sup>. In some embodiments, the porous carbon materials of the present disclosure have densities that range from about 1 g/cm<sup>3</sup> to about 3 g/cm<sup>3</sup>. In some embodiments, the porous carbon materials of the present disclosure have densities that range from about 1 g/cm<sup>3</sup> to about 2 g/cm<sup>3</sup>. In some embodiments, the porous carbon materials of the present disclosure have densities that range from about 2 g/cm<sup>3</sup> to about 3 g/cm<sup>3</sup>. In more specific embodiments, the porous carbon materials of the present disclosure have densities of 1.2 g/cm<sup>3</sup>, 2 g/cm<sup>3</sup>, 2.1 g/cm<sup>3</sup>, 2.20 g/cm<sup>3</sup>, 2.21 g/cm<sup>3</sup>, or 2.5 g/cm<sup>3</sup>.

#### [0089] CO<sub>2</sub> Sorption Capacities

[0090] The porous carbon materials of the present disclosure may also have various sorption capacities. For instance, in some embodiments, the porous carbon materials of the present disclosure have a CO<sub>2</sub> sorption capacity that ranges from about 10% to about 200% of the porous

carbon material weight. In some embodiments, the porous carbon materials of the present disclosure have a CO<sub>2</sub> sorption capacity of about 50% to about 180% of the porous carbon material weight. In some embodiments, the porous carbon materials of the present disclosure have a CO<sub>2</sub> sorption capacity of about 55% to about 90% of the porous carbon material weight. In some embodiments, the porous carbon materials of the present disclosure have a CO<sub>2</sub> sorption capacity of about 55% to about 85% of the porous carbon material weight. In more specific embodiments, the porous carbon materials of the present disclosure have a CO<sub>2</sub> sorption capacity of about 58% or about 82% of the porous carbon material weight.

[0091] In further embodiments, the porous carbon materials of the present disclosure have a CO<sub>2</sub> sorption capacity of about 1 g to about 2 g of porous carbon material per 1 g of CO<sub>2</sub>. In more specific embodiments, the porous carbon materials of the present disclosure have a CO<sub>2</sub> sorption capacity of about 1.5 g of porous carbon material weight per 1 g of CO<sub>2</sub>.

#### **[0092] Physical States**

[0093] The porous carbon materials of the present disclosure may be in various states. For instance, in some embodiments, the porous carbon materials of the present disclosure may be in a solid state. In some embodiments, the porous carbon materials of the present disclosure may be in a gaseous state. In some embodiments, the porous carbon materials of the present disclosure may be in a liquid state.

#### **[0094] Advantages**

[0095] The CO<sub>2</sub> capture methods and the porous carbon materials of the present disclosure provide numerous advantages over prior CO<sub>2</sub> sorbents. In particular, the porous carbon materials of the present disclosure provide significantly higher CO<sub>2</sub> sorption capacities than traditional CO<sub>2</sub> sorbents. For instance, as set forth in the Examples herein, the CO<sub>2</sub> sorption capacities of the porous carbon materials can be nearly 3-5 times higher than that found in zeolite 5A, and 2-3 times higher than that found in ZIF-8.

[0096] Furthermore, unlike traditional CO<sub>2</sub> sorbents, the porous carbon materials of the present disclosure can selectively capture and release CO<sub>2</sub> at ambient temperature without requiring a temperature swing. For instance, unlike traditional CO<sub>2</sub> sorbents that require substantial heating for regeneration, the porous carbon materials of the present disclosure can be spontaneously regenerated through pressure swings. As such, the porous carbon materials of the present disclosure can avoid substantial thermal insults and be used effectively over successive cycles without losing their original CO<sub>2</sub> sorption capacities. Moreover, due to the availability and affordability of the starting materials, the porous carbon materials of the present disclosure can be made in a facile and economical manner in bulk quantities, unlike many metal-oxide framework (MOF) materials.

[0097] As such, the CO<sub>2</sub> capture methods and the porous carbon materials of the present disclosure can find numerous applications. For instance, in some embodiments, the CO<sub>2</sub> capture methods and the porous carbon materials of the present disclosure can be utilized for the capture of CO<sub>2</sub> from subsurface oil and gas fields. In more specific embodiments, the process may take advantage of differential pressures commonly found in natural gas collection and processing streams as a driving force during CO<sub>2</sub> capture and poly(CO<sub>2</sub>) formation. For instance, in some embodiments, the methods of the present disclosure may utilize a natural gas-well pressure (e.g., a natural gas well pressure of 200 to 300 bar) as a driving force during CO<sub>2</sub> capture and poly(CO<sub>2</sub>) formation. Thereafter, by lowering the pressure back to ambient conditions after CO<sub>2</sub> uptake, the poly(CO<sub>2</sub>) is then depolymerized, where it can be off-loaded or pumped back downhole into the structures that had held it for geological timeframes. Moreover, the CO<sub>2</sub> capture methods and the porous carbon materials of the present disclosure can allow for the capture and reinjection of CO<sub>2</sub> at the natural gas sites, thereby leading to greatly reduced CO<sub>2</sub> emissions from natural gas streams.

**[0098] Additional Embodiments**

[0099] Reference will now be made to more specific embodiments of the present disclosure and experimental results that provide support for such embodiments. However, Applicants note that the disclosure below is for illustrative purposes only and is not intended to limit the scope of the claimed subject matter in any way.

[00100] **Example 1. Capture of CO<sub>2</sub> by Sulfur- and Nitrogen-Containing Porous Carbons**

[00101] In this Example, nucleophilic porous carbons are synthesized from simple and inexpensive carbon-sulfur and carbon-nitrogen precursors. Infrared, Raman and <sup>13</sup>C nuclear magnetic resonance signatures substantiate CO<sub>2</sub> fixation by polymerization in the carbon channels to form poly(CO<sub>2</sub>) under much lower pressures than previously required. This growing chemisorbed sulfur- or nitrogen-atom-initiated poly(CO<sub>2</sub>) chain further displaces physisorbed hydrocarbon, providing a continuous CO<sub>2</sub> selectivity. Once returned to ambient conditions, the poly(CO<sub>2</sub>) spontaneously depolymerizes, leading to a sorbent that can be easily regenerated without the thermal energy input that is required for traditional sorbents.

[00102] More specifically, Applicants show in this Example that the new carbon materials can be used to separate CO<sub>2</sub> from various environments (e.g., natural gas), where 0.82 g of CO<sub>2</sub> per g of sorbent (82 wt%) can be captured at 30 bar. A mechanism is described where CO<sub>2</sub> is polymerized in the channels of the porous carbon materials, as initiated by the sulfur or nitrogen atoms that are part of the carbon framework. Moreover, no temperature swing is needed. The reaction proceeds at ambient temperature. Without being bound by theory, it is envisioned that heat transfer between cylinders during the exothermic sorption and endothermic desorption can provide the requisite thermodynamic exchanges.

[00103] In some instances, the process can use the natural gas-well pressure of 200 to 300 bar as a driving force during the polymerization. By lowering the pressure back to ambient conditions after CO<sub>2</sub> uptake, the poly(CO<sub>2</sub>) is then depolymerized, where it can be off-loaded or pumped back downhole into the structures that had held it for geological timeframes.

[00104] **Example 1.1. Synthesis and characterization of porous carbons**

[00105] Sulfur- and nitrogen-containing porous carbons (SPC and NPC, respectively) were prepared by treating bulk precursor polymers with potassium hydroxide (KOH) at 600 °C, as described previously (*Carbon* **44**, 2816-2821 (2006); *Carbon* **50**, 5543-5553 (2012)).

[00106] As shown in **FIG. 2A**, the resulting products were solid porous carbon materials with homogeneously distributed sulfur or nitrogen atoms incorporated into the carbon framework. They exhibited pores and channel structures as well as high surface areas of 2500 and 1490 m<sup>2</sup> g<sup>-1</sup> (N<sub>2</sub>, Brunauer–Emmett–Teller) for the SPC and the NPC, respectively, with pore volumes of 1.01 cm<sup>3</sup> g<sup>-1</sup> and 1.40 cm<sup>3</sup> g<sup>-1</sup>, respectively. The scanning electron microscopy (SEM) and transmission electron microscopy (TEM) images are shown in **FIGS. 2B-D**, and the X-ray photoelectron spectroscopy (XPS) analyses are shown in **FIG. 3**.

[00107] Example 1.2. CO<sub>2</sub> uptake measurements

[00108] For CO<sub>2</sub> uptake measurements, samples were analyzed using volumetric analysis instruments at Rice University and at the National Institute of Standards and Technology (NIST). The measurements were further confirmed with gravimetric measurements.

[00109] **FIG. 4** shows the pressure-dependent CO<sub>2</sub> excess uptake for the SPC sorbent at different temperatures peaking at 18.6 mmol CO<sub>2</sub> g<sup>-1</sup> of sorbent (82 wt%) when at 22 °C and 30 bar. The sorption results measured by volumetric and gravimetric analyses were comparable, as were those measurements on the two volumetric instruments.

[00110] Applicants chose 30 bar as the upper pressure limit in experiments because a 300 bar well-head pressure at 10 mol % CO<sub>2</sub> concentration would have a CO<sub>2</sub> partial pressure of 30 bar. **FIGS. 4B-D** show three consecutive CO<sub>2</sub> sorption-desorption cycles on SPC over a pressure range from 0 to 30 bar, which indicates that the SPC could be regenerated using a pressure swing process while retaining its original CO<sub>2</sub> sorption capacity.

[00111] In the case of microporous materials with negligible external surface area, total uptake is often used as an approximation for absolute uptake, and the two values here are within 10% of

each other. For example, the absolute CO<sub>2</sub> uptake of the SPC was 20.1 and 13.9 mmol g<sup>-1</sup> under 30 bar at 22 and 50 °C, respectively. See FIGS. 5-6 and Example 1.8.

[00112] Similarly, although absolute adsorption isotherms can be used to determine the heat of sorption, excess adsorption isotherms are more often used to calculate the heat of CO<sub>2</sub> sorption (Q<sub>CO<sub>2</sub></sub>) before the critical point of the gas. Thus, the excess CO<sub>2</sub> sorption isotherms measured at two different temperatures, 23 °C and 50 °C (FIG. 4E), were input into the Clausius-Clapeyron equation. At lower surface coverage ( $\leq 1$  bar), which could be expected to be more indicative of the sorbate-sorbent interaction, the SPC exhibits a heat of CO<sub>2</sub> sorption of 57.8 kJ mol<sup>-1</sup>. Likewise, the maximum Q<sub>CO<sub>2</sub></sub> values for nucleophile-free porous materials, such as activated carbon, Zeolite 5A and zeolitic imidazolate framework (ZIF-8, a class of the MOF) were measured to be 28.4, and 31.2, 25.6 kJ mol<sup>-1</sup>, respectively, at low surface coverage (see Example 1.9). Based on this data, the SPC possesses the highest CO<sub>2</sub> sorption enthalpy among these complementary sorbents measured at low surface coverage.

[00113] In order to better assess the sorption mechanism during the CO<sub>2</sub> uptake, attenuated total reflectance infrared spectroscopy (ATR-IR) was used to characterize the properties of the sorbents before and after the CO<sub>2</sub> uptake. A sample vial with ~100 mg of the SPC was loaded into a 0.8 L stainless steel autoclave equipped with a pressure gauge and valves. Before the autoclave was sealed, the chamber was flushed with CO<sub>2</sub> (99.99%) to remove residual air, and the system was pressurized to 10 bar (line pressure limitation). The sorbent was therefore isobarically exposed to CO<sub>2</sub> in the closed system at 23 °C. After 15 min, the system was vented to nitrogen at ambient pressure and the sorbent vial was immediately removed from the chamber and the sorbent underwent ATR-IR and Raman analyses in air.

[00114] FIGS. 7A-B show the ATR-IR spectra of the SPC before (black line) and after exposure to 10 bar of CO<sub>2</sub>, followed by ambient conditions for the indicated times. The two regions that appear in the ATR-IR spectra (outlined by the dashed-line boxes) after the CO<sub>2</sub> sorption are of interest. The first IR peak, located at 2345 cm<sup>-1</sup>, is assigned to the anti-symmetric CO<sub>2</sub> stretch,

confirming that CO<sub>2</sub> was physisorbed and evolving from the SPC sorbent. The other IR band, centered at 1730 cm<sup>-1</sup>, is attributed to the C=O symmetric stretch from the poly(CO<sub>2</sub>) on the SPC. Interestingly, this carbonyl peak is only observed with the porous heteroatom-doped carbon, such as the SPC and NPC. Other porous sorbents without nucleophilic species, such as ZIF-8 and activated carbon, only showed the physisorbed or evolving CO<sub>2</sub> peak (~2345 cm<sup>-1</sup>) (**FIGS. 8-9**). Once the CO<sub>2</sub>-filled SPC returned to ambient pressure, the key IR peaks attenuated over time and disappeared after 20 min. Based on this data, the ATR-IR study confirmed the poly(CO<sub>2</sub>) formation. Raman spectroscopy was further used to probe individual chemical bond vibrations, as shown in **FIG. 7C**. The carbonaceous graphitic G-band and defect-derived diamondoid D-band were at 1590 and 1350 cm<sup>-1</sup>. The peak at 798 cm<sup>-1</sup> can be attributed to the symmetric stretch of the C-O-C bonds, which was not observed for the other nucleophile-free porous materials, suggesting that the poly(CO<sub>2</sub>), with the -(O-C(=O))<sub>n</sub>- moiety, was formed.

[00115] Without being bound by theory, it is envisioned that the monothiocarbonate and carbamate anions within the channels of the SPC and NPC, respectively, were the likely initiation points for the CO<sub>2</sub> polymerization since no poly(CO<sub>2</sub>) was seen in activated carbon (**FIG. 9**). Furthermore, <sup>13</sup>C NMR also confirms the presence of the poly(CO<sub>2</sub>) formation. The sorbent gives a broad signal characteristic of aromatic carbon (**FIG. 7D**, bottom).

[00116] After exposure to CO<sub>2</sub>, a relatively sharp signal on top of the broad sorbent signal appears at 130.6 ppm, which can be assigned to the CO<sub>2</sub> that is evolving from the support. A sharp signal also appears at 166.5 ppm (**FIG. 7D**, middle) that is characteristic of the carbonyl resonance for poly(CO<sub>2</sub>). Both of these signals are gone 19 h later (**FIG. 7D**, top). These assignments are further discussed in detail in Example 1.10.

[00117] Compared to secondary amine-based CO<sub>2</sub> sorbents where maximum capture efficiency is 0.5 mol CO<sub>2</sub> per mol N (2 RNH<sub>2</sub> + CO<sub>2</sub> → RNH<sub>3</sub><sup>+</sup> O<sub>2</sub>CNHR), the SPC and NPC demonstrate a unique mechanism during the CO<sub>2</sub> uptake process resulting in their remarkably higher CO<sub>2</sub>

capacities versus S or N content (8.1 atomic% of S and 6.2 atomic% of N in the SPC and NPC, respectively, by XPS analysis).

[00118] FIGS. 7E-F show illustrations of the aforementioned CO<sub>2</sub>-fixation by polymerization. Dimeric CO<sub>2</sub> uptake has been crystallographically observed in metal complexes, and polymeric CO<sub>2</sub> has been detected previously but only at extremely high pressures of ~15,000 bar. The spectroscopic determination here confirms poly(CO<sub>2</sub>) formation at much lower pressures than formerly observed.

[00119] A series of porous materials with and without the nucleophilic heteroatoms were tested to compare their CO<sub>2</sub> capture performance up to 30 bar at 30 °C (FIG. 10A). The SPC had the highest CO<sub>2</sub> capacity. The NPC, activated carbon, zeolite 5A and ZIF-8 had lower capacities. Although NPC had lower CO<sub>2</sub> capacity than SPC, its uptake performance could be improved by 21 wt% after H<sub>2</sub> reduction at 600 °C, producing reduced-NPC (R-NPC) with secondary amine groups (FIG. 2A).

[00120] Even though the surface area of R-NPC (1450 m<sup>2</sup> g<sup>-1</sup>) is only slightly greater than that of the activated carbon (1430 m<sup>2</sup> g<sup>-1</sup>), the presence of the amine groups induces the formation of the poly(CO<sub>2</sub>) under pressure, promoting the CO<sub>2</sub> sorption efficiency of the R-NPC. The pore volume of R-NPC is 1.43 cm<sup>3</sup> g<sup>-1</sup>.

[00121] Purification of natural gas from wells relies upon a highly CO<sub>2</sub>-selective sorbent, especially in a CH<sub>4</sub>-rich environment. Thus, CH<sub>4</sub> uptake experiments were carried out on three different types of porous materials, SPC, activated carbon and ZIF-8. FIGS. 10B-D compare CO<sub>2</sub> and CH<sub>4</sub> sorption over a pressure range from 0 to 30 bar at 23 °C. In contrast to the CO<sub>2</sub> sorption, the CH<sub>4</sub> isotherms for these three sorbents reached equilibrium while the system pressure was approaching 30 bar. The order of the CH<sub>4</sub> uptake capacities was correlated to the surface area of the sorbents. Comparing these sorbents, the observed molecular ratio of sorbed CO<sub>2</sub> to CH<sub>4</sub> (n<sub>CO<sub>2</sub></sub> / n<sub>CH<sub>4</sub></sub>) for the SPC (2.6) was greater than that for the activated carbon (1.5) and ZIF-8 (1.9). In addition, the density of the SPC calculated using volumetric analysis is

nearly 6-fold higher than in the ZIF-8 (2.21 vs.  $0.35 \text{ g cm}^{-3}$ ) and 3-fold higher than the zeolite 5A (2.21 vs.  $0.67 \text{ g cm}^{-3}$ ). The high CO<sub>2</sub> capacity and high density observed for SPC greatly increase the volume efficiency, which would reduce the volume of the sorption material for a given CO<sub>2</sub> uptake production rate.

[00122] In order to mimic a gas well environment and further characterize the SPC's selectivity to CO<sub>2</sub>, a premixed gas (85 mol% CH<sub>4</sub>, 10 mol% CO<sub>2</sub>, 3 mol% C<sub>2</sub>H<sub>6</sub> and 2 mol% C<sub>3</sub>H<sub>8</sub>) was used with quadrupole mass spectrometry (MS) detection. The MS inlet was connected to the gas uptake system so that it could monitor the gas effluent from the SPC throughout the sorption-desorption experiment. **FIG. 11** shows the mass spectrum recorded during the sorption process. The peaks at 15 and 16 amu correspond to fragment and molecular ions from CH<sub>4</sub>, while the peaks at 28 and 44 amu are from CO<sub>2</sub> in the premixed gas. Other minor peaks can be assigned to fragment ions from C<sub>2</sub>H<sub>6</sub> and C<sub>3</sub>H<sub>8</sub>. Although the peak at 44 amu can also come from C<sub>3</sub>H<sub>8</sub> ions, the contribution is negligible because of the lower C<sub>3</sub>H<sub>8</sub> concentration in the mixed gas, and it is distinguishable by the fragmentation ratios in the MS [C<sub>3</sub>H<sub>8</sub>: m/z = 29 (100), 44 (30); CO<sub>2</sub>: m/z = 44(100), 28(11)]. The observed intensity ratio of two peaks at 16 and 44 amu ( $I_{16} / I_{44} = 9.1$ ) indicates the abundance of CH<sub>4</sub> vs. CO<sub>2</sub> during the sorption and also reflects the relative amount of CH<sub>4</sub> and CO<sub>2</sub> in the premixed gas. Once the sorption reached equilibrium under 30 bar, the desorption process was induced by slowly venting into the MS system. The  $I_{16}/I_{44}$  ratio reduced to ~0.7. The SPC has been shown to have 2.6-fold higher CO<sub>2</sub> than CH<sub>4</sub> affinity at 30 bar when using pure CO<sub>2</sub> and CH<sub>4</sub> as feed gases (**FIG. 10B**).

[00123] If the binding energy of CH<sub>4</sub> and CO<sub>2</sub> were assumed to be similar, and the partial pressure of CH<sub>4</sub> vs. CO<sub>2</sub> in the premixed gas is considered ( $P_{\text{CH}_4} / P_{\text{CO}_2} = 8.5$ ), then it is envisioned that the number of sorbed CH<sub>4</sub> should be ~3.3-times more than that of the sorbed CO<sub>2</sub>. It is also envisioned that CO<sub>2</sub>-selective materials have selective sites and once the CO<sub>2</sub> occupies those sites, the selectivity significantly decreases and the materials behave as physisorbents with lower selectivities at larger pressures. On the contrary, here the SPC

demonstrates much higher CO<sub>2</sub> selectivity than expected since the chemisorbed sulfur-initiated poly(CO<sub>2</sub>) chain displaces physisorbed gas.

[00124] Under the mechanism described here for CO<sub>2</sub> polymerization in the channels of inexpensive nucleophilic porous carbons, these new materials have continuous selectivity toward CO<sub>2</sub>, limited only by the available pore space and pressure.

[00125] Example 1.3. Instrumentations (Rice University)

[00126] An automated Sieverts instrument (Setaram PCTPro) was adopted to measure gas (CO<sub>2</sub>, CH<sub>4</sub> or premixed gas) sorption properties of materials. Typically, a ~70 mg of sorbent was packed into a ~1.3 mL of stainless steel sample cell. The sample was pretreated under vacuum (~ 3 mm Hg) at 130 °C for 6 h and the sample volume was further determined by helium before the uptake experiment. At each step of the measurement, testing gas was expanded from the reference reservoir into the sample cell until the system pressure reached equilibrium. A quadrupole mass spectrometer (Setaram RGA200) was connected to the Sieverts instrument so that it could monitor the gas effluent from the sorbent throughout the entire sorption-desorption experiment. With the assistance of a hybrid turbomolecular drag pump, the background pressure of the MS can be controlled lower than 5 × 10<sup>-8</sup> Torr. All material densities were determined using volumetric analysis on this same instrument.

[00127] XPS was performed using a PHI Quantera SXM Scanning X-ray Microprobe with a base pressure of 5 × 10<sup>-9</sup> Torr. Survey spectra were recorded in 0.5 eV step size and a pass energy of 140 eV. Elemental spectra were recorded in 0.1 eV step size and a pass energy of 26 eV. All spectra were standardized using C1s peak (284.5 eV) as a reference.

[00128] The ATR-IR experiment was conducted using a Fourier transform infrared spectrometer (Nicolet Nexus 670) equipped with an attenuated total reflectance system (Nicolet, Smart Golden Gate) and a MCT-A detector. Raman spectra were measured using a Renishaw in Via Raman Microscope with a 514 nm excitation argon laser.

[00129] Scanning electron microscope (SEM) images were taken at 15 KeV using a JEOL-6500F field emission microscope. High-resolution transmission electron microscope (TEM) images were obtained with a JEOL 2100F field emission gun TEM.

[00130] An automated BET surface analyzer (Quantachrome Autosorb-3b) was used for measurements of sorbents' surface areas and pore volumes based on N<sub>2</sub> adsorption-desorption. Typically, a ~100 mg of sample was loaded into a quartz tube and pretreated at 130 °C under vacuum (~5 mm Hg) in order to remove sorbates before the measurement.

[00131] MAS NMR spectra were recorded on a Bruker Avance III 4.7 T spectrometer with a standard MAS probe for 4 mm outer diameter rotors.

[00132] Example 1.4. Volumetric CO<sub>2</sub> Sorption Experiments (NIST)

[00133] CO<sub>2</sub> sorption measurements were carried out on computer-controlled custom-built volumetric sorption equipment previously described in detail (*J. Phys. Chem. C* **111**, 16131–16137 (2007)) with an estimated reproducibility within 0.5% and isotherm data error bar of less than 2% compared to other commercial instruments. An amount of ~79 mg of sample was used for the experiments. Sample degassing, prior to the CO<sub>2</sub> sorption experiment, was done at 130 °C under vacuum for 12 h.

[00134] Example 1.5. Gravimetric CO<sub>2</sub> Sorption Experiments

[00135] CO<sub>2</sub> sorption measurements were performed on a high pressure thermal gravimetric equipment (Model: TGA-HP50) from TA Instruments. An amount of ~15 mg of sample was used for the experiments. Sample degassing, prior to CO<sub>2</sub> sorption experiment, was done at 130 °C under vacuum for 12 h.

[00136] Example 1.6. Synthesis of S-containing porous carbon (SPC)

[00137] Poly[(2-hydroxymethyl)thiophene] (PTh) (Sigma-Aldrich) was prepared using FeCl<sub>3</sub>. *Microporous Mesoporous Mater.* **158**, 318-323 (2012). In a typical synthesis, 2-

thiophenemethanol (1.5 g, 13.1 mmol) in CH<sub>3</sub>CN (10 mL) was slowly added under vigorous stirring to a slurry of FeCl<sub>3</sub> (14.5 g, 89.4 mmol) in CH<sub>3</sub>CN (50 mL). The mixture was stirred at room temperature for 24 h. The polymer (PTh) was separated by filtration over a sintered glass funnel, washed with distilled water (~1 L) and then with acetone (~200 mL). The polymer was dried at 100 °C for 12 h to afford (1.21 g, 96% yield) of the desired compound.

[00138] The PTh was activated by grinding PTh (500 mg) with KOH (1 g, 17.8 mmol) with a mortar and pestle and then heated under Ar at 600 °C in a tube furnace for 1 h. The Ar flow rate was 500 sccm. After cooling, the activated sample was thoroughly washed 3× with 1.2 M HCl (1 L) and then with distilled water until the filtrate was pH 7. The SPC sample was dried in an oven at 100 °C to afford 240 mg of the black solid SPC. The BET surface area and pore volume were 2500 m<sup>2</sup> g<sup>-1</sup> and 1.01 cm<sup>3</sup> g<sup>-1</sup>, respectively.

[00139] Example 1.7. Synthesis of N-containing porous carbon (NPC)

[00140] Commercial polyacrylonitrile (PAN, 500 mg, average M<sub>w</sub> 150,000, Sigma-Aldrich) powder and KOH (1500 mg, 26.8 mmol) were ground to a homogeneous mixture in a mortar. The mixture was subsequently carbonized by heating to 600 °C under Ar (500 sccm) in a tube furnace for 1 h. The carbonized material was washed 3× with 1.2 M HCl (1 L) and then with distilled water until the filtrate was pH 7. Finally, the carbon sample was dried in an oven at 100 °C to afford 340 mg of the solid black NPC.

[00141] To produce R-NPC, the activated material (270 mg) was further reduced by 10% H<sub>2</sub> (H<sub>2</sub>:Ar = 50:450 sccm) at 600 °C for 1 h to provide 255 mg of the final material. The BET surface area and pore volume were 1450 m<sup>2</sup> g<sup>-1</sup> and 1.43 cm<sup>3</sup> g<sup>-1</sup>, respectively.

[00142] Example 1.8. Conversion of excess uptake to absolute uptake

[00143] Total uptake includes all gas molecules in the adsorbed state, which is the sum of the experimentally measured excess uptake and the bulk gas molecules within the pore volume (**FIG. 5**). For microporous materials with negligible external surface area, the total uptake is

often used as an approximation for absolute uptake and could be represented in the following equation:

$$N_{\text{total}} \approx N_{\text{abs.}} = N_{\text{ex.}} + V_p \bullet \rho_{\text{bulk}}(P, T)$$

[00144] In the above equation,  $V_p$  is the pore volume of porous material and  $\rho_{\text{bulk}}$  is the density of gas in the bulk phase at given pressure and temperature. In the case of SPC, the pore volume was determined to be  $1.01 \text{ cm}^3 \text{ g}^{-1}$  by  $N_2$  adsorption isotherm at 77 K (BET analysis). The  $\text{CO}_2$  density changes from 0.00180 to  $0.06537 \text{ g cm}^{-3}$  in the pressure range between 1 and 30 bar at 22 °C and 0.00164 to  $0.05603 \text{ g cm}^{-3}$  at 50 °C.

**[00145]** Example 1.9. Determination of the heat of  $\text{CO}_2$  sorption (Q)

[00146] The Clausius-Clapeyron equation (*Adsorption* 175, 133-137 (1995)) was used to determine the heat of  $\text{CO}_2$  sorption:

$$\left(\frac{\partial \ln P}{\partial T}\right)_{\theta} = \frac{Q}{RT^2}$$

[00147] In the above equation,  $\theta$  is the fraction of the adsorbed sites at a pressure  $P$  and temperature  $T$ , and  $R$  is the universal constant. The equation can be further derived as the following expression for transitions between a gas and a condense phase:

$$\ln P_2 - \ln P_1 = \frac{Q}{R} \left( \frac{1}{T_1} - \frac{1}{T_2} \right)$$

[00148] **Table 1** below compares the heat of  $\text{CO}_2$  sorption to values in the literature.

	$Q_{CO_2}$ (kJ mol <sup>-1</sup> )	Comparison with reference
<b>SPC</b>	57.8	59.0 <sup>1</sup>
<b>Activated carbon</b>	28.4	28.9 <sup>2</sup>
<b>Zeolite 5A</b>	31.2	33.7 <sup>3</sup>
<b>ZIF-8</b>	25.6	27.0 <sup>4</sup>

**Table 1.** Heat of CO<sub>2</sub> sorption determined in Example 1 versus literature values. Ref. 1: *Carbon* **50**, 5543-5553 (2012). Ref. 2: *J. Natural Gas Chem.* **15**, 223-229 (2006). Ref. 3: *Handbook of Zeolite Science and Technology*, Marcel Dekker, Inc. New York (2003). Ref. 4: *AIChE J.* **59**, 2195-2206 (2013).

**[00149]** Example 1.10. Evaluation of the <sup>13</sup>C NMR assignments

**[00150]** The three NMR spectra in **FIG. 7D** were obtained under identical conditions: 12 kHz MAS, 2.5-μs 90° <sup>13</sup>C pulse, 41-ms FID, 10-s relaxation delay; 480 scans; and 50 Hz of line broadening applied to the FID.

**[00151]** Numerous MAS NMR investigations of CO<sub>2</sub> have reported a signal at 125 ± 1 ppm, regardless of the physical environment for the CO<sub>2</sub> (e.g., free gas, physisorbed on various materials, in a metal organic framework, in a clathrate, dissolved in a glass, etc.) Accordingly, attributing the signal at 130.6 ppm to CO<sub>2</sub> physisorbed on the sorbent seems reasonable, although the reason for the additional deshielding may not be apparent. It is envisioned that this 5-ppm difference does not result from the use of different chemical shift references, as the various reports indicate that either the signal from Si(CH<sub>3</sub>)<sub>4</sub> (TMS) serves as the chemical shift reference (0 ppm) or that the signal from a solid such as adamantane or glycine (this work) relative to TMS at 0 ppm serves as the chemical shift reference. Applicants note that the sorbent is somewhat conductive in that it has a noticeable effect on the tuning and matching of the <sup>13</sup>C and <sup>1</sup>H

channels of the NMR probe (relative to the tuning and matching for glycine). However, spinning is unaffected. Without being bound by theory, it is envisioned that the conductive nature of the sorbent results in the 5-ppm deshielding effect observed for physisorbed CO<sub>2</sub>.

[00152] A chemical shift of 166.5 ppm is rational for poly(CO<sub>2</sub>) in light of various reports of bicarbonate and carbonate species giving signals from 162 to 170 ppm relative to TMS or to [(CH<sub>3</sub>)<sub>3</sub>Si]<sub>4</sub>Si, which is 3.5 ppm relative to TMS at 0 ppm. The carbonyl chemical shift of CH<sub>3</sub>O-CO-O-CO-OCH<sub>3</sub> is extremely sensitive to its environment (the reported shift is 147.9 ppm as a neat liquid at 37°C and 157 ppm in CDCl<sub>3</sub>, both relative to TMS). Applicants are not aware of any reports of chemical shift data for poly(CO<sub>2</sub>) and are hereby reporting the first such example of that chemical shift at 166.5 ppm when entrapped in this carbon matrix.

**[00153] Example 2. CO<sub>2</sub> Absorption Capacities of Different Carbon Materials**

[00154] . In this example, the CO<sub>2</sub> uptake capacities of SPC, R-NPC, rice protein, ZIF-8 and Zeolite 5A were compared. The CO<sub>2</sub> uptake measurements were conducted at 30 °C and 30 bar.

[00155] As shown in FIG. 12, the CO<sub>2</sub> uptake capacities of SPC and R-NPC were significantly higher than the CO<sub>2</sub> uptake capacities of ZIF-8, rice protein, and Zeolite 5A.

[00156] Without further elaboration, it is believed that one skilled in the art can, using the description herein, utilize the present disclosure to its fullest extent. The embodiments described herein are to be construed as illustrative and not as constraining the remainder of the disclosure in any way whatsoever. While the embodiments have been shown and described, many variations and modifications thereof can be made by one skilled in the art without departing from the spirit and teachings of the invention. Accordingly, the scope of protection is not limited by the description set out above, but is only limited by the claims, including all equivalents of the subject matter of the claims. The disclosures of all patents, patent applications and publications

cited herein are hereby incorporated herein by reference, to the extent that they provide procedural or other details consistent with and supplementary to those set forth herein.

**WHAT IS CLAIMED IS:**

1. A method of capturing CO<sub>2</sub> from an environment, wherein the method comprises:
  - associating the environment with a porous carbon material,
    - wherein the porous carbon material comprises a plurality of pores and a plurality of nucleophilic moieties, and
    - wherein the associating results in sorption of the CO<sub>2</sub> to the porous carbon material.
2. The method of claim 1, wherein the environment is selected from the group consisting of industrial gas streams, natural gas streams, natural gas wells, industrial gas wells, oil and gas fields, and combinations thereof.
3. The method of claim 1, wherein the environment is a pressurized environment.
4. The method of claim 3, wherein the environment has a total pressure higher than atmospheric pressure.
5. The method of claim 3, wherein the environment has a total pressure of about 5 bar to about 500 bar.
6. The method of claim 1, wherein the associating occurs by placing the porous carbon material at or near the environment.
7. The method of claim 1, wherein the associating occurs by flowing the environment through a structure that contains the porous carbon materials.

8. The method of claim 1, wherein the sorption of the CO<sub>2</sub> to the porous carbon material occurs by at least one of absorption, adsorption, ionic interactions, physisorption, chemisorption, covalent bonding, non-covalent bonding, hydrogen bonding, van der Waals interactions, and combinations thereof.
9. The method of claim 1, wherein the sorption of the CO<sub>2</sub> to the porous carbon material occurs above atmospheric pressure.
10. The method of claim 1, wherein the sorption of the CO<sub>2</sub> to the porous carbon material occurs at total pressures ranging from about 5 bar to about 500 bar.
11. The method of claim 1, wherein the sorption of the CO<sub>2</sub> to the porous carbon material occurs at a partial CO<sub>2</sub> pressure of about 0.1 bar to about 100 bar.
12. The method of claim 1, wherein the sorption of the CO<sub>2</sub> to the porous carbon material occurs without heating the porous carbon material.
13. The method of claim 1, wherein the sorption of the CO<sub>2</sub> to the porous carbon material occurs selectively over hydrocarbons in the environment.
14. The method of claim 13, wherein the molecular ratio of sorbed CO<sub>2</sub> to sorbed hydrocarbons in the porous carbon material is greater than about 2
15. The method of claim 1, wherein the CO<sub>2</sub> is converted to poly(CO<sub>2</sub>) within the pores of the porous carbon materials
16. The method of claim 1, further comprising a step of releasing the captured CO<sub>2</sub> from the porous carbon material.

17. The method of claim 16, wherein the releasing occurs by decreasing the pressure of the environment.
18. The method of claim 16, wherein the releasing occurs by placing the porous carbon material in a second environment, wherein the second environment has a lower pressure than the environment where CO<sub>2</sub> capture occurred.
19. The method of claim 16, wherein the releasing occurs at or below atmospheric pressure.
20. The method of claim 16, wherein the releasing occurs at total pressures ranging from about 0 bar to about 100 bar.
21. The method of claim 16, wherein the releasing occurs at the same temperature at which CO<sub>2</sub> sorption occurred.
22. The method of claim 16, wherein the releasing occurs without heating the porous carbon material.
23. The method of claim 16, wherein the releasing occurs through depolymerization of formed poly(CO<sub>2</sub>).
24. The method of claim 16, further comprising a step of disposing the released CO<sub>2</sub>.
25. The method of claim 16, further comprising a step of reusing the porous carbon material after the releasing step to capture additional CO<sub>2</sub> from an environment.

26. The method of claim 1, wherein the porous carbon material is selected from the group consisting of nucleophilic polymers, polypeptides, proteins, waste materials, nitrogen-containing porous carbon materials, sulfur-containing porous carbon materials, metal-containing porous carbon materials, metal-oxide containing porous carbon materials, metal sulfide-containing porous carbon materials, phosphorous containing porous carbon materials, and combinations thereof.
27. The method of claim 1, wherein the porous carbon material comprises a nucleophilic polymer.
28. The method of claim 27, wherein the nucleophilic polymer is selected from the group consisting of nitrogen-containing polymers, sulfur-containing polymers, polythiophene (PTH), polythiophene-methanol (2-(hydroxymethyl)thiophene), polyacrylonitrile (PAN), polypyrrole, and combinations thereof.
29. The method of claim 27, wherein the nucleophilic polymer is carbonized.
30. The method of claim 27, wherein the nucleophilic polymer is reduced.
31. The method of claim 1, wherein the nucleophilic moieties are part of the porous carbon material.
32. The method of claim 1, wherein the nucleophilic moieties are embedded within the plurality of the pores of the porous carbon material.
33. The method of claim 1, wherein the nucleophilic moieties are selected from the group consisting of primary nucleophiles, secondary nucleophiles, tertiary nucleophiles and combinations thereof.

34. The method of claim 1, wherein the nucleophilic moieties are selected from the group consisting of oxygen-containing moieties, sulfur-containing moieties, metal-containing moieties, metal oxide-containing moieties, metal sulfide-containing moieties, nitrogen-containing moieties, phosphorous-containing moieties, and combinations thereof.
35. The method of claim 1, wherein the nucleophilic moieties comprise nitrogen-containing moieties.
36. The method of claim 35, wherein the nitrogen-containing moieties are selected from the group consisting of primary amines, secondary amines, tertiary amines, nitrogen oxides, and combinations thereof.
37. The method of claim 1, wherein the nucleophilic moieties comprise sulfur-containing moieties.
38. The method of claim 37, wherein the sulfur-containing moieties are selected from the group consisting of primary sulfurs, secondary sulfurs, sulfur oxides, and combinations thereof.
39. The method of claim 1, wherein the porous carbon material has surface areas ranging from about 1,000 m<sup>2</sup>/g to about 3,000 m<sup>2</sup>/g.
40. The method of claim 1, wherein the plurality of pores in the porous carbon material comprise diameters ranging from about 5 nm to about 100 nm.
41. The method of claim 1, wherein the plurality of pores in the porous carbon material comprise volumes ranging from about 1 cm<sup>3</sup>/g to about 10 cm<sup>3</sup>/g.

42. The method of claim 1, wherein the porous carbon material has a density ranging from about 0.3 g/cm<sup>3</sup> to about 4 g/cm<sup>3</sup>.
43. The method of claim 1, wherein the porous carbon material has a CO<sub>2</sub> sorption capacity ranging from about 10% to about 200% of the porous carbon material weight.
44. The method of claim 1, wherein the porous carbon material has a CO<sub>2</sub> sorption capacity of about 55% to about 90% of the porous carbon material weight.
45. A porous carbon material for CO<sub>2</sub> capture, wherein the porous carbon material comprises a plurality of pores and a plurality of nucleophilic moieties.
46. The porous carbon material of claim 45, wherein the porous carbon material is selected from the group consisting of nucleophilic polymers, polypeptides, proteins, waste materials, nitrogen-containing porous carbon materials, sulfur-containing porous carbon materials, metal-containing porous carbon materials, metal-oxide containing porous carbon materials, metal sulfide containing porous carbon materials, phosphorous containing porous materials, and combinations thereof.
47. The porous carbon material of claim 45, wherein the porous carbon material comprises a nucleophilic polymer.
48. The porous carbon material of claim 47, wherein the nucleophilic polymer is selected from the group consisting of nitrogen-containing polymers, sulfur-containing polymers, polythiophene (PTH), polythiophene-methanol (2-(hydroxymethyl)thiophene), polyacrylonitrile (PAN), polypyrrole, and combinations thereof.
49. The porous carbon material of claim 48, wherein the nucleophilic polymer is carbonized.

50. The porous carbon material of claim 48, wherein the nucleophilic polymer is reduced.
51. The porous carbon material of claim 45, wherein the nucleophilic moieties are part of the porous carbon material.
52. The porous carbon material of claim 45, wherein the nucleophilic moieties are embedded within the plurality of the pores of the porous carbon material.
53. The porous carbon material of claim 45, wherein the nucleophilic moieties are selected from the group consisting of primary nucleophiles, secondary nucleophiles, tertiary nucleophiles and combinations thereof.
54. The porous carbon material of claim 45, wherein the nucleophilic moieties are selected from the group consisting of oxygen-containing moieties, sulfur-containing moieties, metal-containing moieties, metal oxide-containing moieties, metal sulfide-containing moieties, phosphorous containing moieties, nitrogen-containing moieties, and combinations thereof.
55. The porous carbon material of claim 45, wherein the nucleophilic moieties comprise nitrogen-containing moieties.
56. The porous carbon material of claim 45, wherein the nitrogen-containing moieties are selected from the group consisting of primary amines, secondary amines, tertiary amines, nitrogen oxides, and combinations thereof.
57. The porous carbon material of claim 45, wherein the nucleophilic moieties comprise sulfur-containing moieties.

58. The porous carbon material of claim 45, wherein the sulfur-containing moieties are selected from the group consisting of primary sulfurs, secondary sulfurs, sulfur oxides, and combinations thereof.
59. The porous carbon material of claim 45, wherein the porous carbon material has surface areas ranging from about 1,000 m<sup>2</sup>/g to about 3,000 m<sup>2</sup>/g.
60. The porous carbon material of claim 45, wherein the plurality of pores in the porous carbon material comprise diameters ranging from about 5 nm to about 100 nm.
61. The porous carbon material of claim 45, wherein the plurality of pores in the porous carbon material comprise volumes ranging from about 1 cm<sup>3</sup>/g to about 10 cm<sup>3</sup>/g.
62. The porous carbon material of claim 45, wherein the porous carbon material has a density ranging from about 0.3 g/cm<sup>3</sup> to about 4 g/cm<sup>3</sup>.
63. The porous carbon material of claim 45, wherein the porous carbon material has a CO<sub>2</sub> sorption capacity ranging from about 10% to about 200% of the porous carbon material weight.
64. The porous carbon material of claim 45, wherein the porous carbon material has a CO<sub>2</sub> sorption capacity of about 55% to about 90% of the porous carbon material weight.

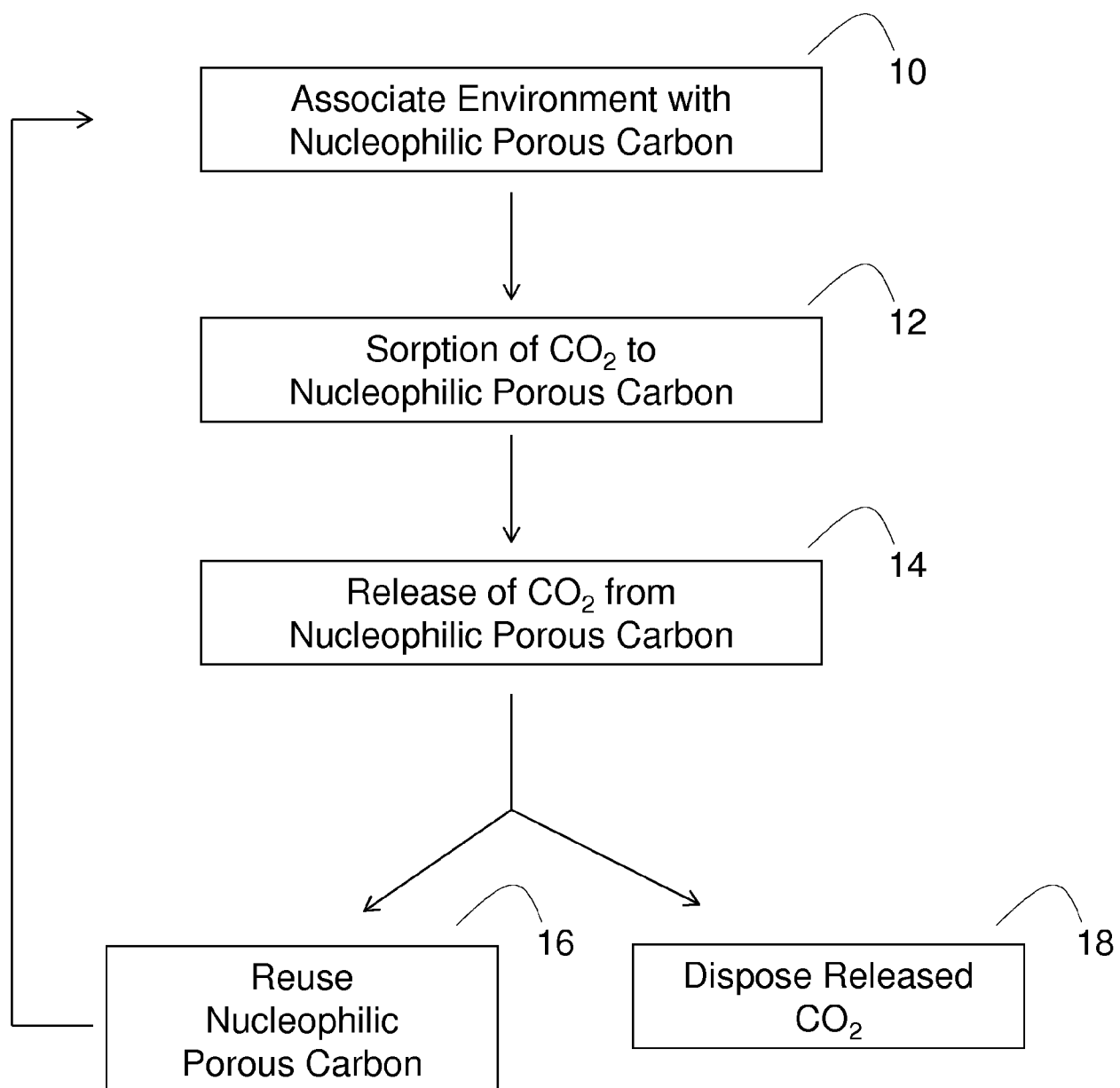
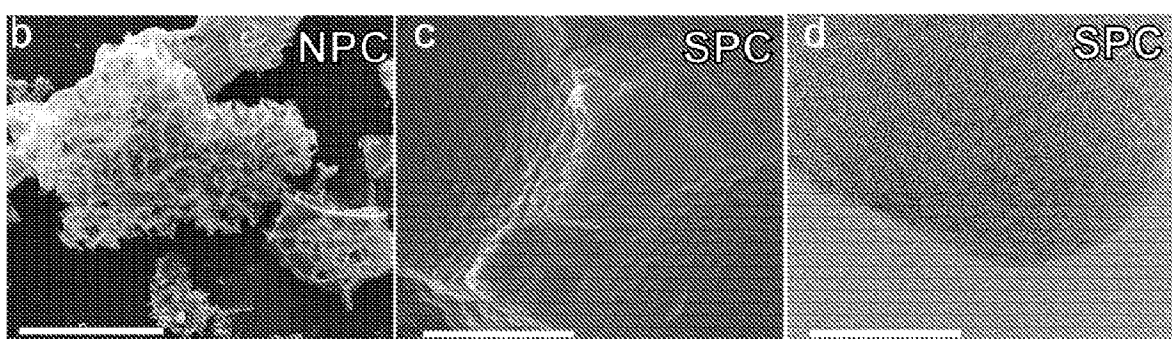
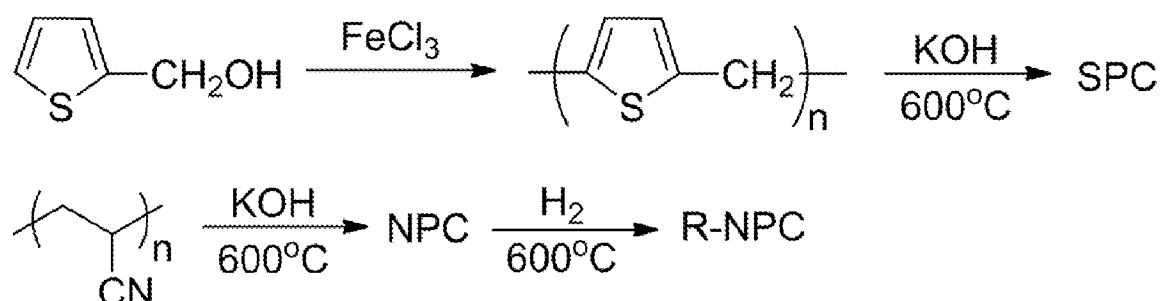


FIG. 1

**a****FIG. 2**

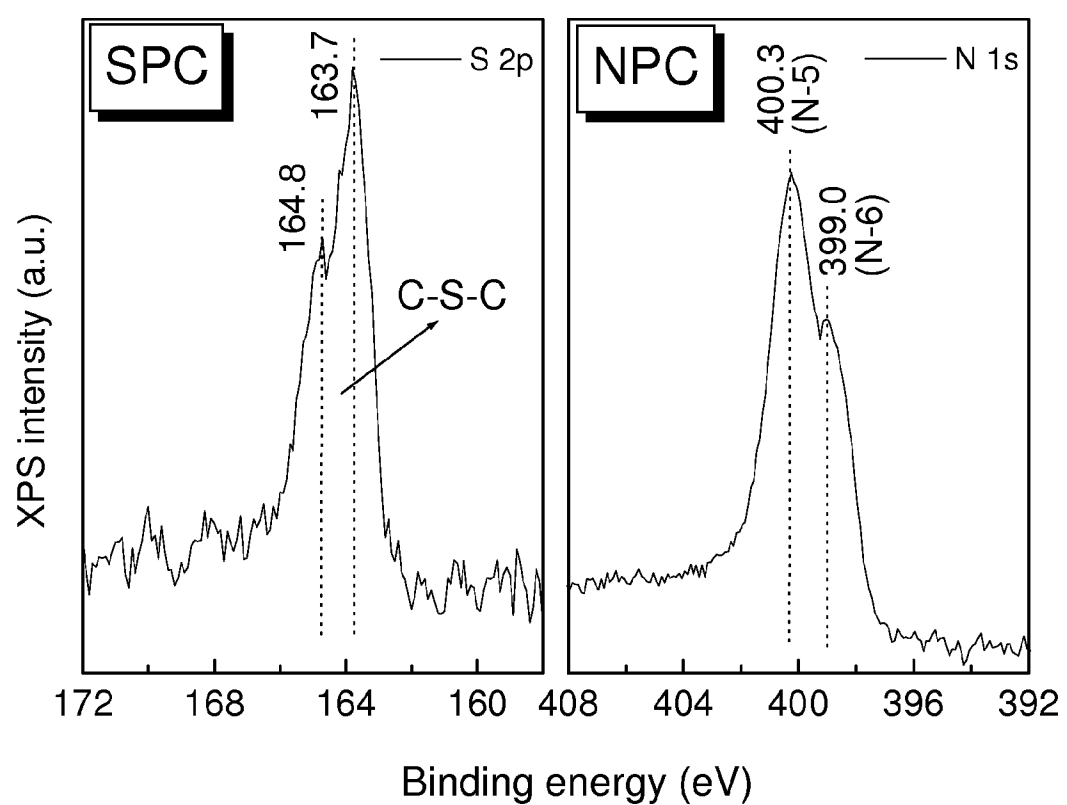


FIG. 3

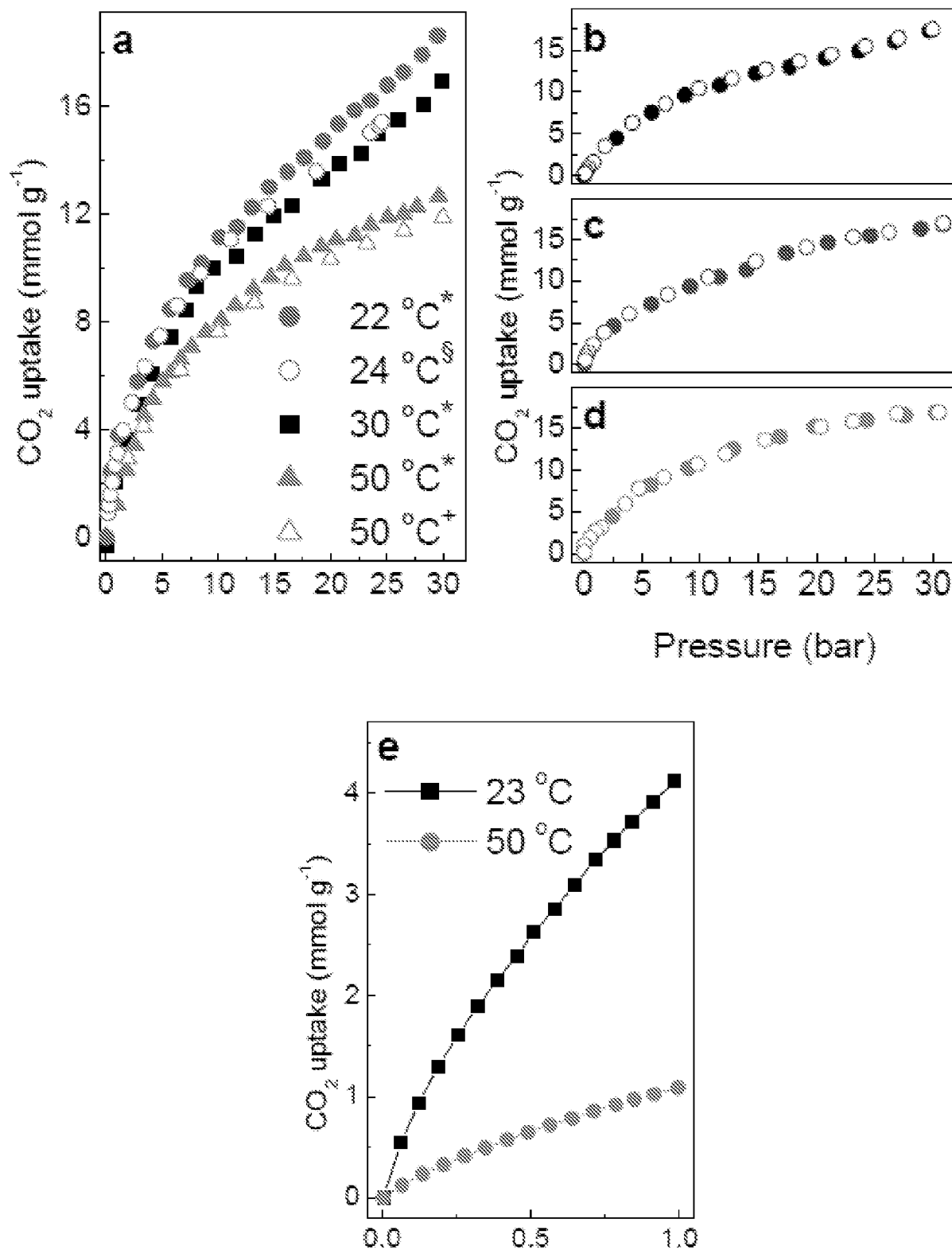


FIG. 4

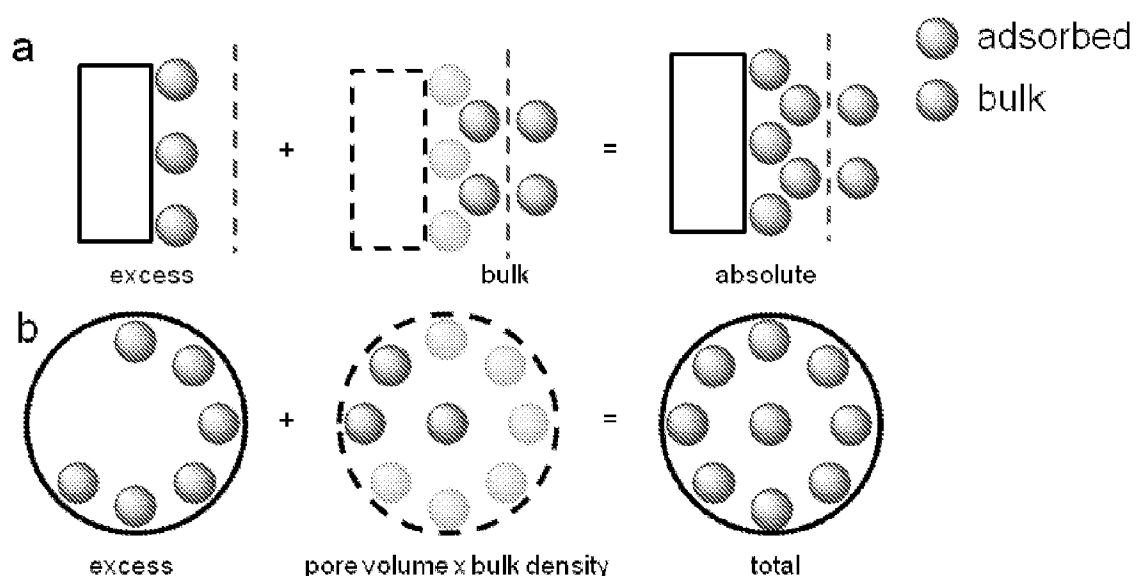


FIG. 5

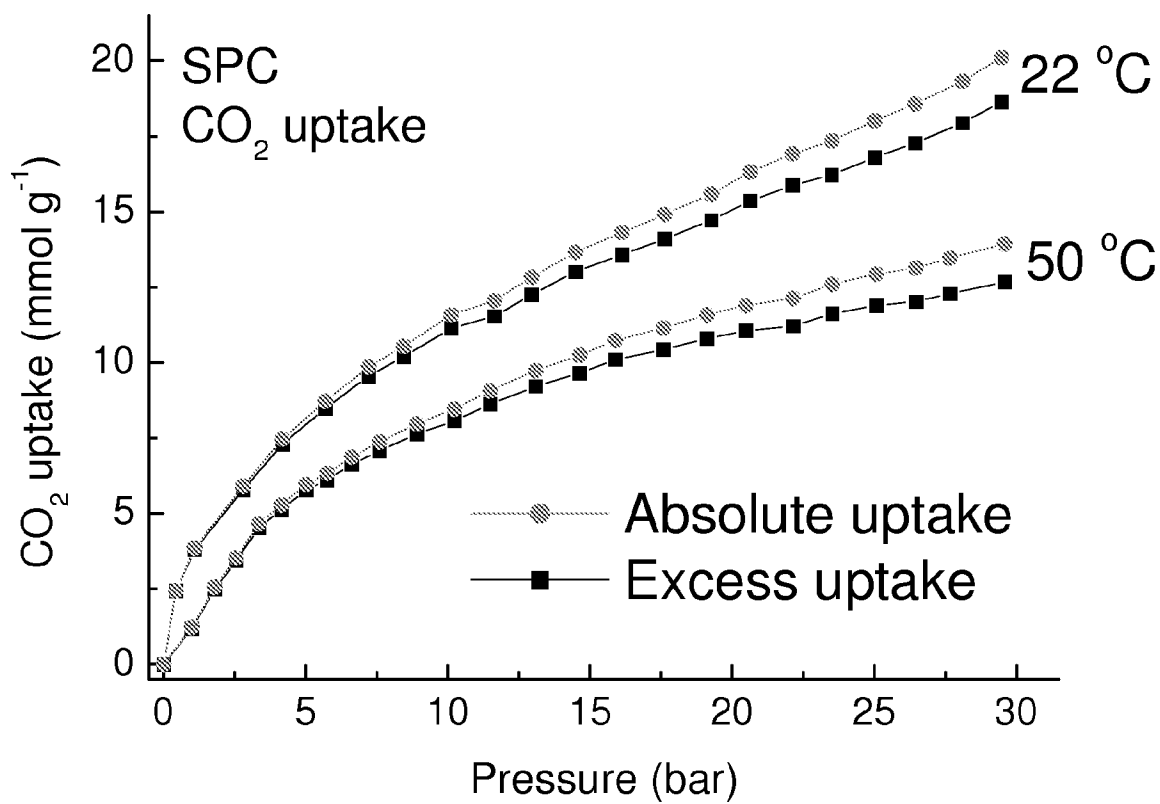


FIG. 6

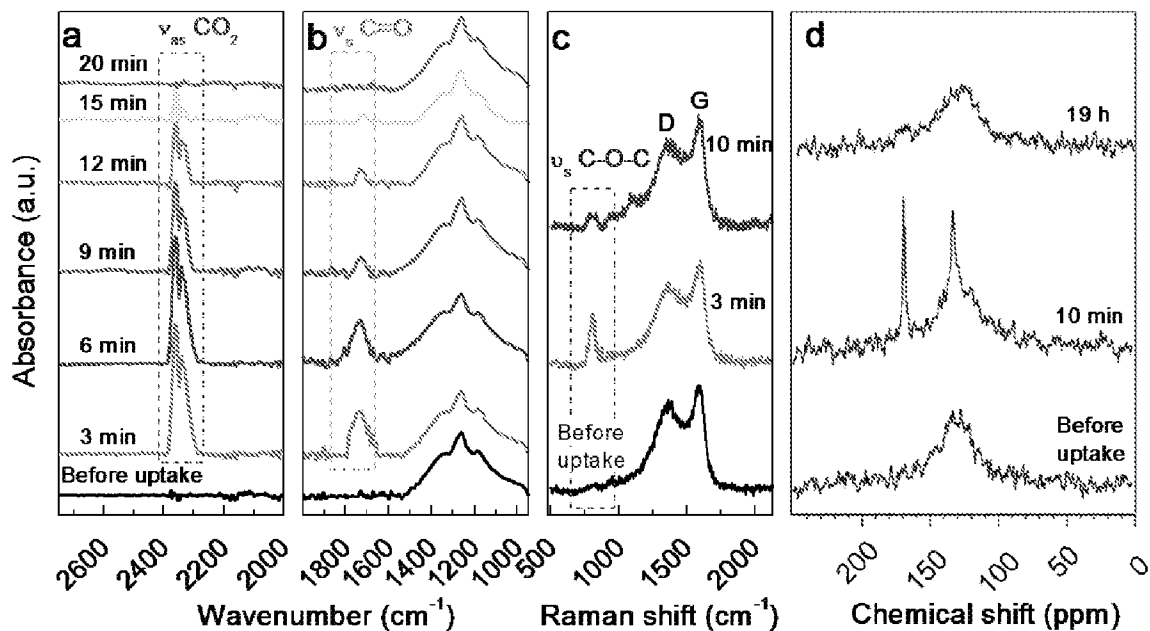


FIG. 7

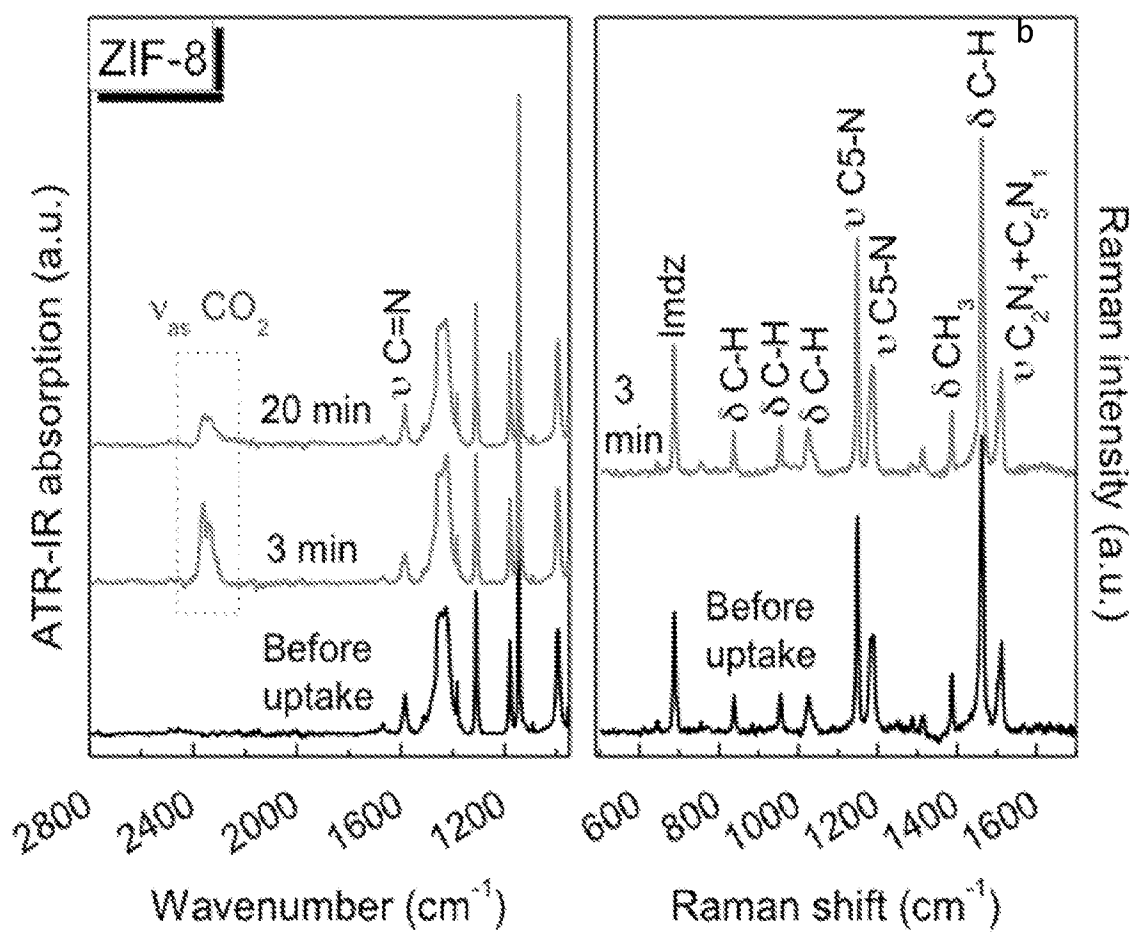


FIG. 8

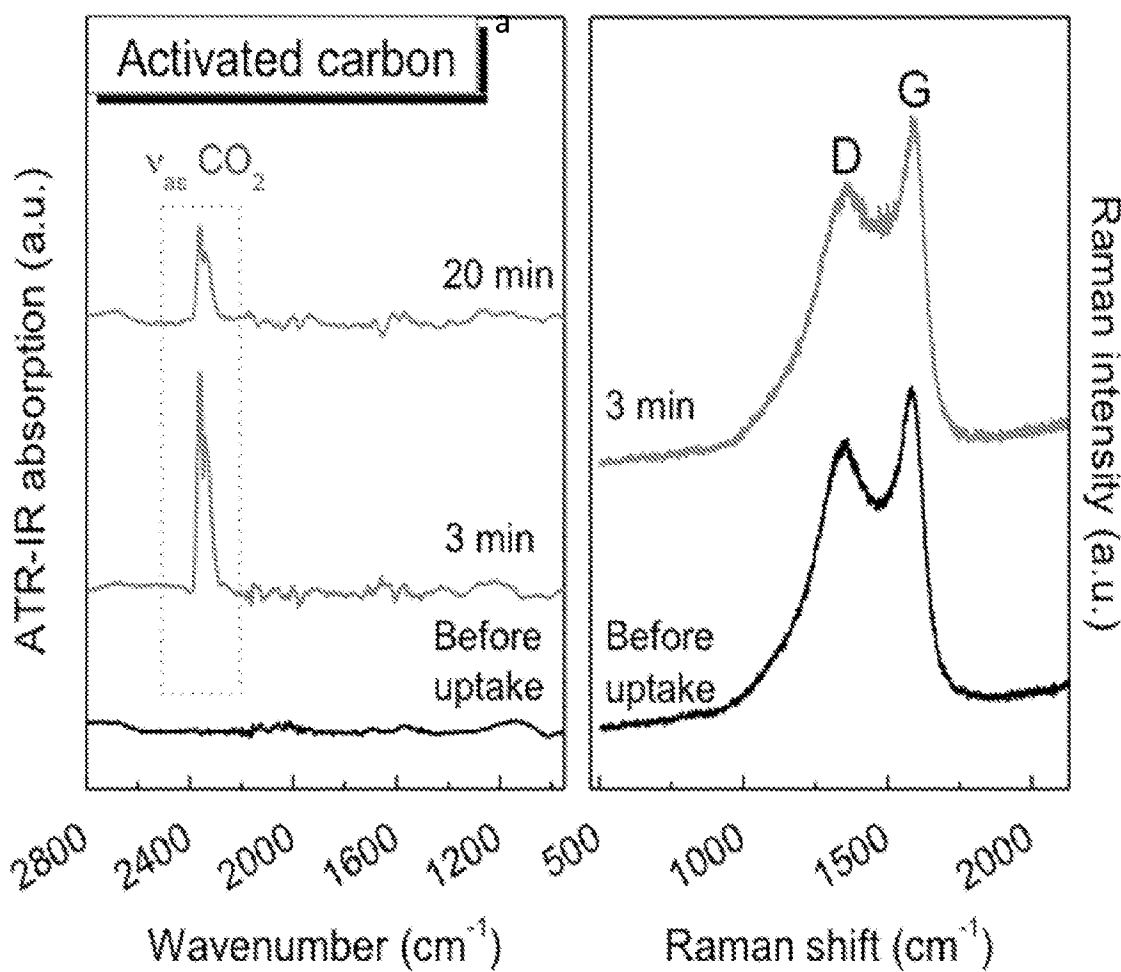


FIG. 9

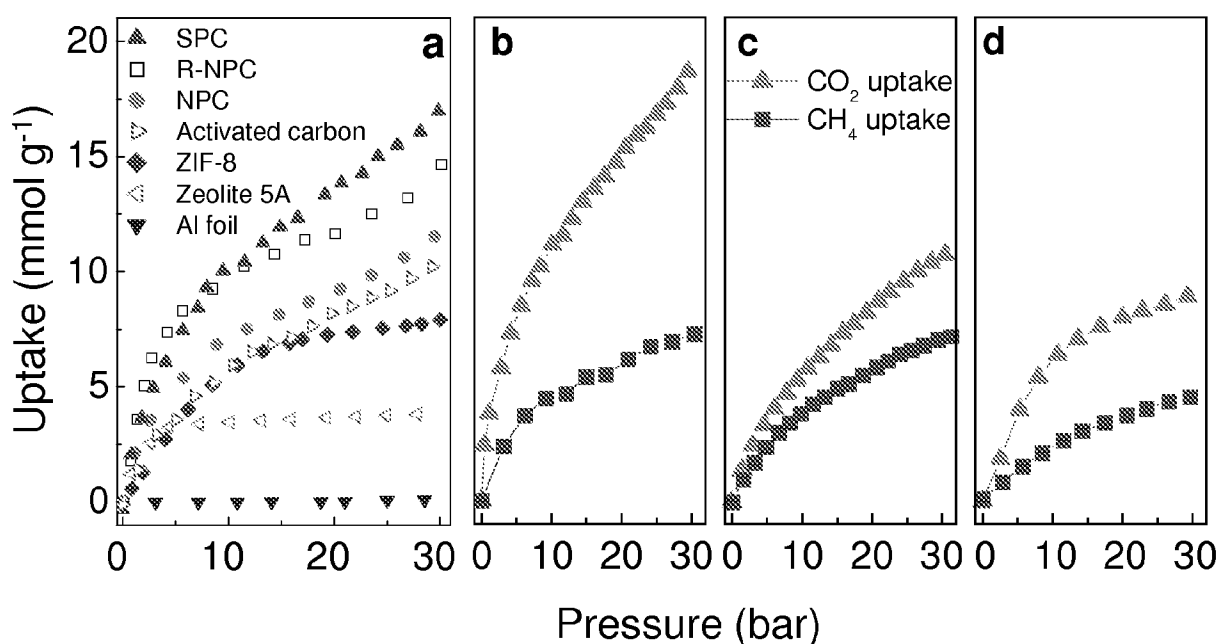


FIG. 10

11/12

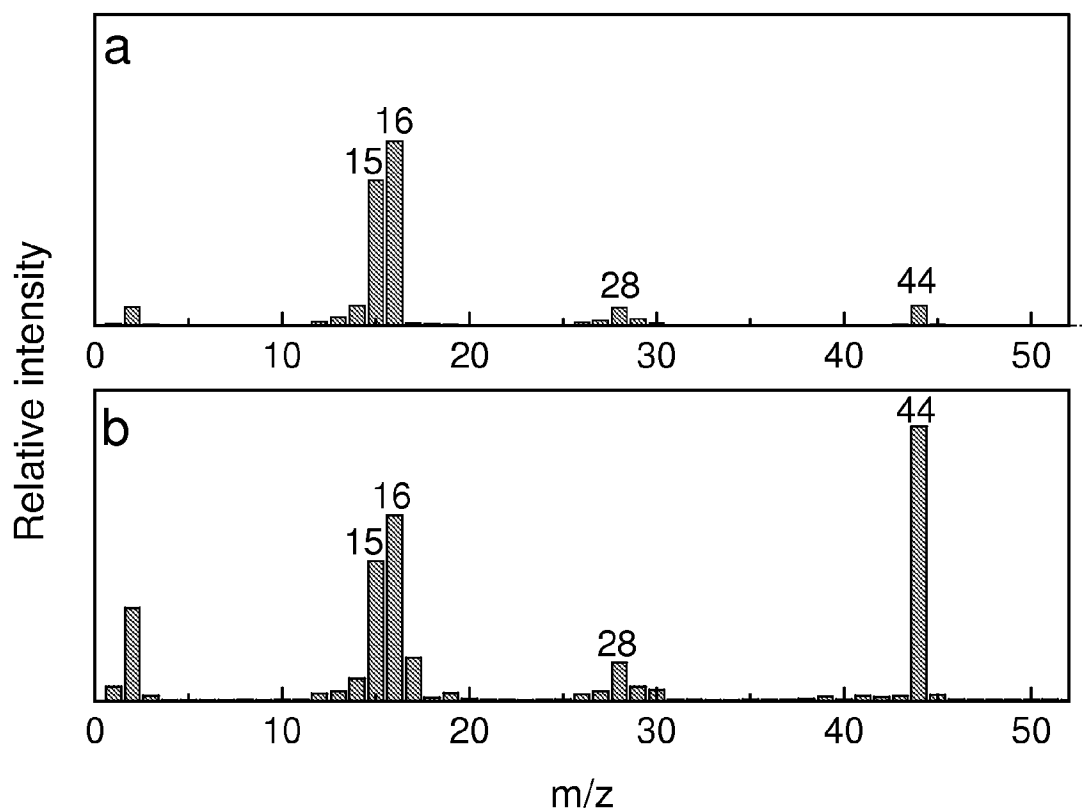


FIG. 11

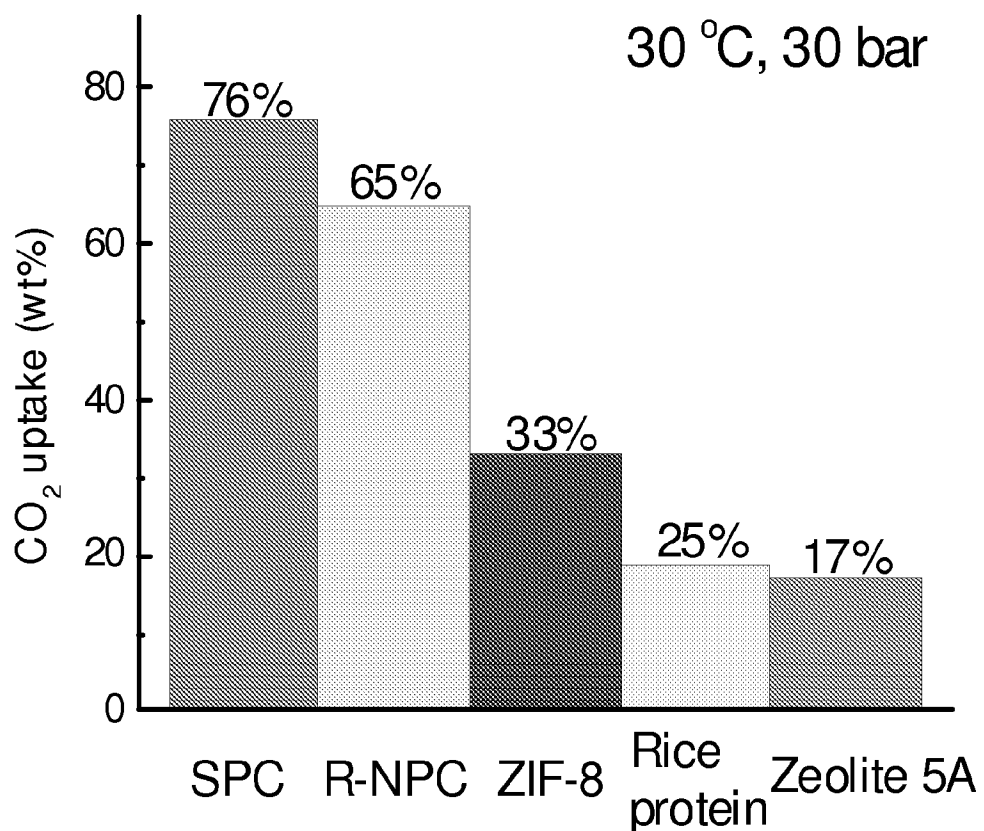


FIG. 12